TOWARDS A UNIFIED MODELLING FRAMEWORK FOR ADAPTIVE NETWORKS

By

Xiaoming Liu

A Thesis Submitted to the Faculty of Natural

Science of University of the Western Cape

in Fulfillment of the Requirements

for the Degree of

DOCTOR OF PHILOSOPHY

Major Subject: Computer Science

Ian Cloete, Thesis Supervisor

Boleslaw K. Szymanski, Thesis Co-Supervisor

Yongxin Xu, Thesis Co-Supervisor

University of the Western Cape
Bellville, Cape Town

November 2014

CONTENTS

LIST OF TABLES

LIST OF FIGURES

ACKNOWLEDGMENT

I would like to thank all the people that continuously support and encourage me during my graduate study at UWC. Without their help, I would not be able to complete my thesis.

I would first like to thank my supervisor Prof. Cloete for his advice, guidance, and encouragement during this research. He has given me a very high degree of freedom to work on topics of my choice. I am very grateful to his firm belief and constant support, without which this thesis would not been possible.

I would also like to thank my co-supervisor Prof. Szymanki, who has been giving me a lot of guidance. Prof. Szymanski has not only high academic standard, but also pleasant and friendly personality. He inspires many ideas and models in this thesis. I also acknowledge the assistance of my co-supervisor Prof. Xu on the fracture network project. He is very nice and always accessible. I have learned a lot from him. I am also grateful to James Connan and Verna Connan that support and help me during the long years.

I am deeply grateful to many people who helped me along the journey, in ways both big and small. It has been a pleasure to get to know and to work with all of them. I would like to thank Jierui Xie, a very active and talented researcher. He has been giving me a lot of helps on the social network project. I would also like to thank Prof. Venter, Prof. Tucker, Liang Xiao, Lixiang Lin, Haili Jia, Sahin Cem Geyik, Wen Dong, Long Yi, Changhong Luo, Fatima Jacobs, Rene Abbott, and Caroline Barnard. I also thank Jing Ma, a friend who give me a lot of support.

I would especially like to thank Prof. Nyongesa for giving me the opportunity to work on this research project and his continued support and help throughout this research.

Last but not least, I thank my parents for their endless love, support, and care. Although they were thousands of miles away from me, I always felt their presence in my heart. I dedicate this thesis to them.

ABSTRACT

Adaptive networks are complex networks with nontrivial topological features and connection patterns between their elements which are neither purely regular nor purely random. Their applications are in sociology, biology, physics, genetics, epidemiology, chemistry, ecology, materials science, the traditional Internet and the emerging Internet-of-Things. For example, their applications in sociology include social networks such as Facebook which have recently raised the interest of the research community. These networks may hide patterns which, when revealed, can be of great interest in many practical applications. While the current adaptive network models remain mostly theoretical and conceptual, however, there is currently no unified modelling framework for implementing the development, comparison, communication and validation of agent-based adaptive network models through using proper empirical data and computation models from different research fields.

In this thesis, a unified framework has been developed that combines agent-based adaptive network models and adaptive control structures. In this framework, the control parameters of adaptive network models are included as a part of the state-topology coevolution and are automatically adjusted according to the observations obtained from the system being studied. This allows the automatic generation of enhanced adaptive networks by systematically adjusting both the network topology and the control parameters at the same time to accurately reflect the real-world complex system.

We develop three different applications within the general framework for agent-based adaptive network modelling and simulation of real-world complex systems in different research fields. First, a unified framework which combines adaptive network models and adaptive control structures is proposed for modelling and simulation of fractured-rock aquifer systems. Moreover, we use this unified modelling framework to develop an automatic modelling tool, Fracture3D, for automatically building enhanced fracture adaptive network models of fractured-rock aquifer systems, in which the fracture statistics and the structural properties can both follow

the observed statistics from natural fracture networks. We show that the coupling between the fracture adaptive network models and the adaptive control structures with iterative parameter identification can drive the network topology towards a desired state by dynamically updating the geometrical states of fractures with a proper adaptive control structure.

Second, we develop a unified framework which combines adaptive network models and multiple model adaptive control structures for modelling and simulation of social network systems. By using such a unified modelling framework, an automatic modelling tool, SMRI, is developed for automatically building the enhanced social adaptive network models through using mobile-phone-centric multimodal data with suitable computational models of behavioural state update and social interaction update. We show that the coupling between the social adaptive network models and the multiple model adaptive control structures can drive the community structure of a social adaptive network models towards a desired state through using the suitable computational models of behavioural state update and social interaction update predetermined by the multiple model adaptive control structure.

Third, we develop a unified framework which combines adaptive network models and support vector machine-based adaptive control structures for modelling and simulation of multicast congestion in mobile ad hoc network systems. Moreover, a multicast congestion detection scheme, WMCD, has been developed for the unified modelling framework, in which the incipient congestions of group members can be predicted by using support vector machine-based prediction models and current traffic states. We show that the network's throughput capacity is efficiently improved through using the unified modelling framework, which dynamically adjusting the group structures according to the updated congestion states of group members generated by the WMCD scheme in order to relieve the high load.

CHAPTER 1
Introduction

1.1 Modelling Complex Systems with Adaptive Networks

This chapter introduces the background and the motivation for the research addressed in this thesis. Complex systems with different nature of the interacting components can generally be considered as an intricate network or physical network whose abstract nodes represent the interacting elements of the system and in which the set of connecting links represent the relations or interactions among the nodes (Zschalera, 2012). Thus, networks provide a powerful abstraction framework to a wide array of complex systems with either physical (real) and/or logical (virtual) interconnected components. The global properties of a complex system can be condensed into a simplified network model which contains the abstract nodes and links by considering its network structure. A network model focuses on the interactions between the components of complex systems and their implications for system behaviour, instead of focusing on their internal details. Such simple, often conceptual network models can help researchers to uncover the generic properties of the studied complex systems and thus build a bridge between different fields and applications (Börner et al., 2007; Zschaler, 2012).

Traditionally, a given network model either describes the dynamics on a certain network (the states of the nodes change in a given network structure) or the dynamics of a certain network (the processes generating particular network structures). Nevertheless, both types of dynamics occur simultaneously in most real-world complex systems. Furthermore, a feedback loop can be established where the states of the nodes and their interaction topology are interdependent (Zschaler, 2012). Networks which exhibit such a feedback loop are called adaptive networks (Gross & Blasius, 2008; Gross & Sayama, 2009).

In most real-world complex systems, many instances of adaptive networks can be found whose states and topologies coevolve. For example, in a computer network, the pattern of data links (the topology of the network) influences the through-

put over a link (the dynamic state). But if network congestions are common on a given link, new links will be created to relieve the high load on the congested nodes. Further examples include power grids (Scirè et al., 2005), the mail network, the Internet or wireless communication networks (Glauche et al., 2004; Krause et al., 2005; Lim et al., 2007), biological networks (Schaper & Scholz, 2003), and chemical networks (Jain & Krishna, 2001). In these adaptive networks, the coupling between state transition of each component and topological transformation of networks can give rise to novel emergent behaviour. Due to their ubiquity, modelling and simulation of complex systems with adaptive network models have been implemented in different scientific domains (Gross & Blasius, 2008; Blasius & Gross, 2009; Gross & Sayama, 2009; Do, 2011; Zschaler, 2012; Sayama et al., 2013; and references therein). However, there is currently no adaptive-network based unified framework for implementing the development, comparison, communication and validation of complex system models across different scientific domains.

1.2 Motivation

In the past few years, network-based modelling and simulation of complex systems have received a boost from the ever-increasing availability of high performance computers and large data collections. These developments have primarily advanced vertically in different scientific disciplines with a variety of discipline-specific approaches and applications (Niazi, 2011). Thus, a set of theories can be used for modelling different aspects of a certain complex system according to various empirical data and various types of network models. However, the nature of many interaction patterns and structure patterns observed both in natural and artificial complex systems are more complicated than their network models (Holthoefer, 2011). A few possibilities have been proposed to improve the performance of the network models, such as collecting a richer set of network data from real-world complex systems with more informative measurements, adjusting parameter regions of the models properly, measuring functional, behavioural and structural features of the models efficiently, and comparing the realizations generated by the models with reference data more comprehensively etc.

Adaptive networks are complex networks with nontrivial topological features and connection patterns between their elements which are neither purely regular nor purely random. Their applications are in sociology, biology, physics, genetics, epidemiology, chemistry, ecology, materials science, the traditional Internet and the emerging Internet-of-Things. For example, their applications in sociology include social networks such as Facebook which have recently raised the interest of the research community. These networks may hide patterns which, when revealed, can be of great interest in many practical applications. In recent years, the rapidly growing research on adaptive networks has opened new avenues to modelling and simulation of complex systems. The adaptive interplay between local and topological dynamics can drive an adaptive network model towards desired target states. Nevertheless, there is no existing unified modelling framework allowing for automatically shaping the network data and the adaptive network models in terms of the observations of a real-world complex system. Having such an automated modelling framework would greatly reduce the human effort and provide a valuable tool for better understanding, description, prediction, and control of the real-world complex systems around us.

1.3 Aims and Objectives

The aim of this research is to developed a unified framework that combines agent-based adaptive network models and adaptive control structures. In this framework, the control parameters of adaptive network models are included as a part of the state-topology coevolution and are automatically adjusted according to the observations obtained from the system being studied. This allows the automatic generation of enhanced adaptive networks by systematically adjusting both the network topology and the control parameters at the same time to accurately reflect the real-world complex system.

This unified framework was applied for modelling and simulation of three different real-world problems, namely fractured-rock aquifer systems, the social community structure generated by mobile phone interactions, and multicast congestion in mobile ad hoc networks. In all cases the unified framework demonstrated im-

proved understanding of the adaptive networks and the capability to model different phenomena using a generalized approach. The key research objectives of this research are listed as follows:

1. Outline the concepts and terminology of adaptive networks as background,
2. Present a critical survey of relevant literature for identifying common elements in different application (case studies) of adaptive networks,
3. Development of a unified modelling framework inspired by the combination of an adaptive network modelling approach and an adaptive control approach, and,
4. Apply the proposed framework to three different applications as case studies to demonstrate that the unified model can accommodate design variants with different features in the same model.

1.4 Contributions and Organization

In this work, a unified framework with the combination of adaptive network models and adaptive control structures is presented for modelling and simulation of real-world complex systems. In this modelling framework, a real-world complex system is represented by an adaptive network model, and the feedback loop formed by the interplay between state and topology is viewed as a dynamical system. An adjustable controller is then used for automatically shaping the network data and the adaptive network models according to the observations of the studied system. By using such a unified modelling framework, the enhanced adaptive network models with desired network structures are built automatically. Further insights into the essential properties of the real-world complex systems can be gained from these adaptive network models, because they present more realistic coevolutionary dynamics between the node states and the network topology in the same framework. Moreover, the modelling framework also provides a guideline for developing the adaptive network models of complex systems spanning multiple scientific disciplines.

In the main part of this thesis, we propose three different applications within the general framework for agent-based adaptive network modelling and simulation

of real-world complex systems in different research fields, such as developing a unified framework which combines adaptive network models and adaptive-control based model parameter identification for modelling fractured-rock aquifer systems, developing a unified framework which combines adaptive network models and multiple model adaptive control for modelling social network systems, and developing a unified framework which combines adaptive network models and support vector machine-based adaptive control structures for modelling wireless ad hoc network systems. Moreover, three automatic adaptive network modelling tools, namely Fracture3D, SMRI, and WMCD have been developed based on this unified modelling framework for different real-world complex systems. With the concept "tool," the meaning is that it is a specific model within the unified framework for a particular application. A tool adapts the parameters and structure of the model automatically based on observational data. Each of the three models have been named for easy reference. These tools demonstrate that the enhanced adaptive network models created by the combination of adaptive network models and adaptive control structures are able to gain more insights in the studied systems. They also show that the unified modelling framework can help multidisciplinary researchers better understand, describe, predict, and control complex systems.

We start in Chapter 2 with a brief overview of the basic concepts and tools from graph and network science used in this work. We introduce adaptive networks with a review of the recent research in this field. In addition, we summarize the basic concepts about adaptive control.

In Chapter 3, the unified modelling framework is introduced. It can automatically shape the network data and the adaptive network models based on the observations of the studied complex system through combining adaptive network models and adaptive control structures. We then introduce three adaptive control structures for modelling complex systems with adaptive network models. Further, a brief introduction of three real-world complex systems will is given.

A unified framework which combines adaptive network models and adaptive control structures with iterative parameter identification is proposed for modelling and simulation of fractured-rock aquifer systems in Chapter 4. In this framework,

the adaptive control structures with iterative parameter identification are used to identify an instance of an adaptive network model with desired topological characteristics, while the natural fracture networks are represented by an adaptive network models with "geometrical state–fracture cluster" coevolution. By using this modelling framework, an automatic modelling tool, Fracture3D, is developed for automatically building the enhanced 3–D fracture adaptive network models, in which the fracture statistics and the structural properties can both follow the observed statistics from natural fracture networks. Through using simple field data and measurements taken on site or in-situ such as length, orientation, and density of measured fractures, the enhanced fracture adaptive network models can be built for rapidly evaluating the connectivity of the studied aquifers on a broad range of scales.

In Chapter 5, we propose a unified framework which combines adaptive network models and multiple model adaptive control structures is proposed for modelling and simulation of social network systems. In this framework, a real-world social network system can be represented as an agent-based adaptive network which is defined by a feedback loop between behavioural state of individuals and community structure of the studied system, where a multiple model adaptive control structure is used for the predetermination of suitable computational models of behavioural state update and social interaction update in order to improve the performance of modelling and simulation. By using such a unified modelling framework, an automatic modelling tool, SMRI, is developed for automatically building the enhanced social adaptive network models whose community structures are similar to the studied real-world social network systems through using mobile-phone-centric multimodal data with suitable computational models of behavioural state update and social interaction update.

In Chapter 6, a unified framework which combines adaptive network models and support vector machine-based adaptive control structures is proposed for modelling and simulation of multicast congestion in mobile ad hoc network systems. In this framework, a mobile ad hoc network system can be represented as an agent-based adaptive network which is defined by a feedback loop between congestion

states of group members and group structure of the network, where the support vector machine-based adaptive control structures are used for the prediction of incipient congestions. Moreover, a multicast congestion detection scheme, WMCD, has been developed for the unified modelling framework, in which the incipient congestions of group members can be predicted by using support vector machine-based prediction models and current traffic states. In this scheme, a congestion prediction model is created by SVMs which quantifies the dynamics of multicast packet flows. The multicast group members then automatically update their congestion states based on the congestion prediction model. By using the updated congestion states, a set of instances of the adaptive network model with updated group structures are generated for dynamically adjusting the network topology and group structure of the mobile ad hoc network system and relieving the high load.

Finally, we summarize our results in Chapter 7. Moreover, we discuss the possible extension of the unified modelling framework and suggest directions for future work. Some additional related works about measurement of structure properties in complex networks , complex network models, and adaptive control are introduced in Appendix A, B, and C respectively. Figure 1.1 illustrates a grouping of the chapters in related subjects.

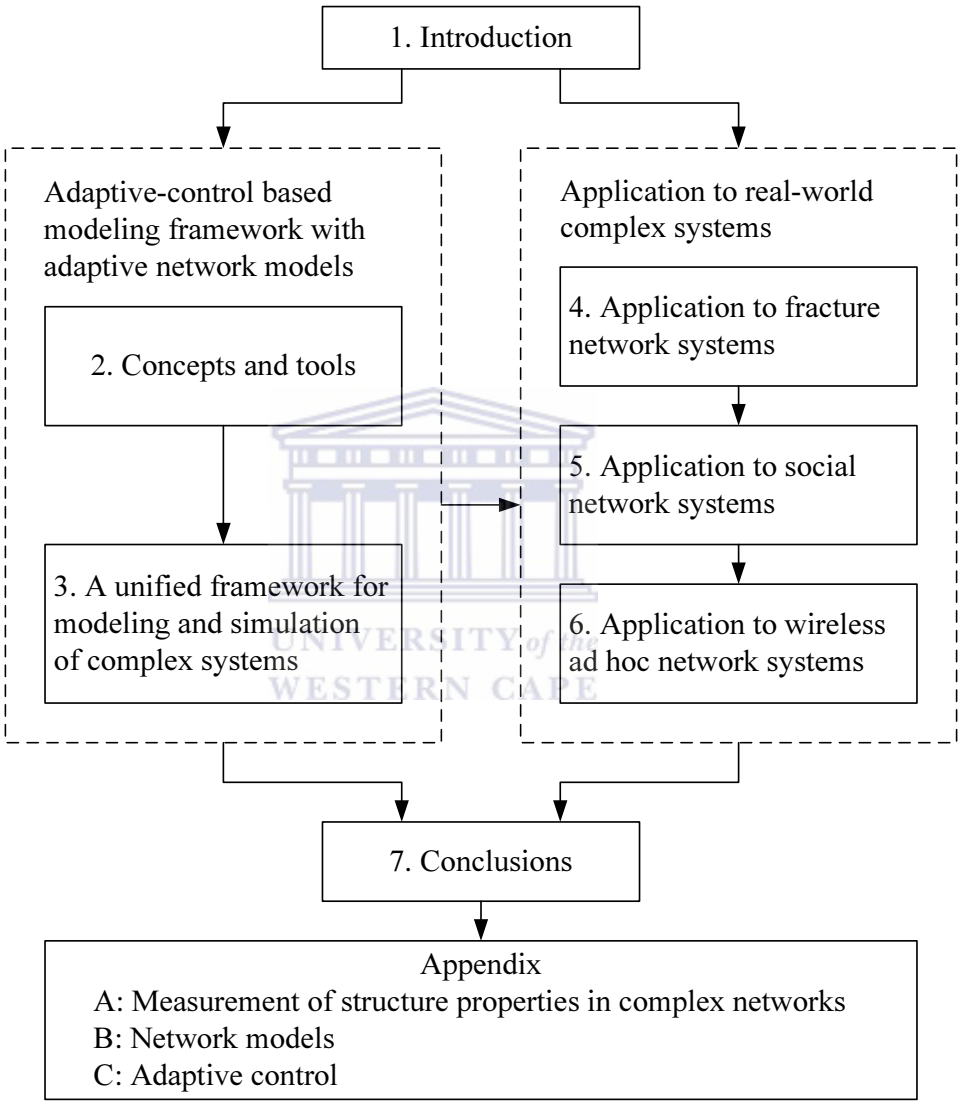

Figure 1.1: Road map of the thesis.

CHAPTER 2
Concepts and Tools

In this chapter we introduce the relevant concepts and approaches. The purpose of this work is to develop a unified modelling framework that automatically shapes the network data and the network models by the combination of adaptive network models and adaptive control structures. Moreover, the real-world applications need to be developed in order to demonstrate how the unified modelling framework can automatically build the enhanced adaptive network models with desired network structures in different real-world complex systems. We chose the pragmatic paradigm as the appropriate research paradigm for this research which spans multiple scientific disciplines. Thus, the selected topics are "research objective-centred." They are presented here for understanding of the thesis and to achieve mathematical rigour. We begin in this chapter with a brief overview of the basic concepts from graph theory and network science. In Section 2.2, we introduce adaptive networks, and review the recent research on adaptive networks. Finally, in Section 2.3 we review the relevant notions from adaptive control.

2.1 Modelling Complex Systems with Network Models

Complex systems, as their name implies, are typically difficult to understand, and hard to control. Traditionally the simplified mathematical models are created and studied by more mathematically oriented sciences such as physics, chemistry, and mathematical biology. These models try to abstract the studied complex systems into a solvable framework, rather than mimic the behaviour of real systems exactly. The rise of interest in understanding global properties of complex systems has paralleled the rise of network science, because the network based approach can create more comprehensive and realistic models of complex systems in nature (Newman, 2011). Networks that represent the interactions between the system's components can be found in each complex system, such as friendship and acquaintance networks in social systems, power grids in electric power systems, trade networks in

economic systems, etc. (Barrat et al., 2008; Boccaletti et al., 2010). As Barabási points out (Barabási et al., 2014), we will never understand complex systems unless we gain a deep understanding of the networks behind them. Network science provides a language through which different research theories, approaches, and applications, from a wide range of research fields can seamlessly interact with each other. This interaction has led to a cross-disciplinary fertilization of tools and ideas which increase our understanding of natural and artificial complex systems (Börner et al., 2007; Barabási et al., 2014).

In the next section, we will review network science by following a conceptual framework, in which a network science approach is used for modelling complex systems. As depicted in Figure 2.1, there are four major processes for developing a network model which explains, describes, and predicts an observed phenomenon in a certain complex system, including network sampling, network modelling, network measurements, and model validation. Firstly, an appropriate dataset is collected or sampled from an observed phenomenon. Next, a network model is created as a simplification of this phenomenon. Subsequently, network measurements are used for identifying essential features of the network model. Model validation is then implemented by the comparison of empirical and modelled data. The network model is considered a good representation of the phenomenon if there is structural similarity between them. Otherwise, a further refinement of the model is required and the process of modelling repeated until the obtained results fits the empirical data. We start with a briefly overview of the essential notions and notations needed to describe networks. Further, the major processes in the modelling of complex systems will be introduced briefly.

2.1.1 Notions and Notations

A complex network is represented as a graph or undirected graph $G = (\mathcal{N}, \mathcal{L})$, formed by a set $\mathcal{N} \equiv \{n_1, n_2, \ldots, n_N\}$ of nodes (or vertices, or points) and a set $\mathcal{L} \equiv \{l_1, l_2, \ldots, l_L\}$ of links (or lines, or edges) $l_k = \{n_i, n_j\}$ that connect the nodes. When the links between pairs of nodes have direction, the graph is represented as

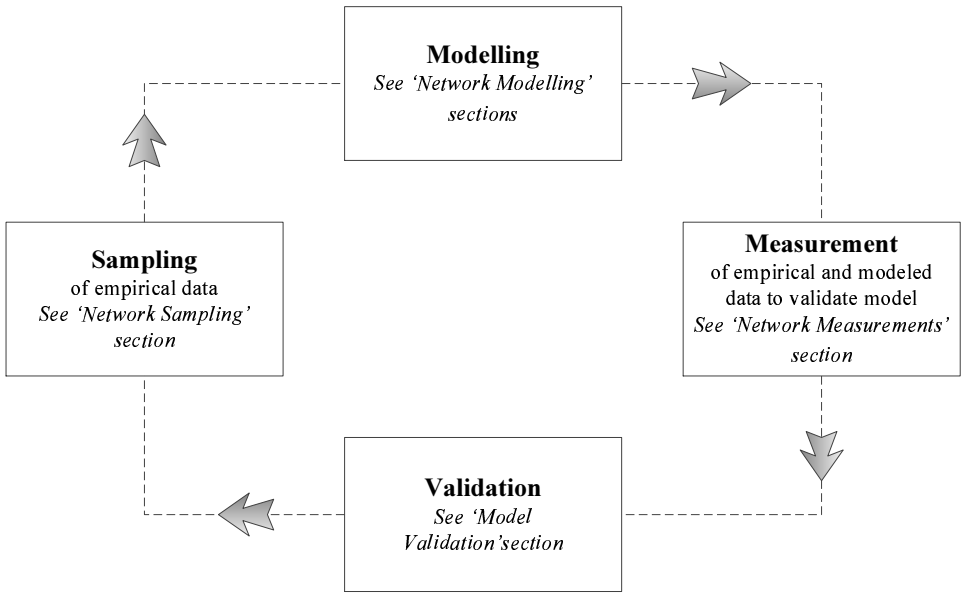

Figure 2.1: General network science research process for modelling of complex systems. There are four major processes for developing a network model which explains, describes, and predicts an observed phenomenon in a certain complex system, including network sampling, network modelling, network measurements, and model validation.

a directed graph $G^{\rightarrow} = (\mathcal{N}, \mathcal{L}^{\rightarrow})$, where $\mathcal{N}$ is the set of nodes and $\mathcal{L}^{\rightarrow}$ is the set of ordered pairs of arcs (or arrows). Each arc can be identified by a pair (i, j) that represents a connection going to node i. In undirected graphs, if nodes i and j are connected and nodes j and k are connected, i and k are also connected. A set of non-overlapping subsets of connected nodes can be found in a graph based on the property. A cluster is one of the subsets. A graph $G^{\star} = (\mathcal{N}^{\star}, \mathcal{L}^{\star})$ is a subgraph of $G = (\mathcal{N}, \mathcal{L})$ if $\mathcal{N}^{\star} \subseteq \mathcal{N}$, $\mathcal{L}^{\star} \subseteq \mathcal{L}$ and the links in $\mathcal{L}^{\star}$ connect nodes in $\mathcal{N}^{\star}$. The network is called connected if there exists a path between any pair of nodes; otherwise it is called disconnected. A weighted graph $G^{w} = (\mathcal{N}, \mathcal{L}, \mathcal{W})$ is formed by a set of N nodes and L links, the set of $\mathcal{W} \equiv \{w_1, w_2, \ldots, w_L\}$ weights that represent the intensity of connections. If the nodes are linked by arcs, the weighted graph $G^{w\rightarrow}$ is directed. A geographical network $G = (\mathcal{N}, \mathcal{L}, \mathcal{D})$ can be defined by a set N of nodes, a set L of links, and a set $\mathcal{D} \equiv \{\overrightarrow{p}_1, \overrightarrow{p}_2, \ldots, \overrightarrow{p}_N\}$, where $\overrightarrow{p}_i$ is an n-dimensional coordinate vector of the node i (Costa et al., 2011).

A graph can be represented by using adjacency lists or adjacency matrices. In the case of using adjacency lists, the graph is represented in terms of a list of links (represented through head and tail). The graph can be also represented by an adjacency matrix A, so that each element $a_{ij} = 1$ expresses an link connecting nodes i and j, and $a_{ij} = 0$ otherwise. A weighted digraph can be represented by a weight matrix W, where the matrix element w_{ij} represents the weight of the connection from node i to node j. The operation of thresholding, represented as $A = \delta_T(W)$, can be used to produce an unweighted counterpart from a weighted digraph; in case $|w_{ij}| > T$ we have $a_{ij} = 1$, otherwise $a_{ij} = 0$, where T is a specified threshold. (Costa et al., 2007).

2.1.2 Network Sampling

In the past few years, network science has received a boost from the ever-increasing availability of high performance computers and large data collections. However, the size, type and richness of empirical data, which consist of observations and measurements of a complex system, are very different in various application domains (Börner et al., 2007). In many cases, the sheer size of empirical data makes it computationally infeasible to study the entire system. In other cases, the size of empirical data may not be large but measurements are required to observe the underlying phenomenon. To create a reliable dataset which demonstrates major properties of a studied complex system, network sampling techniques are used. Thus, network sampling can be considered as the process of acquiring network datasets from gathered empirical data. There are three classes of sampling methods, including node sampling, edge sampling, and topology-based sampling. The sampled subsets may be generated by choosing nodes and/or links which match or exceed a certain threshold, while a sample can also be constructed by using breath-first search (i.e. sampling without replacement) or random walks (i.e. sampling with replacement) over a graph (Börner et al., 2007; Airoldi et al., 2011). To reduce the sampling bias, a large number of techniques have been developed for improving the quality of the recovered samples. More detailed discussion of these approaches can be found in (Börner et al., 2007; Airoldi et al., 2011; Maiya, 2011; and references

therein).

2.1.3 Network Measurements

In order to describe the topology of a network, a large set of measurements have been developed (Costa et al., 2007). By using the measurements described in Appendix A, local analysis can be implemented based on node measurements, while global analysis can be performed based on average measurements for the whole network (Costa et al., 2011). Community identification methods and measurements on complex network are used for intermediate analysis. Community structures can be represented by set of groups whose nodes are more densely interconnected to one another than with the rest of the network (Costa et al., 2007). Many community identification algorithms have been proposed because uncovering the community structure can deepen our understanding of complex systems. After traditional hierarchical clustering methods (Podani et al., 2001; Girvan & Newman, 2002; Ravasz et al., 2002) were applied in some early research (Eckmann et al., 2002; Girvan & Newman, 2002; Maslov & Sneppen, 2002), a quality function called modularity (Newman & Girvan, 2004) was introduced for choosing the optimal partition. A few methods with optimal quality function were then proposed by applying a new heuristic or modifying the quality function (Fortunato, 2010). More alternative methods were also proposed based on different principles, such as percolating cliques (Palla et al., 2005), information compressing (Rosvall & Bergstrom, 2007), and elementary physical dynamics (Raghavan et al., 2007), etc. Multiresolution methods (Danon et al., 2005; Reichardt & Bornholdt, 2006; Delvenne et al., 2010) with a tunable parameter were proposed to resolve clusters under a quite large, network-dependent size, while the original modularity method suffers from an intrinsic resolution limit problem (Fortunato & Barthélemy, 2007; Kumpula et al., 2007). To find clusters inside a cluster, several hierarchical methods (Sales-Pardo et al., 2007; Ruan & Zhang, 2008; Kovács et al., 2010; Rosvall & Bergstrom, 2011) were introduced. Besides communities, there are other types of subgraphs in complex networks, such as motifs (Milo et al., 2002), cycles (Bagrow et al., 2006) and chains (Villas Boas et al., 2008).

2.1.4 Network Modelling

In this section, a brief review of network modelling approaches is provided. The first sub-section starts with an introduction of network formation models. The next sub-section introduces that aim to model the dynamical processes on networks. The third sub-section provides a brief overview of an agent-based modelling approach. A detailed introduction of diverse network modelling approaches can be found in (Wasserman & Faust, 1994; Kumar et al., 2000; Newman, 2003; Carrington et al., 2004; Pastor-Satorras & Vespignani, 2004; Newman et al., 2006; Börner et al., 2007; Newman, 2010; Newman, 2011).

2.1.4.1 Modelling Formation of Networks

In order to study the structure of complex systems, a few statistical models of network formation have been developed based on a set of graphs matching certain statistical threshold of the studied systems. Some structural features observed in complex systems can be reproduced by the network formation models, such as small average path lengths, strong clustering, and scale-free degree distributions (Bollobás, 1998; Zschaler, 2012). Several network models have become a subject of great interest, including Erdös-Rényi random graph, small-world model of Watts and Strogatz, Barabási-Albert scale-free model, and Waxman geographical model (see Appendix B).

2.1.4.2 Modelling Dynamics on Networks

The dynamics of interactions between the constituting elements of a certain complex system can be investigated based on the structure or certain network properties of the system. . In many cases, the evolution of a network's structure is determined by some internal dynamics of the nodes and the interactions between them. Diffusion modelling has been implemented in various applications, including the spreading of diseases, viruses, fashion, rumours, or knowledge (Daley et al., 1999; Tabah, 1999; Liljeros et al., 2001; Pastor-Satorras & Vespignani, 2001; Bettencourt et al., 2005; Keeling & Eames, 2005). In these models, the master equation approach is used for analysis of dynamical processes on networks. This approach

assumes that the states of the nodes can be described by one or more dynamical variables. Transitions of the states are probabilistically obtained from contacts among nodes. Thus, the contact networks provide the underlying interaction geometry in which diffusion occurs (Boccaletti et al., 2006; Börner et al., 2007; Barrat et al., 2008; Zschaler, 2012).

Other dynamical processes have also been studied in artificial complex systems, such as power grid, the Internet, communication systems, for understanding the dynamics of information flow, data flow, and traffic flow. In these systems, the nodes and links are often sensitive to overloading. The failure of one node or one link may increases the burden on other network components, and eventually leading to an avalanche of overloads on them. Modelling dynamics on these networks can provide indications to decrease the undesired effects. Other examples of dynamical processes on networks can be found in neuronal networks and food webs. Synchronization phenomena have been investigated by using an interaction network model which contains a coupled oscillator in conceptual models of neuronal networks. (Kuramoto, 2003; Moreno & Pacheco, 2004). In food webs, dynamical processes are studied by modelling the flow of biomass between predators and their prey. (Camacho et al., 2002; Gross et al., 2009; collective dynamics-Pimm, 2002)(Camacho et al., 2002; Pimm, 2002; Gross et al., 2009).

Most recently modelling dynamical processes often entails using one of two basic methods of developing computational models which use for modelling dynamical process i.e. either use of master equation approach for analysis of dynamical processes on networks or else use of agent-based modelling approach to develop simulation models. In more complicated models, the master equation approach might not lead to solvable equations. Moreover, this approach cannot provide a complete picture of studied system because individual heterogeneity or other possible fluctuations are ignored. In this situation, agent-based models can be applied (Börner et al., 2007; Barrat et al., 2008).

2.1.4.3 Agent-Based Modelling

If analytical solutions cannot be found by the master equation approach in more complicated models, an agent-based modelling approach can be applied for the simulation of complex and varied interactions among the nodes. This approach separately and individually simulate the agents in a complex system and their interactions, allowing the emergent behaviours of the system to appear naturally (Börner et al., 2007; Barrat et al., 2008; Newman, 2011). Agent-based models (Bankes, 2002) have become fashionable in a wide variety of complex systems (Bonabeau, 2002), ranging from biological systems (Folcik et al., 2007; Huang et al., 2007; Devillers et al., 2008; Galvao et al., 2008; Guo et al., 2008; Kiran et al., 2008; Lao & Kamei, 2008; Odell & Foe, 2008; Rubin et al., 2008; Robinson et al., 2008; Santoni et al., 2008; Bailey et al., 2009; Carpenter & Sattenspiel, 2009; Dancik et al., 2010; Galvao & Miranda, 2010; Itakura et al., 2010) to social systems (Gilbert & Troitzsch, 2005; Batty et al., 2007; Chen & Zhan, 2008; Quera et al., 2010), from financial systems (Streit & Borenstein, 2009) to ecosystems (Grimm et al., 2006; Railsback & Grimm, 2011), from supply chains (Zarandi et al., 2008) to modelling of traffic lights (Gershenson, 2005). When modelling dynamical processes using an agent-based modelling approach, each individual node is assumed to be in one of several possible states. A model-specific update procedure that depends on the microscopic dynamics is applied to each node in each discrete time step. The state of a node is changed depending on the state of neighbouring nodes or other dynamic rules. The dynamics of each individual element can be simulated through using Monte Carlo methods, where the random events of the dynamical process are simulated with the use of random number generators. The agent-based modelling approach can be used to reproduce the dynamics occurring in networks, and provides access to the microscopic dynamics of the system that is in general hindered by the mathematical complexity and the large number of degrees of freedom inherent to real-world complex systems. In addition, this approach allows extremely detailed information to be obtained and provide a way to monitor the single state of each agent at any time (Börner et al., 2007; Barrat et al., 2008; Newman, 2011).

A variety of software packages are available for performing agent-based mod-

elling and simulation of complex systems (Newman, 2011; Niazi, 2011). Some of them, such as Repast (North & Macal, 2007) and Mason (Panait & Luke, 2005), are highly advanced programming libraries suitable for cutting edge research, while others are designed as easy-to-use tools requiring little prior knowledge, such as StarLogo (Resnick, 1996), NetLogo (Wilensky, 1999) etc. In addition, some simulators have been developed for the simulation of communication systems, such as NS-2, OPNET (Garrido et al., 2008), J-Sim (Sobeih et al., 2006), TOSSIM (Levis et al., 2003) etc. TOSSIM is a TinyOS simulator. J-Sim and NS-2 have been compared in (Sobeih et al., 2006) and J-Sim is more scalable than NS-2. SensorSim is a simulation framework for wireless sensor networks (Park et al., 2000), while ATEMU (Polley et al., 2004) focuses on simulation of particular sensors. Further examples include Oversim (Baumgart et al., 2007) and PeerSim (Montresor & Jelasity, 2009) for simulation of peer-to-peer networks, Swarm-Bot (Mondada et al., 2004), WebotsTM (Michel, 2004), and LaRosim (Sahin et al., 2008) for simulation of robotic swarms, etc.

Although an agent-based modelling approach can simulate very intricate dynamical processes while fully incorporating stochastic effects, agent-based models are often very complicated. Moreover, it is difficult to study the impact of any given modelling assumption or parameter. Thus, a careful trade-off between the level of details and the interpretation of results is important to modelling and simulation of real-world complex systems. (Börner et al., 2007; Barrat et al., 2008; Newman, 2011).

2.1.5 Model Validation

All models make implicit assumptions about the real-world complex systems based on our understanding of world, while model a certain complex system with all details is impossible. Suitable approximations need to be made according to the corresponding research study objectives and expected outcomes. Dynamic modelling is more suited for modelling large-scale and evolutionary complex systems, while statistical modelling is well suited for modelling the complex systems with the statistical observables. However, all these models need to be validated through the

comparison of modelled data and empirical data for real-world complex systems. By using statistical modelling, the parameters of the statistical models can be obtained based on the statistical measures derived from the empirical data. Moreover, the statistical predictions derived from the generated distributions can be tested by new measurements on the empirical data. In the dynamical approach, the properties of empirical data are used to validate models, while their local dynamic rules normally take no account of the statistical observables (Börner et al., 2007, Barrat et al., 2008). However, agent-based models can be difficult to validate because both the structure of underlying network and local dynamic rules are related to the statistical observables of the studied complex systems. As Niazi points out (Niazi, 2011), a number of issues need to be handled for validation of agent-based models as follows:

- There is no standard way of building agent-based models.
- There is no standard and formal way of validation of agent-based models.
- Agent-based modelling and agent-based simulations are considered in the same manner because there is no formal methodology of agent-based modelling (Macal & North, 2007).
- Agent-based models are primarily pieces of software however no software process is available for development of such models.
- All validation paradigms for agent-based models are based on quantifying and measurable values but none caters for emergent behaviour (Axtell, 1999; Axtell et al., 1999) such as traffic jams, structure formation or self-assembly as these complex behaviours cannot be quantified easily in the form of single or a vector of numbers.

A variety of approaches have been proposed for validation of agent-based models. For example, in the case of Agents in Computation Economics (ACE), empirical validation of agent-based models has been developed by Fagiolo et al. in (Fagiolo et al., 2007). Alternate approaches to empirical validation have been showed by Moss in (Moss, 2008). In Wilensky and Rand's work (Wilensky & Rand, 2007), it has

been found that validation of models is closely related to model replication as noted. An iterative participatory approach, "companion modelling", has been developed by Barreteau et al. in (Barreteau, 2003) where multidisciplinary researchers and stakeholders work together throughout a four-stage cycle. An approach of validation has been discussed in which philosophical truth theories are used in simulations (Schmid, 2005). In addition, agent-based simulation can be used as a means of validation and calibration of other models (Makowsky, 2006).

The general network science research approach has been used for modelling and simulation of complex systems in different real-world applications. However, in this research, the network based approaches (network sampling, modelling, measuring, and validating) are applied to four domains of the adaptive network modelling process for dynamically adjusting their control parameters. Moreover, such a "network structure-centred" modelling framework allows the automatic generation of enhanced adaptive networks by systematically adjusting both the network topology and the control parameters at the same time to accurately reflect the real-world complex system.

2.2 Adaptive Networks

In recent years, the study of networks has received a rapidly increasing amount of attention, with many applications in social, biological and technical systems. Traditionally, most research has taken into account "dynamics of networks" or "dynamics on networks" independently. While the "dynamics of networks" approach focuses on the emergence and evolution of particular network structures, the "dynamics on networks" approach emphasizes on the state transition of nodes on a network with a fixed topology. In this case the network topology can have a strong impact on the dynamics of the nodes (Leidl & Hartmann, 2009; Zschaler, 2012, Sayama et al., 2013).

In real-world complex systems, the underlying networks can provide a static interaction topology for local dynamical process. In many cases, however, these networks also evolve and change due to the ongoing local dynamical process. Moreover, a feedback loop among the dynamics of the network and the dynamics on the

network can be established based on the dynamics of the nodes and the topology of the network that interact with each other and keep changing (see Figure 2.2) (Zschaler, 2012). Networks which present such a feedback loop are called adaptive or coevolutionary networks (Gross et al., 2008). Some examples of "adaptive network" have been shown in Table 2.1. Further examples of this class of networks can be found in (Gross & Blasius, 2008; Gross & Sayama, 2009; Leidl & Hartmann, 2009; Schuster, 2009; Zschaler, 2012; Sayama et al., 2013; and references therein).

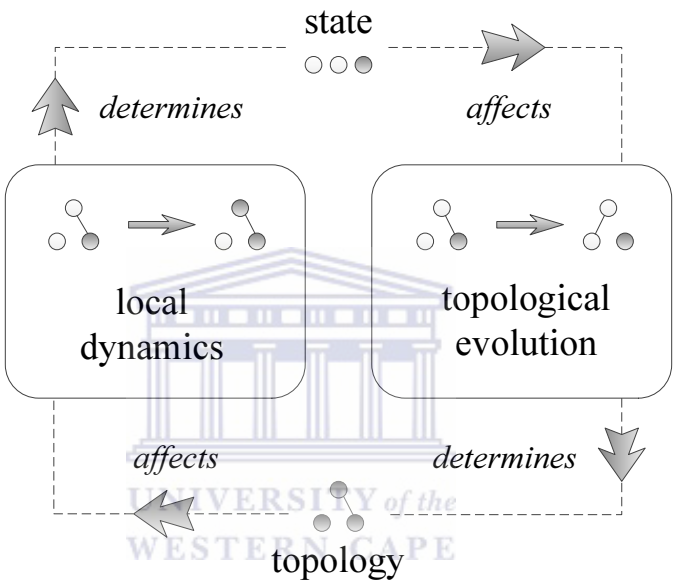

Figure 2.2: In an adaptive network, the evolution of the topology relies on the dynamics of the nodes. A feedback loop is thus created in which a dynamical exchange of information is possible. Figure adapted from (Gross & Blasius, 2008).

In general, the underlying network topology can have a strong impact on dynamical processes that takes place on a fixed network. The network topology is thus mapped to the local dynamics with topological information (Gross & Sayama, 2009; Zschaler, 2012). In certain situations, this topological information may be used to explore topological properties of the network by analyzing the behaviour of dynamical processes on the network (Reichardt & Bornholdt, 2004; Arenas et al., 2006; Hu et al., 2008). In an adaptive network, global topological information

Real-world complex systems	Nodes	Links	Examples of node states	Examples of node addition or removal	Examples of topological changes
Organism	Cells	Cell adhesions, intercellular communications	Gene/protein activities	Cell division, cell death	Cell migration
Ecological community	Species	Ecological relationships (predation, symbiosis, etc.)	Population, intraspecific diversities	Speciation, invasion, extinction	Changes in ecological relationships via adaptation
Epidemiological network	Individuals	Physical contacts	Pathologic states	Death, quarantine	Reduction of physical contacts
Social network	Individuals	Social relationships, conversations, collaborations	Socio-cultural states, political opinions, wealth	Entry to or withdrawal from community	Establishment or renouncement of relationships
Wireless network	Devices	Data communications	Congestion states	Join to or leave from multicast group	Establishment or renouncement of communication channels
Fracture network	Fractures	Intersections	Interconnected states	Fracture initiation and propagation	Fractures intersect due to the growth of size

Table 2.1: Real-world examples of adaptive networks in which the states and the topologies interact with each other and coevolve. Table adapted from (Sayama et al., 2013).

can be accessed locally as the local dynamics of the nodes are ruled by it. Moreover, the nodes can make local changes to the topology depending on this global information, and thus affect the topological dynamics again (Zschaler, 2012). Such a coevolutionary feedback loop can produce novel dynamical phenomena in adaptive networks that would not be seen in other forms of networks (Sayama et al., 2013). Although the range of applications from which adaptive networks emerge is diverse, the reported results demonstrate that several dynamical phenomena recurrently appear: robust dynamical self-organization, spontaneous division of labour, the formation of complex topologies, and complex system-level dynamics (Gross & Blasius, 2008). In the following, a brief introduction of these phenomena will be given, based on the reviews in (Gross et al., 2008; Zschaler, 2012; Sayama et al., 2013). Further details can be found in (Gross & Blasius, 2008; Gross & Sayama, 2009; Leidl & Hartmann, 2009; Schuster, 2009; Zschaler, 2012; Sayama et al., 2013).

2.2.1 Robust Self-Organization

The adaptive feedback with the coevolution of the local dynamics and network topologies provides a robust mechanism for global self-organization. It allows an adaptive network to robustly organize into a state with special topological or dynamical properties (Leidl & Hartmann, 2009). Moreover, the coupling of local dynamics and network topologies can provide a dynamical self-organization, in which the local dynamics drives the network topologies towards a critical point (Christensen et al. (1998.

Bornholdt and Rohlf (2000) considered a Boolean threshold network, where a topological update rule determined the local dynamics. Their investigation illustrated that the topological information can be accessed locally and affect the local dynamics of the topology. The local dynamics then drove the topological dynamics towards the critical state. Thus, the interplay of two local processes can give rise to a highly robust global self-organization without the impact of the initial conditions and the specific control parameters. (Gross et al., 2008; Zschaler, 2012; Sayama et al., 2013;). This dynamical self-organization behaviour has also been found in different complex network models (Christensen et al., 1998; Bornholdt & Roehl, 2003; Liu & Bassler, 2006), including some models for the investigation of self-organized criticality in adaptive neural systems (Chialvo & Bak, 1999; Beggs & Plenz, 2003; Liu & Bassler, 2006; Kitzbichler et al., 2009; Levina et al., 2009; Meisel & Gross, 2009; Pearlmutter & Houghton, 2009; Meisel et al., 2012), in which the generality of the underlying mechanism is highlighted.

2.2.2 Spontaneous Division of Labour

In adaptive networks, the adaptive interplay between the node states and the network topology can produce different classes of nodes from an initially homogeneous population (Gross et al., 2008). This spontaneous "division of labour" phenomenon was shown by Ito and Kaneko (Ito & Kaneko, 2001) in an adaptive network of coupled oscillators. They investigated a weighted directed network which consists of a few one-dimensional chaotic oscillators. The states of the nodes were updated based on the states of the their neighbours, while the network topology

can be modified through using a update rule of link weights. Moreover, this update rule increases link weights between oscillators with similar states, and still keeps the total weight of all incoming links of each node constant at the same time (Zschaler, 2012; Gross et al., 2008).

In a certain parameter region, two classes of nodes with distinct effective out-degree (high/low) can be observed. Moreover, a node generally remain in one class over a long period of time despite the ongoing rewiring of individual links. Thus, the nodes with high out-degree have more influences on other nodes than the low out-degree nodes because all nodes are impacted by their incoming connections (Gross et al., 2008; Zschaler, 2012). In this regard, the two classes of nodes in a system can be considered as a spontaneous "division of labour" with "leaders" and "followers". Similar phenomena have also observed in different complex networks. In some dynamical models of neural network, the topology is changed through a strengthening of connections among nodes with similar state (Gong & van Leeuwen, 2004; van den Berg & van Leeuwen, 2004). In addition, emergent "leadership" has also been found when researchers studied the Prisoner's Dilemma game on adaptive network 2004; Eguíluz et al., 2005). In these models, the nodes generally follow other nodes in self-organized hierarchical structures (Zschaler, 2012).

2.2.3 Formation of Complex Topologies

In adaptive networks, heterogeneous structures can arise from initially homogeneous conditions through the coevolution of the local dynamics and the topological dynamics. Furthermore, highly complex topologies produced by this coevolution have been observed in different complex network models (Zschaler, 2012). For example, Holme and Newman (2006) and Zanette and Gil (2006) have studied collective opinion formation on adaptive networks. In these models, the agents can have many possible opinions and update their states depending on their neighbours' opinions, when the competing opinions are diffused in a social network. Moreover, the adaptive voter model (Kozma & Barrat, 2008) shown that the coevolution of state and topology can drive the population towards consensus or a fragmentation. In order to investigate the fragmentation transition, in which the long term

outcomes change from consensus to fragmentation, several approaches (Kimura & Hayakawa, 2008; Böhme & Gross, 2011; Zschaler et al., 2012) have been proposed for the analytical computation of the transition point. Detailed discussion of the fragmentation transition can be found in the work of Vazquez et al. (2008) and Kimura and Hayakawa (2008).

Similar fragmentation transition phenomena have also been found in agent-based adaptive network models (Centola et al., 2007; Centola, 2010; Centola, 2011) of more realistic cultural drift and dissemination processes, in which social network structures interact with human behaviours. Further examples include the works of Huepe et al. (2011) and Couzin et al. (2011) which have demonstrated voter-like models can deep our understanding of the dynamics of decision making.

Complex topologies have also been observed in different game-theoretic models of cooperation in adaptive networks. For instance, the minority game on adaptive networks has been investigated by Paczuski, Bassler, and Corral (2000), while Skyrms and Pemantle (2000) have studied the various coordination and cooperation games on adaptive networks. In addition, a study of the Prisoner's dilemma on adaptive networks has been implemented by Zimmermann et al. (2000). Further, the interactive between coevolutionary dynamics and the evolution of cooperation in adaptive networks have been investigated in different works. For example, Pacheco et al. (2006) and van Segbroeck et al. (2011) have shown that coevolution can increase levels of cooperation by combining the underlying beneficial structures and the dynamics of cooperation. Zschaler et al. (2010) have demonstrated that full cooperation can be achieved by an unconventional dynamical mechanism.

Another class of games in adaptive networks has also been investigated, in which nodes aim to obtain an advantageous position instead of some optimal benefit (Bala & Goyal, 2001; Holme & Ghoshal, 2006). In these models, the nodes use locally available information to maximize their centralities with reasonable costs (i.e., maintaining reasonable connections) through adaptively modifying their links (Sayama et al., 2013). The coupling between the states of nodes and network topologies can drive the network state towards a critical point of the transition between well-connected and fragmented states. Furthermore, Do et al. (2010) has also found

that the local dynamics can give rise to emergent global topology in a game-theoretic model of cooperation.

2.2.4 Complex System-Level Dynamics

In many adaptive networks, the state-topology coevolution can give rise to new dynamical phenomena. The resulting interplay can describe complex dynamics and produce new phase transitions. This has been shown in a number of epidemiological models on adaptive networks, where the agents rewire their social contacts in response to the epidemic state of other agents (Gross et al., 2006; Zschaler, 2012).

Gross et al. (2006) proposed the adaptive Susceptible-Infected-Susceptible (SIS) model, in which the transition points can be computed analytically through using moment closure approximation. In this model, the node-level coevolution can give rise to the emergence of system-level dynamics. This model has been used as a performance baseline in different adaptive network research (Gross & Kevrekidis, 2008; Guerra & Gomez-Gardenes, 2010; Marceau et al., 2010; Wieland et al., 2012). Moreover, inspired by the SIS model, social impact and policy responses to epidemics on disease propagation has been investigated in (Wang et al., 2007; Shaw & Schwartz, 2008; Zanette & Risau-Gusmán, 2008).

In addition, several applications (Epstein et al., 2008; Funk et al., 2009; Shaw & Schwartz, 2010) of adaptive networks have also been developed for real-world epidemiological practice. These adaptive social models can present more realistic dynamics of social network, while people change their social behaviours depending on epidemiological states of their neighbours (Funk et al., 2010). The node-level dynamics can give rise to the emergence of complex system-level dynamics in adaptive networks has also been found in many different models. For instance, the fragmentation transition between well-connected and fragmented states can be driven by the state-topology coevolution has been observed in the voter-like models and models of opinion formation. (Gil & Zanette, 2006; Kimura & Hayakawa, 2008; Böhme & Gross, 2011).

In a number of models from game-theory, phase transitions driven by network adaptivity has also been observed (Pacheco et al., 2006; Santos et al., 2006; Szolnoki

et al., 2009; van Segbroeck et al., 2009; Demirel et al., 2011; van Segbroeck et al., 2011).

In recent years, the rapidly growing research on adaptive networks has opened new avenues to modelling and simulation of complex systems. The adaptive interplay between local and topological dynamics can drive an adaptive network model towards desired target states. Nevertheless, there is no existing unified modelling framework allowing for automatically shaping the network data and the adaptive network models in terms of the observations of a real-world complex system. In this research, a unified framework that combines agent-based adaptive network models and adaptive control structures has been developed . In this framework, the control parameters of adaptive network models are included as a part of the state-topology coevolution and are automatically adjusted according to the observations obtained from the system being studied. Having such an automated modelling framework would greatly reduce the human effort and provide a valuable tool for better understanding, description, prediction, and control of the real-world complex systems around us.

2.3 Adaptive Control

Adaptive control consists of a number of techniques which provide a systematic approach for automatically adjusting the controller settings in non-linear dynamical systems. Moreover, the desired system performance can be achieved or maintained through modifying a controller's behaviour in response to changes in the dynamics of the process and the character of the disturbances (Kuramoto, 2011; Aström & Wittenmark, 2013). As depicted in Figure 2.3, an adaptive control system is considered as having two loops: a conventional feedback loop with the process and the controller and a parameter adjustment loop (Aström & Wittenmark, 2013). Furthermore, a certain performance index can be measured based on the inputs/output, the states, and the disturbances of the system. Through the comparison of the measured performance index and the desired performance, in order to drive the adaptive control system towards a desired state, a adaptation mechanism is used to dynamically adjust the parameters of the adjustable controller according to the

comparison result of the measured performance index and the desired performance. A basic configuration of an adaptive control system is shown in Figure 2.4, in which the basic adaptation scheme consists of three fundamental blocks, including adaptation mechanism, performance measurement, and comparison-decision (Kuramoto, 2011).

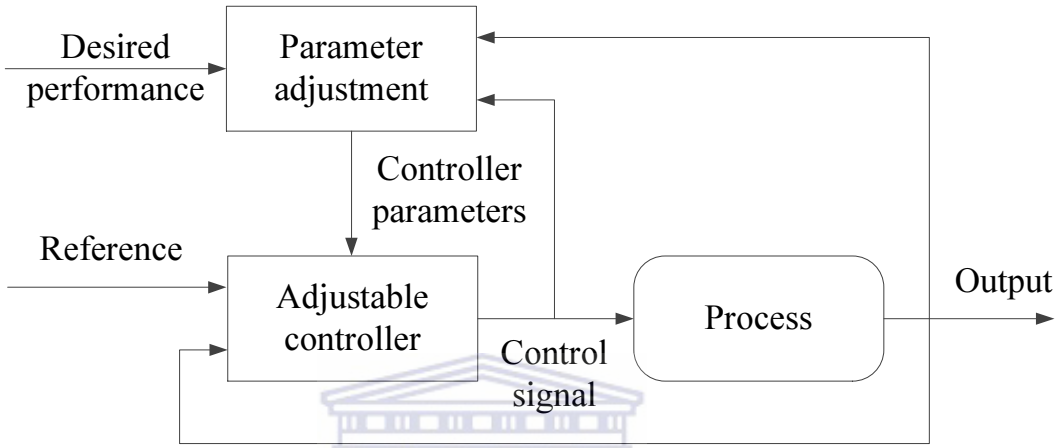

Figure 2.3: Block diagram of an adaptive system which consists of two loops: a conventional feedback loop with the process and the controller and a parameter adjustment loop. Adapted from (Aström & Wittenmark, 2013)

In recent years, adaptive control methodologies have become more and more popular as a way of improving performance and functionality of control systems. However, only three adaptive control structures which were used in the present work are presented in the following subsections, while a brief introduction of other adaptive control methodologies is given in Appendix C. In the following, we will briefly review three types of adaptive control systems, including parameter adaptation with self-tuning regulators, model-reference adaptive systems with learning machines, and multiple model adaptive control with switching. Detailed discussion of various adaptive control systems and their applications can be found in (Ioannou & Sun, 1996; Landau et al., 2011; Nguyen-Tuong & Peters, 2011; Aström & Wittenmark, 2013).

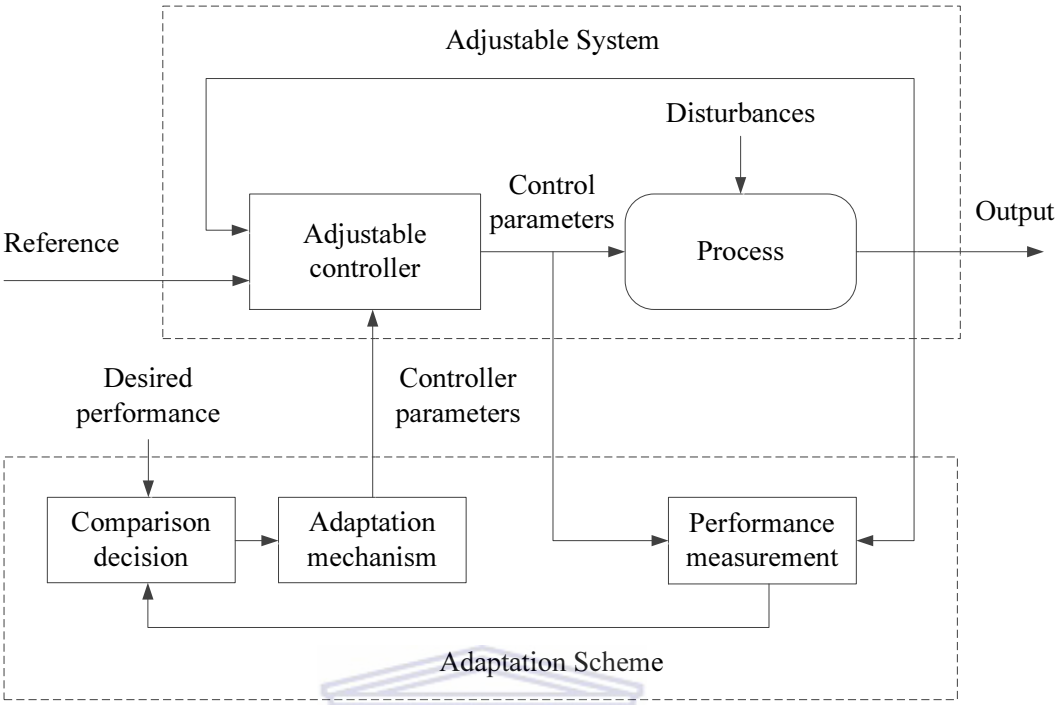

Figure 2.4: Basic configuration for an adaptive control system, in which the basic adaptation scheme consists of three fundamental blocks, including adaptation mechanism, performance measurement, and comparison-decision. Adapted from (Kuramoto, 2011).

2.3.1 Parameter Adaptation with Self-Tuning Regulators

Self-tuning regulators (STR) (Aström & Wittenmark, 2013) are one of the most commonly used and well studied adaptive controllers, in which the parameters of the controller can be dynamically adjusted in each time step depending on the current estimated plant model (Landau et al., 2011). As depicted in Figure 2.5, the adaptive controller consists of two loops: the inner loop which is composed of the process and an ordinary feedback controller, and the outer loop, which consists of a recursive parameter estimator and a design calculation. The parameter estimator may be considered as an observer for the parameters. The "Controller Design" represents an on-line solution to an underlying design problem for a system with known parameters. However the controller parameters can be updated directly without the design calculations. The STR approach can also be viewed as an automation of process modelling and design, when the process model and the control

design are updated periodically (Aström & Wittenmark, 2013).

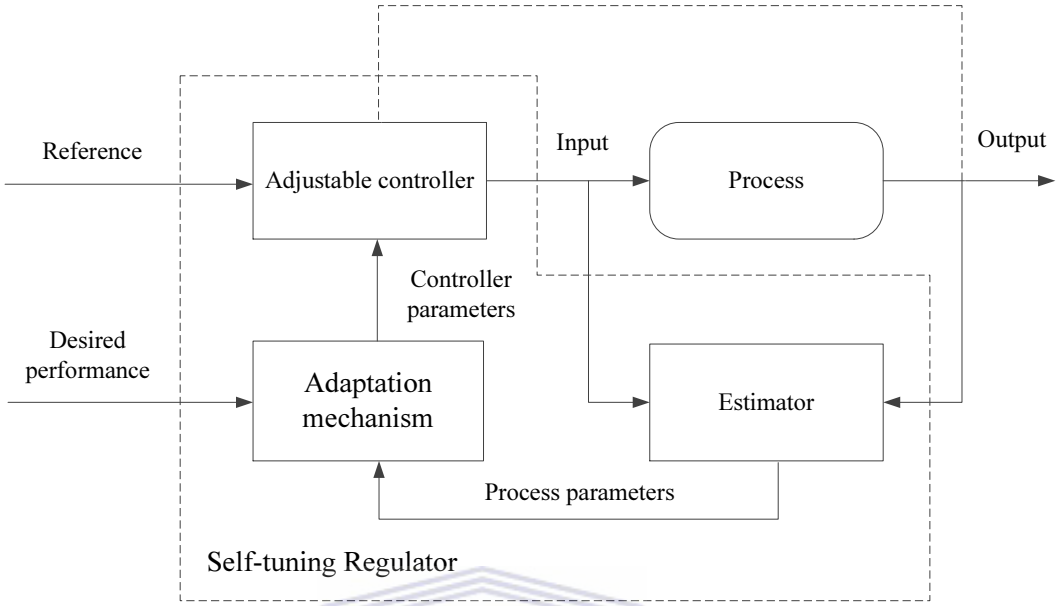

Figure 2.5: Block diagram of a self-tuning regulator, in which the parameters of the controller can be dynamically adjusted in each time step depending on the current estimated plant model. Adapted from (Aström & Wittenmark, 2013).

In the STR, the controller parameters or the process parameters can be dynamically adjusted in each time step depending on the current estimated plant model (Landau et al., 2011). However, the controller parameters can also be updated every N sampling instants according to the parameter estimation in closed loop,. This adaptive control approach is called iterative identification in closed loop and controller redesign (Bitmead, 1993; Trentelman & Willems, 1993; van den Hof & Schrama, 1995), in which parameter identification is performed in closed loop for controller tuning depending on the possible dynamical change in the plant model (Landau et al., 2011).. The performances of a controller can be improved based on a more accurate plant model identified in closed loop. Detailed discussions of STR schemes and iterative identification techniques can be found in (Landau et al., 2011; Aström & Wittenmark, 2013).

2.3.2 Model Reference Adaptive Control with Learning Machines

Model reference adaptive control (MRAC) is one of the main approaches to adaptive control in which the performance specifications are given according to a reference model. As depicted in Figure 2.6, the adaptive control system can be thought of as consisting of two loops. The inner loop is an ordinary feedback loop with the process and the controller, while the outer loop modifies the controller parameters by the comparatione of the output of the plant model and the reference model. MRAC has been widely used for control of nonlinear systems in the presence of significant modelling uncertainties (Narendra & Annaswamy, 1989; Ioannou & Sun, 1996; Kim & Calise, 1997; Tao, 2003; Cao & Hovakimyan, 2008; Lavretsky, 2009; Chowdhary et al., 2012; Aström & Wittenmark, 2013). In general, two types of MRAC schemes can be used for achieving and maintaining the desired performance: direct MRAC and indirect MRAC. On the one hand, the parameter of the controller can be updated directly by an adaptive law in direct MRAC. On the anther hand, in indirect MRAC, this parameter can be modified based on an adaptive law that relates the parameter with the on-line estimates of the plant output.

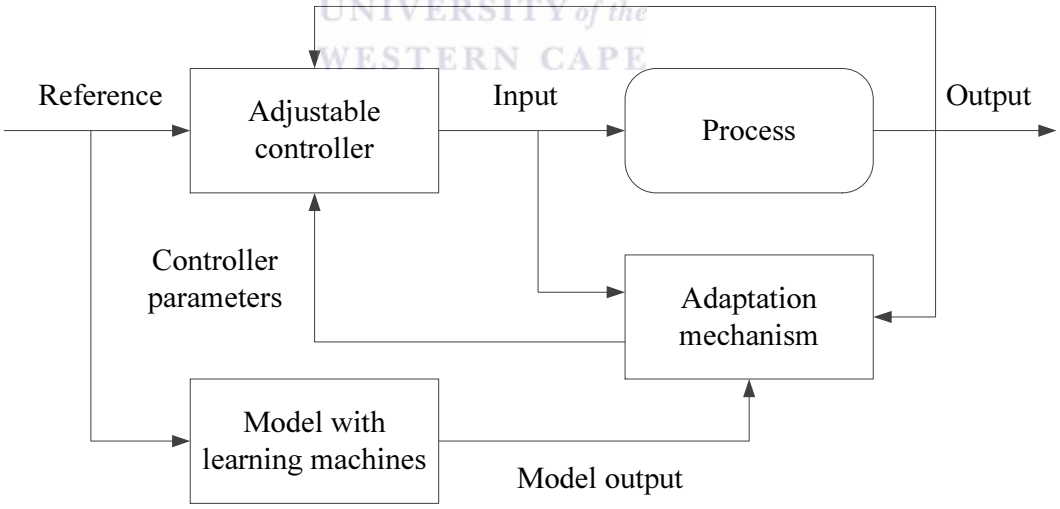

Figure 2.6: Block diagram of a model reference adaptive control. The adaptive control system can be thought of as consisting of two loops. The inner loop is an ordinary feedback loop with the process and the controller, while the outer loop modifies the controller parameters by the comparatione of the output of the plant model and the reference model. Adapted from (Aström & Wittenmark, 2013)

In some cases, the reference model has been used for predicting future desired states of the adaptive control system depending on the measurements derived from the plant model. These models can be incorporated into a learning control framework for predicting the next state of a dynamic system. This prediction is then used for automatic adjustment of the controllers. In direct model learning approach, for example, direct model learning can be implemented using most standard regression techniques which learn a direct mapping from input data to output data, such as least (Ljung, 2004), neural networks (Haykin, 1999; Steil, 2004; Butz et al., 2007) or statistical approximation techniques (Schölkopf & Smola, 2002; Rasmussen & Williams, 2006; Lopes & Damas, 2007). More details of modelling learning and its applications can be found in (Nguyen-Tuong & Peters, 2011; Calliess et al., 2013).

2.3.3 Multiple Model Adaptive Control with Switching

In order to handle large and rapid parameter variations, the multiple model adaptive control scheme has been developed (Isidori, 1995; Narendra & Balakrishnan, 1997; Karimi & Landau, 2000). This scheme can be used for the predetermination of a suitable plant model from several priori known models at every instant. The updated control parameters generated by the corresponding predesigned controller are then applied to the plant model. Thus, a more accurate plant model can be found by on-line adaption for improvement of performance (Landau et al., 2011). As shown in Figure 2.7, the system is composed of a bank of fixed models, an adaptive model estimator and an adjustable controller. In the estimator, an error criterion can be generated by a closed-loop type parameter estimation. Based on this error criterion, the model with smallest error is rapidly chosen by the supervisor (switching). The parameters of the model are updated using a parameter adaptation algorithm (tuning). More details of multiple model adaptive control can be found in (Karimi & Landau, 2000; Karimi et al., 2001; Landau et al., 2011; and references therein).

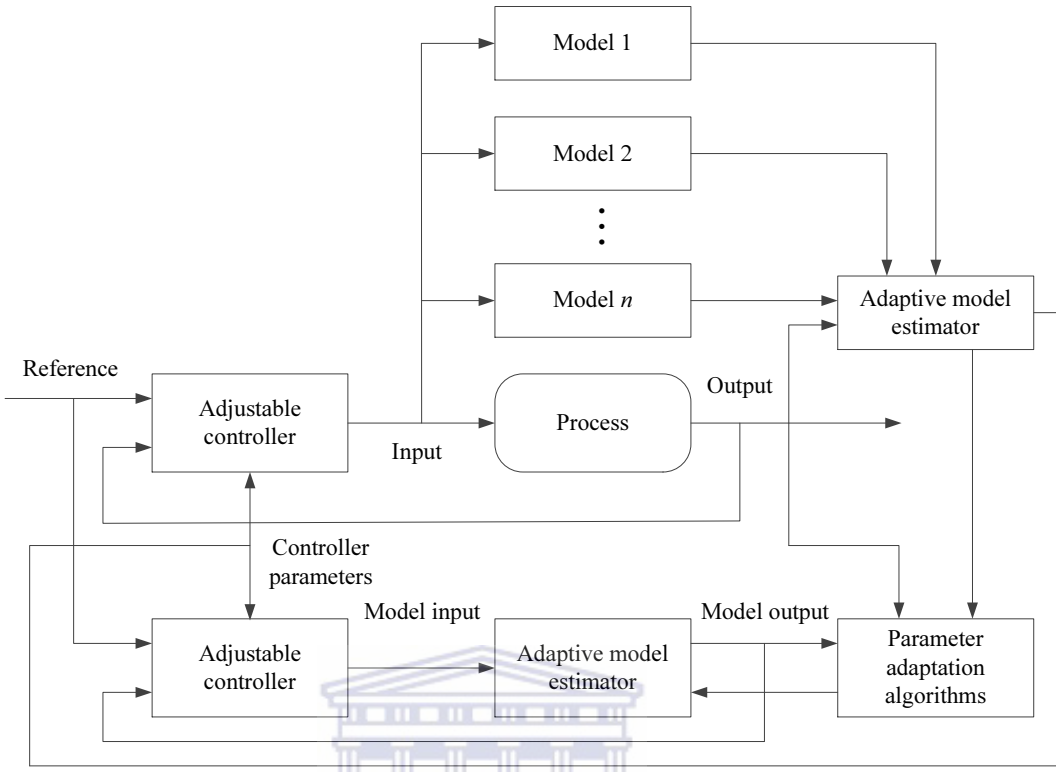

Figure 2.7: Block diagram of a multiple-model adaptive control approach. The adaptive control system is composed of a bank of fixed models, an adaptive model estimator and an adjustable controller. In the estimator, an error criterion can be generated by a closed-loop type parameter estimation. Based on this error criterion, the model with smallest error is rapidly chosen by the supervisor (switching). The parameters of the model are updated using a parameter adaptation algorithm (tuning). Adaptive from (Landau et al., 2011)

In recent years, adaptive controllers have become more and more popular as a way of improving performance and functionality of control systems, because it provides a systematic approach for automatic adjustment of controllers in non-linear dynamical systems. Nevertheless, there is no existing unified modelling framework allowing for automatically shaping the network data and the adaptive network models in terms of the observations of a real-world complex system. In the present work, a unified framework has been proposed for modelling and simulation of complex systems using a combination of adaptive network models and adaptive control

structures. While the process of modelling and simulation is considered as a control system with a state-topology feedback, this framework is not only able to automatically generate enhanced adaptive network models based on the observations of real-world complex systems, but also provide a systematic approach for automatic adjustment of control parameters in order to achieve or to maintain a desired topological property for the corresponding adaptive network models.

2.4 Summary

The review of various approaches presented above now permits the identification of common elements of a unified framework that combines adaptive network models and adaptive control structures. This idea is developed in Chapter 3 based on the reviews presented in this chapter.

CHAPTER 3
A Unified Framework for Modelling and Simulation of Complex Systems

In this chapter, we propose a unified framework for modelling and simulation of complex systems using a combination of adaptive network models and adaptive control structures. This framework is not only able to automatically generate adaptive network models that are based on information which is extracted from the data streams accessible to multidisciplinary researchers, but also provide a systematic approach for automatic adjustment of controllers in order to achieve or to maintain a desired topological property for the corresponding adaptive network models, while the process of modelling and simulation of complex systems is considered as a control system with a state-topology feedback. Moreover, through tracing various reference values, the generated adaptive network models can have different structures which are similar to the studied complex systems when the systems change. While this chapter can be considered a generalized methodology, we discuss how this unified framework can be useful for modelling and simulation of complex systems by combining adaptive network models and adaptive control structures.

3.1 A Unified Framework for Modelling and Simulation of Complex Systems

The adaptive network model-based approach provides a powerful abstraction of many different real-world complex systems, which targets the interplay between local dynamics and topological coevolution and its implications for system behaviour. More insights of complicated system behaviours can be gained from the adaptive network models because they present more realistic coevolutionary dynamics between the node states and the network topology in the complex systems. In order to generate meaningful adaptive network models from observations

of real-world complex systems, a set of analytical modelling approaches have been developed. In more complicated adaptive network models, however, the analytical approaches might not lead to solvable equations. Moreover, these analytical modelling approaches cannot provide a complete picture of the studied adaptive system because individual heterogeneity or other possible fluctuations are ignored. In this situation, an agent-based adaptive network modelling approach can be applied for the modelling and simulation of complex and varied coevolution of node states and network topology in adaptive systems. This approach separately and individually simulates the agents in a adaptive system and their adaptive interactions, allowing the emergent behaviours of the system to appear naturally (Börner et al., 2007; Barrat et al., 2008; Newman, 2011). In recent years, agent-based adaptive network models have become fashionable in a wide variety of real-world complex systems.

Although an agent-based modelling approach can simulate very intricate dynamical processes while fully incorporating stochastic effects, the agent-based models are often very complicated and it is difficult to study the impact of any given modelling assumption or parameter. Moreover, the adaptive network models may be rendered impractical due to the unrealistic assumptions and poor sample quality, and their accuracy suffers significantly from a lack of knowledge about the conditions of real-world complex systems or other useful information related to the assumptions. A more accurate adaptive network model whose topological properties are similar to the studied complex system might be made through automatically obtaining more knowledge from empirical data or dynamically adjusting the control parameters of the adaptive network models properly. This calls for a unified modelling framework which allowing for automatically determining the suitable control parameters and generating enhanced adaptive network models with desired network states in real-world adaptive systems.

In recent years, adaptive controllers have become more and more popular as a way of improving performance and functionality of control systems, because it provides a systematic approach for automatic adjustment of controllers in non-linear dynamical systems. Moreover, a desired level of control system performance can be achieved or maintained through modifying a controller's behaviour in response to

changes in the dynamics of the studied systems. In order to develop a unified modelling framework allowing multidisciplinary researchers to better understand, describe, predict, and control real-word complex systems, a network structure-centred approach is used for modelling and simulation of complex systems. As shown in Figure 3.1, this research paradigm places "the network structure" centrally and uses the combination of adaptive network models and adaptive control structures to achieve the desired network structure. Furthermore, the network based approaches (network sampling, modelling, measuring, and validating) can be applied to four domains of the adaptive network modelling process for dynamically adjusting their control parameters.

In this thesis, the network structure-centred research paradigm is used for addressing the issue of the applicability of the model by looking at three case studies which are relevant in practical situations. The overall research approach includes the following steps: background research on adaptive networks, adaptive control and their applications in different fields, derivation of a framework to guide the study, case study of practical modelling of complex state-topology coevolution into adaptive networks with simulation results revealing the performance of the model.

3.2 Generalized Methodology

In the present work, a unified framework has been proposed for modelling and simulation of complex systems using a combination of adaptive network models and adaptive control structures. While the process of modelling and simulation is considered as a control system with a state-topology feedback, this framework is not only able to automatically generate enhanced adaptive network models based on the observations of real-world complex systems, but also provide a systematic approach for automatic adjustment of control parameters in order to achieve or to maintain a desired topological property for the corresponding adaptive network models. Moreover, through tracing various reference values, the generated adaptive network models can have different structures which are similar to the studied

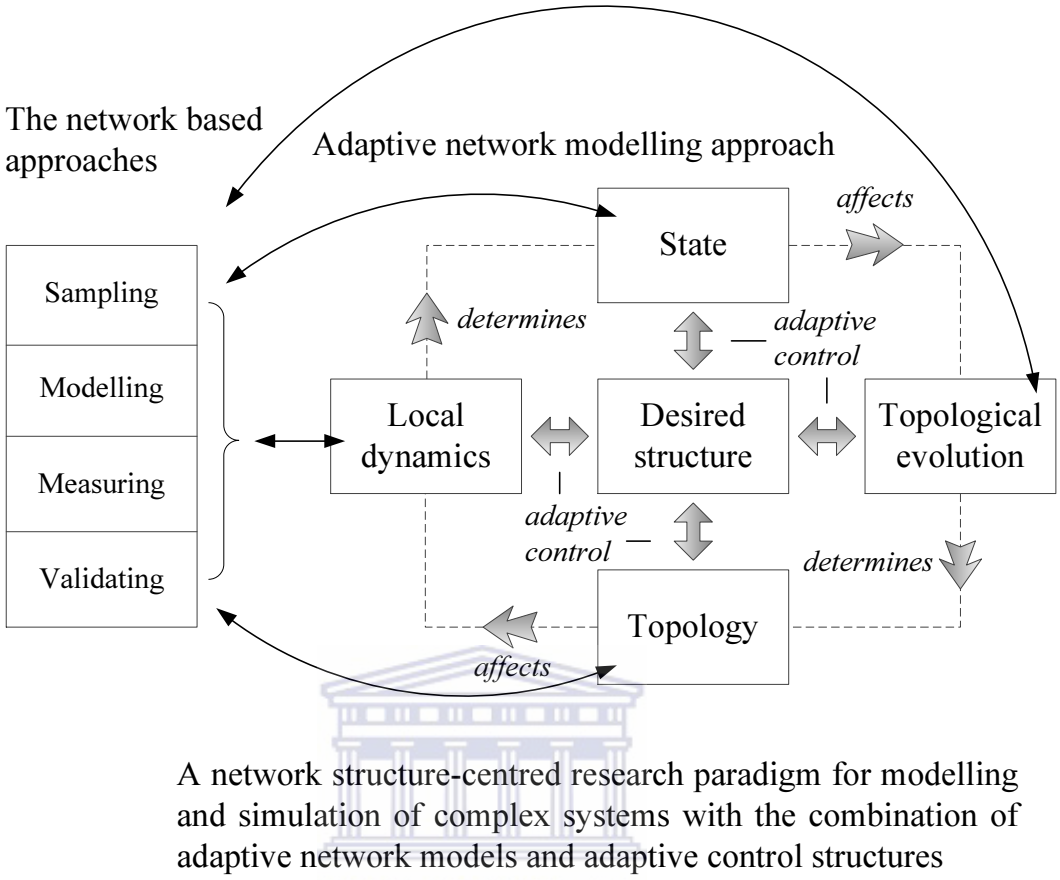

Figure 3.1: A network structure-centred research paradigm for modelling and simulation of complex systems with the combination of adaptive network models and adaptive control structures. Moreover, the network based approaches can be applied to four domains of the adaptive network modelling process for dynamically adjusting their control parameters.

complex systems when the systems change. While this chapter can be considered a generalized methodology, we discussed how this unified framework can be useful for modelling and simulation of complex systems by the combination of adaptive network models and adaptive control structures.

As depicted in Figure 3.2b, modelling and simulation of complex systems with ordinary adaptive network models can be considered as a feedback control system, while modelling and simulation with ordinary network models can be thought of as a simple input-output model (see Figure 3.2a). This feedback control system with ordinary adaptive network models consists of a state-topology feedback loop and

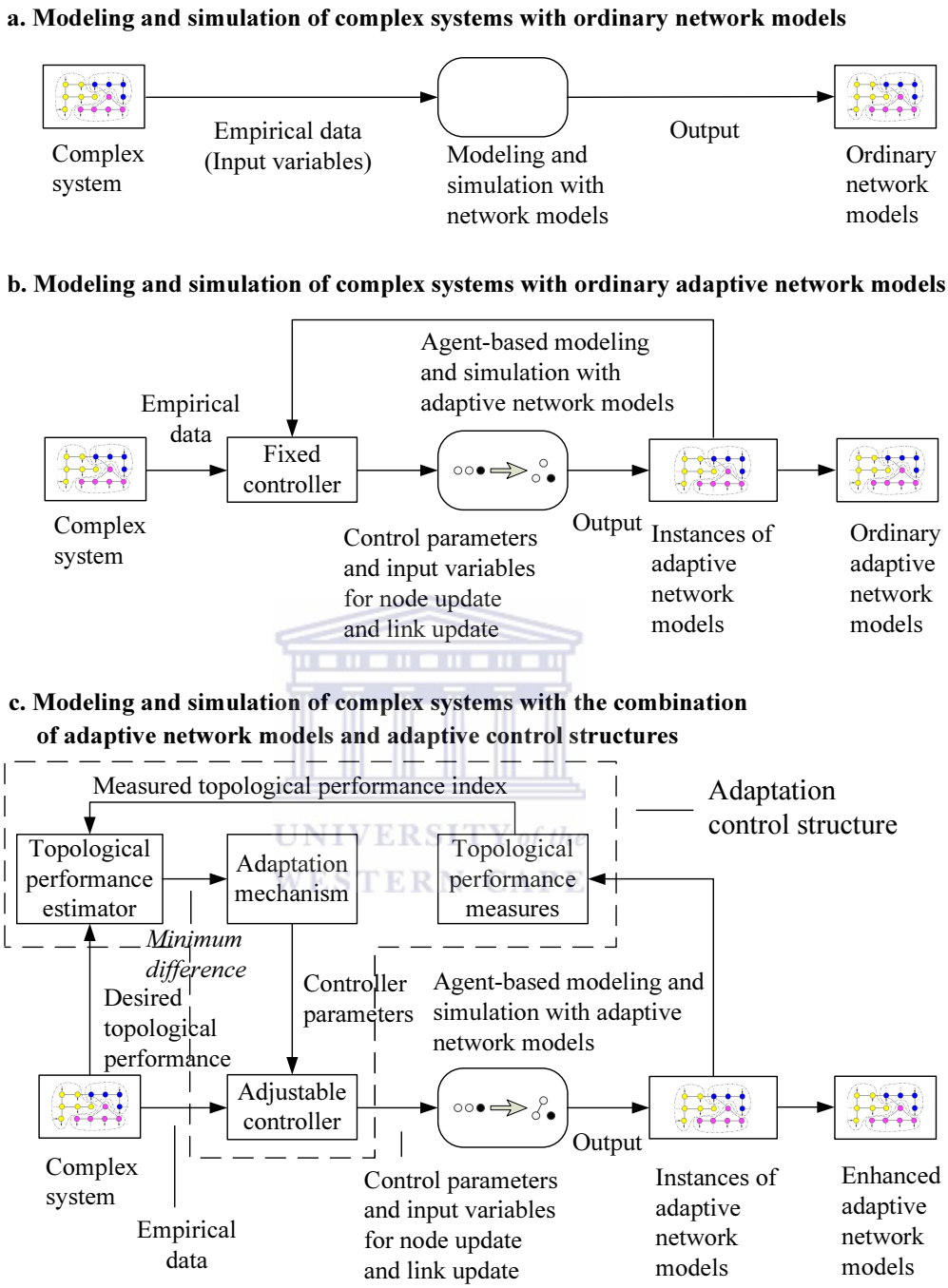

Figure 3.2: Modelling and simulation of complex systems with network models. a, Modelling and simulation of complex systems with ordinary network models. b, Modelling and simulation of complex systems with ordinary adaptive network models. c, Modelling and simulation of complex systems with the combination of adaptive network models and adaptive control structures.

a fixed controller. When applying adaptive network models to agent-based modelling and simulation of complex systems, it is necessary to specify how the states of nodes will be changed to generate new topologies of the network. Adaptive network models may have control parameters for node update and link update which greatly determine the quality of the generated network models. Choosing suitable control parameter values is, frequently, a problem-dependent task and requires previous experience of the multidisciplinary researchers (Maruo et al., 2005). However, there is no consistent methodology for determining the control parameters of an adaptive network model, which are arbitrarily selected within some predefined ranges most of the time (Maruo et al., 2005). In ordinary adaptive network models, these control parameters are not included as a part of the state-topology coevolution, when they are considered as external fixed parameters. Moreover, the adaptive network models make implicit assumptions for modelling and simulation of complex systems. The adaptive network models may be rendered impractical due to these unrealistic assumptions and poor sample quality, and their accuracy suffers significantly from a lack of knowledge about the conditions of real-world complex systems or other useful information related to the assumptions.

In order to achieve or to maintain a desired topological property for the corresponding adaptive network models, we propose a unified framework for modelling and simulation of complex systems using a combination of adaptive network models and various adaptive control structures. As shown in Figure 3.2c and 3.3, the unified modelling framework can be thought of as having two loops. One loop is an ordinary state-topology feedback with the process of modelling and simulation and the adjustable controller. The other loop is the parameter adjustment loop, in which control parameters are included into the state-topology coevolution and updated according to the topological performance estimation of the difference between the generated instances of an adaptive network model and the desired topological performance. The input variables of the adaptive control system can be generated from the empirical data derived from the studied complex systems. These empirical data may be some summarized statistical data or detailed records which are generated by using different data collection methods. Typically such data would present

important relations of some kind between various components of a certain complex system (Niazi, 2011). Moreover, the desired topological performance can also be generated from the empirical data for a comparative evaluation of the generated adaptive network models, such as the desired topologies of networks, the desired values of links, or desired classes of nodes.

To achieve or maintain a level of desired topological performance, the process of adaptive-network based modelling and simulation is controlled by a controller that has adjustable parameters. Through using a suitable adaptive control structure, the controller can be adjusted properly for node update and link update, when the characteristics of the process of modelling and simulation and the studied complex system are unknown or changing. The process of adaptive-network based modelling and simulation typically consists of two types of operations: state update of nodes and weight update of links, whose control parameters can be modified in the adjustable controller. Given the current states of the nodes and the current weights of the links, the instance of the adaptive network model in a certain discrete time step can be generated. A performance index can then be established according to the topological measurements of the generated instances for topological performance estimation. The measured performance index will be compared to the desired performance index which is desired topological characteristics of a reference network model, and their difference can be used for the adjustment of the adaptation mechanism. The parameters of the controller will be updated based on the output of the adaptation mechanism in order to improve the performance of modelling and simulation (Landau et al., 2011). The adaptive state-topology feedback loop will stop at some point once a certain level of desired topological performance is achieved. An enhanced adaptive network model can then be created based on an instance with desired topological characteristics. This procedure can be repeated.

In general, through combining adaptive network models and adaptive control structures, the unified modelling framework measures a certain performance index of the adaptive control system which is the topological characteristics of an instance generated by the current input valuables and control parameters. In or-

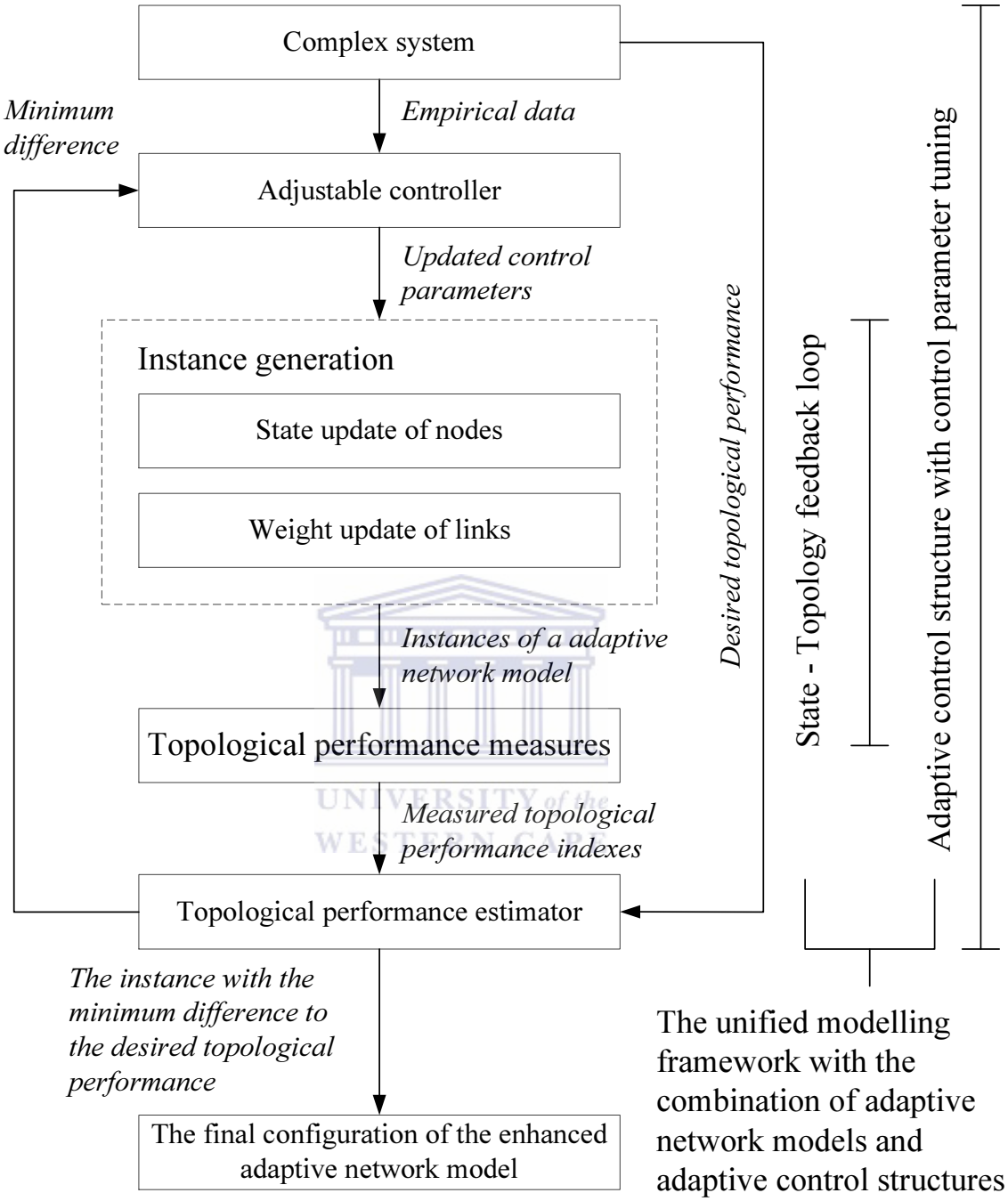

Figure 3.3: Model of the unified modelling framework with a combination of adaptive network models and various adaptive control structures. The unified modelling framework can be thought of as having two loops. One loop is an ordinary state-topology feedback with the process of modelling and simulation and the adjustable controller. The other loop is the parameter adjustment loop, in which control parameters are included into the state-topology coevolution and updated according to the topological performance estimation of the difference between the generated instances of an adaptive network model and the desired topological performance.

der to generate the final configuration of the adaptive network model with desired topological characteristics, the control parameters of the adjustable controller can be dynamically updated according to the topological performance estimation of the difference between the generated instances of an adaptive network model and the desired topological performance. Through using such a unified modelling framework, the enhanced adaptive network models with desired topologies can be created automatically which are able to provide further insights about the basic principles in the studied complex systems. Moreover, this unified framework also provides a guideline for developing the adaptive network models of complex systems spanning multiple scientific disciplines.

3.3 Adaptive Control Structures

A number of well-studied adaptive control schemes can be used to determine suitable controller parameters. In this section, however, we will introduce three adaptive control structures for modelling and simulation of real-world complex systems with adaptive network models, including adaptive control with iterative parameter identification, multiple model adaptive control, and support vector machine-based adaptive control.

3.3.1 Iterative Parameter Identification

In order to identify an instance of an adaptive network model with desired topological characteristics, an adaptive control structure with iterative parameter identification can be used for agent-based adaptive network modelling and simulation of complex systems. As shown in Figure 3.4, this adaptive control structure consists of two loops: the inner loop which is composed of the process of agent-based adaptive network modelling and simulation and a state-topology feedback controller, and the outer loop, which consists of a recursive parameter estimator for controller tuning. Through using such an adaptive control structure, suitable control parameters can be identified for generating an enhanced adaptive network model with desired topology.

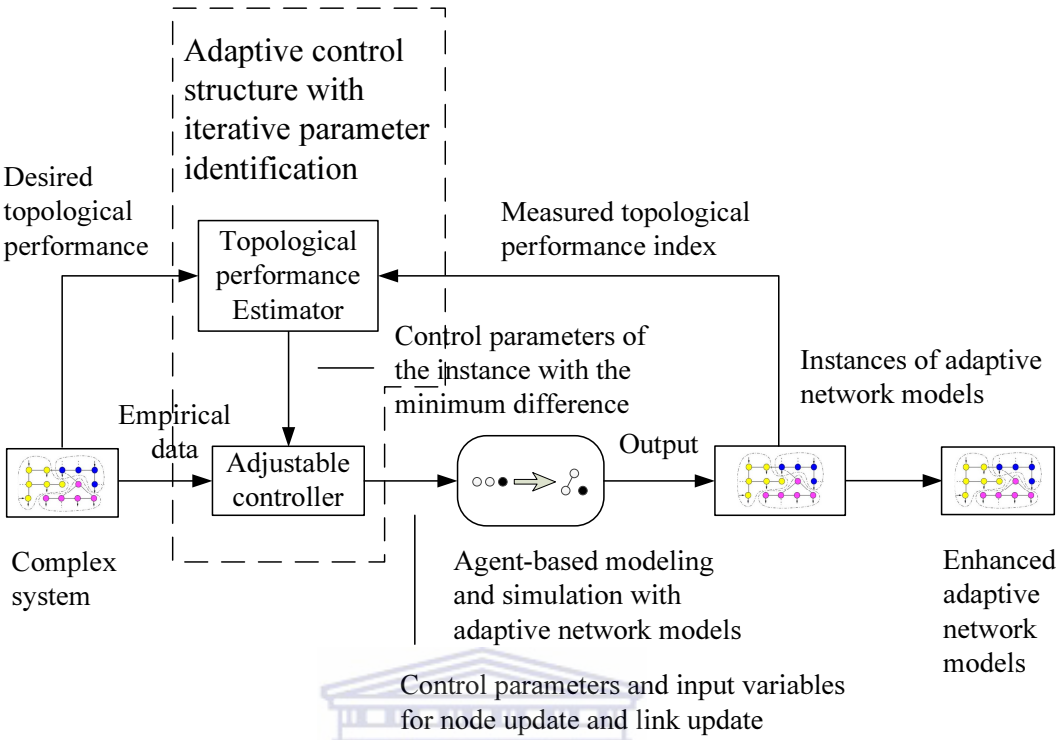

Figure 3.4: Block diagram of an adaptive control structure with iterative parameter identification for modelling and simulation of complex systems with adaptive network models. This adaptive control structure consists of two loops: the inner loop which is composed of the process of agent-based adaptive network modelling and simulation and a state-topology feedback controller, and the outer loop, which consists of a recursive parameter estimator for controller tuning.

In this adaptive control structure, a set of control parameters of state update and weight update are adjusted in each time step. By using the current states of nodes and the current weights of links, the instance of the adaptive network model in a certain discrete time step can be generated. A performance index can then be established in N time steps according to the topological measurements of the generated instances. The measured performance index will be compared to the desired performance index which is the desired topological characteristics derived from empirical data of real-world complex system, and the corresponding control parameters of the instance whose difference is the minimum will be fed into the controller. The states of nodes and the weights of links can then be updated in order to generate

an enhanced adaptive network model with desired topological characteristics. The adaptive state-topology feedback loop will stop at some point once a certain level of desired topological performance is achieved. The final configuration of the enhanced adaptive network model can then be created based on an the instance with desired topological characteristics. This procedure can be repeated until a set of enhanced adaptive network models are generated for all given desired values. Thus, through tracing various desired values, the generated adaptive network models can have different structures which are similar to the studied complex system when the system changes. In Chapter 4, a unified framework which combines adaptive network models and adaptive control structures with iterative parameter identification is proposed for modelling and simulation of fractured-rock aquifer systems.

3.3.2 Multiple Model Adaptive Control

Agent-based modelling and simulation of complex systems with adaptive network models subjected to abrupt and large parameter variations are generally very difficult to control. A fixed controller normally leads to poor performances due to large uncertainties (Karimi et al., 2001). In order to improve the performance of modelling and simulation, multiple model adaptive control structure can be used for the predetermination of a suitable computational model of the state update of nodes and the weight update of links (Figure 3.5).

In this adaptive control structure, we suppose that a set of computational models for the state update of nodes and the weight update of links is a priori known. By using the current control parameters and the current input data, a set of instances of the adaptive network model can be generated based on various computational models. In the model estimator, a performance index can be established according to the topological measurements of the generated instances. The measured performance index will be compared to the desired performance index which is desired topological characteristics derived from empirical data of the studied complex system. The corresponding control parameters of the instance whose difference is the minimum will be fed into the controller, and the corresponding

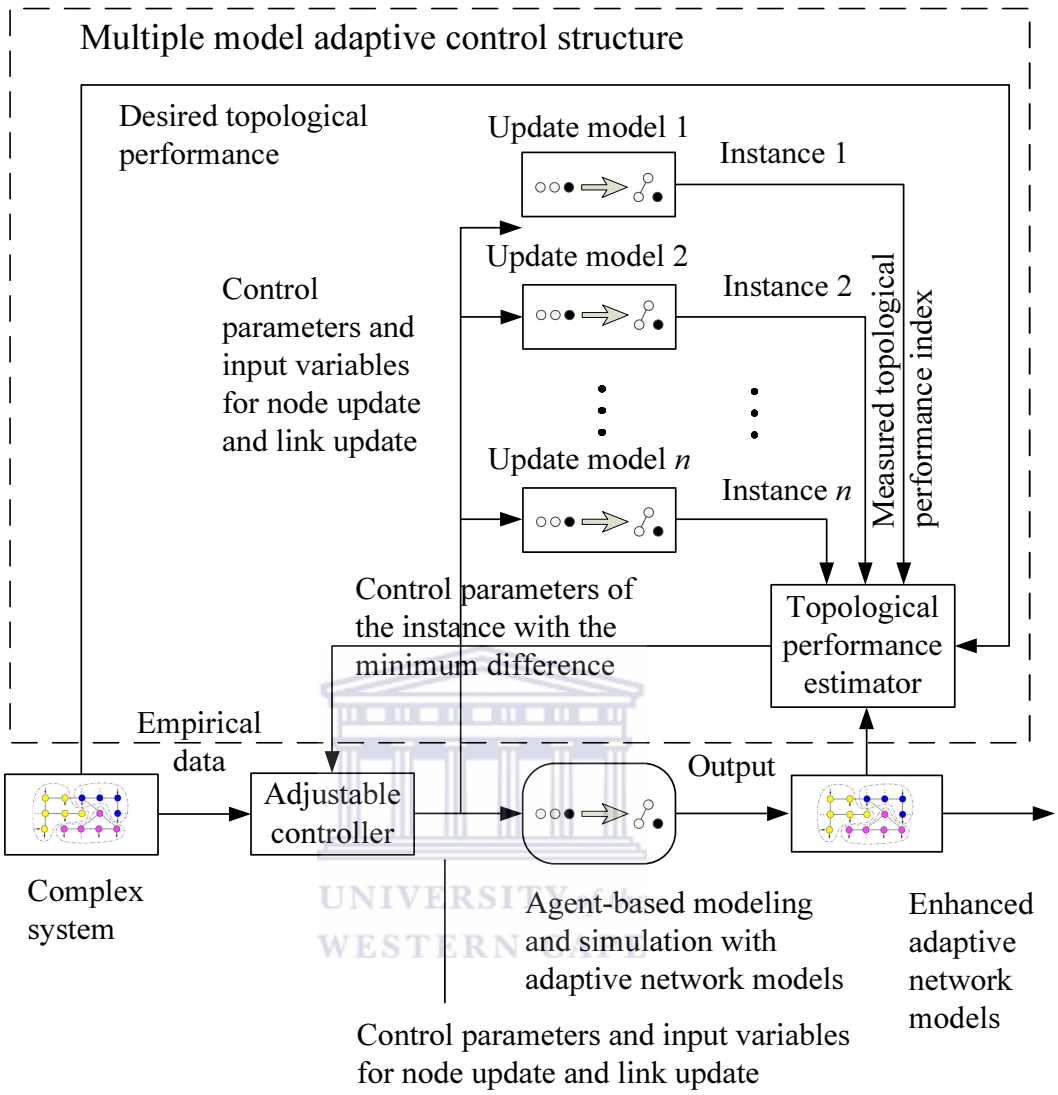

Figure 3.5: Block diagram of a multiple model adaptive control structure for modelling and simulation of complex systems with adaptive network models. This adaptive control structure is composed of a set of update models, a topological performance estimator and an adjustable controller. In the model estimator, a performance index can be established according to the topological measurements of the generated instances. The measured performance index will be compared to the desired performance index which is desired topological characteristics derived from empirical data of the studied complex system. The corresponding control parameters of the instance whose difference is the minimum will be fed into the controller, and the corresponding computational model of the instance will be applied to the process of agent-based adaptive network modelling and simulation.

computational model of the instance will be applied to the process of agent-based adaptive network modelling and simulation. The states of nodes and the weights of links can then be updated with a suitable computational model in order to generate an enhanced adaptive network model with desired topological characteristics. By using such a multiple model adaptive control structure, the adaptive state-topology feedback loop can be performed for modelling and simulation of the studies complex system with a suitable a suitable computational model of the state update of nodes and the weight update of links. In Chapter 5, we propose a unified framework which combines adaptive network models and multiple model adaptive control structures is proposed for modelling and simulation of social network systems.

3.3.3 Support Vector Machine-Based Adaptive Control

While it has been widely used for control of complex systems in the presence of significant modelling uncertainties, a support vector machine-based adaptive control structure can be used for agent-based modelling and simulation of complex systems with adaptive network models. As depicted in Figure 3.6, this adaptive control structure can be thought of as consisting of two loops. The inner loop is composed of the process of agent-based adaptive network modelling and a state-topology feedback controller, while the outer loop modifies the controller parameters based the output of a support vector machine-based prediction model. In this adaptive control structure, future behaviour of the system can be predicted by using a support vector machine-based prediction model depending on empirical data of the studied complex system. An instance with desired topology can be generated in each time step by using the current input variables and control parameter, while the states of the nodes and weights of the links are dynamically adjusted according to the future behaviour of the studied system. Moreover, a set of control actions will be implemented based on the generated instances in order to improve the system performance. In Chapter 6, a unified framework which combines adaptive network models and support vector machine-based adaptive control structures is proposed for modelling and simulation of multicast congestion in mobile ad hoc network systems.

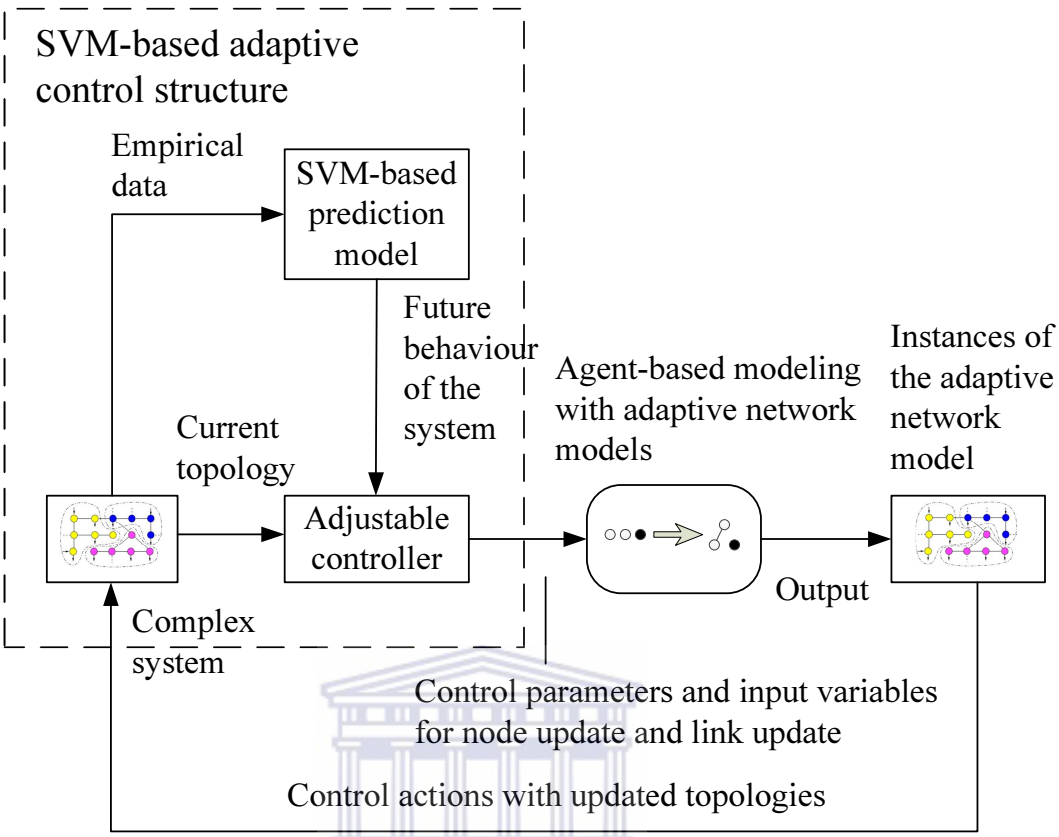

Figure 3.6: Block diagram of a support vector machine-based adaptive control structure for modelling and simulation of complex systems with adaptive models. This adaptive control structure can be thought of as consisting of two loops.The inner loop is composed of the process of agent-based adaptive network modelling and a state-topology feedback controller, while the outer loop modifies the controller parameters based the output of a support vector machine-based prediction model.

3.4 Modelling Real-World Complex Systems with A Unified Framework

By using the unified modelling framework introduced in Section 3.1, three different real-world applications (fractured-rock aquifer systems, social network systems, and wireless ad hoc network systems) have been modelled in this framework. In the following, a brief introduction of the three real-world complex systems will be given, while further details of modelling and simulation of the systems with the unified modelling framework can be found in Chapter 4, Chapter 5, and Chapter 6.

3.4.1 Fracture Network Systems

A fracture network is a set of fractures (cracks) in brittle materials. Two approaches are used for generating fracture networks. The first approach gives the fracture's path of propagation by inducing disorder into the studied system (say intact rock) (Kachanov, 1987; Renshaw & Pollard, 1994; Alava et al., 2006; Bonamy & Bouchaud, 2011). The second approach generates fracture networks based on the statistics derived from controllable laboratory tests and field data. The orientation, the size and the aperture are assigned to the fracture based on the statistical distribution functions, while the centre of a fracture is located at random according to the Poisson distribution (Ghaffari et al., 2011). The number of generated fractures is determined based on the density of the fracture network and the size of model space. The generated fracture networks should satisfy the same characteristics (features or attributes) for the fracture system (Ghaffari et al., 2011), such as distribution law over density, length, directionality, distance, fractal dimension, and permeability (Sornette et al., 1993; Berkowitz & Adler, 1998; Berkowitz et al., 2000; Bour, 2002). In a fracture network, the fractures represented by the nodes occupy a precise position in two or three-dimensional Euclidean space, and the connections of the fractures represented by the links are real physical connections. Fracture networks thus can be also called geographical or spatial networks. An excellent review on spatial networks has been presented in (Barthelemy, 2010).

Fracture networks research can be conceptualized as lying at the intersection between graph theory and statistical mechanics. In (Ghaffari et al., 2011), fracture networks were mapped into graphs, and the characteristics of the generated graphs were compared with the main spatial fracture networks. However, there is no existing unified modelling framework allowing for automatically shaping the fracture data and the fracture network models in terms of the observations of a real-world fracture network. In this research, we focus on using a unified modelling framework, which combines adaptive network models and adaptive control structures, to automatically search for desired configurations of the adaptive network models based on the observations of natural fractured-rock aquifer systems. Having such an automated modelling framework would greatly reduce the human effort and provide a valuable

tool for better understanding, description, and prediction of the groundwater flow and transport processes in fractured-rock aquifer systems.

3.4.2 Social Network Systems

A social network is a set of people (individuals or social groups) and different types of relationships (friendship, trust, kinship, status, sexual, business or political) among them (Wasserman & Faust, 1994; Scott, 2012). Different social, diplomatic, commercial and even cultural networks can be defined by hidden and clear relationships or interactions between any groups of people (Costa et al., 2011). Although many sociometric researches (Wellman, 1926; Simon, 1955; Price, 1965; Milgram, 1967; Travers & Milgram, 1969; Price, 1976; Freeman, 1977; Freeman, 1979; Wasserman & Faust, 1994; Degenne & Forsé, 1999; Ball, 2002; Baldi et al., 2003; Watts, 2003; Social Network Journal, 2007; Scott, 2012) have contributed to the understanding of society, traditional social network studies often suffer from problems of inaccuracy, subjectivity, and small sample size (Newman, 2003). In the conventional studies, social contacts were established based on extensive questionnaires and cross comparison of the responses. However, new forms of social contacts have been generated due to the fast development of communication systems, such as the telephone or the Internet (Wellmanet et al., 1996; Wellman, 2001). With tools like blogs, photoblogs, messengers, emails, and social network services, a large amount of extensive electronic databases can provide extremely abundant statistical sample and a complete picture of the complex social system they represent (Costa et al., 2011). Benefiting from the massive amounts of online data, reliable social networks can be generated faster and more accurately than ever (González & Barabási, 2007; Watts, 2007).

Recent developments in sensing technologies have enabled us to examine the nature of human social behaviour in greater detail. However, there is no existing unified modelling framework allowing for automatically obtaining more knowledge from multidimensional mobile sensing data and adjusting the control parameters of the adaptive network models properly. In this thesis, we propose a unified framework which combines adaptive network models and multiple model adaptive control struc-

tures for modelling and simulation of social network systems. In this framework, a real-world social network system can be represented as an agent-based adaptive network which are defined by a feedback loop between the behavioural state of individuals and the community structure of the studied system, when a multiple model adaptive control structure is used for the predetermination of suitable computational models of behavioural state update and social interaction update in order to improve the performance of modelling and simulation.

3.4.3 Wireless Ad Hoc Network Systems

In real systems, modelling the dynamics of flows of the physical quantities is also important, because a completed characterization of a network need to consider the relationship between structure and dynamic of complex networks (Boccaletti et al., 2006). The dynamics models of a complex network can be generated by quantifying the transmission capacities and loads of its components (Boccaletti et al., 2006). In the present work, we focus on multicast congestion in mobile ad hoc networks (MANETs).

Mobile ad hoc networks use a shared broadcast medium. All the nodes within a collision domain share the medium capacity, which is therefore a scarce resource. Multicast communication is thus of particular interest in these networks, since it helps saving resources when delivering data to multiple destinations. Congestion is one of the most important issues impeding the development and deployment of Internet Protocol multicast and multicast applications in MANETs. Congestion phenomena are common in wireless communication networks, where some nodes occasionally malfunction or they are overloaded. A few congestion control models have been proposed to tackle multicast congestion for MANETs. However, most of these congestion control models (Lee et al., 1999; Tang et al., 2002; Tang et al., 2002; Tang et al., 2003; Baumung et al., 2004; Gossain et al., 2004; Baumung, 2005; Jain & Das, 2006; Scheuermann et al., 2007; Kang et al., 2009) suffer from the same problems as Transmission Control Protocol model suffers in wireless networks, which is unnecessarily reducing the transmission rate in response to link errors. This is because they use losses as the indication of the congestions but cannot distinguish

between wireless losses and congestion losses. In wireless networks, packet losses are not only caused by overflow but can also be caused by link errors. In these models, the MANETs react in the same way to losses due to congestion losses and due to wireless losses. They reduce their transmission rate systematically at each packet loss. Thus, the sending rate can be restricted even when there is no congestion.

To increase its throughput, the multicast sender should prevent it from reducing its rate when it faces a loss due to a link error. One strategy is to suppress wireless losses with the support of the network by splitting the multicast connection or retransmitting in link layer. Another strategy is to classify the packet loss causes by using a classification algorithm at the receiver. The transmission rate is reduced only if the loss is classified as a congestion loss. Several congestion detection models, with classification algorithms for packet loss causes, have been proposed for MANETs multicast. In Peng and Sikdar (2003) and Rajendran et al. (2004)'s models, congestion loss is detected by monitoring MAC layer queue state, while congestion can be detected by monitoring network queuing delay in Kang et al.'s work (Kang et al., 2009).

In order to capture more realistic dynamics of wireless communication networks with the interplay between network state and topology, several adaptive-network based models have also been developed for routing and congestion control in wireless communication networks. In these adaptive network models, the control parameters are not included as a part of the state-topology coevolution, because they are considered as external fixed parameters. Moreover, the adaptive network models make implicit assumptions for modelling and simulation of wireless communication network systems. The adaptive network models may be rendered impractical due to the unrealistic assumptions and poor sample quality, and their accuracy suffers significantly from a lack of knowledge about the conditions of the networks or other useful information related to the assumptions. However, we use a unified framework which combines adaptive network models and support vector machine-based adaptive control structures for modelling and simulation of multicast congestion in mobile ad hoc network systems. In this framework, a mobile ad hoc network system can be represented as an agent-based adaptive network which is defined by a feed-

back loop between the congestion states of group members and the group structure of the network, when the support vector machine-based adaptive control structures are used for the prediction of incipient congestions.

CHAPTER 4
Towards A Unified Framework for Modelling and Simulation of Fractured-Rock Aquifer Systems

In this chapter, the unified framework which combines adaptive network models and adaptive control structures has been applied for modelling and simulation of fractured-rock aquifer systems. We start in Section 4.1 with brief introduction to the background of modelling and simulation of fractured-rock aquifer systems. In Section 4.2, we propose a unified framework which combines adaptive network models and adaptive control structures with iterative parameter identification for modelling and simulation of fractured-rock aquifer systems. In this framework, the adaptive control structures with iterative parameter identification are used to identify an instance of an adaptive network model with the desired topological characteristics, while the natural fracture network can be represented by an adaptive network model with "state-topology" coevolution. In Section 4.3, by using this modelling framework, an automatic modelling tool, Fracture3D, is developed for automatically building the enhanced 3–D fracture adaptive network models, in which the fracture statistics and the structural properties can both follow the observed statistics from natural fracture networks. In Section 4.4, a set of experiments and simulations are conducted in order to verify the validity of the proposed unified modelling framework and modelling tool Fracture3D.

4.1 Modelling and Simulation of Fractured-Rock Aquifer Systems

The fractured-rock aquifer systems that would carry and circulate water generally contain a set of fractures in rocks. Fractures control the magnitude and direction of hydraulic conductivity in the aquifer systems. They can act as conduits or barriers to groundwater flow; and the understanding of fracture connectivity is critical for understanding subsurface flow and transport processes (Margolin et al.,

1998). Although it is an intrinsic factor controlling groundwater flow and transport processes, the connectivity of fractured-rock aquifer systems has no generally accepted definition. It is normally used to describe the subjective appearance of a fractured-rock aquifer system; and highly connected fractures tend to be more permeable (National Research Council, 1996). Generally, the connectivity of a certain fractured-rock aquifer system can be determined by orientation, length and density of fractures, which is the probability that any specific fracture is connected to the conducting portion of the aquifer system (Berkowitz, 1995).

In order to study the connectivity of fractured-rock aquifer systems, a number of network-based applications for modelling and simulation have been developed. In these applications, fractured-rock aquifer systems were generally viewed as intricate networks that encode the interactions between the fractures. These applications often entail using one of two basic methods of developing computational models for modelling fractured-rock aquifer systems i.e. either use a master equation approach for analysis of groundwater flow and transport processes on networks or else use an agent-based modelling approach to develop simulation models. For example, a master equation-based mathematical model of connectivity and conductivity in underground reservoirs has been developed in (Nayak et al., 2012), in which percolation theory (Stauffer & Aharony, 1992) was used to delineate the connectivity of a fracture network system. In these models, an occupancy function "p" is used to describe mathematically how the number and the size of the clusters of fractures vary in a certain natural fracture network system, and the finite size clusters bridged and grow in size as this occupancy probability is increased (Nayak et al., 2012). A critical value exists (called the percolation threshold, p_c) at which one large cluster (so called the spanning, percolating or infinite cluster) spans the whole region and allows flow to move from one side to the other.

In more complicated models, the master equation approach might not lead to solvable equations. Moreover, this approach cannot provide a complete picture of a studied fracture-rock aquifer system, because it is intrinsically considering a coarse grained perspective that does not take into account the heterogeneity of fractures or other possible fluctuations. In this situation, agent-based models can be applied

(Börner et al., 2007; Barrat et al., 2008). The discrete fracture network (DFN) models have been applied to the research of natural fracture network systems in (Baecher, 1983; Rouleau & Gale, 1985; Cacas et al., 1990a; Cacas et al., 1990b; Willis-Richards et al., 1996; Lin & Xu, 2006). Spatial statistics derived from observed fracture data can be measured and used to generate 3–D fracture network models with the similar spatial properties. By using agent-based modelling approach with DFN models, the estimation of connectivity of the studied fracture networks can provide vital information for studying the hydrological behaviour in fractured-rock aquifer systems. Several stochastic fracture simulators, such as FracMan (Golder Associates), Meyer (Baker Hughes), FracaFlow (Beicip-Franlab) etc., have been developed for generating stochastic DFN models. By using these simulators, the statistical data derived from field measurements such as orientation, length, and density of fractures can be used for studying 3D-connectivity of the studied fractured-rock aquifer systems (Bradbury & Muldoon, 1994). When these statistical data are incorporated with other parameters such as aperture and particularly connectivity of fractures, the hydraulic properties of the studied fractured-rock aquifer systems could be estimated (Mourzenko et al., 1998; de Dreuzy et al., 2000).

Although agent-based modelling and simulation approach can simulate very complicated groundwater flow and transport processes with fully incorporating stochastic effects, agent-based models are often very intricate and the impact of any given modelling assumption or parameter is difficult to study. A poor fracture network model may be generated because of parameter uncertainty and poor or incorrect geological and hydrological assumptions, in which the fracture statistics can follow the observed statistics, but the structural properties are totally different with observations. In the study of fracture system at a uranium mine in France, for instance, Long and Billaux (1987) found that only 0.1% fractures out of 65,740 generated ones contribute to flow at the site scale. In other cases (Karasaki et al., 2000; Halihan et al., 2005), situ borehole tests have also shown that fractures developed in a rock mass are not always fully connected. Fracture interconnection may depend on both geometric and physical properties such as orientation, aperture, length, termination, and fracture filling. This calls for a unified modelling framework which allows for

automatically determining the suitable control parameters and generating the 3–D fracture adaptive network models with desired structure in terms of field data and measurements taken on site or in-situ. Having such an automated modelling framework would greatly reduce the human effort and provide a valuable tool for better understanding, description, and prediction of the groundwater flow and transport processes in fractured-rock aquifer systems.

In the following sections, we present a framework for modelling and simulation of fractured-rock aquifer systems based on the unified modelling framework described in Chapter 3. In this framework, the adaptive control structures with iterative parameter identification are used to identifying an instance of an adaptive network model with the desired topological characteristics, while the natural fracture network can be represented by adaptive network models with "geometrical state–fracture cluster" coevolution. Moreover, we use this modelling framework to develop an automatic modelling tool for automatically building the enhanced fracture adaptive network models of fractured-rock aquifer systems, in which the fracture statistics and the structural properties can both follow the observed statistics from natural fracture networks.

4.2 A Unified Framework for Modelling and Simulation of Fractured-Rock Aquifer Systems

Most of fracture network modelling tools make implicit assumptions for modelling and simulation of fractured-rock aquifer systems, such as shape of fractures, size scale between field data and simulated data, and size of the stochastic fractures, while these properties cannot be easily determined in the field by any direct measurements. The fracture network models may be rendered impractical due to these impractical assumptions and poor sample quality, and their accuracy suffers significantly from a lack of knowledge about real geological and hydrological conditions of natural fracture networks or other useful information related to the assumptions. The control parameters of the network models, such as, profile of fractures, size of fractures, position of fractures, and scale of fracture network models, may vary greatly depending on different geological and hydrological conditions. In order to

achieve or maintain a desired topological property for the corresponding 3–D fracture network models of fractured-rock aquifer systems, we proposed a framework which combines adaptive network models and adaptive-control based model parameter identification for modelling and simulation of fractured-rock aquifer systems based on the unified modelling framework introduced in Chapter 3. While the process of modelling and simulation of fractured-rock aquifer systems is considered as a control system with a geometrical state–fracture cluster feedback loop and a control parameter–topological estimates feedback loop, this framework provides a systematic approach for automatic generation of the enhanced 3–D fracture adaptive network models, in which the fracture statistics and the structural properties can both follow the observed statistics from natural fracture networks.

In this framework, an adaptive control structure with iterative parameter identification is used for identifying an instance of an adaptive network model with the desired topological characteristics. The enhanced fracture adaptive network models can then be used in estimating the 3D-connectivity of the studied fractured-rock aquifer systems. As depicted in Figure 4.1, the unified modelling framework consists of two loops: the inner loop which is composed of the process of agent-based adaptive network modelling and simulation and a geometrical state–fracture cluster feedback controller, and the outer loop, which consists of a recursive topological estimator for control parameter tuning. Through using such an adaptive control structure, suitable control parameters can be identified for generating the final configuration of the enhanced 3–D fracture adaptive network model with similar topological properties to the studied natural fracture network system.

In this framework, a fractured-rock aquifer system is considered as an adaptive network which are defined by a feedback loop between the geometrical states (size and position) of the fractures and the fracture clusters of the studied fracture network. Moreover, such a "geometrical state–fracture cluster" coevolution can self-organize towards non-trivial topologies. A set of control parameters, such as *Ratio* (the ratio of length to width of a fracture) and *Scale* (the ratio of original value to final value of length of a fracture), for geometrical state update and interconnection

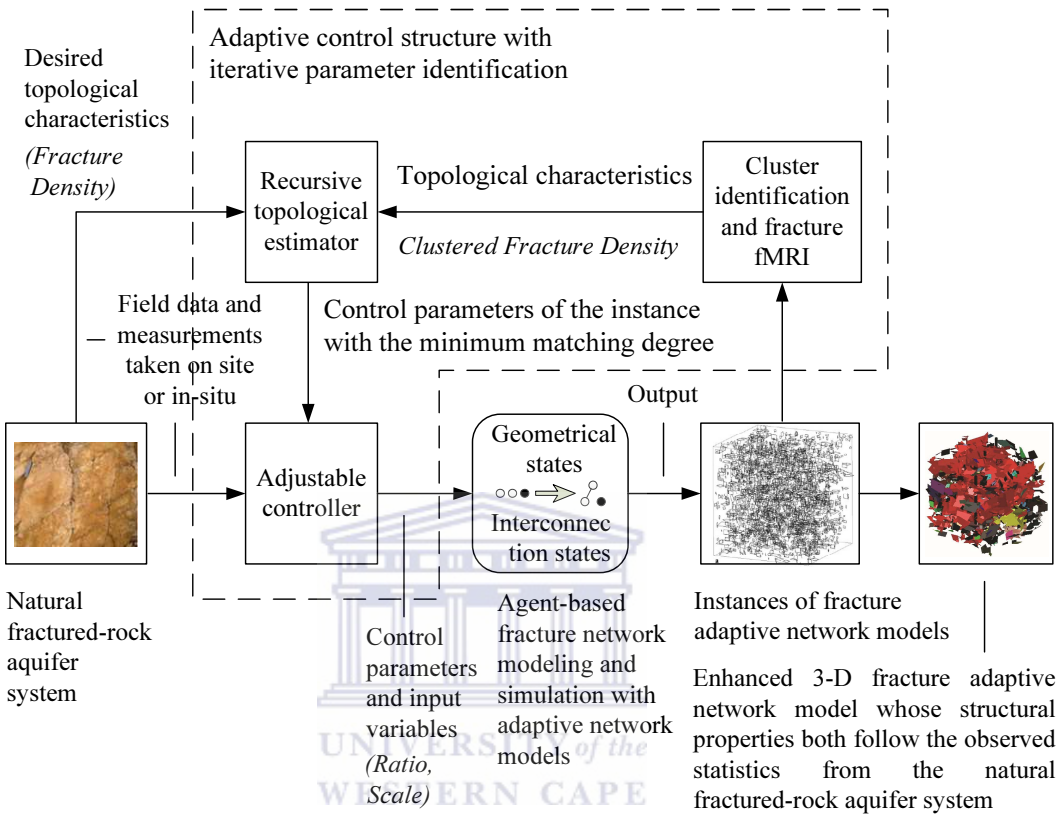

Figure 4.1: Block diagram of a unified framework for modelling and simulation of fractured-Rock aquifer systems which combines adaptive network models and an adaptive control structure with iterative parameter identification. The unified modelling framework consists of two loops: the inner loop which is composed of the process of agent-based network modelling and simulation and a state-topology feedback controller, and the outer loop, which consists of a recursive parameter estimator for controller tuning. Through using such an adaptive control structure, suitable control parameters can be identified for generating for generating the final configuration of the enhanced 3–D fracture adaptive network model with similar topological properties to the studied natural fracture network system.

state update of fractures are adjusted in each time step. Based on the statistical data derived from field data such as length, orientation, and density of measured natural fractures and the updated control parameters, the size and position of fractures are determined. The intersection analysis is then implemented for determining if two fractures intersect. By using the current sizes, positions and intersections of fractures, the instance of the adaptive network model in a certain discrete time step can be generated, in which the fractures can be represented by abstract nodes and the intersections among them by links. A performance index (clustered fracture density of the generated 3–D instances) can then be established in N time steps according to the topological measurements of the generated instances. The measured performance index is compared to the desired topological characteristics (area density of a 3–D reference fracture network) derived from field data, and the corresponding control parameters of the instance whose matching degree is the maximum is fed into the adjustable controller. The sizes, positions and intersections of fractures can be updated in order to generate an enhanced adaptive network model with similar topological properties to the studied natural fracture network system. This procedure can be repeated until a set of enhanced fracture adaptive network models are automatically generated for all given input variables, such as various field measurements, model sizes, seeds of random number generator, etc. Thus, through tracing various desired values, the generated 3–D fracture adaptive network models can have different structures which are similar to the studied fractured-rock aquifer systems with different geological and hydrological conditions.

4.3 Fracture3D, An Automatic 3–D Fracture Modelling Tool by Using Field Fracture Measurements

Through using the unified framework which combines adaptive network models and adaptive control structures, Fracture3D, an automatic 3–D fracture adaptive network modelling tool is conceptualized and programmed in spreadsheets for modelling and simulation of fractured-rock aquifer systems and connectivity analysis. Based on a limited amount of field data and suitable control parameters, the enhanced 3–D fracture adaptive network models can be created by Fracture3D, in

which the fracture statistics and the structural properties can both follow the observed statistics from natural fracture networks. The model of Fracture3D is shown in Figure 4.2. The simple field data can be gathered from field measurements of natural fractures, including fracture density, fracture orientation (dip angle and dip direction), and fracture diameter (length) (Table 4.1). The statistical data of the field data will be used as input variables of the process of modelling and simulation, when the mean and standard deviation of "Dip direction", "Dip angle", and "Length" are calculated respectively according to varied "Density". According to the input variables and the given control parameters, the size and position of fractures and the intersections among them can be determined in the process of agent-based adaptive network modelling and simulation. An instance of the adaptive network model is thus built. The label-propagation based cluster identification and Fracture Mapping and Realization Imaging (FMRI) are used for generating topological characteristics (clustered fracture density) of the 3–D instance. The adaptive-control based iterative parameter identification is implemented in order to identify an instance with the minimum topological difference to field data from a set of instances of the fracture adaptive network models, while the instances are automatically generated through using a set of adjustable control parameters. The final configuration of the enhanced 3–D fracture adaptive network model is then built through using the control parameters of the identified instance. In the following, several key algorithms of Fracture3D will be introduced, including geometrical state update, interconnection state update, label-propagation based cluster identification, topology measurement with FMRI, and adaptive-control based iterative parameter identification.

4.3.1 Geometrical State Update of Fractures

In the present work, an agent-based adaptive network modelling approach is used for modelling and simulation of fractured-rock aquifer systems with adaptive network models, when each individual fracture is assumed to be one possible ge-

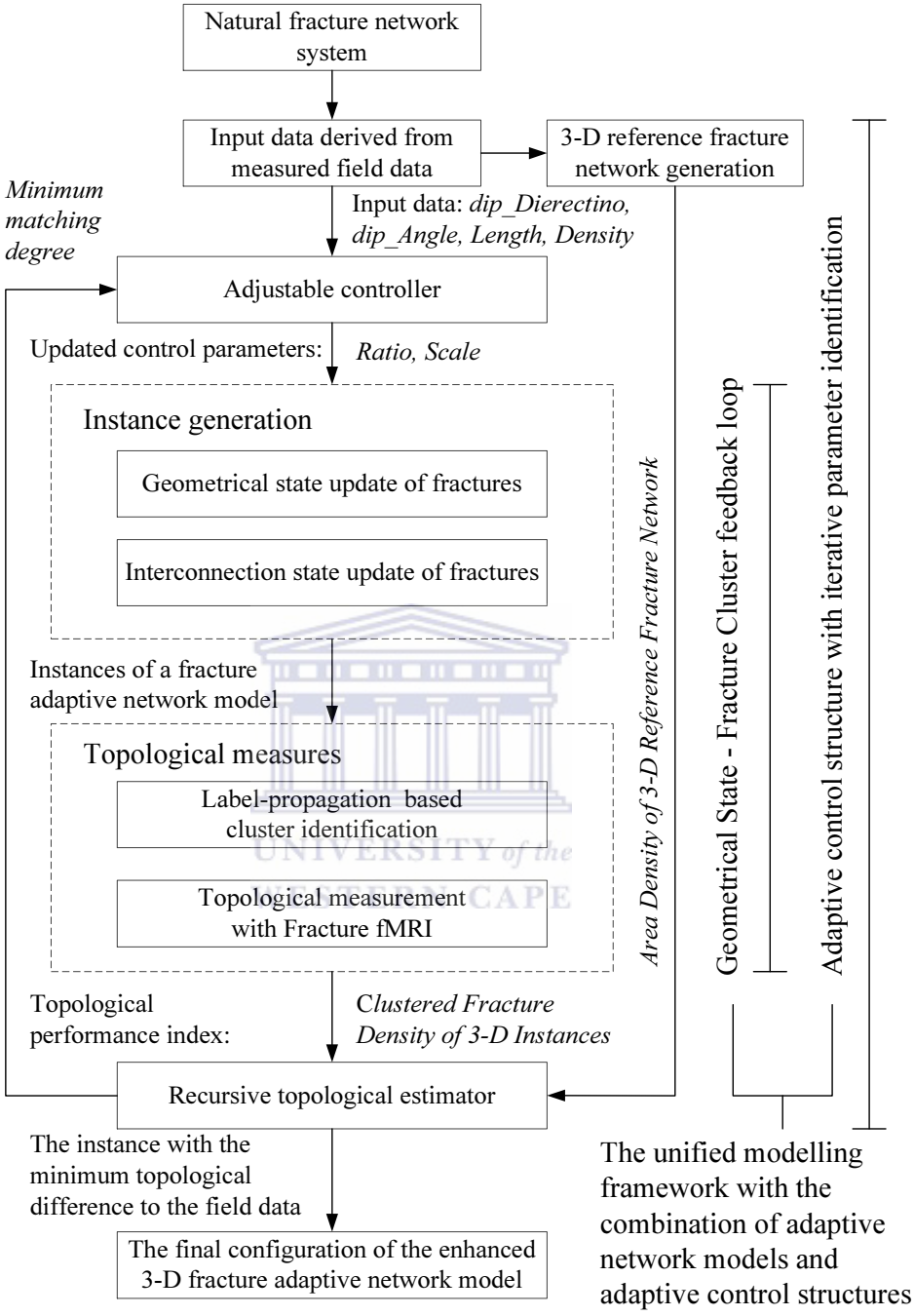

Figure 4.2: Model of Fracture3D. Through using a limited amount of field data and the unified framework which combines adaptive network models and adaptive control structures, a set of enhanced 3–D fracture adaptive network models are automatically created by Fracture3D, in which the fracture statistics and the structural properties can both follow the observed statistics from natural fracture networks.

ID	Dip direction	Dip angle	Length	Density
1	242	38	21	2.45
2	245	32	25	2.45
3	247	38	33	2.45
4	247	32	12	2.45
5	252	40	15	2.45
6	247	40	25	2.45
7	237	38	10.5	2.45
8	242	42	12	2.45
9	237	50	9	2.45
10	232	60	45	2.45
11	252	55	20.7	2.45
12	254	45	23	2.45
13	242	36	12.5	2.45
14	236	43	13.6	2.45
15	246	37	9	2.45
16	253	41	9	2.45
17	253	38	11.9	2.45
18	256	35	6.5	2.45
19	230	55	10.9	2.45
20	243	23	27	2.45

Table 4.1: Example of field data. The field data can be gathered from field measurements of natural fractures, including dip direction, dip angle, length, and length density of natural fractures.

ometrical state. Moreover, we also assume that fracture length obeys log-normal distribution, and fracture density follows uniform distribution, when dip angle and dip direction are assumed as normal distribution. A geometrical state update scheme which is specified by DFN models and the given control parameters is applied to each fracture in each discrete time step. The geometrical state (size and position) of a fracture is updated in each time step depending on the current control parameters (*Scale*, *Ratio*, and *Length*) and statistics of field data (see Figure 4.3).

The update scheme of geometrical states of fractures is depicted in Figure 4.4. Consider K fracture datasets measured from various sites in a field dataset (fracture mapping on rock exposures and/or borehole logging). One fracture dataset $S(\mathcal{M}, \mathcal{A}, \mathcal{D}, \mathcal{L}, P)$ is defined by a set $\mathcal{M} \equiv \{m_1, m_2, \ldots, m_M\}$ of measured fractures, a set $\mathcal{A} \equiv \{a_1, a_2, \ldots, a_M\}$ of values of dip angles, a set $\mathcal{D} \equiv \{d_1, d_2, \ldots, d_M\}$ of values of dip direction, a set $\mathcal{L} \equiv \{l_1, l_2, \ldots, l_M\}$ of values of length, and one dimensional fracture density P. Based on a DFN model, 3–D stochastic fracture network dataset $F(\mathcal{I}, \mathcal{X}^A, \mathcal{X}^D, \mathcal{X}^L, \mathcal{X}^W, \mathcal{X}^x, \mathcal{X}^y, \mathcal{X}^z)$ is generated with control parameters *Scale*, *Ratio*, and *Length*, formed by a set $\mathcal{I} \equiv \{i_1, i_2, \ldots, i_I\}$ of generated

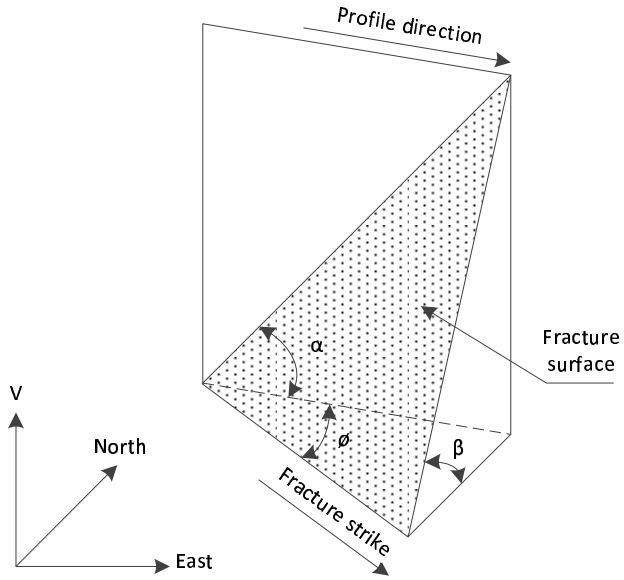

Figure 4.3: Relationship between fracture orientation and profile direction, in which φ is the included angle of fracture strike and profile direction, β is the fracture dip angle, and α is the apparent dip angle of fracture projected on the profile. Thus, a 3–D fracture-trace model can be generated based on the 2–D fracture-trace map. Adapted from (Lin, 2007).

fractures, and $I = P * Length$, a set $X^A \sim \mathcal{N}(u^A, o^A)$ of values of dip angle, a set $X^D \sim \mathcal{N}(u^D, o^D)$ of values of dip direction, a set $X^L \sim EXP(\mathcal{N}(u^L, o^L)) * Scale$ of values of length, a set $X^W = X^L * Ratio$ of values of width, a set $X^x = RNG * Length$ of values of x-axis coordinates, a set $X^y = RNG * Length$ of values of y-axis coordinates, and a set $X^z = RNG * Length$ of values of z-axis coordinates, where u and o is the mean and standard deviation of measured data regarding to dip angle, dip direction, and length respectively, RNG is a variable generated by a random number generator, $Scale$ is scale of length for modelling, $Ratio$ is scale of width for modelling, $Length$ is length of a cube space for modelling. This update procedure will be repeated K times for K fracture datasets. Based on dataset F, the stochastic DFN coordinate dataset with 3–D coordinates of four vertices of each fracture $G(\mathcal{I}, \mathcal{X}^x_{v1}, \mathcal{X}^y_{v1}, \mathcal{X}^z_{v1}, \mathcal{X}^x_{v2}, \mathcal{X}^y_{v2}, \mathcal{X}^z_{v2}, \mathcal{X}^x_{v3}, \mathcal{X}^y_{v3}, \mathcal{X}^z_{v3}, \mathcal{X}^x_{v4}, \mathcal{X}^y_{v4}, \mathcal{X}^z_{v4})$ is then generated by using an algorithm as shown in Figure 4.5.

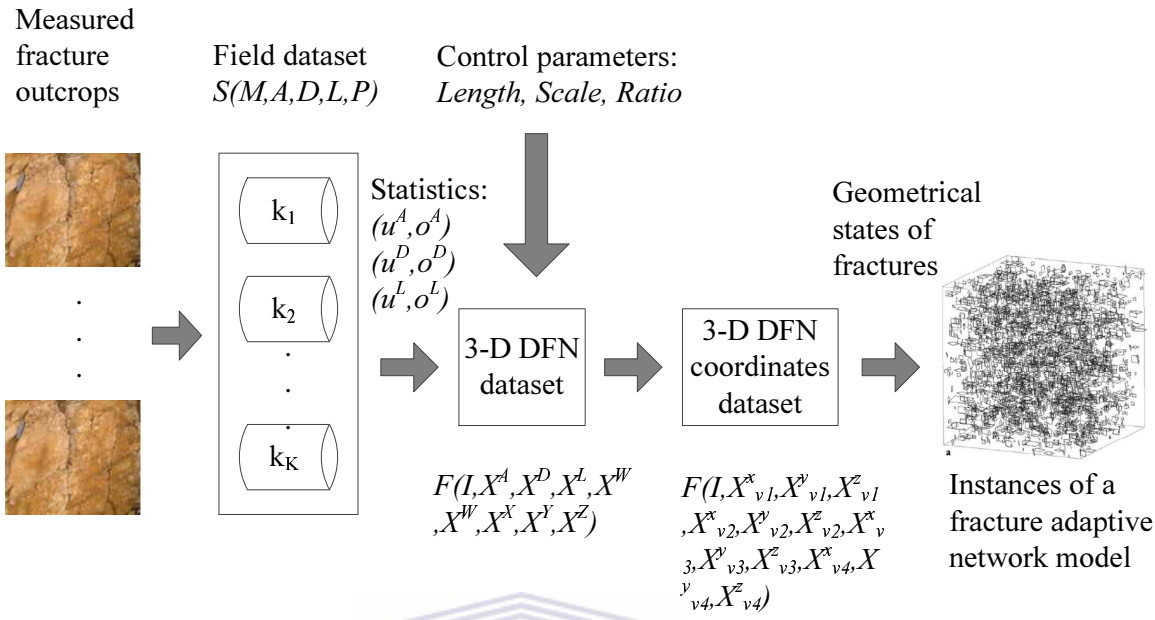

Figure 4.4: Block diagram of Geometrical State Update Scheme.

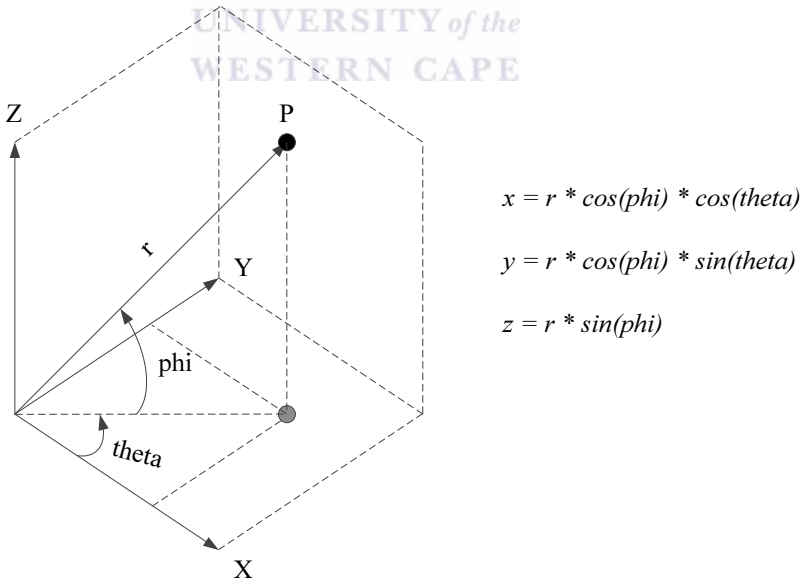

Figure 4.5: Algorithm for vertex calculations. 3–D coordinates of other three vertices of a generated fracture can be calculated based on coordinates of one vertex, dip angle, dip direction, and distance between two vertices.

4.3.2 Interconnection State Update of Fractures

After geometrical states of fractures are updated with the current control parameters, an intersection analysis algorithm is implemented for updating interconnection states of fractures according to their geometrical information. As shown in Figure 4.6, single fracture intersection test is used to determine if two fractures intersect through a fast and reliable 3–D triangle-triangle intersection test algorithm. Möller's method (Möller, 1997) is implemented for 3–D triangle-triangle intersection tests by checking the mutual intersection of each triangle with the plane of the other. It determines for each triangle on which side of the other triangle's supporting plane its vertices lie. If all vertices of one triangle lie on the same side and no vertex is on the plane, the intersection is rejected. Otherwise, the input triangles are guaranteed to intersect the line of intersection of the two planes.

Multiple fracture intersection tests are implemented to identify all neighbours of a fracture who intersect this fracture. The interconnection states of fractures can then be updated. Through using the current geometrical states and interconnection states of fractures, an instance of an adaptive network model is created. This generated instance can be represented by an ordered pair $G = (\mathcal{N}, \mathcal{E})$, where $\mathcal{N}$ is a set $\mathcal{N} \equiv \{n_1, n_2, \ldots, n_N\}$ of generated fractures and $\mathcal{E}$ is a set $\mathcal{E} \equiv \{e_1, e_2, \ldots, e_E\}$ of links $e_k = \{n_i, n_j\}$. A link $e_k = \{n_i, n_j\}$ is established when the fracture n_i intersects the fracture n_j. An adjacency matrix can be established for cluster identification according to the results of intersection detection, in which each element $a_{ij} = 1$ expresses a fracture i intersects fracture j, and $a_{ij} = 0$ otherwise.

4.3.3 Label-Propagation Based Cluster Identification

A fracture cluster is a maximal complete subnetwork of three or more fractures, i.e. a subnetwork of fractures all of which intersect each other, and such that no other fracture intersects all of them. By using the adjacency matrix with the current interconnection states, a label-propagation based cluster identification algorithm can be implemented for generating topological characteristics of measured instances of adaptive network models. The label of each fracture is initialized with its *ID*. An

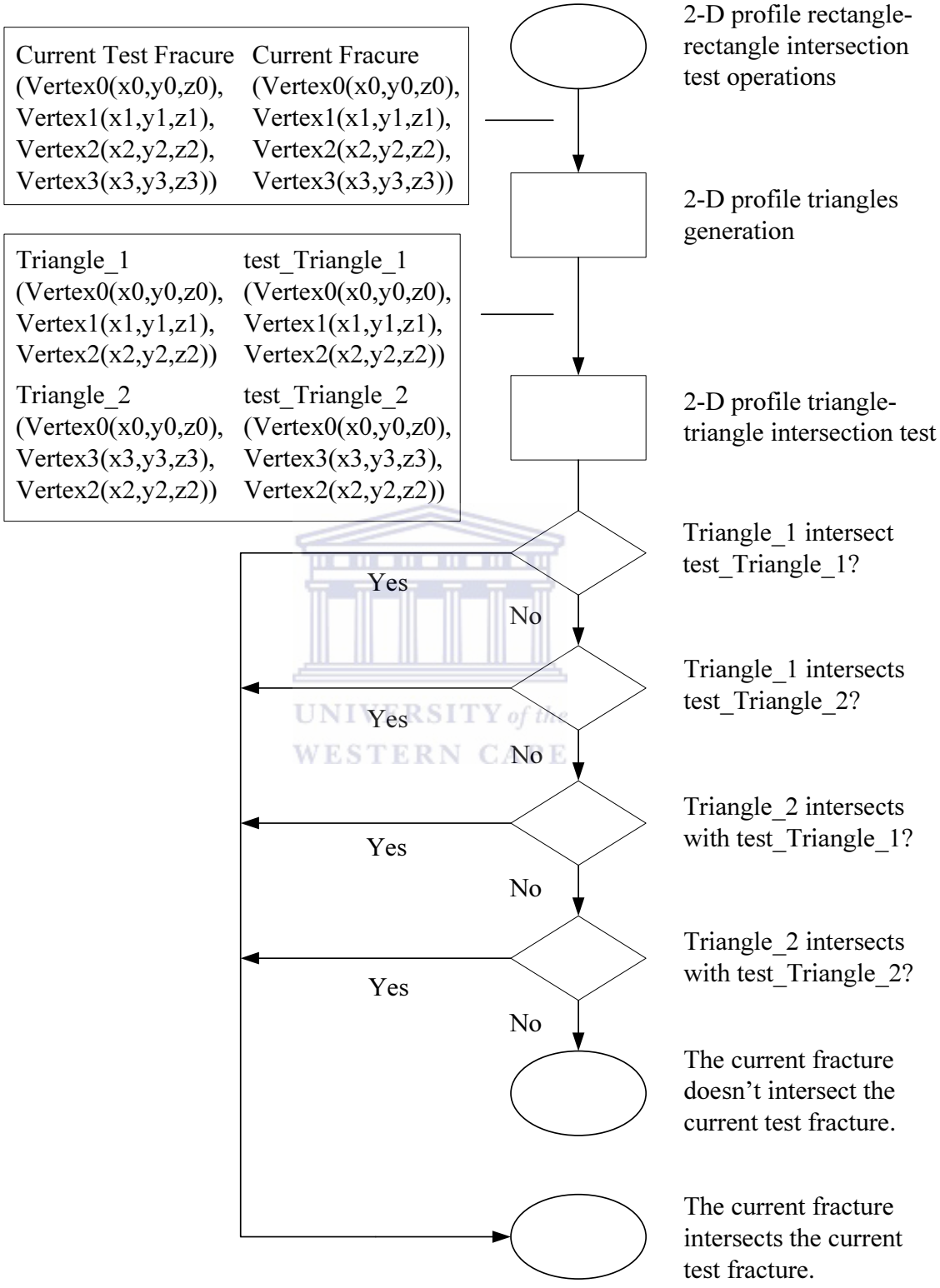

Figure 4.6: Multiple fracture intersection test operations.

originator of a cluster can be a fracture with an initial label. The neighbours of an originator are called the propagators. The neighbours of a propagator can be new propagators. The label propagating process ends when no more new propagators are found. All propagators update their initialized *ID* with the label of their originator. Next fracture that had an initial label is a new originator. This procedure can be repeated until there is no more new originator and new propagator. In this iterative process, the fracture clusters are identified when interconnected fractures (directed or undirected) are labelled with a unique *ID*. A simple example of the label propagating processes will be given in the following.

Suppose that a fracture n is an originator and carries its initial label $L_n = ID_n$. If the fracture n intersects its neighbours n_1,n_2,...,n_i, the fractures n_1,n_2,...,n_i can then be propagators and update their labels to ID_n. If the fracture n_i intersects n_1^i, n_2^i,...,n_j^i, the fractures n_1^i, n_2^i,...,n_j^i can also be propagators and update their labels to ID_n. This procedure can be repeated until there is no more new originator and new propagator. At the end of the propagation process, fractures what have the same label are grouped together as one cluster.

4.3.4 Topological Measure with FMRI

In order to identify an instance with the similar structural properties to field data from a set of generated instances, the topological characteristics of the generated instances need to be extracted and compared with field data. In this work, we assume that the fracture density of the maximum fracture cluster in a "good" instance of a 3–D fracture adaptive network model should be similar with the 1–D fracture density obtained from the 2–D fracture outcrops. Moreover, a topological measure algorithm, FMRI, has been used in Fracture3D for measuring the fracture density of each generated instance.

Functional magnetic resonance imaging is a brain-scanning technique for monitoring the flow of blood to different areas of the brain. In this work, a similar idea, Fracture Mapping and Realization Imaging, or FMRI, is used for measuring topological characteristics of the instances of fracture adaptive network models. The FMRI technique uses Clustered Fracture Density (CFD) as indicators of hydraulic

activity in simulated fracture networks. This idea is based on a hypothesis that the hydraulic properties of a sampling space depend on the clustered fracture density of the space. Moreover, only the fractures from the maximum cluster are scanned. A region with the maximum amount of interconnected fractures is located through global sampling and local sampling. A slice plane is then generated in this region. The value of CFD on this slice plane is computed according to the amount of intersected fractures and the length of the plane. Thus, the 2–D density information can be extracted from a 3–D instance of a certain fracture adaptive network model. An example for measuring the CFD of a generated instance is presented as Figure 4.7.

To generate proper sampling regions for FMRI scans, the sampling scale need to be determined according to the size of a reference space. This reference space is established based on the mean of measured densities which can be extracted from input data. The mean of length of a fracture set is $L_i = N_i/D_i$, where N_i is number of fractures of this fracture set, and D_i is density of this fracture set. The mean of length for all fracture sets is $\overline{L} = \frac{1}{k}\sum_{i=1}^{k} L_i$, where k is number of the fracture sets. Thus, a 3–D reference cube space is established, and the length of the cube is $\overline{L}$. The sampling cubes for FMRI scans are generated according to the length of this reference cube space. The sampling scale of FMRI is $S = \|(\frac{L_m}{\overline{L}})^{1/2}\|$, and L_m is the length of the modelling cube space. Several parameters are then calculated, including the number of global sampling cubes $i = S^3$, the length of global sampling cubes $L_g = L_m/S$, the number of local sampling cubes $j = S^3$, and the length of local sampling cubes $L_l = L_g/S$. The 3–D coordinates of each vertex are then generated for these sampling cubes.

Global sampling is implemented to locate one global sampling cube with the maximum amount of clustered fractures. The fractures that intersect this global sampling cube are labelled for local sampling. Local sampling is then performed to locate one local sampling cube with the maximum number of clustered fractures in this global sampling cube. The fractures that intersect this local sampling cube are labelled for slice sampling. The number of the fractures that intersect a sampling cube can be detected by using a fracture locating algorithm (see Algorithm 4.1).

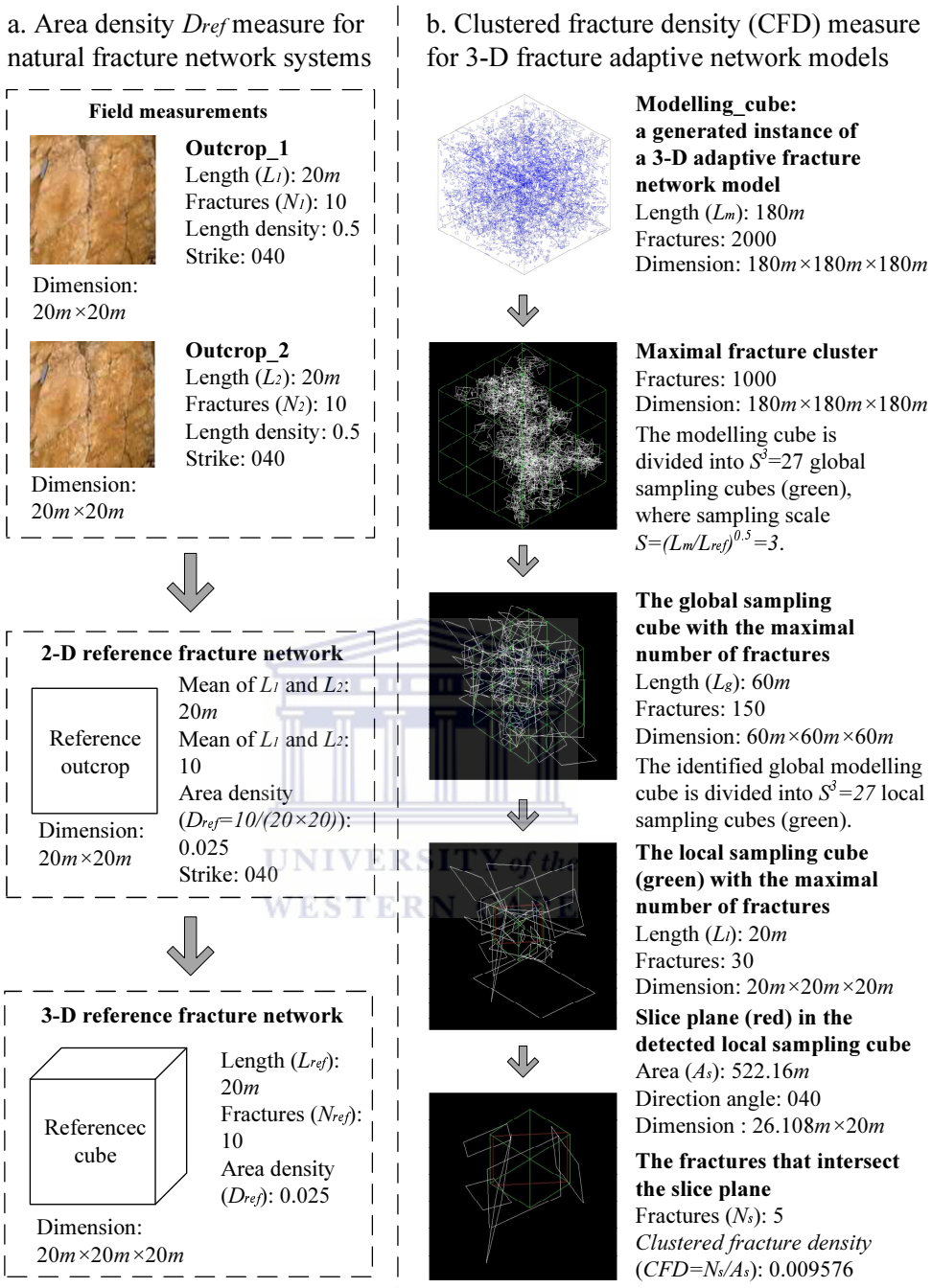

Figure 4.7: An example for the measurement of the Clustered Fracture Density of a generated instance by using FMRI. A region with the maximum amount of interconnected fractures is located through global sampling and local sampling. A slice plane is then generated in this region. The value of CFD on this slice plane is computed according to the amount of intersected fractures and the length of the plane. Thus, the 2–D density information can be extracted from a 3–D instance of a certain fracture adaptive network models.

Algorithm 1: Fracture locating in a sampling cube

```
x _v1…8, y_v1…8, z_v1…8:  x,y,z coordinates for eight vertex of a sampling cube.
x_max_cube, y_max_cube, z_max_cube:  maximal x,y,z coordinates of a sampling cube.
x_ f1…4, y_ f1…4, z_f1…4,:  x,y,z coordinates for four vertex of a clustered fracture.
x_max_frac, y_max_frac, z_max_frac:  maximal x,y,z coordinates of a clustered fracture.

for each cubes do
  x_max_cube  =  max (x_v1, x_v2, ..., x_v8)
  y_max_cube  =  max (y_v1, y_v2, ..., y_v8)
  z_max_cube  =  max (z_v1, z_v2, ..., z_v8)
  for each fracture do
    x_max_frac = max(x_f1, x_f2, x_f3, x_f4)
    y_max_frac = max(y_f1, y_f2, y_f3, y_f4)
    z_max_frac =  max (y_f1, y_f2, y_f3, y_f4)
      if x_max_frac ≥ x_min_cube && x_min_frac ≥ x_max_cube &&
       y_max_frac ≥ y_min_cube && y_min_frac≥ y_max_cube &&
       z_max_frac ≥ z_min_cube && z_min_frac ≥ z_max_cube then
          current_fracture ∩ current_cube
      end if
  end for
end for
```


A vertical slice plane is generated in the local sampling cube with the maximum amount of clustered fractures. The direction angle of reference cube space is given according to the strike angle of the measured fracture plane from field measurements. The direction angle of this slice plane is the same as the direction angle of reference cube space. The fractures labelled by local sampling are detected if they intersect the slice plane. The clustered fracture density is then calculated as: $CFD = N_s/A_s$, where N_s is the number of labelled fractures, and A_s is the area of slice plane.

4.3.5 Adaptive-Control Based Iterative Parameter Identification

While an instance of a 3–D fracture adaptive network model can be generated and its topological characteristics are measured by using the algorithms mentioned above, an adaptive-control based iterative parameter identification algorithm is used for automatically generating a set of instances of a 3–D fracture adaptive

network models based on a set of adjustable control parameters. An instance with the minimum topological difference to the studied natural fracture network is then be identified from the generated instances based on the dynamical topological estimation to the natural fracture network. Thus, the coupling of fracture adaptive network models ("geometrical state–fracture cluster" coevolution) and adaptive control structures ("control parameter–topological estimate" coevolution) can give rise to a dynamical self-organization such that topological properties of the generated 3–D instances closed to a desired state, where the geometrical states of the fractures changed qualitatively.

4.3.5.1 Adjustable Controller

An ordinary 3–D fracture network models can be built with the fixed control parameters, such as the ratio of length to width of a fracture and the ratio of original value to final value of length of a fracture. However, a poor fracture network model may be generated because of parameter uncertainty and poor or incorrect geological and hydrological assumptions, in which the fracture statistics may follow the observed statistics, but the structural properties are totally different compared to the observations. An example of the network models with fixed control parameters is shown as Figure 4.8a, in which there are only 16 interconnected fractures in the maximum cluster (see Figure 4.8b). It has been found that the hydrological properties of the studied fractured-rock aquifer derived from these ordinary fracture network model with fixed control parameters cannot be explained by field observations, in-situ hydraulic tests (packer test and pumping test), and the models established through using other flow modelling approaches (Lin, 2007). In Fracture3D, however, an adjustable controller has been used for automatic generation of a set of enhanced 3–D fracture adaptive network models, in which the fracture statistics and the structural properties can both follow the observed statistics from natural fracture networks.

In the adjustable controller, two control parameters need to be updated in each time step for generating the instances of fracture adaptive network models,

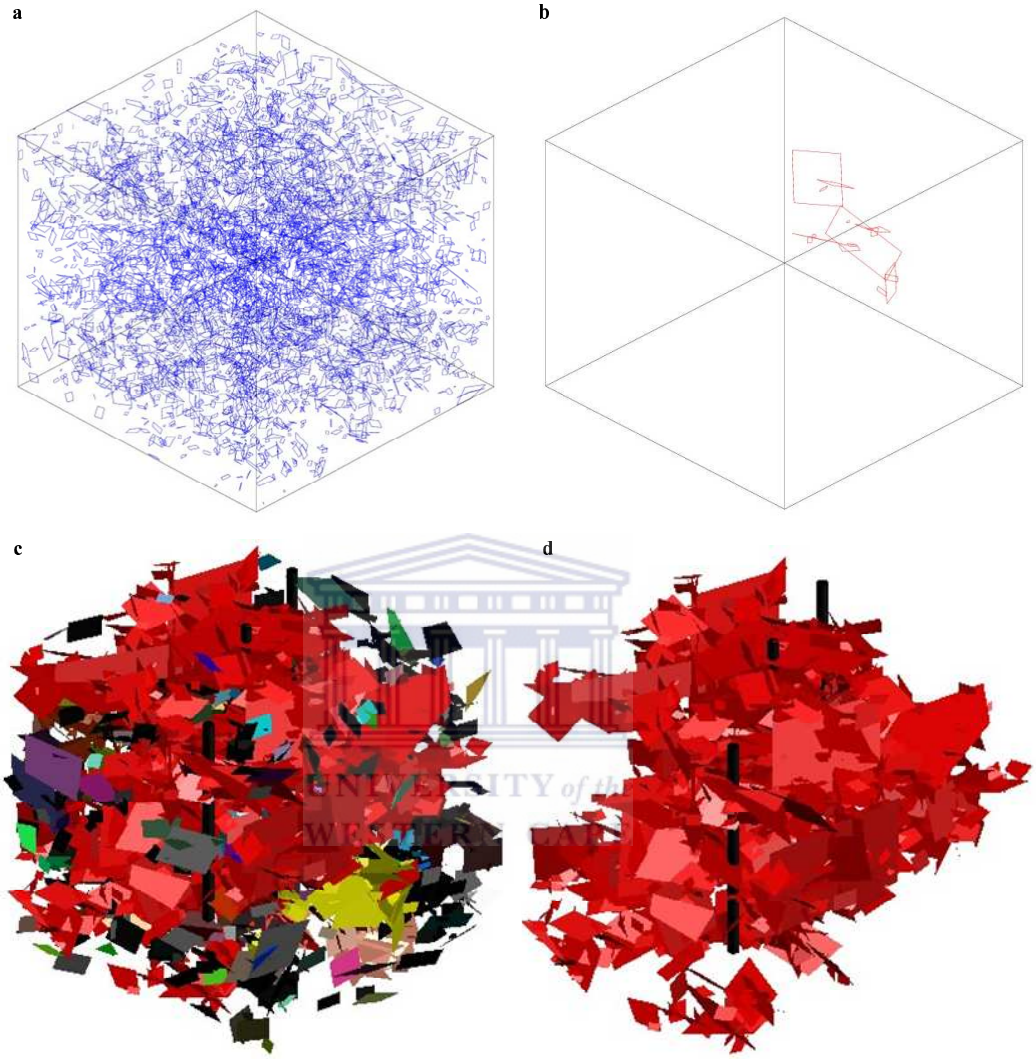

Figure 4.8: 3–D fracture network model generated by using various control parameters. a, an ordinary 3–D fracture network model generated by using fixed control parameters (*Size*=300, *Ratio*=1.5, and *Scale*=1); b, the maximum cluster of the ordinary network model which contains 16 fractures. c, the final configuration (*Size*=300, *Ratio*=0.7, and *Scale*=1.4) of an enhanced 3–D fracture adaptive network model generated by Fracture3D with control parameter tuning; d, the maximum cluster of the fracture adaptive network model has 1,255 fractures.

including *Ratio* (the ratio of length to width of a single stochastic fracture), *Scale* (the ratio of original value to final value of length of a generated fracture), when the current value of *Size* (the length of one side of a 3–D model space) is given. An adaptive control scheme for control parameter update is implemented. In the present work, the update scheme consists of 18 parameter pairs (*Ratio* and *Scale*) for generating 18 instances of a fracture adaptive network model, while 9 control parameter pairs *Scale=1, 1.25, 1.5, 1.75, 2, 2.25, 2.5, 2.75, 3* and all *Ratio=1* are given in advance. In 1-9 time steps, nine control instances are automatically generated by using field data and these control parameters respectively. According to the results of recursive topological estimation, the corresponding control parameter *Scale* (S_o) of the instance whose matching degree is the maximum is fed into the adjustable controller. In 10-18 time steps, another nine control instances are automatically generated by using field data and the control parameters respectively, while *Scale* is setup as $S_o * \sqrt{0.2}$, $S_o * \sqrt{0.4}$, $S_o * \sqrt{0.6}$, $S_o * \sqrt{0.8}$, $S_o * \sqrt{1}$, $S_o * \sqrt{2}$, $S_o * \sqrt{3}$, $S_o * \sqrt{4}$, and $S_o * \sqrt{5}$ respectively, and *Ratio* is setup as 0.2, 0.4, 0.6, 0.8, 1, 2, 3, 4, and 5 respectively. The corresponding control parameter pairs of the instance whose matching degree is the maximum is then used to generate the final configuration of the fracture adaptive network model, in which the fracture statistics and the structural properties can both follow the observed statistics from natural fracture networks. An example of the final configuration of the enhanced fracture adaptive network models is shown in Figure 4.8c, in which there are 1,255 fractures in the maximum cluster (see Figure 4.8d).

4.3.5.2 Recursive Topological Estimator

In order to identify an instance of a 3–D fracture adaptive network model with the desired topological characteristics, a simple absolute-error estimator is used. Although this desired topological characteristics cannot be directly obtained from natural fracture networks, we can build a 3–D reference fracture network by using field data (see Figure 4.7a). The area density of the 3–D reference fracture network is $D_{ref} = \overline{N}/(\overline{L} * \overline{L})$, where $\overline{N}$ is mean of number of fractures of all measured fracture sets, $\overline{L}$ is mean of length of all measured fracture sets. Given a set of

$CFD(CFD_1, CFD_2, \ldots, CFD_i)$ measured from i generated instances, the *matching degree* (M) of i instances can be calculated as $M_i = 1 - |CFD_i - D_{ref}| / Max(|CFD_1 - D_{ref}|, |CFD_2 - D_{ref}|, \ ldots, |CFD_i - D_{ref}|)$. The maximum value of matching degree is 1 as $CFD_i = D_{ref}$ and the minimum value is 0 as $CFD_i = CFD_{max}$. The corresponding control parameters of the instance whose matching degree is the maximum are then fed into the adjustable controller for controller tuning.

4.3.6 Programming

Visual Basic for Applications is a fast, powerful, and portable tool for enhancing Microsoft Excel. By using Visual Basic for Applications, Fracture3D, a spreadsheet based fracture network modelling tool is developed for 3–D fracture random realization and fracture connectivity analysis. The fracture field measurements collected from the study site were imported to an Excel worksheet, which includes dip direction, dip angle, length, and density of natural fractures. A set of user-defined control parameters were also imported to another Excel worksheet, including *Size* (the length of one side of a 3–D model space), *Scale* (the ratio of original value to final value of length of a generated fracture), and *Ratio* (the ratio of length to width of a single stochastic fracture). Based on these input data and control parameters, a set of 3–D fracture network models with different model sizes are generated by using Fracture3D. An AutoCAD macro is then be implemented for 3–D visualization by using the 3–D coordinate data of the generated fractures.

4.4 Experiments on Fracture Field Measurement Dataset

In order to verify the validity of the proposed unified modelling framework and automatic modelling tool Fracture3D, we have applied them on a real-world fractured-rock aquifer systems. Through using simple fracture field measurements taken on site and Fracture3D, a set of the enhanced 3–D fracture adaptive network models, whose fracture statistics and structural properties can both follow the observed statistics from natural fracture networks, have been built for the Table Mountain Group (TMG) fractured aquifer. We compared the topological characteristics of the 3–D instances to demonstrate how Fracture3D with a unified modelling

framework can drive the 3–D fracture adaptive network models towards a desired state. Moreover, we also compared the 3–D fracture adaptive network models generated by our Fracure3D with control parameter tuning to ordinary 3–D fracture network models generated by using fixed control parameters, and ordinary 3–D fracture adaptive network models generated by using preset control parameters.

4.4.1 Field Data and Control Parameters

The field data were collected from the TMG area, South Africa. The study site is a groundwater research and monitoring site with a five-borehole network located in the Gevonden farm, 6 km west of Rawsonville, Western Cape, South Africa. Based on the field observations through borehole core logging, groundwater observations, hydraulic test, and the examination of fracture characteristics, the hydraulic properties of the TMG fractured aquifer have been investigated in this study site by (Lin, 2007). Moreover, the fracture field measurements were gathered including dip direction, dip angle, and length of 216 natural fractures on five different outcrops (see Figure 4.9). The fracture density (1–D length density) of the outcrops was also measured. More details about the study site and the fracture measurement on the outcrops can be found in (Lin, 2007).

Figure 4.9: A TMG sandstone outcrop for fracture measurement.

In simulations, we compared the generated 3–D fracture adaptive network models generated by our Fracure3D with control parameter tuning to ordinary 3–D fracture network models generated by using fixed control parameters, and ordinary

3–D fracture adaptive network models generated by using preset control parameters. In the simulations with Fracture3D, the fracture field measurements collected from the study site were imported to an Excel worksheet, which includes dip direction, dip angle, length, and density of natural fractures. A set of control parameters were also imported to another Excel worksheet, including *Size=100m, 200m, 300m, 500m, 800m*, *Scale=1, 1.25, 1.5, 1.75, 2, 2.25, 2.5, 2.75, 3*, and *Ratio=1, 1, 1, 1, 1, 1, 1, 1, 1*, where *Size* is the length of one side of a 3–D model space, *Scale* is the ratio of original value to final value of length of a generated fracture, and *Ratio* is the ratio of length to width of a single stochastic fracture. Based on these input data and control parameters, five 3–D fracture network models with different model sizes were generated by using Fracture3D. While 3–D adaptive fracture network models were automatically generated by Fracture3D with control parameter tuning, five ordinary 3–D fracture network models with various model sizes have also been generated for performance evaluation by using fixed control parameters (*Scale=1* and *Ratio=1*). Furthermore, another five ordinary 3–D fracture adaptive network models were also generated by only using the preset control parameters, which were *Scale=1, 1.25, 1.5, 1.75, 2, 2.25, 2.5, 2.75, 3*, and *Ratio=1, 1, 1, 1, 1, 1, 1, 1, 1*, in order to evaluate the performance of adaptive-control based control parameter tuning.

4.4.2 Performance Metrics

We use the following three metrics to compare the 3–D fracture network models: percentage error, interconnection ratio, and interconnection ratio of the maximum cluster. Percentage error can be computed as $\delta = |CFD - D_{ref}|/D_{ref}$, which is the relative magnitude of the difference between CFD of a generated 3–D fracture network model and a 3–D reference fracture network model. In all simulations, the 3–D reference fracture network model and the measured D_{ref} were the same because the same field data were used. Interconnection ratio is the proportion of interconnected fractures among all generated fractures. Interconnection ratio of the maximum cluster is the proportion of interconnected fractures in the maximum cluster among all generated fractures.

4.4.3 Comparison of the Generated Instances

Through using Fracture3D with control parameters tuning, we generated the five enhanced 3–D adaptive fracture network models with various model sizes based on the field data and the preset control parameters. Given a certain model size, the final configuration of the 3–D fracture adaptive network model is generated by using the control parameters of the instance whose matching degree is the maximum among 18 instances. Matching degrees, interconnection rate, and interconnection rate of the maximum fracture cluster of the 1–9 instances with different model sizes are shown in Figures 4.10, 4.11, and 4.12 separately, while the 10–18 instances are shown in Figures 4.13, 4.14, and 4.15 respectively.

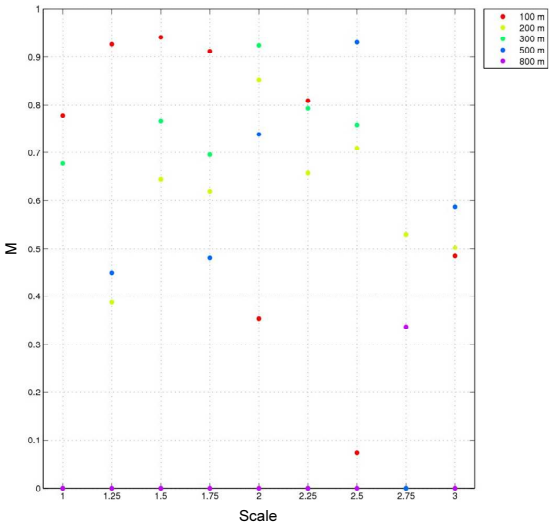

Figure 4.10: Matching degree (M) of 1-9 instances with different model sizes.

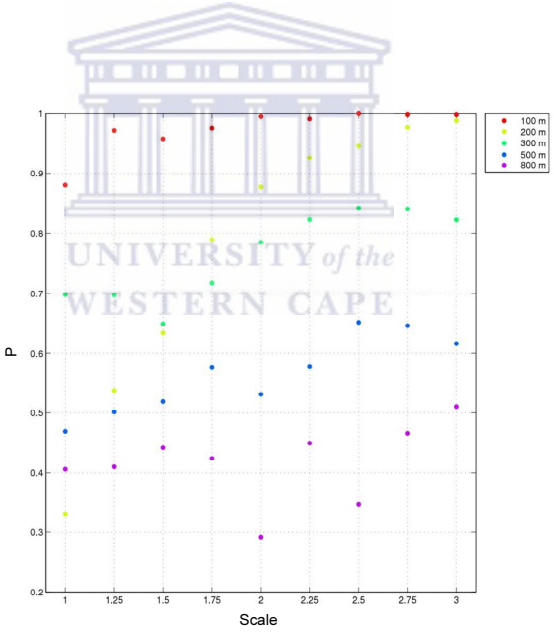

Figure 4.11: Interconnection rate (P) of 1-9 instances with different model sizes.

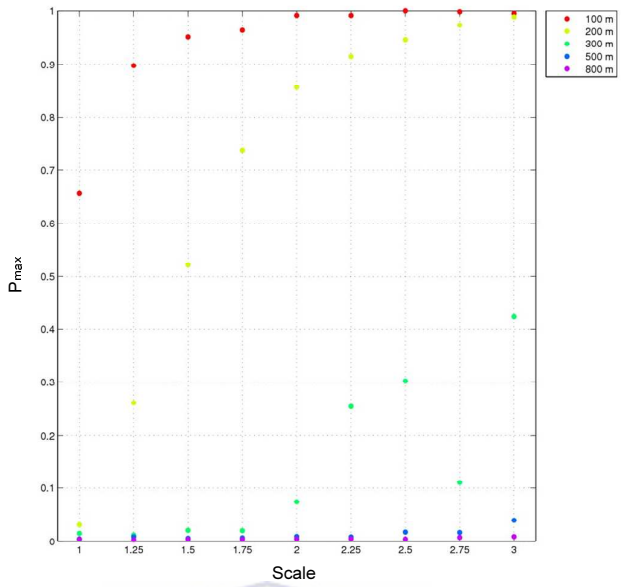

Figure 4.12: Interconnection rate of the maximum fracture cluster (P_{max}) of 1-9 instances with different model sizes.

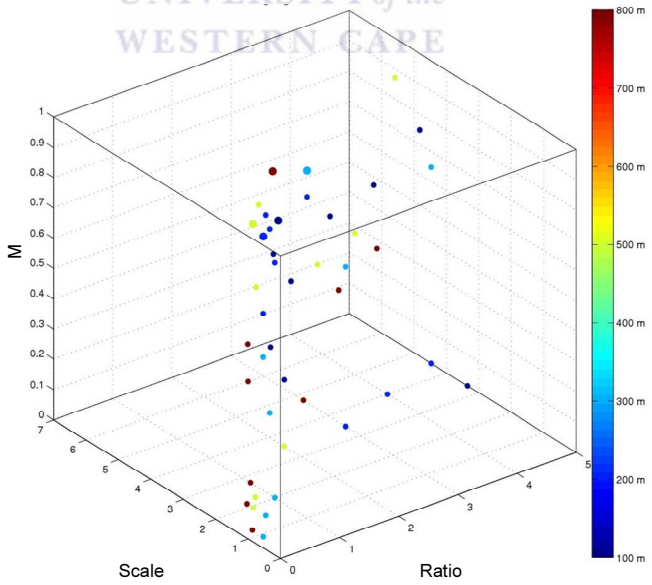

Figure 4.13: Matching degree (M) of 10-18 instances with different model sizes. The maximum values of M are shown with larger marking points.

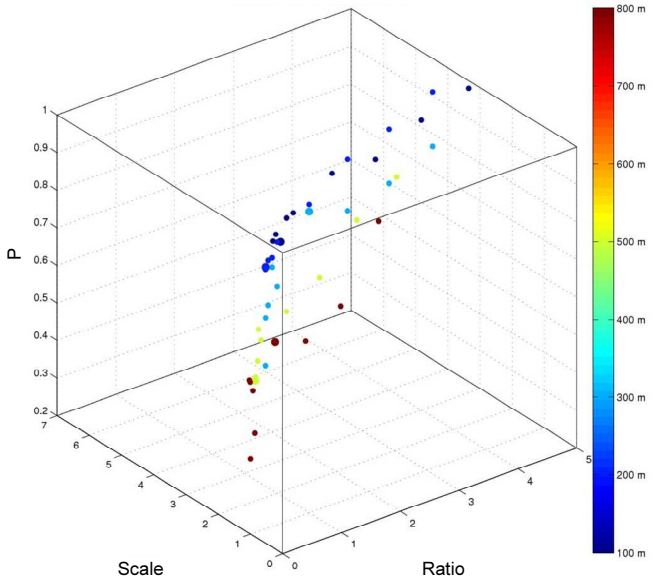

Figure 4.14: Interconnection rate (P) of 10-18 instances with different model sizes. The maximum values of P are shown with larger marking points.

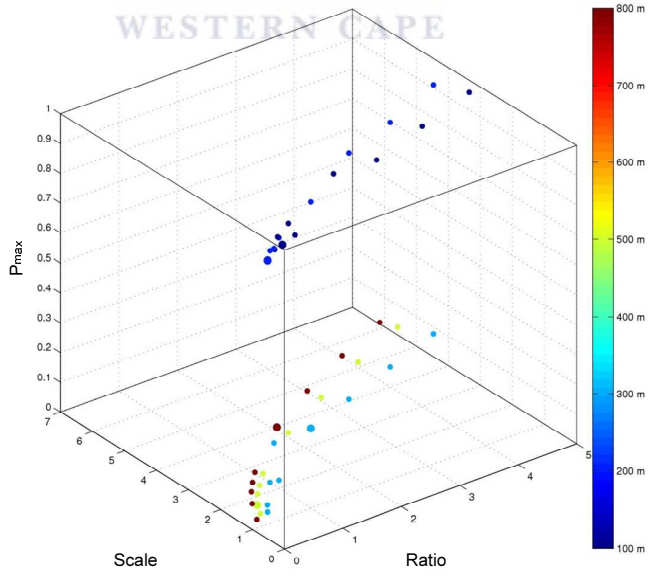

Figure 4.15: Interconnection rate of maximum fracture cluster (P_{max}) of 10-18 instances with different model sizes. The maximum values of P_{max} are shown with larger marking points.

Figures 10, 11, 12, 13, 14, and 15 show that the range of the control parameter *Scale* and the corresponding matching degree are $1.5 - 2.75$ and $0.33712 - 0.9418$ respectively, while *Ratio* is a fixed control parameter (all *Ratio*=1). However, as it is shown in Figure 13, 14, and 15, we can observe that the values of the control parameters *Ratio* and *Scale* span quite a wide range ($0.2 - 2$ and $0.8944 - 3.8891$), while the generated 3–D fracture adaptive network models have better matching degree ($0.8838 - 0.9991$). In order to demonstrate how the "geometrical state–fracture cluster" coevolution with control parameter tuning can drive the 3–D fracture adaptive network models towards a desired state, we compared the topological characteristics of the generated instances of five 3–D fracture adaptive network models (see Figure 16). In Figure 16a, we show the percentage errors of the first instance with *Ratio=1* and *Scale=1*, the instance whose matching degree is the minimum among 1-9 instances, and the instance whose matching degree is the minimum among 10–18 instances in five enhanced 3–D fracture adaptive network models with various model sizes. Clearly, the instance whose matching degree is the minimum among 10–18 instances achieves lower percentage error than other instances. The instances whose matching degrees are the minimum among 10–18 instances of the fracture adaptive network models with different model sizes achieved $89.2\% - 99.7\%$ improvements in percentage error over the first instances, while the instances whose matching degrees are the minimum among 1–9 instances achieved $64\% - 93\%$ improvements. Moreover, the instances whose matching degrees are the minimum among 10–18 instances achieved $59.9\% - 98.9\%$ improvements over the instances whose matching degrees are the minimum among 1-9 instances. Hence, by using the control parameters of the instances whose matching degrees were the minimum among 10–18 instances, the final configurations of the 3–D fracture adaptive network models have been generated, in which the fracture statistics and the structural properties both followed the observed statistics from natural fracture networks.

In Figure 4.16b and 4.16c, we also observe that the network topology is dynamically changed by the geometrical states of the fractures, while the geometrical states of the fractures are dynamically updated by using adaptive-control based

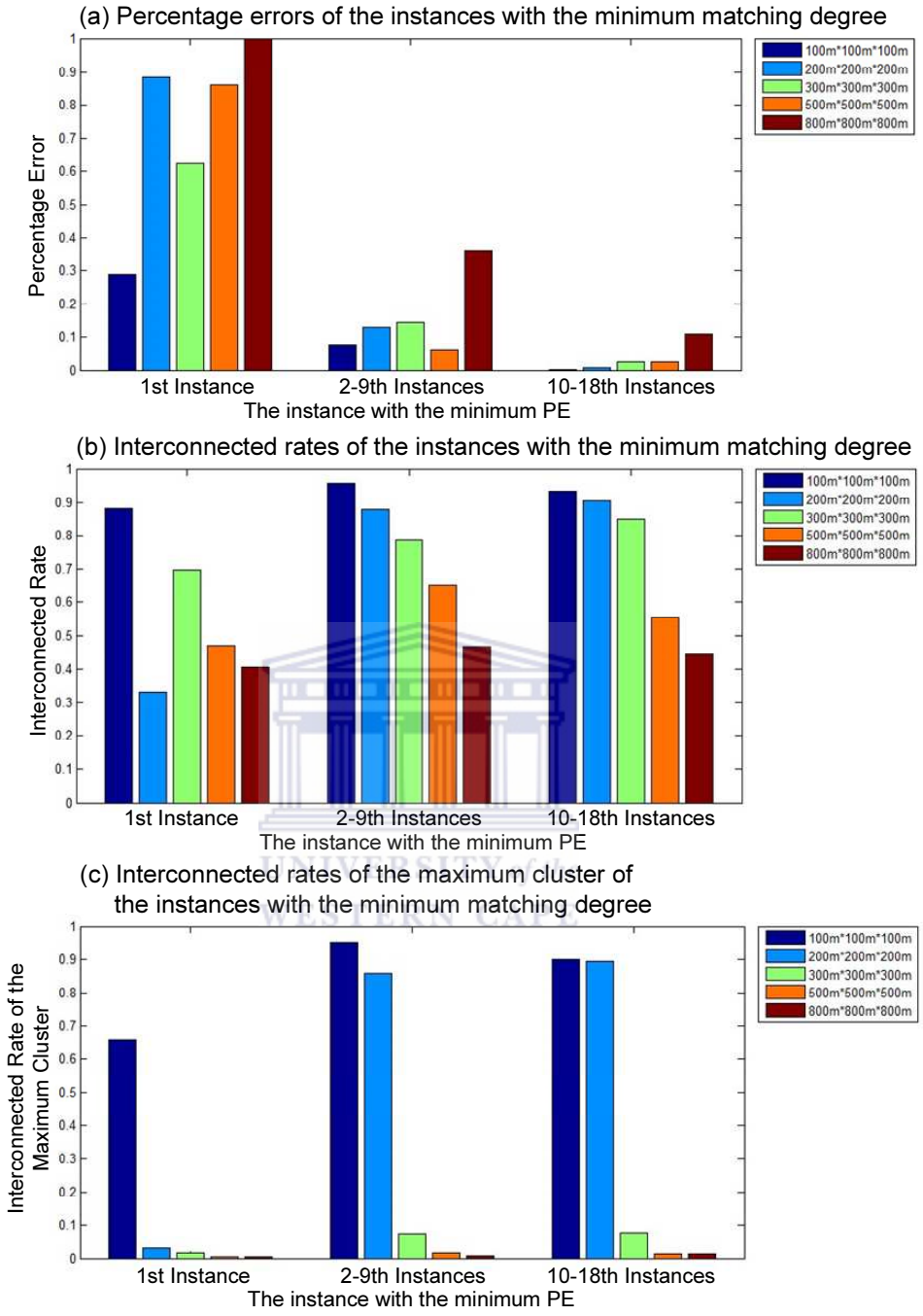

Figure 4.16: Comparison of topological characteristics of instances of the enhanced 3–D fracture adaptive network models with various model sizes. a, comparison of percentage errors of the instances whose matching degrees are the minimum; b, comparison of interconnected rates of the instances whose matching degrees are the minimum; c, comparison of interconnected rates of the maximum cluster of the instances whose matching degrees are the minimum.

control parameter tuning. The interconnected rates of the instances whose matching degrees are the minimum among 1–9 instances were higher than the first instances $8.8\% - 165.5\%$, while the instances whose matching degrees are the minimum among 10–18 instances were higher than the first instances $6.1\% - 173.5\%$. Moreover, the interconnected rates of the maximum cluster of the instances whose matching degrees are the minimum among 1–9 instances were higher than the first instances $44.9\% - 2684.4\%$, while the instances whose matching degrees are the minimum among 10–18 instances were higher than the first instances $35.9\% - 2803.1\%$. However, the difference of the interconnected rates and the interconnected rates of the maximum cluster between the two types of instances are relatively small ($-14.9\% - +8.1\%$ and $-18.7\% - +59.9\%$). These results show that the adaptive control structures modify the network topology in a wide range by using the preset control parameters at first, and then dynamically adjust the network topology in a narrow range by using control parameter tuning such that topological properties of the generated 3–D instances closed to a desired state. For example, given a model size $300m \times 300m \times 300m$, the first instance ($Ratio = 1$ and $Scale = 1$) has 2210 interconnected fractures in 186 fracture clusters respectively, 47 fractures in the maximum cluster, 11 fractures that intersect the slice plane, and its percentage error is 62.4%. The eighth instance ($Ratio = 1$ and $Scale = 2$) whose matching degree is the minimum among 1–9 instances has 2484 interconnected fractures in 139 clusters, 234 fractures in the maximum cluster, 25 fractures that intersect the slice plane, and its percentage error is 14.6%. The fifteenth instance ($Ratio = 2$ and $Scale = 2.83$) whose matching degree is the minimum among 10–18 instances has 2686 interconnected fractures in 103 clusters, 244 fractures in the maximum cluster, 30 fractures that intersect the slice plane, and its percentage error is 2.5%. While the number of total fractures is 3166 in all 18 instances, the instance whose matching degree is the minimum among 10–18 instances achieved 96.0% and 83.0% improvements over the first instance and the instance whose matching degree is the minimum among 1–9 instances respectively by using adaptive-control based iterative parameter identification.

4.4.3.1 Comparison of the Generated Network Models

In order to evaluate the performance of our Fracture3D, we generated five enhanced 3–D fracture adaptive network models with various model sizes by using Fracure3D with control parameter tuning, five ordinary 3–D fracture network models by using fixed control parameters, and five ordinary 3–D fracture adaptive network models by using preset control parameters. We ran each simulation 10 times with different seeds and collected statistics in each run. All results plotted in Figure 4.17 show the averages of results obtained in all runs. Figure 4.17a compares the percentage errors of three types of 3–D fracture network models with various model sizes. We can observe that the enhanced 3–D fracture adaptive network models generated by using Fracure3D with control parameter tuning achieves lower percentage error than other network models. The enhanced 3–D fracture adaptive network models achieved $49.3\% - 97.1\%$ improvements over the ordinary 3–D fracture network models, while the ordinary 3–D fracture adaptive network models achieved $35.0\% - 88.0\%$ improvements. Furthermore, the enhanced 3–D fracture adaptive network models also achieved $19.2\% - 73.3\%$ improvements over the ordinary 3–D fracture adaptive network models.

As shown in Figure 4.17b and 4.17c, we can observe the impact of the geometrical states of the fractures on fracture network topology, while the geometrical states are updated based on fixed or adjustable control parameters. The average interconnected rates of the enhanced 3–D fracture adaptive network models were higher than the ordinary 3–D fracture network models ($10.5\% - 150.2\%$), while the ordinary 3–D fracture adaptive network models were higher than the ordinary 3–D fracture network models $10.2\% - 147.7\%$. Moreover, the average interconnected rates of the maximum cluster of the enhanced 3–D fracture adaptive network models were higher than the ordinary 3–D fracture network models $103.6\% - 2419.8\%$, while the ordinary 3–D fracture adaptive network models were higher than the ordinary 3–D fracture network models $102.1\% - 2376.6\%$. However, the difference of the average interconnected rates and the average interconnected rates of the maximum cluster between the ordinary and enhanced 3–D fracture adaptive network

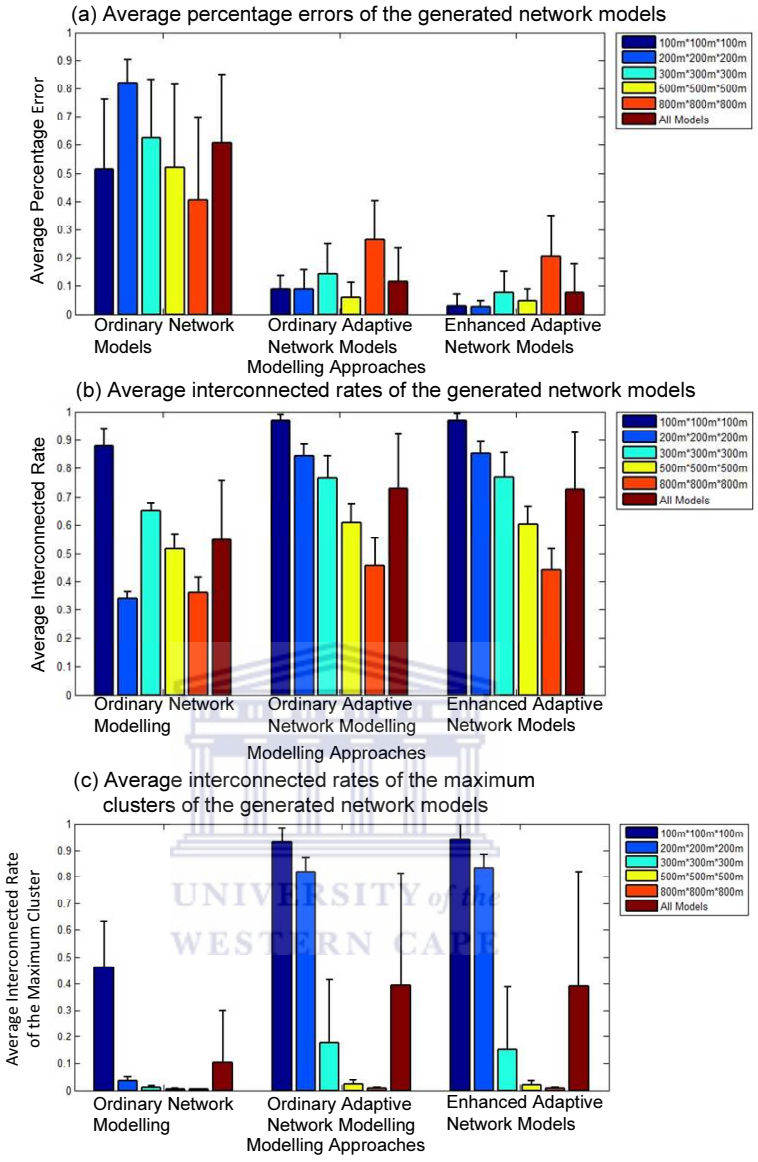

Figure 4.17: Comparison of topological characteristics of the different 3–D fracture network models with various model sizes, including the enhanced 3–D fracture adaptive network models generated by using Fracure3D with control parameter tuning, the ordinary 3–D fracture network models generated by using fixed control parameters, and the ordinary 3–D fracture adaptive network models generated by using preset control parameters. a, comparison of average percentage errors of the generated 3–D fracture network models; b, comparison of average interconnected rates of the generated 3–D fracture network models; c, comparison of average interconnected rates of the maximum cluster of the generated 3–D fracture network models.

models were relatively small ($-3.3\% - +0.4\%$ and $-12.8\% - +12.7\%$). These results show that our Fracture3D can drive the network topology towards a desired state by dynamically updating the geometrical states of fractures (size and profile of fractures) with a proper adaptive control structure. For example, given a model size $800m \times 800m \times 800m$, the ordinary 3–D fracture network model with fixed control parameters has 3,425 interconnected fractures in 202 fracture clusters respectively, 35 fractures in the maximum cluster, 0 fracture that intersect the slice plane, and its percentage error is 100%. The ordinary 3–D fracture adaptive network model with preset control parameters has 3,933 interconnected fractures in 219 clusters, 62 fractures in the maximum cluster, 28 fractures that intersect the slice plane, and its percentage error is 36.0%. The enhanced 3–D fracture adaptive network model with control parameter tuning has 3,758 interconnected fractures in 211 clusters, 99 fractures in the maximum cluster, 39 fractures that intersect the slice plane, and its percentage error is 10.8%. While the number of total fractures was 8,442 in all three types of 3–D fracture network models, the enhanced 3–D fracture adaptive network model with control parameter tuning achieved 89.2% and 69.9% improvements over the ordinary 3–D fracture network model and the ordinary 3–D fracture adaptive network model separately. The ordinary 3–D fracture network model shows that only 0.4% of fractures at the measurement scale are probably involved in the groundwater flow system. However, the connectivity pattern of this model cannot be explained by in-situ hydraulic tests (packer test and pumping test), although its fracture statistics are similar to the field data. In the enhanced 3–D fracture adaptive network model whose fracture statistics and the structural properties both follow the observed statistics from natural fracture networks, the maximum fracture cluster has more fractures (282.9% increase in the number of fractures in the maximum cluster) than the ordinary 3–D fracture adaptive network model. Moreover, the results from the estimation of the aquifers' hydraulic properties (hydraulic conductivity and transmissibility) based on the connectivity pattern of the enhanced 3–D fracture adaptive network model can be interpreted by in-situ pumping test results and packer test results. Hence, the enhanced 3–D fracture adaptive network model generated by Fracture3D may help researchers have better

understanding, description, and prediction of the groundwater flow and transport processes in fractured-rock aquifer systems without relevant hydraulic test data.

4.5 Summary

We have described a unified framework which combines adaptive network models and adaptive control structures for modelling and simulation of fractured-rock aquifer systems. In this framework, an adaptive control structure with iterative parameter identification is used to identify an instance of a fracture adaptive network model with the desired topological characteristics, while the natural fracture network can be represented by fracture adaptive network models with "geometrical state–fracture cluster" coevolution. By using this modelling framework, an automatic modelling tool, Fracture3D, has been developed for automatically building the enhanced fracture adaptive network models, in which the fracture statistics and the structural properties can both follow the observed statistics from natural fracture networks. Through using simple field data and measurements taken on site or in-situ such as length, orientation, and density of measured fractures, the enhanced fracture adaptive network models can be built for rapidly evaluating the connectivity of the studied aquifers on a broad range of scales, especially in the early groundwater development state when data are very limited. Moreover, having such an automated 3–D fracture adaptive network modelling tool would greatly reduce the human effort and improve the 3–D fracture network model which might be affected by parameter uncertainty and varied geological and hydrological conditions.

For illustration purpose, a set of simulations and experiments have been conducted for verifying the validity of the proposed unified modelling framework and modelling tool Fracture3D. A set of the enhanced 3–D fracture adaptive network models with the desired topological characteristics have been have been built for the TMG fractured aquifer by using Fracture3D. We compared the topological characteristics of the 3–D instances to demonstrate how Fracture3D with a unified modelling framework can drive the 3–D fracture adaptive network models towards a desired state. Moreover, we also compared the 3–D fracture adaptive network models generated by our Fracure3D with control parameter tuning to ordinary 3–D

fracture network models generated by using fixed control parameters, and ordinary 3–D fracture adaptive network models generated by using preset control parameters. The simulations have clearly shown that our Fracture3D can drive the network topology towards a desired state by dynamically updating the geometrical states of fractures (size and profile of fractures) with a proper adaptive control structure.

The unified modelling framework and the automatic 3–D fracture adaptive network modelling tool can be used to conceptualize an order magnitude of the fracture connectivity of the fractured-rock aquifer of interest. It can also serve as crosscheck for other results obtained from conventional software and methods when fracture connectivity must be assessed within reasonable accuracy. Moreover, it provides a starting point for future research in this direction for TMG type of aquifer systems.

CHAPTER 5
Towards A Unified Framework for Modelling and Simulation of Social Network Systems

In this chapter, the unified framework which combines adaptive network models and adaptive control structures has been applied for modelling and simulation of social network systems. We start in Section 5.1 with brief introduction to the background of modelling and simulation of social network systems. In Section 5.2, we propose a unified framework which combines adaptive network models and multiple model adaptive control structures for modelling and simulation of social network systems. In this framework, a real-world social network system can be represented as an agent-based adaptive network which is defined by a feedback loop between the behavioural state of individuals and the community structure of the studied system, where a multiple model adaptive control structure is used for the predetermination of suitable computational models of behavioural state update and social interaction update in order to improve the performance of modelling and simulation. In Section 5.3, by using such a unified modelling framework, an automatic modelling tool, SMRI, is developed for automatically building enhanced social adaptive network models through using mobile-phone-centric multimodal data with suitable computational models of behavioural state update and social interaction update. In Section 5.4, a set of simulations and experiments on real-world mobile-phone-centric multimodal dataset are conducted in order to verify the validity of the proposed unified modelling framework and modelling tool SMRI.

5.1 Modelling and Simulation of Social Network Systems

Recent developments in sensing technologies have enabled us to examine the nature of human social behaviour in greater detail. Especially, the pervasiveness of mobile phones has made them ubiquitous social sensors of location, proximity and communications (Aharony et al., 2011a). Because of this, extremely detailed sensing and imaging of social network systems can be implemented through mobile-phone-

centric social and behavioural sensing system (Aharony et al., 2011a; Aharony et al., 2011b). Thus, mobile phone records have proven to be particularly valuable. The mobile-phone-centric datasets enable us to construct multiple network modalities of the studied social network system, such as the phone communication network, physical face-to-face encounters network, online social network, self-reported network, and more. Similar to Magnetic Resonance Imaging in the medical realm, social relationship imaging (Social MRI) has been used to sense and image the social systems based on various network modalities of the social network system (Aharony et al., 2011a; Aharony et al., 2011b). A few schemes have been developed for various social network analysis requirements according to different mobile-phone-centric datasets. For example, Gonzáles et al. showed that cellular-tower location information can be used to characterize human mobility and that humans follow simple reproducible mobility patterns (González et al., 2008). Eagle et al. found that the diversity of individuals' relationships is strongly correlated with the economic development of communities (Eagle et al., 2010). Eagle and Pentland (2006) defined the term "Reality Mining" to describe collection of sensor data pertaining to human social behaviour. They showed that using call records, cellular-tower IDs, and Bluetooth proximity logs, collected via mobile phones, the subjects' social network can be accurately detected, as well as regular patterns in daily activity (Eagle & Pentland, 2006; Eagle et al., 2009). This initial study was then expanded by Madan et al. (2010), who conducted a similar experiment and showed that mobile social sensing can be used for measuring and predicting the health status of individuals based on mobility and communication patterns. They also investigate the spread of political opinion within the community (Madan et al., 2011). Aharony et al. (2011a) developed a mobile-phone-centric social and behavioural sensing system that is deployed with 130 adult members of a young-family living community for over a year. A dataset with 25 phone-based signals is generated which includes location, accelerometry, Bluetooth-based device proximity, communication activities etc. Other examples for using mobile phones for social sensing are those by Montoliu and Gatica-Perez (2010) and Lu et al. (2010). However, there is currently no adaptive-network based unified framework for implementing the development, comparison, communication

and validation of social network models though using mobile-phone-centric data.

Adaptive networks have produced significant implications for studying real-world social network systems, as they can present more realistic dynamics of social network, while people change their social behaviours depending on epidemiological states of their neighbours (Funk et al., 2010). The effect of social responses to epidemics on social networks has been investigated in detail in a class of adaptive-network based epidemic models. As a pioneering model in this direction, the adaptive Susceptible-Infected-Susceptible model studied by Gross et al. (Gross et al., 2006) can provide detailed analytical insights into the emergence of system-level phenomena from the node-level coevolution by a so-called moment closure approximation. In order to investigate opinion formation and collective behaviour in social network systems, adaptive-network based models have been developed (Holme & Newman, 2006; Zanette & Gil, 2006). In these models, the diffusion of competing opinions occurs through a networked population, when agents modify their contacts depending on the opinions held by their neighbours (Sayama et al., 2013). Moreover, the fragmentation transition in opinion formation has also been investigated by using adaptive-network based model (Kozma & Barrat, 2008; Vazquez et al. 2008; Zimmermann et al. 2000), in which the social network breaks into distinct components of opposing agents. Besides opinion formation, different classes of social games have also been investigated on adaptive networks. For example, the work of Pacheco et al. (2006) and van Segbroeck et al. (2011) showed clearly that coevolution can lead to increased levels of cooperation, where agents aim to optimize some abstract payoff by building up beneficial structure. The work of Poncela et al. (2009) demonstrated that coevolutionary dynamics can also facilitate cooperation through the dynamics of growth itself. In other cases, adaptive-network based models have been proposed for studying social games, in which agents struggle for an advantageous position in the network (Bala & Goyal, 2001; Holme & Ghoshal, 2006; 2010). In addition, organizational dynamics on adaptive networks have also been investigated by Buskens and van de Rijt (2008), when social network evolution was described by actors striving for structural holes.

In some cases, these mathematical models above fall short of the complexity

of the studied real-world social network systems, and that hence no connection to real-world observations and experiments can be made. In this situation, agent-based adaptive network models can be applied, where mechanisms of the coevolution of social network topologies and individuals' behavioural states can be a lot more complex and detailed than other more abstract mathematical models (Sayama et al., 2013). In the work of Centola et al. (2007), for example, similar dynamics including the fragmentation transition have been found by using agent-based adaptive network models of more realistic cultural drift and dissemination processes. The interactions between the social network structures and the human behaviours have also been experimentally examined by Centola (2010; 2011) when voter-like models have been used to investigate the dynamics of decision making in the collective motion of swarms of locusts (Huepe et al., 2011) and schools of fish (Couzin et al., 2011). Agent-based models have also been used for computational modelling of complex organizational behaviour, including the evolution of organizational networks, information/knowledge/culture sharing and trust formation within a group or corporation (Sayama et al., 2013). For example, the work of Dionne et al. (2010) showed the nontrivial effects of team network topology and other parameters on the overall team performance after the team development process. In this work, an agent-based model of team development dynamics have been developed, in which agents exchange their knowledge through social ties and then update their self-confidence and trust to other team members dynamically. Moreover, the self-confidence (node state) and trust (link weight) were represented by a complex function defined over a continuous knowledge domain (modelling complex systems). Another example can be found in the work of Lin and Desouza (2010), which showed that knowledgeable individuals do not necessarily gain many connections in the network, and that when high knowledge diversity exists in the organization, the network tends to evolve into one with small characteristic path lengths. In this work, an agent-based computational model has been used for addressing organizational dynamics at a larger scale on the coevolution of informal organizational network and individual behaviour, where a node state includes behavioural patterns and knowledge an individual has, and the knowledge is transferred through informal social links that are changed adaptively

(Sayama et al., 2013).

Although an agent-based modelling and simulation approach can simulate very complicated state-topology coevelution processes in social network systems, agent-based models are often very intricate and the impact of any given modelling assumption or parameter is difficult to study. When applying adaptive network models to agent-based modelling and simulation of social network systems, it is necessary to specify how the states of nodes will be changed to generate new topologies of the network. Adaptive network models may have control parameters for node update and link update which greatly determine the quality of the generated network models. Choosing suitable parameter values is, frequently, a problem-dependent task and requires previous experience of the researchers (Maruo et al., 2005). In ordinary adaptive network models, these control parameters are not included as a part of the state-topology coevolution, because they are considered as external fixed parameters. In real-world applications, however, the control parameters of the social adaptive network models may vary greatly depending on different assumptions and conditions. In the present work, we used a multiple model adaptive control structure for modelling real-world social network system through using mobile-phone-centric behavioural data and adaptive-network based modelling approach, where the predetermination of suitable computational models is implemented for the state update of nodes and the weight update of links.

5.2 A Unified Framework for Modelling and Simulation of Social Network Systems with Mobile-Phone-Centric Data

Recent developments in sensing technologies have enabled us to examine the nature of human social behaviour in greater detail. However, the social network models may be rendered impractical due to these impractical assumptions and poor sample quality, and their accuracy suffers significantly from a lack of knowledge about real social network conditions or other useful information related to the assumptions. Moreover, mechanisms of the coevolution of community structures and individuals' behavioural states can be a lot more complex and detailed than other more abstract mathematical models, when computational models of adaptive net-

works are hybrids of dynamical networks and agent-based models. Such models subjected to abrupt and large parameter variations are generally very difficult to control.

Based on the unified modelling framework described in Chapter 3, a unified framework which combines adaptive network models and multiple model adaptive control structures has been developed in this work in order to achieve a desired topological property for the corresponding adaptive network models of social network systems. Through using mobile-phone-centric behavioural data, the studied social network system can be represented as an adaptive network which contains a feedback loop between the behavioural states of individuals and the community structures of the system. Moreover, a multiple model adaptive control structure has been used for the predetermination of suitable computational models of behavioural state update and social interaction update in order to improve the performance of modelling and simulation. The modelling framework then automatically identifies desired configurations of the adaptive network models based on a benchmark network model derived from collected self-report data. The generated enhanced social adaptive network models can promote better understanding of the inner workings of the studied social network system. Having such an automated modelling framework would greatly reduce the human effort and provide a valuable systematic modelling tool for understanding, description, prediction, and control of the real-world social network systems through using mobile-phone-centric behavioural data.

As depicted in Figure 5.1, a real-world social network system is considered as an agent-based adaptive network which are defined by a feedback loop between the behavioural state of individuals and the community structure of the studied system. Moreover, such a state-topology coevolution can self-organize towards non-trivial topologies. The input data are obtained from different measurements through using various mobile-phone-centric behavioural data such as call logs, Bluetooth proximity logs, cellular-tower transition logs, which quantify different behavioural states of people or various types of social interactions between people. We suppose that a set of computational models for behavioural state update and social interaction

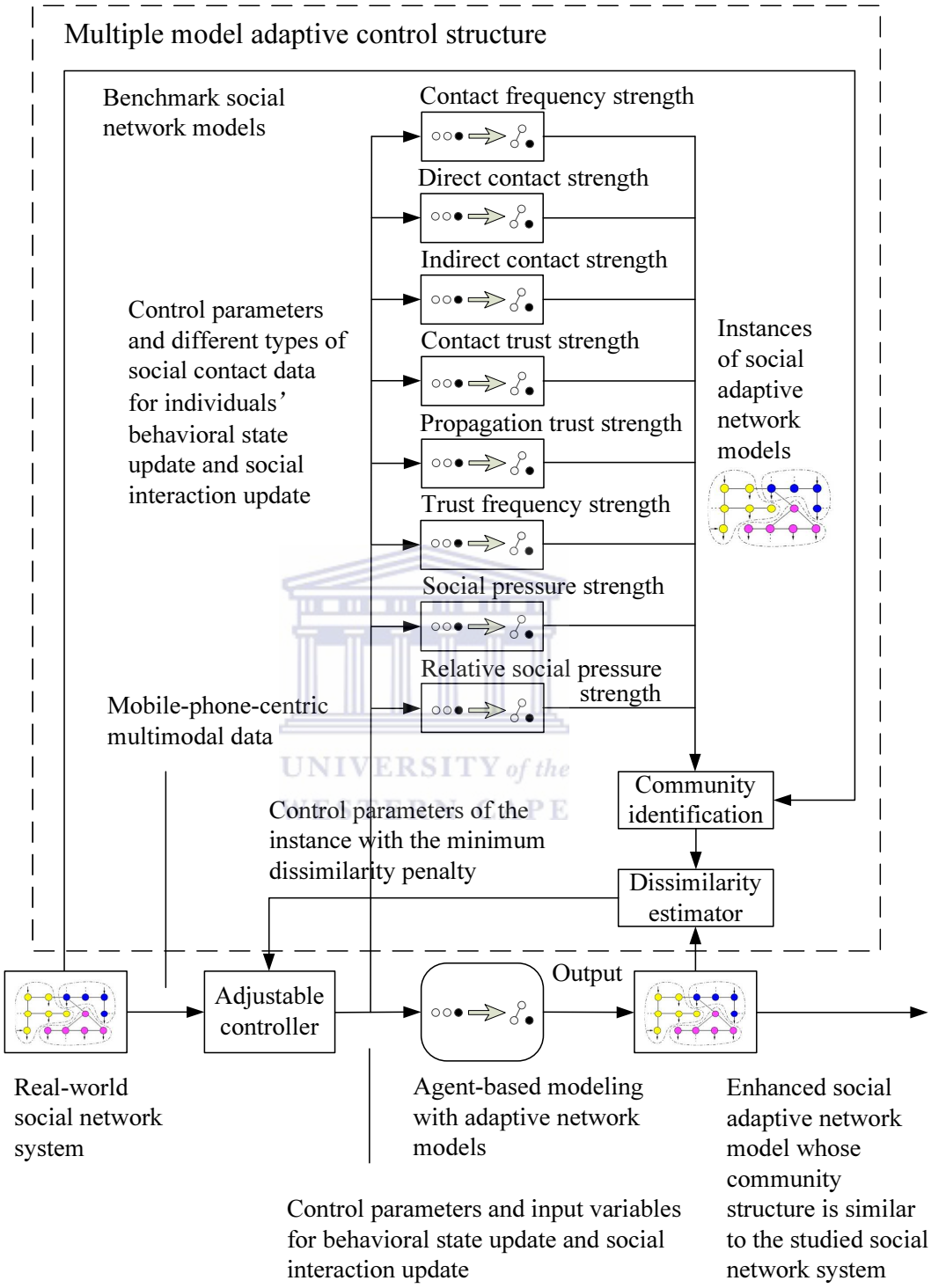

Figure 5.1: Block diagram of a unified framework which combines adaptive network models and adaptive control structures for modelling real-world social network systems with mobile-phone-centric multimodal data.

update is a priori known. By using the current control parameters and the current input data, a set of instances of an adaptive network model are generated based on various computational models. In the model estimator, the dissimilarity between the discovered communities of a generated instances and the discovered communities of benchmark network model built by using self-report data is measured. A performance index is established according to the dissimilarity measurements of the generated instances. The corresponding control parameters of the instance whose dissimilarity score is the minimum are fed into the controller, and the corresponding computational model of the instance is applied to the process of agent-based modelling and simulation. The behavioural states of individuals and social interactions among them are then updated with a suitable computational model in order to generate an enhanced social adaptive network model whose community structure is similar to the studied social network system. By using such a multiple model adaptive control structure, the adaptive-network based framework can be used for modelling and simulation of the studied social network system with suitable computational models of behavioural state update and social interaction update.

5.3 SMRI, An Automatic Social Network Modelling Tool by Using Mobile-phone-centric Multimodal Data

Through using the mobile-phone-centric multimodal data and the unified framework which combines adaptive network models and multiple model adaptive control structures, an automatic modelling tool, SMRI, is developed for automatically building the enhanced social adaptive network models whose community structures are similar to the real-world social network systems. Moreover, a multiple model adaptive control structure is used for the predetermination of suitable computational models of behavioural state update and social interaction update in order to achieve a desired topological property for the social adaptive network models. The model of SMRI is shown in Figure 5.2. A mobile-phone-centric multimodal dataset which contains call logs, Bluetooth proximity logs and cellular-tower transition logs is used for modelling of social network systems with adaptive network models, when

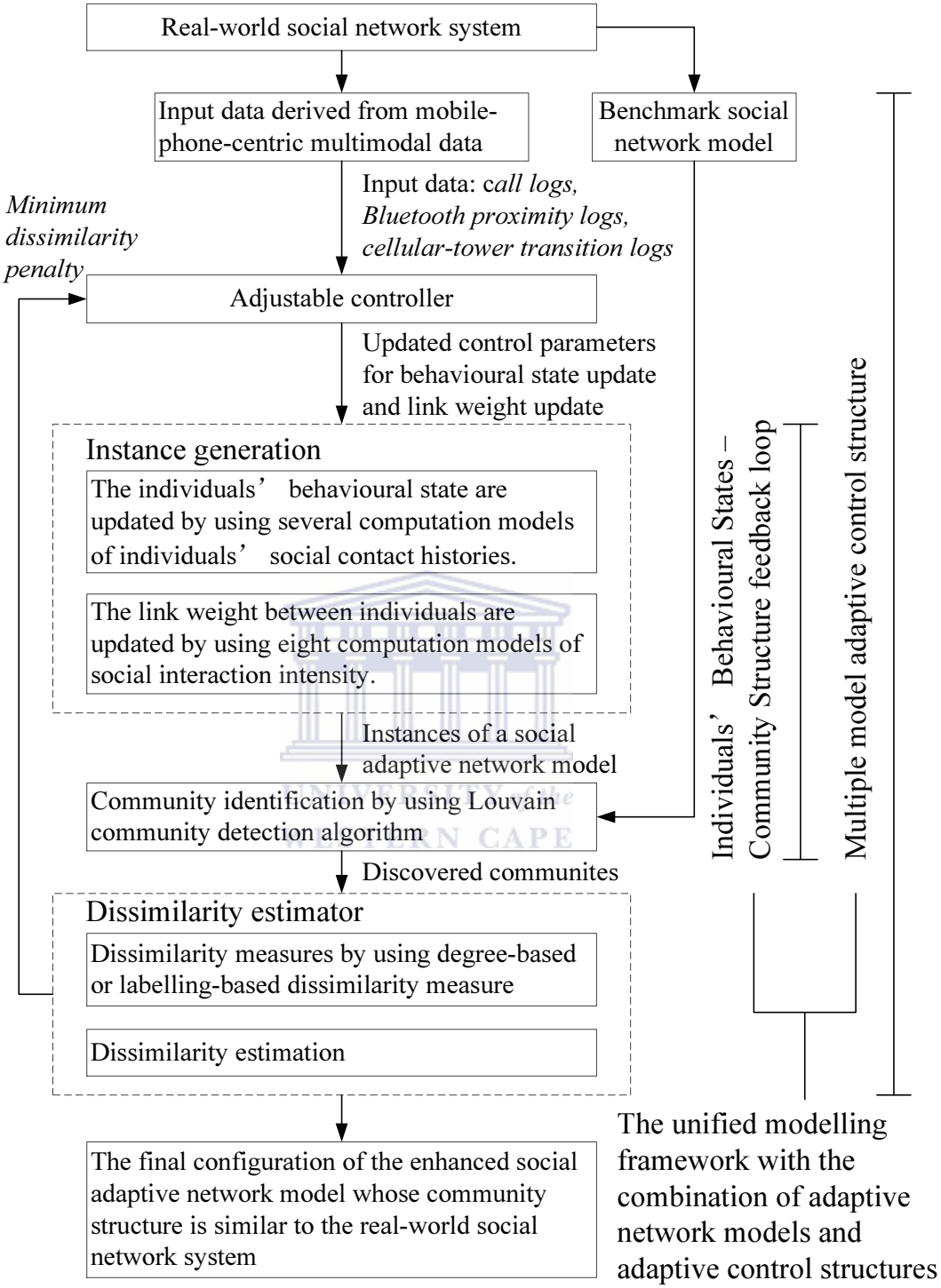

Figure 5.2: Model of SMRI. Through using the mobile-phone-centric multimodal data and the unified framework which combines adaptive network models and multiple model adaptive control structures, a set of enhanced social adaptive network models are automatically built, in which the community structures are similar to the real-world social network systems.

individuals' behavioural states are extracted from these data. In the process of agent-based modelling, individuals' behavioural states are updated by using several computation models of indivduals' social contract histories through using the current control parameters and certain sampled data, while the link weight between the individuals update by using eight computation models of social interaction intensity. A set of instances of a social adaptive network model are then generated by using various computation models of behavioural state update and link weight update. The Louvain community detection algorithm (Blondel et al., 2008) is used for community identification of the generated instances and the benchmark social network model built by using self-report data. In the dissimilarity estimator, the discovered communities are used for the measurement of dissimilarity penalty between the generated instances and the benchmark network model by using degree-based network model dissimilarity measure or labelling-based network model dissimilarity measure. The corresponding control parameters and computation models of the instance whose dissimilarity penalty is the minimum are then used for generating the final configuration of the enhanced social adaptive network model with desired topological characteristics. In the following, several key algorithms of this modelling framework will be introduced, including behavioural states update, link weight update, community identification, and dissimilarity estimation.

5.3.1 Behavioural State Update

In the past few years, mobile-phone-centric behavioural data such as call log data, GPS-based location data, and mobile-sensing based detailed proximity data have been used for agent-based social network modelling. In the present work, we assume that a social action occurs when a direct/indirect contact is recorded by using different mobile sensing techniques. Thus, a mobile-phone-centric multimodal dataset which contains call logs, Bluetooth proximity logs and cellular-tower transition logs can be used for modelling of social network systems with adaptive network models (Table 5.1), when individuals' behavioural states are extracted from these data. Such a behavioural state can be represented by a vector which contains a set of social contacts with four tuples: $\langle contactID, timestamp, duration, direction \rangle$. The

behavioural states of individuals are updated with modified vectors depending on the current control parameters and certain sampled data. Three types of contact histories including voice-call based contacts, detailed-proximity based contacts, and coarse-proximity based contacts are generated according to various mobile-phone-centric behavioural data (Table 5.2). Moreover, in order to capture the impact of temporal changes of social relations, the periodic contact histories can also be generated according to four time periods in a day, 00:00–08:00, 08:00–16:00, 16:00–24:00, and 00:00–24:00 (the union of the other three periods for a comparative analysis).

Mobile-phone-centric data	*Individual's ID*	*Contract ID*	*Timestamp*	*Duration*	*Direction*	*Area ID*
Call logs	Calling party ID	Called party ID	Timestamp	Duration	Incoming /outgoing	
Bluetooth proximity logs	Scanner ID	Neighbor ID	Timestamp	Duration		
cellular-tower transition logs	Mobile phone ID		Timestamp	Duration		Cellular tower ID

Table 5.1: Formats of mobile-phone-centric multimodal data.

Individual's social contact histories	*Contract ID*	*Timestamp*	*Duration*	*Direction*
Voice-call based contacts	Called party ID	Timestamp	Duration	Incoming/outgoing
Detailed-proximity based contacts	Neighbor ID	Timestamp	Duration	Scanner ID, Neighbor ID, Area ID, Timestamp
Coarse-proximity based contacts	Mobile phone ID, Area ID, Timestamp	Timestamp	Duration	Area ID, Timestamp

Table 5.2: Formats of various social contact data. Various individual's social contact histories are generated by using mobile-phone-centric multimodal data.

5.3.1.1 Voice-Call Based Contact Data

The ordinary call detail records (CDR) can be specified by a set of communication 5-tuples: $\langle callingpartyID, calledpartyID, Timestamp, Duration, Direction\rangle$. The voice-call based contacts are directly generated from CDR data. However, in some cases, the called party ID of each record may not be available due to technical difficulties or privacy concerns. In this work, the called party ID is identified through comparing the timestamps of all voice call events. We sorted all voice call events over all individuals by timestamp, and match the incoming/outgoing calls occurring within a small time window ($\triangle t$).

5.3.1.2 Detailed-Proximity Based Contact Data

The detailed-proximity based contact data can be built according to Bluetooth proximity logs and cellular-tower transition logs. Bluetooth proximity logs can provide encounter information of people. However, the movement direction of people can not be measured directly in an encounter event without accurate position information. In this work, the coarse location information (Area ID) derived from cellular-tower transition logs was used for measuring the movement direction of people. The movement status of a mobile phone is labelled as "static" for each record in Bluetooth proximity logs if the mobile phone is still in the range of the same cellular tower for a specific time period (five minutes); otherwise "active" is labelled. The records of Bluetooth proximity logs can then be labelled with "incoming/outgoing" when the movement status labels of scanner ID and neighbour ID are different. Furthermore, we assume that a social action occurs when a Bluetooth scan record is labelled with "incoming/outgoing". Thus, a set of detailed-proximity based contacts can be established based on Bluetooth proximity logs and cellular-tower transition logs.

5.3.1.3 Coarse-Proximity Based Contact Data

In this work, we assume that a social contact happens when two persons who know each other are in the same area. Thus, a set of coarse-proximity based contacts can be created according to cellular-tower transition logs. Although movement direction of people can not be directly obtained from cellular-tower transition logs,

the movement direction may be detected by using coarse location information (Area ID) derived from cellular-tower transition logs. Through comparing Timestamp and Area ID of each record in cellular-tower transition logs, the coarse-proximity based contacts are labelled with "incoming/outgoing" by detecting who enters this area earlier.

5.3.2 Link Weight Update

Social contact happens when one person communicates with another person. In Hossmann et al.'s work (Hossmann et al., 2011), they represented the complex resulting pattern of who meets whom, how often and for how long, in a compact and tractable way. We borrow their idea for measuring social contact strength based on mobile-phone-centric data. This allows us to quantify structural properties beyond pairwise statistics such as inter-contact and contact time distributions. We aggregate the entire sequence of social contacts of all individuals to a weighted instance of a social adaptive network model. In this instance, the weight of a link represents the strength of the relationship between two persons. A key question is how to derive the tie strength between two persons, i.e., what metric to use for computing the weight of a link in a social network model, based on the observed social interactions. This weight should represent the amount of social interactions between two persons. Various metrics, such as the age of last contact (Dubois-Ferriere et al., 2003), contact frequency (Hui et al., 2011), or aggregate contact duration (Hui et al., 2011) have been used as tie strength indicators in delay-tolerant-networking routing. In this work, we suppose that a set of computational models for measuring the intensity of social interactions is a priori known. By using the current control parameters and the current behavioural states of individuals, an instances of the social adaptive network model can be generated in a time step based on a certain computational model of social interaction intensity. A brief introduction of the computational models will be given subsequently:

5.3.2.1 Contact Frequency Strength

Traditionally, contact frequency strength (CFS) has been considered as an important metric for modelling real-world social networks. Frequent contacts may

imply many meetings and hence many information forwarding opportunities (short delays). In this work, we mapped this feature to a scalar weight according to current behavioural states of individuals. Each pair of individuals i, j is assigned to a feature vector w_{ij}^{CFS}, which is the number of social contacts between individuals i and j.

5.3.2.2 Direct Contact Strength

Similar to (Hossmann et al., 2011), we consider both contact frequency and contact duration, when direct contact strength (DCS) is computed. They capture different aspects, both of which are important for modelling social networks. Frequent contacts imply many meetings and hence many information forwarding opportunities (short delays) and long contacts imply meetings where a large amount of information can be transferred (high throughput). Since most community detection algorithms require one dimensional tie strengths, we map these two features to a scalar weight. We first assign each pair of individuals i, j a two-dimensional feature vector, $z_{ij} = (\frac{f_{ij}-\overline{f}}{\sigma_f}, \frac{t_{ij}-\overline{t}}{\sigma_t})$, where f_{ij} is the number of contacts in the log between individuals i and j, and t_{ij} is the sum of the durations of all contacts between the two individuals. $\overline{f}$ and $\overline{t}$ are the respective empirical means, and σ_f and σ_t, the empirical standard deviations. We normalize the values by their standard deviations to make the scales of the two metrics comparable. We then transform the two-dimensional feature vector to a scalar feature value, using the principal component, i.e., the direction in which the feature vectors of all node pairs $Z = \{z_{ij}\}$, $i, j \in N$ has the largest variance. This is the direction of the eigenvector v_1 (with the largest corresponding eigenvalue) of the 2×2 covariance matrix of frequency and duration. We then define the tie strength between i and j as the projection of z_{ij} on the principal component $w_{ij}^{DCS} = v_1^T z_{ij} + w_0$, where we add $w_0 = v_1^T(-\frac{\overline{f}}{\sigma_f}, -\frac{\overline{t}}{\sigma_t})$ (the projection of the feature value for a pair without contacts) in order to have positive tie strengths. The obtained weight is a generic metric that combines the frequency and duration in a scalar value and captures the heterogeneity of node pairs with respect to frequency and duration of various social contacts (Hossmann et al., 2011).

5.3.2.3 Indirect Contact Strength

By applying an information theoretic method to the conversation event log, Takaguchi et al. (2011) found that sequences of conversation events have deterministic components. Long contacts may imply meetings where a large amount of information can be transferred. We thus assume that individual l has an indirect contact with individual j, when individual i contacts with individual l after contacting with individual j. Thus, indirect contact strength (ICS) of a pair of individuals (w_{ij}^{ICS}) can be measured, which is the number of indirect contacts between individuals i and j.

5.3.2.4 Contact Trust Strength

Behavioural trust in social networks has been studied by Adali et al. in (Adali et al., 2010; Adali et al., 2012). Based on the sender-receiver-time data derived from the communication stream of a social network, trusting relationships among people can be captured and quantified, when text analysis is in general expensive and fairly sophisticated tools are needed (see Figure 5.3). Suppose we are working on a set of social contacts $\mathcal{C} = \{C_1, C_2, \ldots, C_l\}$ between individuals A and B; contract trust strength (CTS) can be measured as follows: $w_{ij}^{CTS} = l \cdot H(C)$, where l is the number of the social contacts, and $H(C)$ is a measure of the balance in the set of contacts. We use the entropy function to measure balance: $H(C) = -p \log p - (1-p) \log(1-p)$, where $p(C)$ is the fraction of contacts in the set of contacts C that were sent by individual A.

5.3.2.5 Propagation Trust Strength

A measure of propagation trust has been developed based on the propagation of information in (Adali et al., 2010; Adali et al., 2012). In the present work, a similar measure was implemented through using various social contact histories. We assume that indirect trust is established and information is propagated, when individual A makes a contact with individual B, and B makes another contact with some third person X within some time interval δ. Thus, the valid propagations can

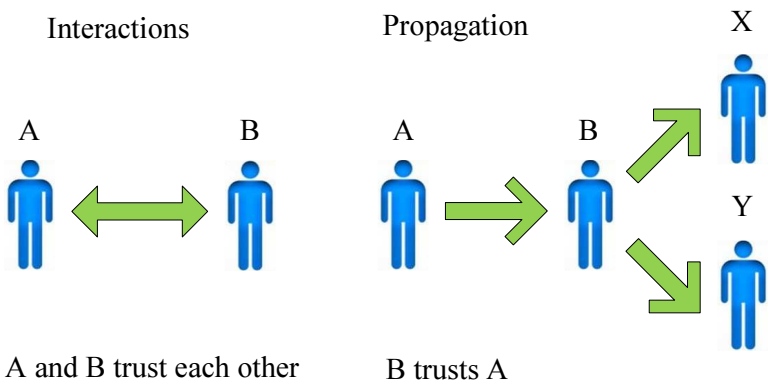

Figure 5.3: Two social behaviours as an expression of trust: interaction and propagation. Specifically, if two persons have interactions, then they are more likely to trust each other. If one person propagates information from another then it suggests that the propagator trusts the information. Figure adapted from (Adali et al., 2010).

be identified based on behavioural states of individuals. Given the valid propagations of individuals i and j, the propagation trust strength (PTS) can be computed as follows: $w_{ij}^{PTS} = prop_{ij}/prop_j + prop_{ji}/prop_i$, where $prop_j$ is the number of propagations by j; $prop_{ij}$ is the number of contacts in which i makes contacts with j, and a propagation then happens; $prop_i$ is the number of propagations by i; $prop_{ji}$ is the number of contacts in which j makes contacts with i, and a propagation then happens.

5.3.2.6 Trust Frequency Strength

Given the valid propagations of individuals i and j, the trust frequency strength (TFS) can also be computed as follows: $w_{ij}^{TFS} = prop_{ij} + prop_{ji}$, where $prop_{ij}$ is the number of contacts in which i makes contacts with j, and a propagation then happens; $prop_{ji}$ is the number of contacts in which j makes contacts with i, and a propagation then happens.

5.3.2.7 Social Pressure Strength

Social pressure metric (SPM)(Bulut & Szymanski, 2012) has been used for studying friendship relations in mobile social networks, which can detect the quality of friendships between individuals by using mobile-phone-centric data. In this work,

given a set of social contacts derived from behavioural states of individuals, social pressure strength of a pair of individuals i and j can be computed as follows

$$SPM_{i,j} = \frac{\int_{t=0}^{T} f(t)dt}{T} \quad and \quad w_{i,j}^{SPS} = \frac{1}{SPM_{i,j}} \tag{5.1}$$

where $f(t)$ represents the time remaining to the next contact of the two individuals i and j at time t. As depicted in Figure 5.4, if at time t, the individuals are in contact, then $f(t) = 0$, otherwise, $f(t) = t_{next} - t$, where t_{next} is the time of the next contact between individuals i and j. Hence, each inter-meeting time t_{inter} contributes the term $t_{inter}^2/(2T)$ to SPM. If there are n contacts in the time period T, then $SPM_{i,j} = (\sum_{x=1}^{n} t_{inter,x}^2)/(2T)$ and $w_{ij}^{SPS} = (2T)/(\sum_{x=1}^{n} t_{inter,x}^2)$.

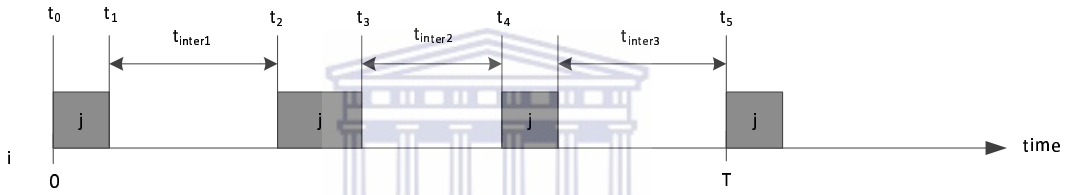

Figure 5.4: Social contacts between individuals i and j in $[0, T]$ for social pressure strength measure. Adapted from (Bulut & Szymanski, 2012).

5.3.2.8 Relative Social Pressure Strength

In order to find indirect friendships between individuals according to their social contact histories, relative social pressure metric (RSPM) (Bulut & Szymanski, 2012) is also measured. Each indirect information passing consists of two stages (see Figure 5.5). The first one starts at the last contact of individual i with individual j and ends at the time individual i's next call with individual j. Here, if there are several subsequent contacts with j before any contact between j and k, then the last one is considered. We denote duration of this stage as $t_{a,x}$, where x denotes the number of indirect information passing occurring. During this stage, individual i transfers messages to individual j. The second stage starts when the first one ends and it finishes when individual j meets individual k. The duration of this session

is denoted $t_{b,x}$. During this stage, the messages accumulated at j merely wait for the contact with the destination (without accumulating further at individual j). Denoting the number of such sessions as n, $RSPM_{i,k|j}$ is computed as:

$$RSPM_{i,k|j} = \left(\sum_{x=1}^{n} \int_{0}^{t_{a,x}} (t_{b,x} + t_{a,x} - t)dt \right) /T \tag{5.2}$$

$$= \frac{\sum_{x=1}^{n} (2t_{b,x}t_{a,x} + t_{a,x}^2)}{2T}. \tag{5.3}$$

We then have $w_{ik}^{RSPM} = 1/RSPM_{ik}$, where $RSPM_{ik}$ is sum of all $RSPM_{i,k}$ with different intermediaries.

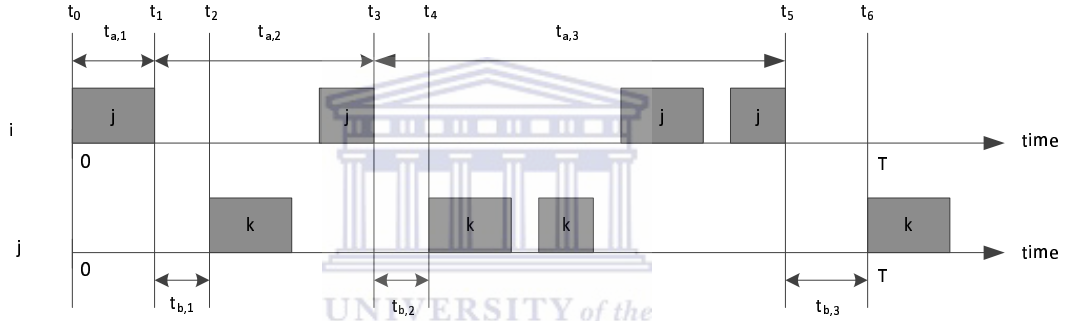

Figure 5.5: Social contacts between individuals i and j and between individuals j and k in the same time interval $[0, T]$ for relative social pressure strength measure. Adapted from (Bulut & Szymanski, 2012).

5.3.2.9 Feature-Fused Social Contact Strength

In real-world social network systems, there exists various types of social interactions, such as voice calling, face-to-face oral communication, text messaging, email, etc. Various features of social interactions among people can be extracted based on different measurements and sampled data. For example, social mechanisms of real-world social network systems have been investigated by Aharony et al. (2011a; 2011b). In their works, a set of social activity features were captured

through using mobile-sensing based social fMRI technique and mobile-phone-centric multimodal datasets. A set of social network models can then be built respectively according to the features derived from different types of mobile sensing data. However, some social interaction information is typically lost in such social network models since it is rarely possible to represent the features of all types of social interactions at once. In order to lose as little as possible interaction information for modelling real-world social network systems, information-based feature enhancement is performed by using voice-call based contact data, detailed-proximity based contact data, and the features of social interaction introduced above.

In this work, we suppose that social interaction information can be measured based on the quantity of the social contacts. The higher frequency of social contacts contains more social interaction information. The information content can be expressed by the equation: $I(f) = \log(f)$, where f is the frequency of the social contacts. Through the log function the information $I(f)$ is higher for a type social contact with a higher frequency. The feature fusion can then be implemented in a way to weight voice-call based contacts and detailed-proximity based contacts. To formalize this weighting we introduce the equation: $\gamma(\dot{f}, \ddot{f}) = \frac{I(\ddot{f})}{I(\dot{f})+I(\ddot{f})}$, where $\dot{f}$ is the number of all voice-call based contacts, and $\ddot{f}$ is the number of all voice-call based contacts. If the value of γ is 0.5, both types of social contacts contain the same amount of social interaction information.

Given a pair of values $\dot{w}_{ij}^{CFS}$ and $\ddot{w}_{ij}^{CFS}$ which are contact frequency strength of individual i and j derived from voice-call based contact data and detailed-proximity based contact data respectively, the fusion of two values can be implemented by the following equation: $w_{ij}^{fCFS} = (1-\gamma) * \dot{w}_{ij}^{CFS} + \gamma * \ddot{w}_{ij}^{CFS}$. Thus, feature-fused contact strength can be generated for each type of the various social interaction features.

5.3.3 Community Identification

In real-world social network systems, people naturally tend to form groups within their work environment, family, and friends (Fortunato, 2010). Such subgroups are called social communities whose members are all "friends" to each other (Luce & Perry, 1949). Communities are typical for the structure of social networks,

which contain a set of individuals with stronger social connections between them than towards other individuals. The existence of strong communities in the contact based social network models may imply high potential for human cooperation and community-based trust mechanisms (Hossmann et al., 2011). Since community structure is one of the most relevant features of network models representing real-world complex systems, a few community detection algorithms have been developed by a large interdisciplinary community of scientists (Fortunato, 2010). A thorough introduction of community detection in network models has been given by Fortunato (2010).

In the present work, the widely used Louvain community detection algorithm (Blondel et al., 2008) has been used for community identification according to various instances of social adaptive network models and the social network model built by using self-report data. The Louvain community detection algorithm is a modularity-based method with greedy optimization technique for the general case of weighted network models. This algorithm has two steps that are repeated iteratively. In the first step, every node is assigned to the local community that yields the largest modularity increase. The second step consists of a successive transformation of the communities into nodes of a smaller communities (Fortunato, 2010). According to a comparative analysis of community detection methods carried out by Lancichinetti and Fortunato (2009), the Louvain algorithm has good performance, and can be deployed to large systems.

5.3.4 Dissimilarity Estimation

In the dissimilarity estimator, the discovered communities are used for the measurement of dissimilarity penalty between the generated instances and the benchmark network model by using degree-based network model dissimilarity measure or labelling-based network model dissimilarity measure. The corresponding control parameters and computation models of the instance whose dissimilarity penalty is the minimum are then used for generating the final configuration of the enhanced social adaptive network model with desired topological characteristics.

In order to check the performance of a community detection algorithm, several

measures for comparing community structure have been developed. As discussed in (Traud et al., 2011), these methods can be classified roughly into three categories: measures based on *pair counting*, *cluster matching* and *information theory*. Pair-counting methods (Rand, 1971; Fowlkes & Mallows, 1983; Wallace, 1983; Mirkin, 1996; Meilă, 2007; Traud et al., 2011) depend on the number of pairs of nodes which fall in the same or in different groups in the two partitions, when similarity measures based on cluster matching (Meilă & Heckerman, 2001; van Dongen, 2000) try to find the largest overlaps between pairs of clusters of different partitions (Fortunato, 2010). In addition, similarity measures with information-theoretic techniques (Stanley, 1997; Gusfield, 2002; Mackay, 2003; Donon et al., 2005; Gustafsson et al., 2006; Zhang et al., 2006; Fan et al., 2007; Meilă, 2007; Palla et al., 2007; Karrer et al., 2008; Lancichinetti et al., 2009) have also been developed based on the assumption that very little information is needed to infer one partition given the other if they are similar (Fortunato, 2010). In this work, however, we focus on pair-counting methods due to their convenient algebraic description and computational simplicity. To estimate the performance of computational models of social interaction strength, two dissimilarity-comparing measures based on pair counting have been developed in this work: degree-based measure and labelling-based measure. The implementation details of these two measures are presented in the following subsections.

5.3.4.1 Data for Similarity-Comparing Measures

A set $\mathcal{C} \equiv \{c_1, c_2, \ldots, c_C\}$ of communities can be generated through using Louvain community detection algorithm and an instance generated by a ceratin social interaction strength measure. Each community C_i is formed by a set $\mathcal{C}^* \equiv \{v_1, v_2, \ldots, v_{C^*}\}$ of nodes and a set $\mathcal{F}^* \equiv \{f_1, f_2, \ldots, f_{F^*}\}$ of links $e_s = \{v_i, v_j\}$. We can also get a set $\mathcal{K}^C \equiv \{k_1^C, k_2^C, \ldots, k_K^C\}$ of number of nodes in each community.

By using the Louvain community detection algorithm and a benchmark network model built by using self-report data, a set $\mathcal{T} \equiv \{t_1, t_2, \ldots, t_T\}$ of communities can be generated. Each community T_i forms by a set $\mathcal{T}^* \equiv \{u_1, u_2, \ldots, u_{T^*}\}$ of nodes and a set $\mathcal{E}^* \equiv \{e_1, e_2, \ldots, e_{E^*}\}$ of links $e_r = \{u_i, u_j\}$ that connect the nodes. A set $\mathcal{K}^T \equiv \{k_1^T, k_2^T, \ldots, k_K^T\}$ of the number of nodes in each community can be also

obtained.

5.3.4.2 Degree-Based Dissimilarity Measure

The degree-based method is a measure of dissimilarity between the discovered communities of generated instances ("discovered" communities) and the discovered communities of benchmark network model built by using self-report data ("true" communities). The dissimilarity penalty to an instance which contains a set of "discovered" communities P is composed of two parts, *split penalty* P_s for breaking links in "true" communities, and *merge penalty* P_m for imposing non-existent links in "true" communities. If an instance has the same community structure with the benchmark network model (same number of communities with same members), the penalty is $P_s = 0$. If any node in a benchmark network model can not be found in an instance, the penalty is the maximum possible number of links in the benchmark network model: $P_s = u_T(u_T - 1)$, where u_T is number of nodes in a "true" community. If u_T nodes in a certain "true" community are split into c "discovered" communities with v_i nodes in the i-th "discovered" community, thus $u_T = \sum_{i=1}^{c} v_i$, the *split penalty* of the "true" community is $P_s^T = \sum_{i=1}^{c} v_i(u_T - v_i)$. The *split penalty* of an instance which contains t "true" communities can then be calculated as: $P_s = \sum_{h=1}^{t} P_s^h$.

If v_C nodes in a "discovered" community are split into t "true" communities with k_j nodes in the j-th "true" community, so that $v_C = \sum_{j=1}^{t} k_j$, the *merge penalty* of the "discovered" community is $P_m^C = \sum_{j=1}^{t} k_j \cdot \sum_{i \neq j}^{t} k_i/2 = \sum_{j=1}^{t} k_j(n_c - k_j)/2$. The *merge penalty* of an instance which contains c "discovered" communities can then be calculated as: $P_m = \sum_{h=1}^{c} P_m^h$. The *total penalty* to an instance is $P = P_s + P_m$.

5.3.4.3 Labelling-Based Dissimilarity Measure

In this work, the dissimilarity between the generated instances and the benchmark network model can also be measured by a labelling-based method. The dissimilarity penalty to an instance which contains a set of "discovered" communities P is composed of two parts as well, *split penalty* P_s for splitting links in "true" communities, and *merge penalty* P_m for merging two disjoint "true" communities

within one "discovered" community. A set of labels $\mathcal{L}^C \equiv \{l_1^C, l_2^C, \ldots, l_n^C\}$ which are community ID of the nodes can be generated through using the Louvain community detection algorithm and an instance built by a ceratin social interaction strength measure. We can also obtain a set of labels $\mathcal{L}^T \equiv \{l_1^T, l_2^T, \ldots, l_n^T\}$ from a benchmark network model with the same nodes, when different community IDs are assigned to each node. The *split penalty* P_s can then be computed by using a labelling-based algorithm (see Algorithm 5.1).

Algorithm 5.1: Calculation of *Split Penalty* (*Ps*) for labeling-based measure

n: number of nodes in a benchmark network model

l_j^C: community ID of node *j* derived from an instance with a social interaction strength

l_i^C: community ID of node *i* derived from an instance with a social interaction strength

l_j^T: community ID of node *j* derived from a benchmark network model

for *i = 1* to *n*
 for *j = 1* to *n*
  if $l_j^C <> l_i^C$ *and* $l_j^C <> l_j^T$ *and* $l_j^C <> 0$ **then**
   P_s++
  end if
 next *j*

If the nodes in a certain "discovered" community come from t "true" communities, the *merge penalty* of the "discovered" community is $P_m = t(t-1)/2$. The *merge penalty* of an instance which contains c "discovered" communities can then be calculated as: $P_m = \sum_{h=1}^{c} P_m^h$. Thus, the *total penalty* to an instance is $P = P_s + P_m$.

5.4 Experiments on Mobile-phone-centric Multimodal Dataset

In order to verify the validity of the proposed unified modelling framework and automatic modelling tool SMRI, we have applied it on a real-world social network

system. In this work, the studied real-world social network system is considered as an agent-based adaptive network which are defined by a feedback loop between the behavioural state of individuals and the community structure of the studied system, when mobile phones are used as in-situ social sensors to map social interactions and social relations of users. Two experiments have been implemented through using MIT Reality Mining multimodal dataset and our automatic modelling tool SMRI, namely modelling of social network system based on periodic social contact data and modelling of social network system based on fused data and fused features. Through using SMRI, a set of enhanced social adaptive network models whose community structure is similar to the studied social network system were automatically built based on various mobile-phone-centric social contact data and computational models of social interaction strength. In the first experiment, the generated social adaptive network models helped us evaluate the performance of social adaptive network modelling with the temporal changes of individuals' social interactions. In the second experiment, the performances of the proposed data and feature enhancement methods were evaluated based on the generated social adaptive network models. Moreover, the performance of the computational models for modelling and simulation of real-world social network systems, such as mobile-sensing based social contact data generation, periodic social contact data generation, social interaction strength measure, network dissimilarity measures, were also evaluated based on these enhanced social adaptive network models.

5.4.1 Mobile-Phone-Centric Multimodal Dataset

Traditionally, the study of social network systems has been an arduous process, involving extensive surveys, interviews, ethnographic studies, or analysis of online behaviour. However, more insights about the dynamics of both individual and group behaviour can be obtained through using the unprecedented amount of information, such as continuous proximity, location, communication and activity data, generated by pervasive mobile phones, which are used as in-situ social sensors to map social interactions and social relations of users. The MIT Reality Mining project (Eagle & Pentland, 2006; Eagle et al., 2009) was conducted from 2004–2005 at the MIT Media

Laboratory for the study of human social behaviour with mobile sensing techniques. There are 83 participants who are either students or faculty at MIT. Through using a custom logging software and various mobile sensing techniques, a mobile-phone-centric multimodal dataset, MIT Reality Mining dataset (Eagle & Pentland, 2006; Eagle et al., 2009), has been generated which includes call logs, Bluetooth proximity logs and cellular-tower transition logs (Eagle, 2005).

5.4.2 Self-Report Data

In the MIT Reality Mining project (Eagle & Pentland, 2006; Eagle et al., 2009), self-report relational data which contains their friendship with others were also collected from each user. The relationship between two users is labelled as "1" if they are friends. A benchmark network model which contains 52 nodes and 57 links was generated based on these self-report data.

5.4.3 Modelling with Periodic Social Contact Data

Considering the fact that main activities of people are periodic in a social network system, mobile-phone based social interactions often change periodically with time. Normally, the social interactions among people happen in some specific periods of the day. If two persons were frequently in contact in a particular time period, then they are likely to make next contact in the same time period. For example, in MIT Reality dataset, human subject 28 meets with subject 38 usually between $9am$ to $7pm$ while subject 28 meets with subject 48 usually between $1pm$ to $7pm$ (Bulut & Szymanski, 2012). Similar behaviour is also seen in the Haggle dataset (Haggle, 2006–2010). Temporal correlation of social interactions has been used for making routing decisions in delay tolerant networks (Bulut & Szymanski, 2012; Bulut et al., 2014). However, there is no analysis and explicit usage of periodic mobile-sensing data for modelling real-world social network systems with adaptive network models.

In order to capture the impact of temporal changes of social interactions among people on the performance of network models, a set of enhanced social adaptive network models have been automatically generated by using SMRI according to various periodic social contact data and different social interaction strength measures. The

temporal correlation between the behaviour dynamics of individuals and the structure of social networks can then be analyzed based on the generated social adaptive network models.

5.4.3.1 Input Data

By using the MIT Reality Mining multiple model dataset, three types of social contact histories were generated, including voice-call based contacts, detailed-proximity based contacts, and coarse-proximity based contacts. Because of privacy concerns, the called party ID in each voice call record is not available in the MIT Reality Mining dataset. However, we sorted all voice call records over all individuals by their timestamp, and matched the incoming/outgoing calls occurring within a small time window $\triangle t$. In this work, 11,899 voice-call contacts were generated, when $\triangle t$ is setup as $120.96s$. We also generated 172,568 detailed-proximity based contacts by using the Bluetooth proximity logs and the cellular-tower transition logs, and 231,074 coarse-proximity based contacts through using the cellular-tower transition logs. Four periodic social contact data can then be generated for each type of social contacts, including the contacts in period (00:00–24:00), the contacts in period (00:00–08:00), the contacts in period (08:00–16:00), and the contacts in period (16:00-24:00). Thus, twelve periodic social contact data were used as input data in this experiment.

5.4.3.2 Modelling with SMRI

By using SMRI, a set of enhanced social adaptive network models were automatically generated based on various periodic social contact data. The behavioural state of each node is updated with a certain periodic contact history which is extracted from current input data. In each time step, the weights of links are updated based on one of eight measures of social interaction strength. Thus, eight instances of the social adaptive network model are generated for each periodic social contact data. In the dissimilarity estimator, the dissimilarity between the discovered communities of the generated instances and the discovered communities of benchmark network model built by using self-report data is measured. The corresponding control parameters of the instance whose dissimilarity penalty is the minimum are fed

into the controller, and the corresponding computational model of the instance are applied to the generation of the final configuration of the enhanced social adaptive network model of the studied real-world social network system.

5.4.3.3 Simulation Results

Through using 12 periodic social contact data and SMRI, we generated 24 enhanced social adaptive network models. The adaptive network model generated by using contact trust strength measure and periodic detailed-proximity contact data (16:00-24:00), and the social adaptive network model obtained through using direct contact strength measure and periodic detailed-proximity contact data (00:00-08:00) have the greatest similarity to the community structure of the benchmark network model according to corresponding dissimilarity measures (see Table 5.3). This means that friendship relations can be efficiently captured by measuring behavioural trust among people based on periodic detailed proximity mobile-sensing data (00:00–08:00), and measuring contact strength combined frequency and duration based on periodic detailed proximity mobile-sensing data (16:00–24:00). Moreover, this is a further indication that when more longer contacts and more contacts occur in 00:00–08:00 and 16:00–24:00, they imply closer relationships between people. As shown in Figure 5.6a and 5.6b, the final configuration of the enhanced social adaptive network model generated by using contact trust strength measure and periodic detailed-proximity contact data (00:00–08:00) has 29 nodes, 32 links, and 7 communities, and its modularity is 0.45, degree-based dissimilarity penalty is 624 (normalized value is 0.23), labelling-based dissimilarity penalty is 39 (normalized value is 0.28), while the final configuration generated by using contact trust strength measure and periodic detailed-proximity contact data (16:00–24:00) has 49 nodes, 239 links, and 7 communities, and its modularity is 0.35, degree-based dissimilarity penalty is 502 (normalized value is 0.18), and labelling-based dissimilarity penalty is 40 (normalized value is 0.28). The final configuration generated by using contact trust strength measure and periodic detailed-proximity contact data (00:00–24:00) has 52 nodes, 368 links, and 5 communities, and its modularity is 0.37, degree-based dissimilarity penalty is 602 (normalized value is 0.22), while labelling-based

dissimilarity penalty is 43 (normalized value is 0.3); and the benchmark network model derived from self-report data has 52 nodes, 57 links, and 12 communities, and its degree-based/labelling-based dissimilarity penalty is 0 (normalized value is 0) (see Figure 5.6c and 5.6d).

Periodic social contact data		*Degree-based dissimilarity measure*		*Labeling-based dissimilarity measure*	
		Social interaction strength	*Total penalty*	*Social interaction strength*	*Total penalty*
Voice-call based contact	00:00-24:00	RSPS	1230	RSPS	69
	00:00-08:00	RSPS	1365	RSPS	74
	08:00-16:00	PTS	1415	PTS	86
	16:00-24:00	SPS	1435	SPS	88
Detailed-proximity based contact	00:00-24:00	CTS	602	CTS	43
	00:00-08:00	CTS	624	DCS	**39**
	08:00-16:00	CFS	690	TFS	49
	16:00-24:00	CTS	**502**	CTS	40
Coarse-proximity based contact	00:00-24:00	RSPS	1699	RSPS	94
	00:00-08:00	SPS	1675	SPS	95
	08:00-16:00	SPS	1461	SPS	95
	16:00-24:00	ICS	1830	ICS	102

Table 5.3: Statistics of the enhanced social adaptive network models generated by using various periodic social contact data. The minimum values of total dissimilarity penalty are highlighted in bold.

The normalized values of the generated instances generated were separately calculated through using scale normalization which can be defined as: $\hat{x}_{sn} = (x - min(x))/((max(x) - min(x))$. As shown in Figure 5.7, the community structures of instances derived from detailed-proximity based contact data are more similar to the benchmark network model than other instances generated by using voice-call based contact data and coarse-proximity based contact data. This implies that encounter-

(a) The final configuration generated by using contact trust strength measure and periodic detailed-proximity contact data (00:00-08:00)

(b) The final configuration generated by using contact trust strength measure and periodic detailed-proximity contact data (16:00-24:00)

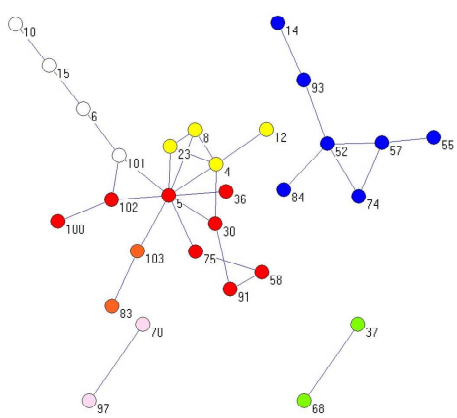

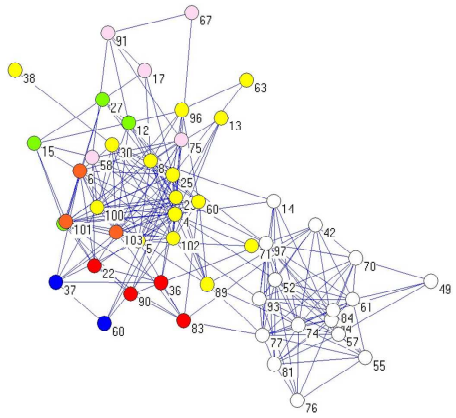

(c) The final configuration generated by using contact trust strength measure and periodic detailed-proximity contact data (00:00-24:00)

(d) The benchmark network model derived from self-report data

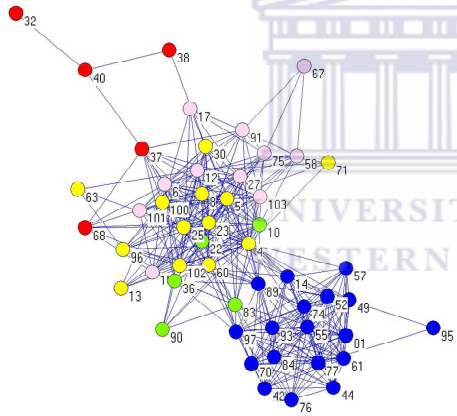

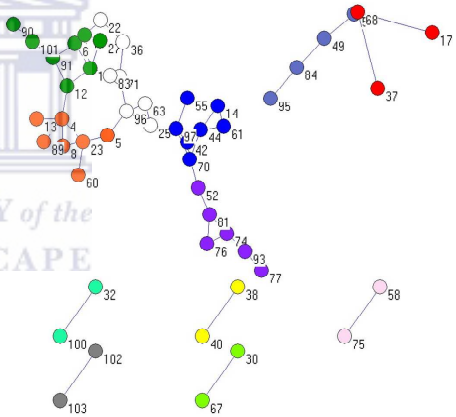

Figure 5.6: The final configurations of the enhanced social adaptive networks generated by using different periodic social contact data and social contact strength measures. a, the final configuration generated by using contact trust strength measure and periodic detailed-proximity contact data (00:00–08:00), which has the minimum dissimilarity penalty according to labelling-based measure; b, the final configuration generated by using contact trust strength measure and periodic detailed-proximity contact data (16:00–24:00), which has the minimum dissimilarity penalty according to degree-based measure; c, the final configuration generated by using contact trust strength measure and periodic detailed-proximity contact data (00:00–24:00); d, the benchmark network model derived from self-report data.

based social adaptive network models can effectively represent friendship circles in social network systems. However, the performance of social adaptive network models derived from voice-call based contact data should be improved by using complete call log with called party ID.

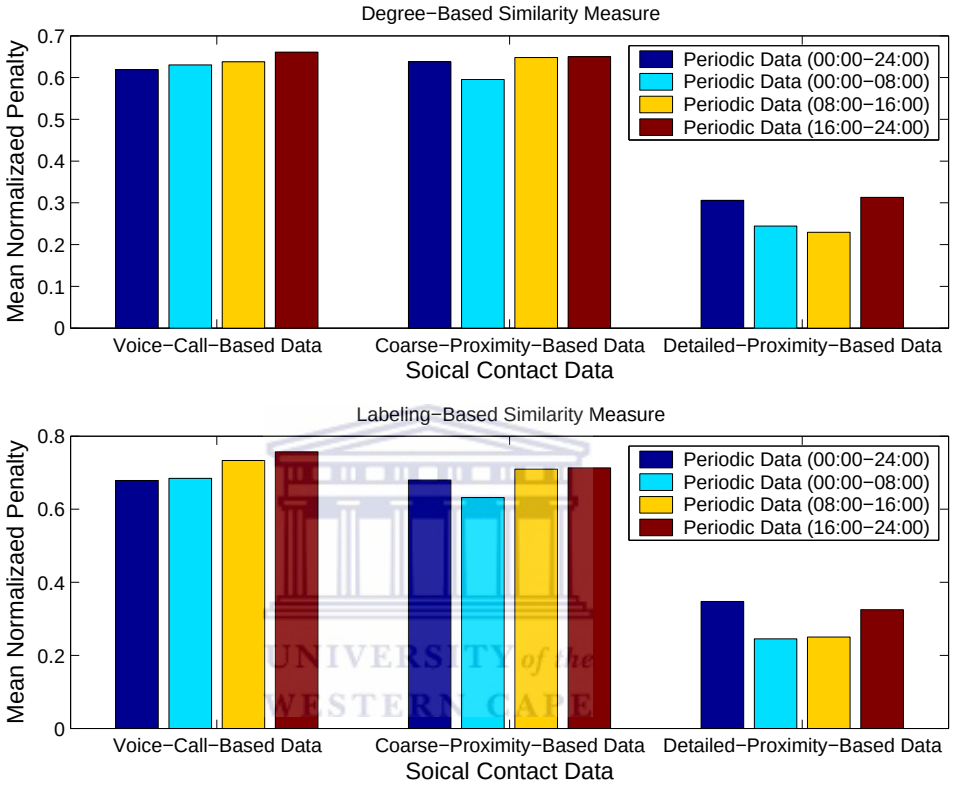

Figure 5.7: The comparison of the mean normalized penalty of the generated instances for three periodic types social contact data, including voice-call based periodic social contact data, coarse-proximity based periodic social contact data, and detailed-proximity based periodic social contact data.

In Figure 5.8, it can be observed that the instances generated by using contact trust strength measure (CTS), trust frequency strength measure (TFS), and direct contact strength measure (DCS) have higher matching degrees to the benchmark network model. As depicted in Figure 5.9, the dissimilarity of the instances derived from periodic contact data (00:00–08:00) to the benchmark network model are lower

than other instances. Thus, social relations in a certain social network system may be efficiently captured through measuring individuals' behaviours in time period 00:00–08:00.

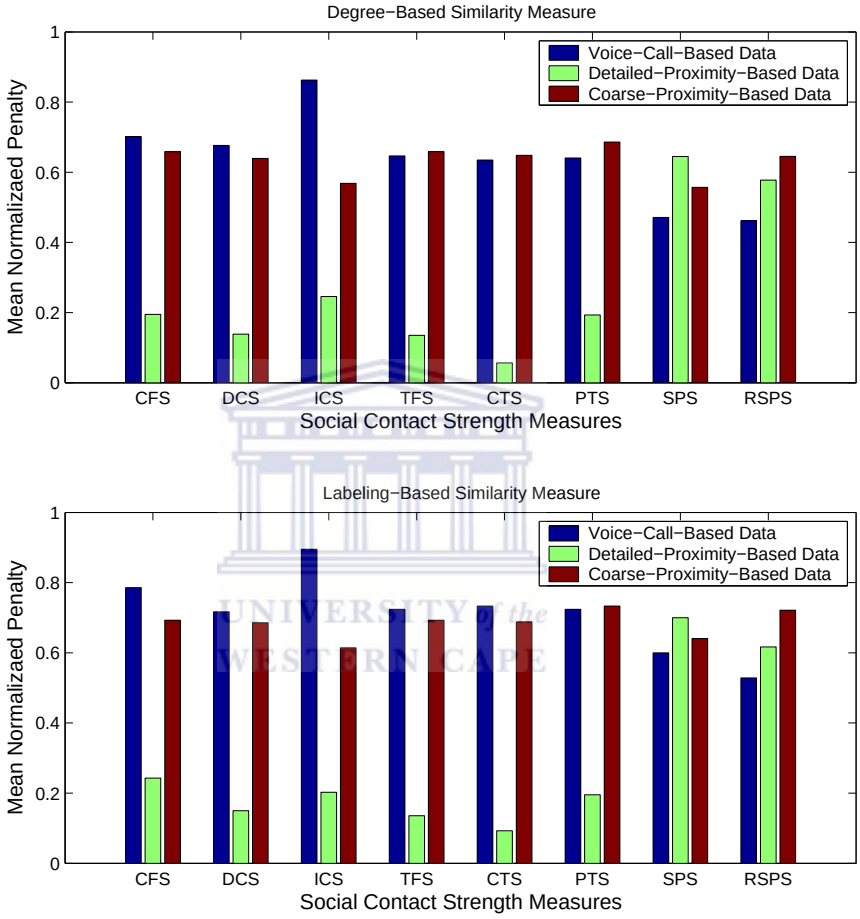

Figure 5.8: The comparison of the mean normalized penalty of the generated instances for eight social contact strength measures, including contact frequency strength measure (CFS), direct contact strength measure (DCS), indirect contact strength measure (ICS), trust frequency strength measure (TFS), contact trust strength measure (CTS), propagation trust strength measure (PTS), social pressure strength measure (CPS), and relative social pressure strength measure (RSPM).

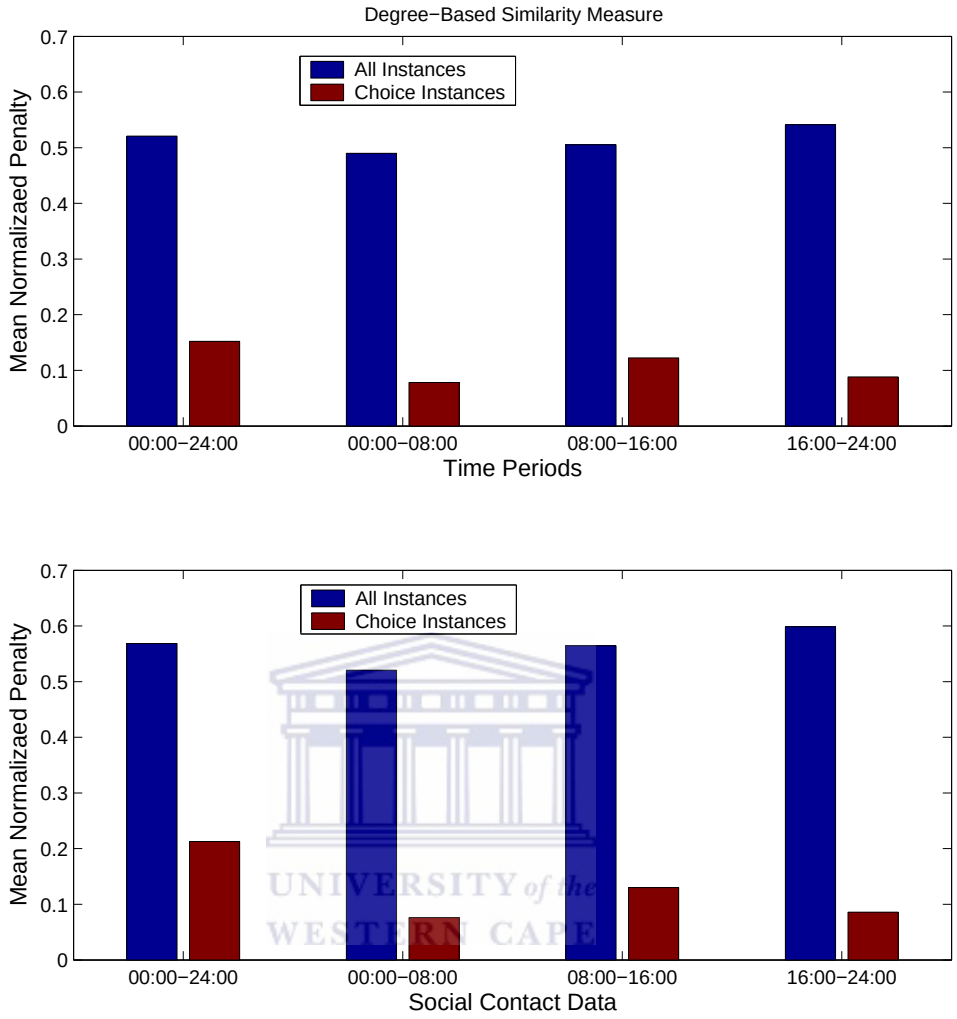

Figure 5.9: The comparison of the mean normalized penalty of the all instances and choice instances generated by using contact trust strength measure (CTS), trust frequency strength measure (TFS), and direct contact strength measure (DCS) for four time periods, including 00:00–24:00, 00:00–08:00, 08:00–16:00, and 16:00–24:00.

According to these simulation results, the enhanced social adaptive network models whose community structures are similar to the studied real-world social network systems can be automatically built through using SMRI and periodic social contact histories of individuals, when these social contact data are generated from various mobile-sensing based data sources. Moreover, the experimental results also

demonstrated that the coupling between the social adaptive network model and the multiple model adaptive control structures can drive the community structure of a social adaptive network models towards a desired state through using suitable computational models of behavioural state update and social interaction update predetermined by the multiple model adaptive control structure.

5.4.4 Modelling with Fused Data and Fused Features

Social network models can be established based on mobile-phone-centric multimodal dataset which provides large amount of information about the studied social network system. Thus, the extraction of useful information from raw data is a major goal. This can be achieved by quantifying the information content or importance of a certain part of the data set. Fused data and features are chosen in a way to enhance parts of the data which may contain more information about the social network system. A set of enhanced social adaptive network models can then be built based on these fused data and features. In this experiment, the performances of the data and feature enhancement methods were evaluated according to the enhanced social adaptive network models generated by our automatic modelling tool SMRI.

5.4.4.1 Input Data

By using the periodic voice-call-based contact data (00:00–24:00) and the periodic detailed-proximity-based contact data (00:00–24:00) as original datasets, fused voice-call-based contact data and fused detailed-proximity-based contact data were generated in a way to enhance parts of the data which may contain more information about the studied social network system.

The raw data of the call logs and Bluetooth proximity logs are normally noisy when they are used for studying of social relations among people. For example, a person call/meet another person several times does not mean they must be friends. However, the noise of voice-call based contact data may be filtered by using the social interactions derived from detailed-proximity based contact data and vice versa. The fused voice-call-based contact data only involves matched voice-call based social contacts between two persons when there exists social interactions between these two persons according to the original detailed-proximity-based contact data. Further-

more, we also generated the fused detailed-proximity-based contact data by using the same method based on the original voice-call-based contact data.

5.4.4.2 Modelling with SMRI

We generated a set of enhanced social adaptive network models by using SMRI and four social contact datasets, including original/fused voice-call-based contact datasets, and original/fused detailed-proximity-based contact datasets. The behavioural state of each node is updated with a certain periodic contact history which is extracted from current input data. In each time step, the weights of links are updated based on a certain social interaction strength measure. Thus, eight instances of the social adaptive network model are then generated for a certain social contact data. Moreover, by using the information-based feature fusion method with $\gamma = 0.56236$ (see Section 5.3.2.9), fused social interaction strength are generated based on the measurements of social interaction strength derived from fused voice-call-based contact data and fused detailed-proximity-based contact data respectively. Thus, extra eight instances are generated based on these fused social interaction strength. In the dissimilarity estimator, the dissimilarity between the discovered communities of the generated instances and the discovered communities of benchmark network model built by using self-report data is measured. The corresponding control parameters of the instance whose dissimilarity penalty is the minimum are fed into the controller, and the corresponding computational model of the instance are applied to the generation of the final configuration of the enhanced social adaptive network model.

5.4.4.3 Simulation Results

We have generated ten enhanced social adaptive network models when the four social contact datasets and two dissimilarity measures were used. As shown in Table 5.4, the social adaptive network models generated by using original/fused detailed-proximity-based contact data have the greatest similarity to the community structure of benchmark network model according to the labelling-based dissimilarity measure, while the dissimilarity penalty of the social adaptive network model generated by using the original detailed-proximity-based contact data is the mini-

mum according to degree-based dissimilarity measure. In Figure 5.10a and 5.10b, the final configuration of the enhanced social adaptive network model generated by using propagation trust strength measure and fused detailed-proximity-based contact data has 52 nodes, 477 links, and 7 communities, and its modularity is 0.31, the degree-based dissimilarity penalty is 686 (normalized value is 0.23), and the labelling-based dissimilarity penalty is 43 (normalized value is 0.3), while the final configuration generated by using contact trust strength measure and original detailed-proximity-based contact data has 52 nodes, 368 links, and 5 communities, and its modularity is 0.37, degree-based dissimilarity penalty is 602 (normalized value is 0.2), and labelling-based dissimilarity penalty is 43 (normalized value is 0.3). The final configuration generated by using direct contact strength measure and feature-fused contact data has 51 nodes, 487 links, and 2 communities, and its modularity is 0.26, degree-based dissimilarity penalty is 745 (normalized value is 0.25), and labelling-based dissimilarity penalty is 45 (normalized value is 0.31); while the benchmark network model derived from self-report data has 52 nodes, 57 links, and 12 communities, and its degree-based/labelling-based dissimilarity penalty is 0 (normalized value is 0) (see Figure 5.10c and 5.10d). We also observed that the mean dissimilarity penalties of all generated instances with fused data and features to the benchmark network model are higher than the network models with original social contact data in Figure 5.11. They could be the possible reasons that the contact frequencies of original voice-call based contact data and original detailed-proximity based contact data are similar ($\gamma = 0.56236$), and the raw voice call data are incomplete (without called party ID). However, through using data fusion and feature fusion, the similarity values of instances generated by direct contact strength measure, trust frequency strength measure, and social pressure strength measure can be improved (see Figure 5.12).

The experiment results with different social adaptive network models having different computation models of data and feature processing show that our automatic modelling tool SMRI with data-fusion based and feature-fusion based feature enhancement methods can be used for improving the performance of ceratin computational models when raw data are noisy. Moreover, it also demonstrates that

the SMRI which combines adaptive network models and multiple model adaptive control structures can be used for implementing the development, comparison, communication and validation of mobile-phone-centric computational models in social network research.

Social contact data	*Degree-based dissimilarity measure*		*Labeling-based dissimilarity measure*	
	Social interaction strength	*Total penalty*	*Social interaction strength*	*Total penalty*
Fused voice-call based contact	TFS	2110	DCS	111
Fused detailed-proximity based contact	PTS	686	PTS	**43**
Feature-Fused contact	DCS	745	DCS	45
Original voice-call based contact	RSPS	1230	RSPS	69
Original detailed-proximity based contact	CTS	**602**	CTS	**43**

Table 5.4: Statistics of the enhanced social adaptive network models generated by using various social contact data with/without feature enhancement, including original/fused voice-call based social contact data, original/fused voice-call based social contact data, and feature-fused social contact data. The minimum values of the total dissimilarity penalty are highlighted in bold.

(a) The final configuration generated by using propagation trust strength measure and fused detailed-proximity-based contact data

(b) The final configuration generated by using contact trust strength measure and original detailed-proximity-based contact data

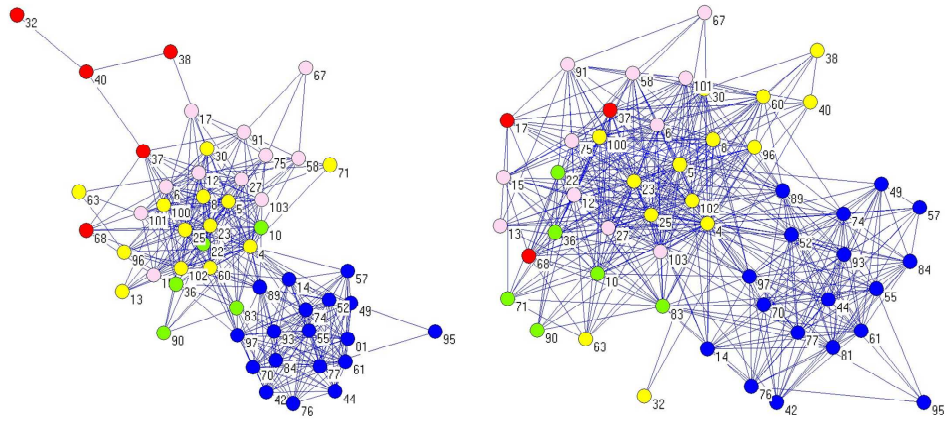

(c) The final configuration generated by using direct contact strength measure and feature-fused contact data

(d) The benchmark network model derived from self-report data

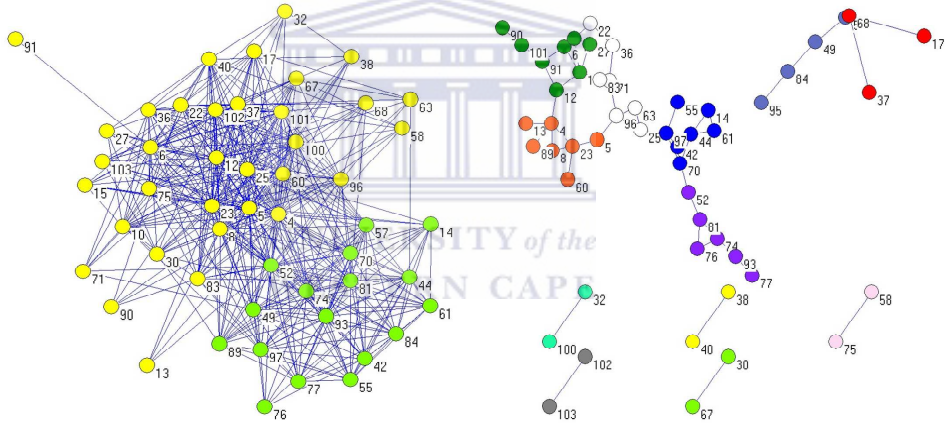

Figure 5.10: The final configurations of the enhanced social adaptive networks generated by using various social contact data with/without feature enhancement and social contact strength measures. a, the final configuration of the enhanced social adaptive network model generated by using propagation trust strength measure and fused detailed-proximity-based contact data, which has the minimum dissimilarity penalty according to labelling-based measure; b, the final configuration generated by using contact trust strength measure and original detailed-proximity-based contact data, which also has the minimum dissimilarity penalty according to labelling-based measure; c, the final configuration generated by using direct contact strength measure and feature-fused contact data, which has the minimum dissimilarity penalty according to degree-based measure; d, the benchmark network model derived from self-report data.

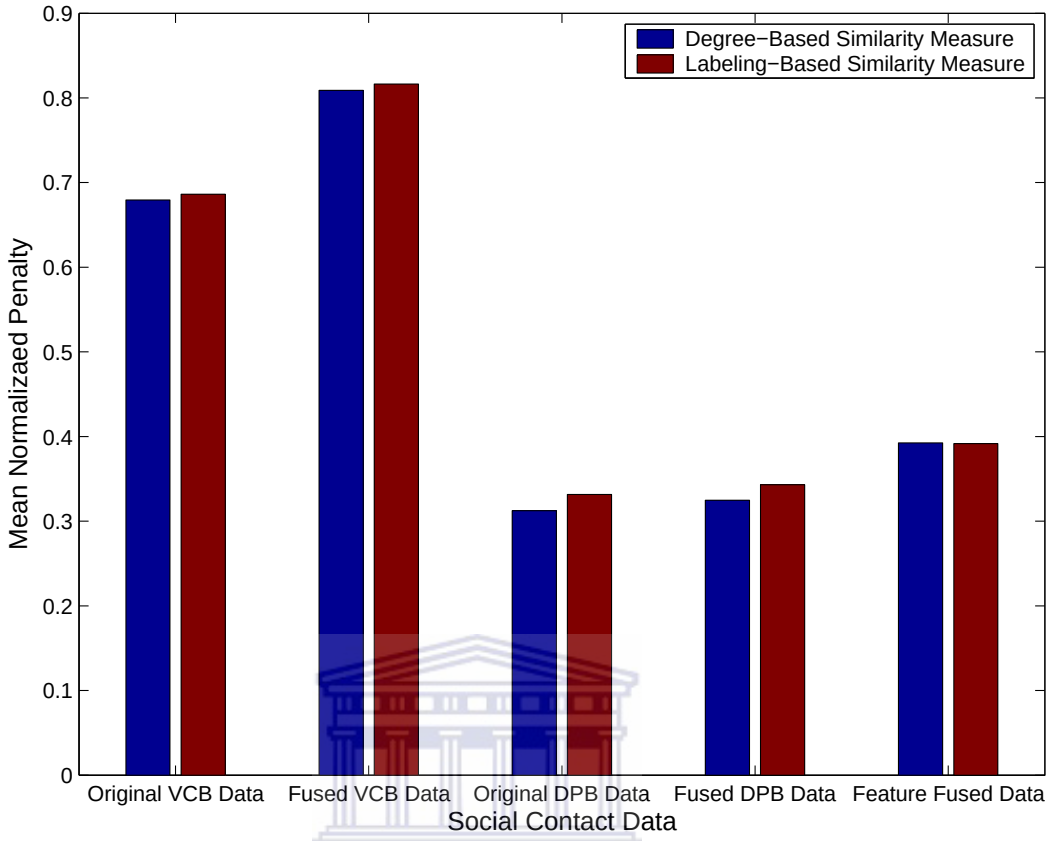

Figure 5.11: The comparison of the mean normalized penalty of the generated instances for the five social contact data with/withouth feature enhancement, including original voice-call-based social contact data (Original VCB Data), fused voice-call-based social contact data (fused VCB Data), original detailed-proximity-based social contact data (Original DPB Data), fused detailed-proximity-based social contact data (fused DPB Data), and feature-fused social contact data (Feature-Fused Data).

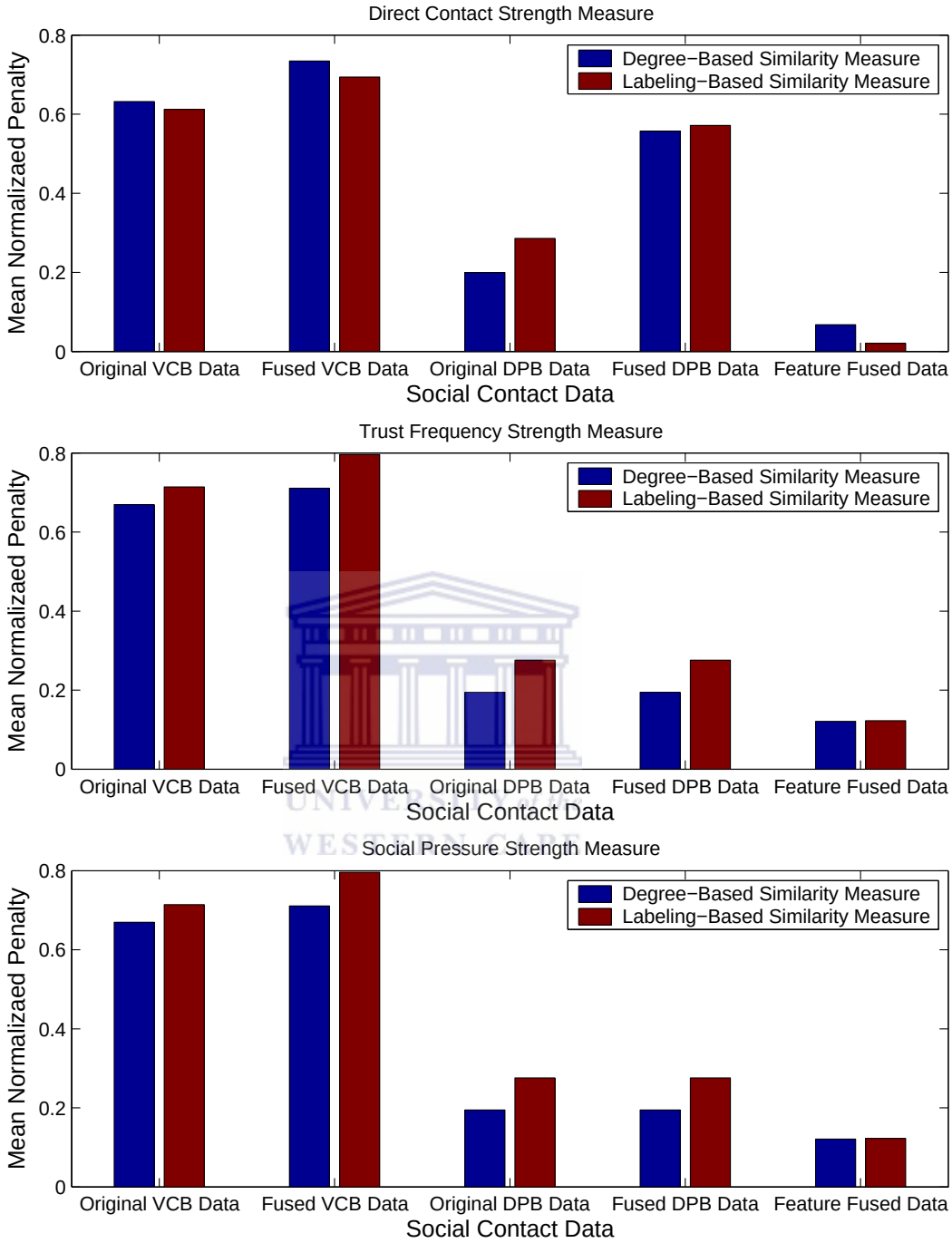

Figure 5.12: The comparison of the normalized penalty of instances generated by three various social contact strength measures, including direct contact strength measure, trust frequency strength measure, and social pressure strength measure, for five social contact data with/withouth feature enhancement.

5.5 Summary

In this chapter, we have described a unified framework which combines adaptive network models and multiple model adaptive control structures for modelling and simulation of real-world social network systems. In this modelling framework, the studied social network system can be represented as an adaptive network which contains a feedback loop between the behavioural states of the individuals and the community structures of the system, while a multiple model adaptive control structure was used for the predetermination of suitable computational models of behavioural state update and social interaction update in order to drive the community structures of the social adaptive network model towards a desired state. By using this modelling framework, an automatic modelling tool, SMRI, has been developed for automatically generating the enhanced social adaptive network models whose community structures are similar to real-world social network systems by using mobile-phone-centric multimodal data. Having such an automated modelling tool would greatly reduce the human effort and provide a valuable systematic modelling tool for understanding, description, prediction, and control of the real-world social network systems through using mobile-phone-centric behavioural data.

We have applied our SMRI on a real-world social network system by using a mobile-phone-centric multimodal dataset. Two experiments were performed for demonstrating how to conduct a research case study on social network modelling by using the automatic modelling tool. In the first experiment, the simulation results demonstrate that the enhanced social adaptive network models whose community structures are similar to the studied real-world social network systems can be automatically built through using SMRI and periodic social contact histories of individuals derived from various mobile-sensing based data sources. In the second experiment, the experiment results with different social adaptive network models having different computation models of data and feature processing show that our automatic modelling tool SMRI with data-fusion based and feature-fusion based feature enhancement methods can be used for improving the performance of ceratin computational models when raw data are noisy. Moreover, the results of both experiments also demonstrated that the coupling between the social adaptive network

models and the multiple model adaptive control structures can drive the community structure of a social adaptive network models towards a desired state through using suitable computational models of behavioural state update and social interaction update predetermined by the multiple model adaptive control structure.

By using the multimodal datasets with richer and more complete social behaviour data and our automatic modelling tool SMRI, we would like to do more work in the future in order to investigate temporal correlation between the social behaviours of individuals for better modelling and simulation of evolving social network systems. As a future work of our study, we would also like to apply the unified modelling framework and the automatic modelling tool SMRI to more real-world social network systems. Moreover, through using richer and more accurate mobile sensing data and more computational models derived from different scientific disciplines, a more complete picture of the studied social network systems can be captured based on the enhanced social adaptive network models which are automatically generated by SMRI.

CHAPTER 6
Towards A Unified Framework for Modelling and Simulation of Mobile Ad Hoc Network Systems

In this chapter, the unified framework which combines adaptive network models and adaptive control structures has been applied for modelling and simulation of multicast congestion in mobile ad hoc network systems (MANETs). We start in Section 6.1 with a brief introduction to the background of modelling and simulation of multicast congestion in mobile ad hoc network systems. In Section 6.2, we propose a unified framework which combines adaptive network models and support vector machines for modelling and simulation of multicast congestion in MANETs. In this framework, a mobile ad hoc network system can be represented as an agent-based adaptive network which is defined by a feedback loop between the congestion states of group members and the group structure of the network, where the support vector machine-based adaptive control structures are used for the prediction of incipient congestions. In Section 6.3, a multicast congestion detection scheme, WMCD, is developed for the unified modelling framework, in which the incipient congestions of group members can be predicted by using support vector machine-based prediction models and current traffic states. In Section 6.4, a set of simulations and experiments are conducted in order to verify the validity of the proposed unified modelling framework and modelling tool WMCD.

6.1 Multicast Congestion in Mobile Ad Hoc Network Systems

In real systems, modelling the dynamics of flows of the physical quantities is also important, because a completed characterization of a network need to consider the relationship between structure and dynamics of complex networks (Boccaletti et al., 2006). The dynamics model of a complex network can be generated by quantifying the transmission capacities and loads of its components (Boccaletti et

al., 2006). However, in the present work, we focus on modelling multicast congestion based on the adaptive interplay between the dynamics of the packet streams and the dynamics of the network structure in mobile ad hoc networks.

Several adaptive-network based models have been developed for routing and congestion control in wireless communication networks, where they captured more realistic dynamics of wireless communication networks with the interplay between network state and topology. In these models, network congestion caused by high load on a given component can be handled through the adjustment of communication routes. For example, in the work of Glauche et al., (Glauche et al., 2004), end-to-end routes were dynamically adjusted according to the congestion state of each node which can be measured based on end-to-end time delay of packets and single-node relaxation times. In the work Krause et al. (Krause et al., 2006), the network structures and end-to-end routes can be modified according to the number of routes that pass through a node and it's neighbours. A pruning-based network formation adjustment mechanism has been developed by Lim et al., (Lim et al., 2007) which allows for reducing the transition distances by automatically adjusting the transmission radii of nodes. Although the adaptive-network-based modelling and simulation approach can simulate very complicated state-topology coevelution processes in wireless communication network systems, adaptive network models are often very intricate and the impact of any given modelling assumption or parameter is difficult to study. When applying adaptive network models to modelling and simulation of wireless communication network systems, it is necessary to specify how the states of nodes will be changed to generate new topologies of the network. The adaptive network models may have control parameters for node update and link update which greatly determine the quality of the generated network models. Choosing suitable parameter values is, frequently, a problem-dependent task and requires previous experience of the researchers (Maruo et al., 2005). In ordinary adaptive network models, these control parameters are not included as a part of the state-topology coevolution, because they are considered as external fixed parameters. Moreover, the adaptive network models make implicit assumptions for modelling and simulation of wireless communication network systems. The adaptive

network models may be rendered impractical due to the unrealistic assumptions and poor sample quality, and their accuracy suffers significantly from a lack of knowledge about the conditions of the networks or other useful information related to the assumptions. A more accurate wireless network model might be made through obtaining more knowledge from empirical data or adjusting the control parameters of the adaptive network models properly. In the present work, we use a unified framework with the combination of adaptive network models and adaptive control structures for modelling the multicast congestion in wireless ad hoc networks, where the incipient congestions of group members can be predicted by using support vector machine-based prediction models and current traffic states. The group structure of the network is then anatomically adjusted according to the updated congestion states of group members in order to relieve the high load.

6.2 A Unified Framework for Modelling Multicast Congestion in Mobile Ad Hoc Network Systems

Based on the unified modelling framework described in Chapter 3, a unified framework which combines adaptive network models and support vector machine-based adaptive control structures is proposed for modelling multicast congestion in mobile ad hoc network systems. In this framework, a mobile ad hoc network system can be represented as an agent-based adaptive network which are defined by a feedback loop between the congestion states of group members and the group structure of the system, where the support vector machine-based adaptive control structures are used for the prediction of incipient congestions in this network. Moreover, the group structure of the network is anatomically adjusted according to the updated congestion states of group members in order to relieve the high load. For example, a set of nodes in a multicast network can be assigned to three multicast groups with fixed transmission rate (high, moderate, and low) according to the end-to-end time delay of control packets in time step T_1 (see Figure 6.1). The incipient congestion at a group member in the group with high transmission rate is detected by using the samples of packet streams and the support vector machine-based prediction model in time step T_2. According to the updated congestion state, all group members

in the group with high transmission rate leave this group and join the group with moderate transmission rate in time step T_3 through the modification of their group memberships in order to relieve the high load. In addition, the nodes can also leave the current group and join another group with higher transmission rate in order to improve the network's throughput capacity if there is no congestion in a certain time period. By using such a unified modelling framework, a set of instances of a wireless adaptive network model with updated group structures can be generated through using structural situation information derived from multicast packet streams. Moreover, such a wireless adaptive network model can make the multicast congestion control protocols "cognitive" in mobile ad hoc network systems by perceiving current network conditions and making adjustment and actions properly.

As depicted in Figure 6.2, this adaptive control structure can be thought of as consisting of two loops. The inner loop is composed of the process of agent-based modelling with wireless adaptive network models and a congestion state–group structure feedback controller, while the outer loop modifies the controller parameters through using the updated congestion states of group members. In this adaptive control structure, the incipient congestions of group members are predicted by using support vector machine-based prediction models and current traffic states. By using the current congestion states of group memberships, the current network topology and group structure, and the current control parameters, an instance of the wireless adaptive network model with updated group structure is generated in each time step. Thus, depending on the generated instance, the network topology and group structure of the mobile ad hoc network system are modified in order to relieve the high load.

6.3 WMCD, A Multicast Congestion Detection Scheme for the Unified Modelling Framework

In the present work, we focus on using support vector machines (SVMs) to detect incipient multicast congestion in advance which is the first step towards to the

unified modelling framework introduced above. Support vector machines (Vapnik, 1998) have already been successfully applied in a number of areas, and has given useful results. Here we address MANET multicast congestion problem with end-to-end assumptions. We cannot obtain accurate congestion information directly from inside the network. In this case, support vector machines are particularly appropriate due to the absence of packet loss information and the unpredictable

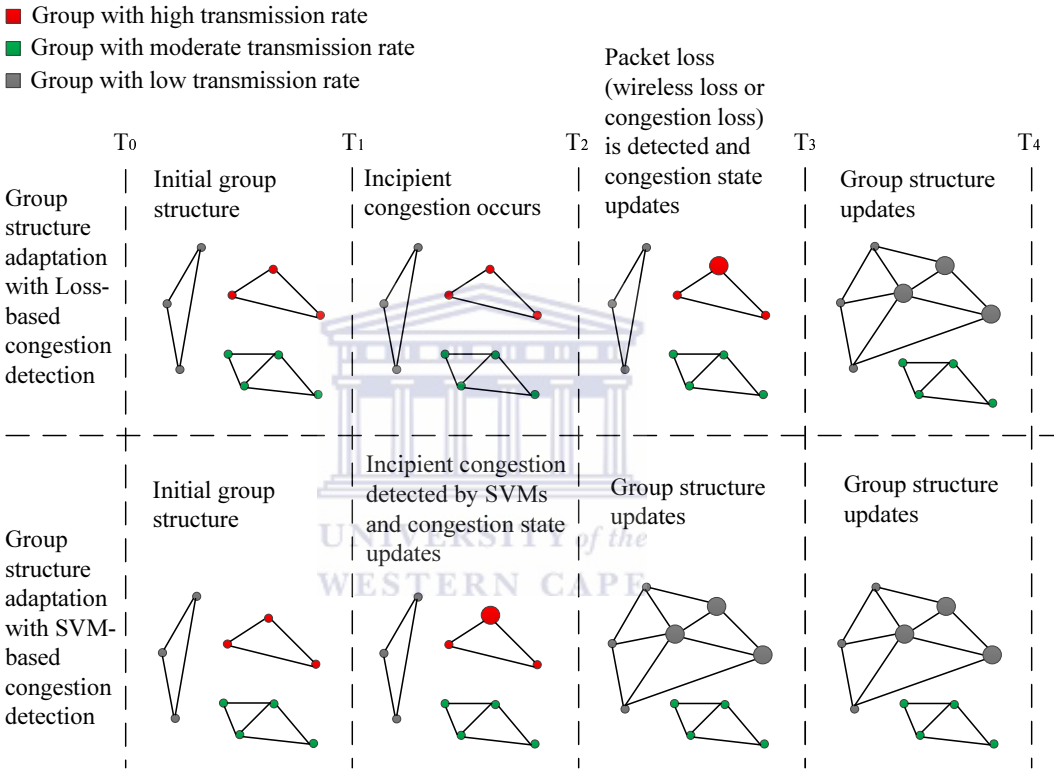

Figure 6.1: Wireless adaptive network model for multicast congestion control with loss-based and support vector machine-based congestion detection methods. The mobile ad hoc network system is represented by a wireless adaptive network model with a multicast congestion state–group structure feedback loop. The loss-based congestion detection method modifies their group structure when packet losses are detected, including wireless losses and congestion losses. Thus, the transmission rate can be restricted even when there is no congestion. However, the support vector machine-based congestion detection method adjusts their group structure when incipient congestions are detected and the high load is relieved before packet loss occurs.

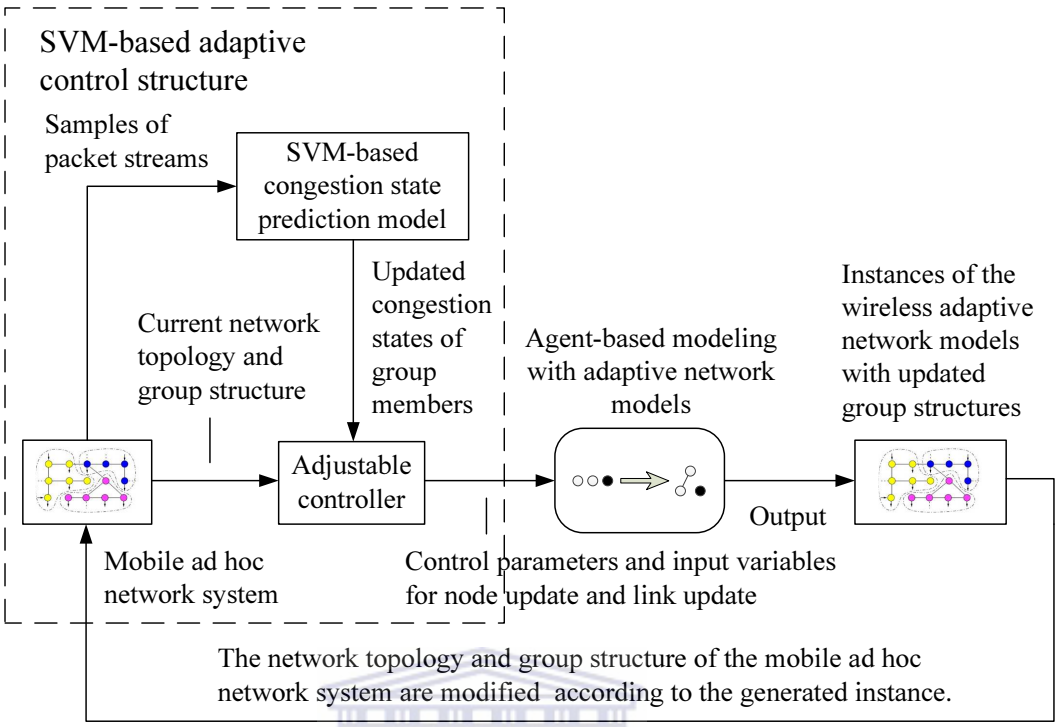

Figure 6.2: Block diagram of a unified framework which combines adaptive network models and support vector machine-based adaptive control structures for modelling and simulation of multicast congestion in mobile ad hoc network systems. In this modelling framework, a mobile ad hoc network system can be represented as a wireless adaptive network model which contains a multicast congestion state–multicast group structure feedback loop. The adaptive control structure consists of two loops. The inner loop is composed of the process of agent-based modelling with wireless adaptive network models and a congestion state–group structure feedback controller, while the outer loop modifies the controller parameters through using the updated congestion states of group members.

variance of network congestions. In learning to detect multicast congestion, the output is a simple yes/no tag. Thus, multicast congestion detection is viewed as a binary classification problem. Support vector machines are used to detect incipient multicast congestion with good accuracy in an end-to-end MANET after training by using structural situation information about the network. Moreover, the group structure adaptation can only be implemented when network congestion is detected at the group members. All the wireless losses are ignored.

By using support vector machines, a multicast congestion detection scheme, WMCD, is developed for the unified modelling framework, in which the incipient congestions of group members are predicted according to support vector machine-based prediction models and current traffic states. As shown in Figure 6.3, a SVM-based congestion prediction model is created by WMCD which quantifies the dynamics of packet flows in MANETs and identify incipient congestions for each group member. The multicast group members automatically update their congestion states based on the congestion prediction model. By using the current congestion states of group memberships, the current network topology and group structure, and the current control parameters, an instance of the wireless adaptive network model with updated group structure is generated in each time step. Thus, depending on the generated instance, the network topology and group structure of the mobile ad hoc network system are modified in order to relieve the high load.

As it is depicted in Figure 6.4, in WMCD scheme, incipient congestions are detected by using SVMs at each multicast group member according to the structural situation information extracted from multicast data packet streams. To obtain the training samples where our SVM learns about incipient congestion, congestion state measurement and interpolation computation are executed at all group members. The sender multicasts data packets to the group members. The receivers detect "local congestion" using MAC layer queue state measure, while "global congestion" is detected by checking if there is a "congestion" flag in multicast data packets forwarded from intermediate nodes. The congestion flag is set by any intermediate node when their MAC queue grows beyond a threshold of the maximum MAC queue size. The time of "local congestion" or "global congestion" is then recorded. Meanwhile, the number of the packets received at fixed intervals is also recorded as the sample. The estimation value of the number of the packets received is calculated using the interpolation algorithm while every packet arrives. We can then compute the sample mean and variance depending on the estimated number of the packets. Structural situation information is generated based on the estimated statistics. After that, the structural situation information is labelled as "congested" or "uncongested" accord-

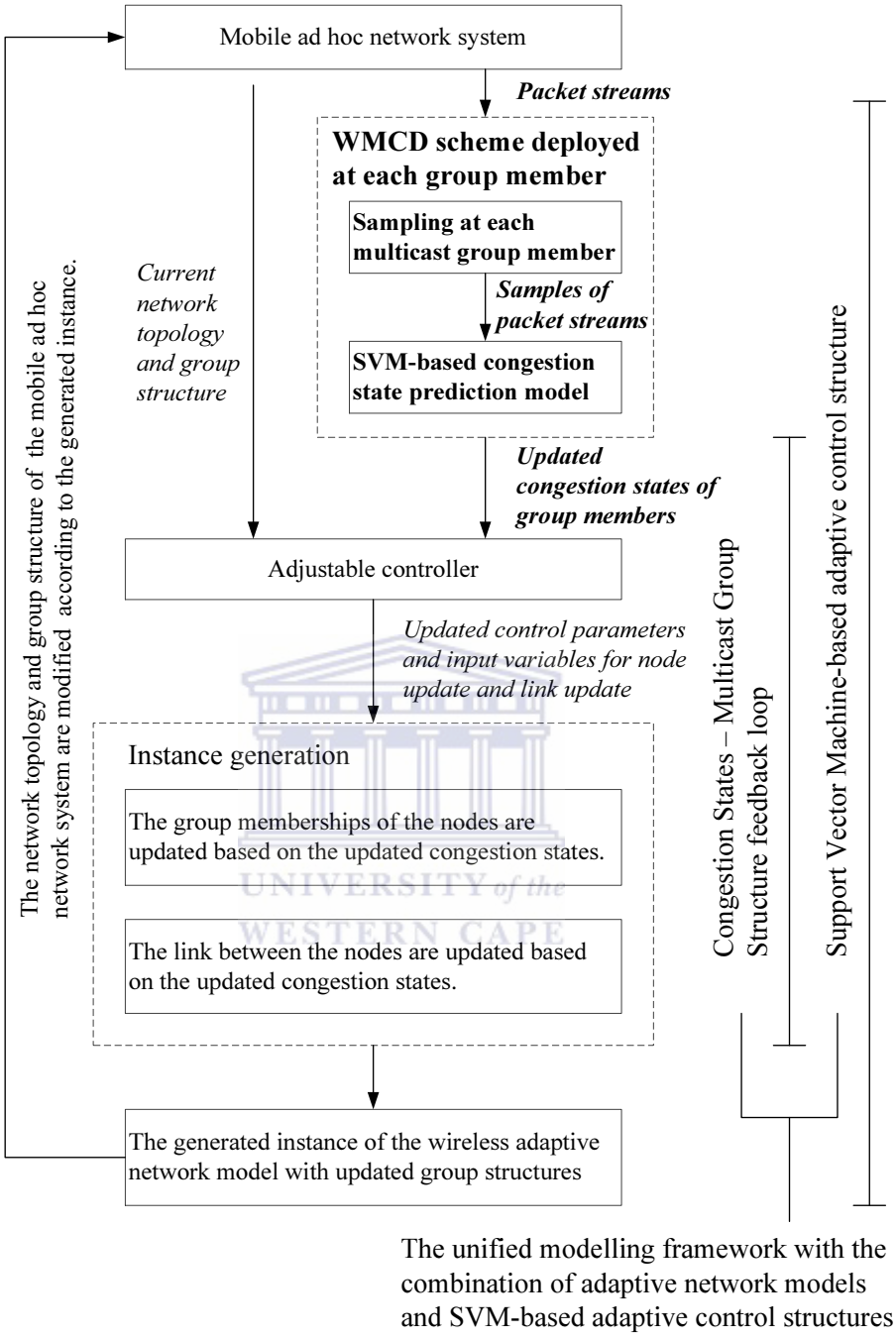

Figure 6.3: The unified modelling framework with WMCD scheme. By using support vector machines, a multicast congestion detection scheme, WMCD, is developed for the unified modelling framework with the combination of adaptive network models and SVM-based adaptive control structures, in which the incipient congestions of group members are predicted according to SVM-based prediction models and current traffic states. The WMCD scheme is highlighted in bold.

ing to the detection results of the congestion state measurement. Our training set is generated using the labelled situation information.

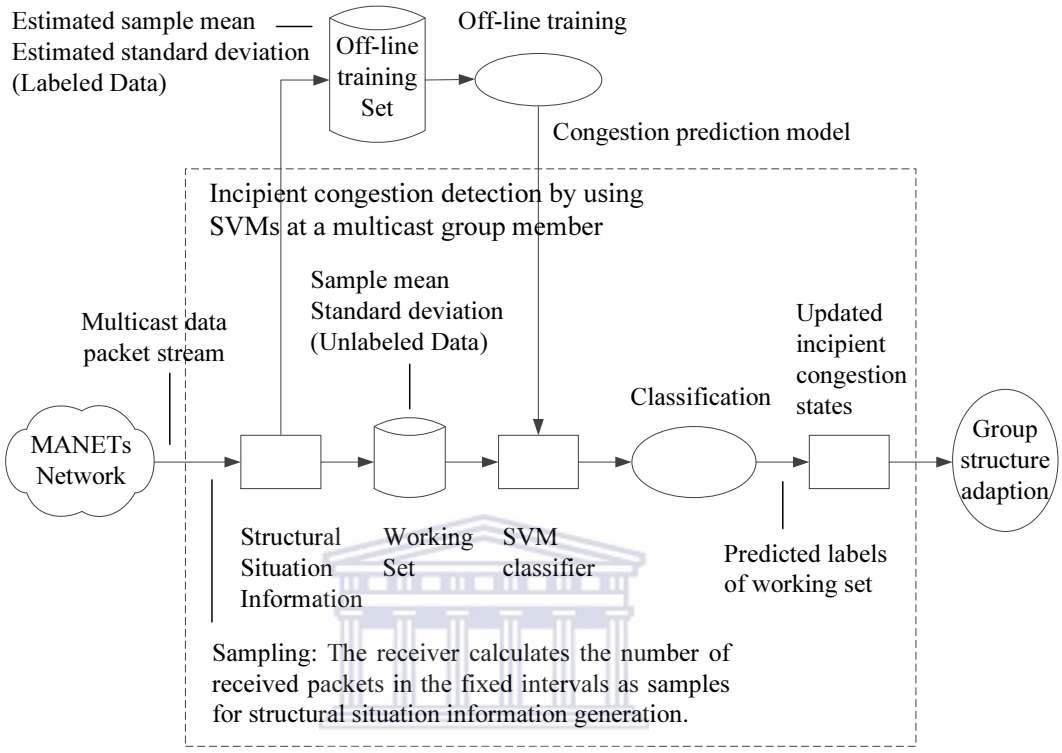

Figure 6.4: Model of WMCD. Incipient congestion detection by using SVMs at a multicast group member. The group structure adaptation is implemented based on the updated congestion states.

The senders multicast data packets to all receivers in a ceratin multicast group after our SVM is trained. At each receiver, the number of the packets received at fixed intervals is sampled. Two parameters, the average of the number of the packets received at fixed intervals and the variance, are computed as structural situation information of the multicast stream when every sample is recorded. The unlabelled data is also the working set of the SVM classification. The C-Support Vector Classification algorithm (Schölkopf et al., 1997) is used to classify the working set and arbitrate the congestion. The congestion state of the group member is updated according to the results of the classification. Group structure adaption is then implemented based on the updated congestion states of all group members in

the network in order to relieve the high load.

In the following, four key algorithms of WMCD will be introduced, including MAC layer congestion measure, interpolation estimation algorithm, structural situation information generation algroithm, and SVM classification algorithm. We present the details in the following sections. We compare the performance of the WMCD scheme to the plain MAC layer queue state measure method in Section 6.4. Further, the conclusion and a short outlook are given.

6.3.1 MAC Layer Congestion State Measure

In order to manage and maintain communications between 802.11-based wireless stations, the Medium Access Control (MAC) Layer provides a set of functions for coordinating access to a shared radio channel and deploying protocols that enhance communications quality over a wireless medium. The MAC layer congestion state measure is implemented for training sample collection. This algorithm is explained by Figure 6.5, 6.6, and the following specifications.

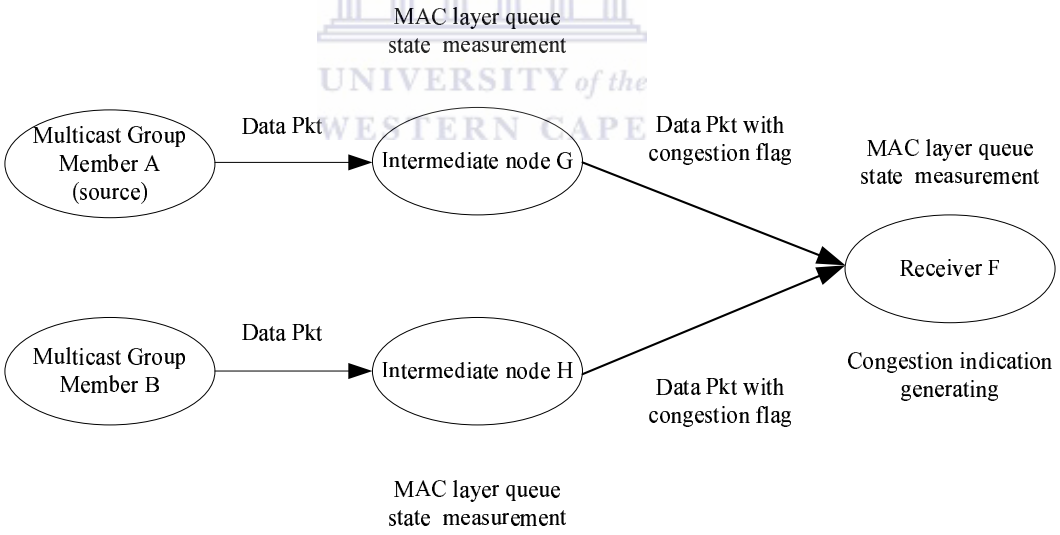

Figure 6.5: Block diagram of MAC layer congestion state measure.

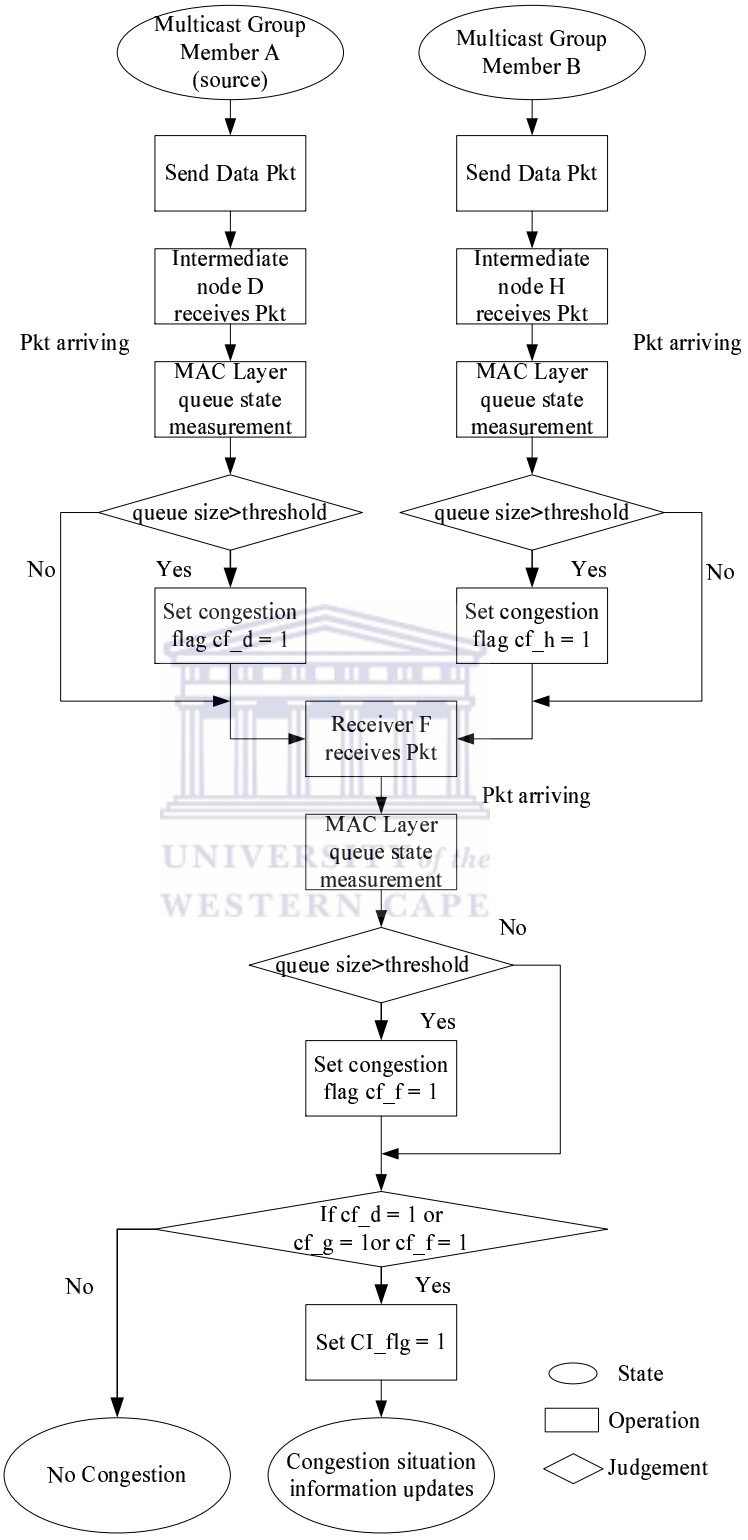

Figure 6.6: Flowchart of MAC layer congestion state measure.

Two types of incipient congestion are detected by using the MAC layer queue state measure (Rajendran et al., 2004). The Internet Protocol option field in the multicast data packet is used to carry congestion situation information. This field is updated as the packet is forwarded to the group. Global congestion is detected by a multicast group member when the multicast data packet arrives with the "*global_congestion*" flag. This flag is set if any intermediate node on the path to the group member has MAC queue size beyond the *congestion_threshold*. Local congestion is detected by the group member when its queue size is beyond a congestion threshold. The congestion threshold is set at 95% for local and global congestion detection, while it is set at 100% for local congestion loss detection. Time is recorded when global congestion or local congestion is detected. After that, we use an interpolation technique to obtain the estimated value of the statistics about the multicast stream when incipient congestion is detected.

6.3.2 Interpolation Estimation

In generation of the training set, we gather two types of labelled data ("congested" and "uncongested") as training samples for SVM classification. At a multicast group member, local congestion and global congestion are detected as every multicast data packet arrives. MAC layer queue state is measured to detect local congestion, while global congestion is detected by checking if the multicast data packet carries the congestion flag. Using the interpolation technique, we estimate values of the statistical information about the multicast stream according to the data packet arrival time.

Although the time of the congestions can be collected at each multicast group member, it is difficult to directly measure the statistics about the multicast stream at that moment. Thus, we use the interpolation estimation algorithm to obtain the estimated values. During training set generation, the number of the packets received at fixed intervals ($20ms$) is recorded. Two variables are obtained from the sampling, namely the number of the packets received at fixed intervals $Y_i = \{Y_1, Y_2, \ldots, Y_n\}$ and the time of the sampling $X_i = \{X_1, X_2, \ldots, X_n\}$, where n is

the number of the samples. We then establish a lookup table with X_i and Y_i. By using spline interpolation, we can calculate the estimated number of the packets $\hat{Y}_j = \hat{Y}_1, \hat{Y}_2, \ldots, \hat{Y}_m$ and the time of the congestions $\hat{X}_j = \hat{X}_1, \hat{X}_2, \ldots, \hat{X}_m$ where m is the number of the congestions.

6.3.3 Situation Information Generation

In our scheme, structural situation information is collected at all nodes in the network for constructing the training set as well as the working set. We obtain the structural situation information (the sample mean and variance) using simple statistical techniques. The details of this process are presented in the following discussion.

6.3.3.1 Congestion Situation Information Generation for Training Set

In our scheme, structural situation information is collected at all nodes in the network for constructing the training set as well as the working set. We obtain the structural situation information (the sample mean and variance) using simple statistical techniques. The details of this process are presented in the following discussion. The training set is generated by using two types of training samples labelled as "congested" or "uncongested". As shown in Figure 6.7, incipient congestion is detected by MAC layer queue state measure (local congestion detection) or congestion flag detection (global congestion detection) when a packet arrives; the estimated number of the packets, relating to the packet arrival time, is then computed using the interpolation estimation algorithm. Depending on the number of the packets, the estimated statistics are obtained for training set generation when every packet is received. The estimated statistics are labelled as "congested" or "uncongested" according to the results of the congestion detection.

At each multicast group member, the number of packets received at fixed intervals are recorded as samples during training set generation. Two parameters, sample mean, $\overline{Y_k}$ and sample variance, S_k, are computed as the estimated statistics when every packet is received. We have $\overline{Y_k} = \frac{1}{n+1}\sum_{i=1}^{n+1} Y_i + \frac{\hat{Y}_i}{n+1}$, where Y_i is the

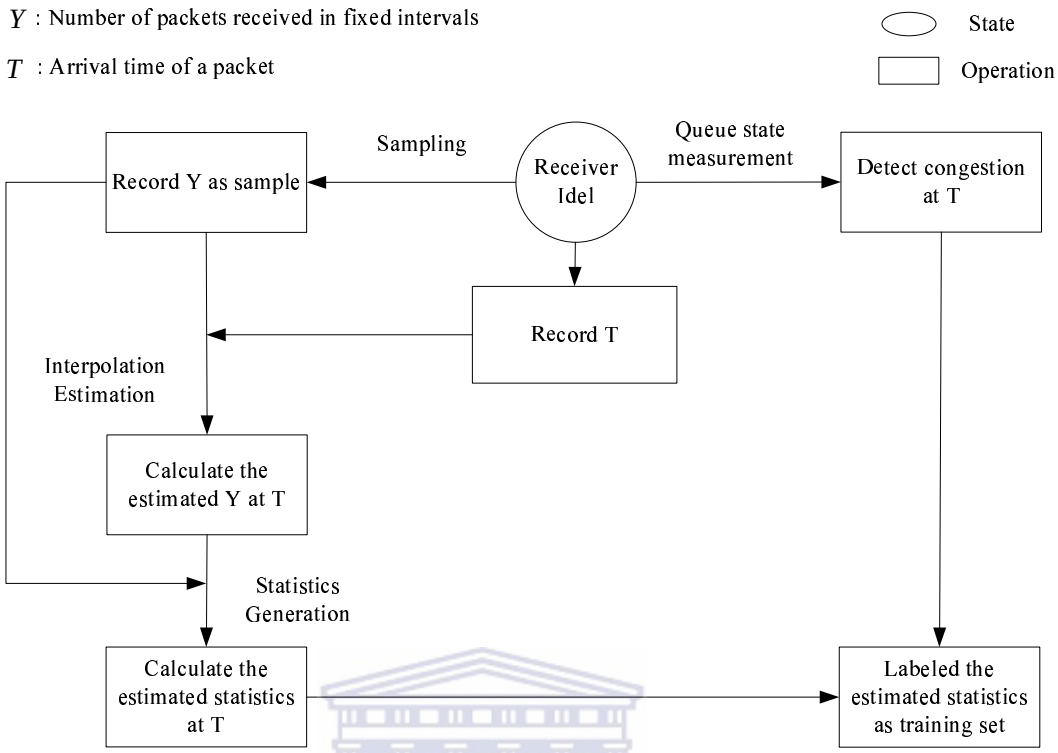

Figure 6.7: Training set generation by using congestion situation information.

number of the packets received at fixed intervals before the packet arrives; $\hat{Y}_i$ is the estimated number of the packets as the packet arrives; n is the sampling number before the packet arrives. Let the unbiased variance, $S = \frac{1}{n-1}\sum_{i=1}^{n}(X_i - \overline{X})^2$, the estimated variance, S_k is then given by $S_k = \frac{1}{n}\sum_{i=1}^{n+1}(\hat{Y}_i - \overline{Y_k})^2$. The estimated sample mean, $\overline{Y_k}$ and the estimated variance, S_k will be computed to create the training dataset where our SVM learns about incipient congestion.

6.3.3.2 Situation Information Generation for Working Set

During SVM classification, the number of the packets received is recorded as a sample at each multicast group member. Two parameters $\overline{Y_t}$ and S_t are computed as the statistics of the multicast stream when every sample is recorded. The unlabelled data is also the working set of the SVM classification. We have, $\overline{Y_t} = \frac{1}{n}\sum_{i=1}^{n} Y_i$, where $\overline{Y_t}$ is the sample mean; Y_i is the number of the packets received at fixed intervals; n is the sampling number. The unbiased formula is also used for the sample variance. We have, $S_t = \frac{1}{n-1}\sum_{i=1}^{n}(Y_i - \overline{Y_t})^2$, where S_t is the sample variance;

Y_i is the number of the packets received at the fixed intervals; $\overline{Y_t}$ is the sample mean and n is the sampling number.

6.3.4 Support Vector Classification

Support Vector Machines (Vapnik, 1998) is one type of learning method constructed by Vapnik and Cortes. It is used in our scheme to detect incipient congestion that occurs within a time series. We chose to use the SVM since it has been successfully applied in many fields, such as word sense disambiguation, text classification, part-of-speech tagging, web page classification, and question classification (Vapnik, 1998). SVM first maps input space into some high dimensional feature space, then constructs a linear decision surface in this feature space that relates to a non-linear decision surface in the original input space. The comparison between SVM and other classification methods is given by (Rumelhart & Hinton, 1986; Bennett & Blue, 1997; Chang & Lin, 2001). In our scheme, a congestion prediction model generated by using Schölkopf et al.'s C–Support Vector Classification algorithm (Schölkopf et al., 1997) is used to classify the statistics of multicast stream and arbitrate the congestion according to the dynamics of multicast packet streams.

6.4 Simulations and Experiments

To evaluate our WMCD scheme, we performed a set of simulations for different scenarios that may affect the performance of the proposed scheme. First of all, we collected congestion situation information of packet streams from several QualNet (Scalable Networks) simulations, and established a training set by using the situation information. After off-line training, the generated SVM-based congestion prediction model was used for congestion detection in different simulation scenarios. In order to estimate the classification accuracy of the WMCD scheme, a set of simulations was implemented which compared the classification results of the WMCD scheme to the detection results of the MAC layer queue state measure method. We also performed a set of simulations with group structure adaptation for evaluating the performance of our WMCD scheme, while the unified modelling framework was used for multicast congestion control in MANETs.

6.4.1 Stream Situation Information Collection

In all QualNet (Scalable Networks) simulations, on-demand multicast routing protocol (ODMRP) (Lee et al., 1999) and ad hoc on-demand distance vector routing (AODV) (Perkins & Royer, 1999) are used as the underlying multicast and unicast routing protocols, respectively. The link bandwidth is 112,000 *bps*. The MAC protocol used is IEEE Standard 802.11*b*, (1999). The simulation time is 60 seconds. We first collect the samples and record each packet's arrival time on the simple topology in Figure 6.8. Ten multicast group members are placed randomly in a $100m \times 100m$ field and they can join or leave the two multicast groups with different transmission rates (high and low) in the same time according to the updated congestion states. Five randomly selected group members continuously send multicast constant bit rate (MCBR) traffic throughout the whole duration of the simulation with payload size of 512 bytes, while another five group members are receivers. The results are averaged over 10 runs and presented with 95% confidence. Three QualNet (Scalable Networks) simulation scenarios are established for WMCD performance evaluation, including local congestion detection, global congestion detection, and local congestion loss detection. At this group member, the number of the packets received at fixed intervals ($20ms$), is recorded as a sample. The arrival time of each packet is also gathered for training set generation. The time samples are labelled as "congested" or "uncongested" based on the results of the congestion detection.

6.4.2 Training Set Generation and SVM Training

After obtaining the congestion situation information from QualNet (Scalable Networks), we generate the training set for our SVM using statistical methods (see Section 6.3.3.1). Chang and Lin's LIBSVM (Chang & Lin, 2001) is used to train and optimize our SVM. LIBSVM is an integrated software package for support vector classification (C-SVC, nu-SVC), regression (epsilon-SVR, nu-SVR) and distribution estimation (one-class SVM). To choose the best parameters of our SVM, grid.py, a model selection tool in LIBSVM is used for C-SVM classification. It

uses cross validation techniques to estimate the accuracy of each parameter combination in the specified range. The statistics of the generated training sets in various scenarios are shown in Table 6.1, including ID of the slowest group member, number of congestions, number of samples, SVM control parameters c and g, and classification accuracy at the slowest group member. For example, one of the training sets generated by Simulation 10 in the local congestion detection scenario ($seed\_of\_random\_node\_placement\_model$ = 1027) contains 14,617 samples (16,638 samples are labelled as 0, 979 samples are labelled as 1) which are collected at the slowest group member 7.

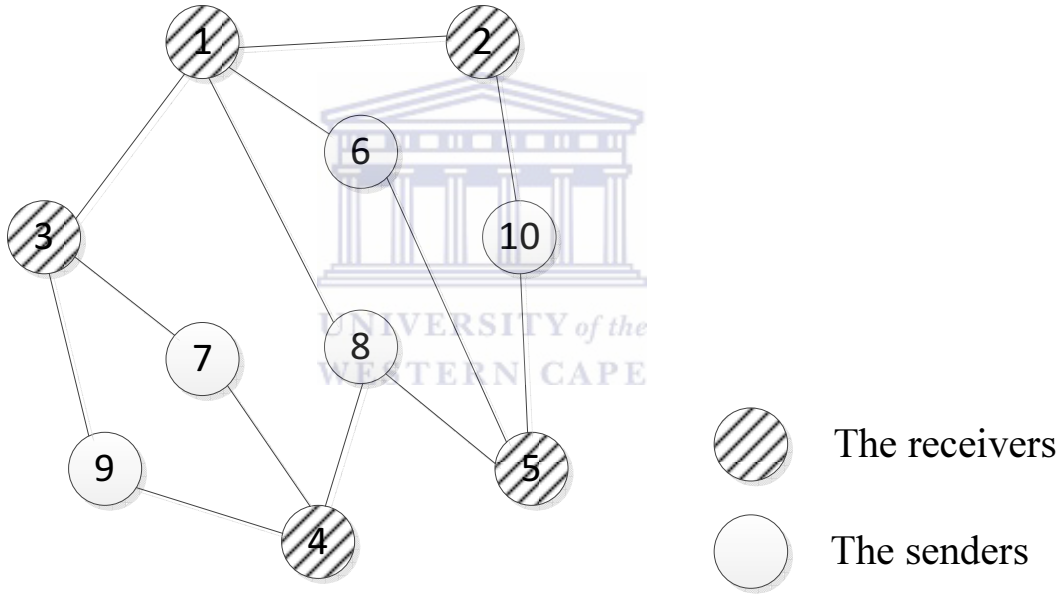

Figure 6.8: Ten multicast group members are placed randomly in a $100m \times 100m$ field and they can join or leave the two multicast groups with different transmission rates (high and low) in the same time according to the updated congestion states. Five randomly selected group members continuously send multicast constant bit rate traffic throughout the whole duration of the simulation with payload size of 512 bytes, while another five group members are receivers.

Sim.	ID of the slowest group member	Number of congestions	Number of samples	*c*	*g*	Classification accuracy (%)	Scenarios
1	6	5335	13659	32768	8	87.76	Local congestion detection
2	6	4350	12536	32768	8	87.80	Local congestion detection
3	6	973	14917	32768	8	97.53	Local congestion detection
4	9	5302	13549	32768	8	87.38	Local congestion detection
5	10	1013	14563	32768	8	95.06	Local congestion detection
6	6	975	14821	512	8	97.29	Local congestion detection
7	7	3992	11197	32768	8	84.03	Local congestion detection
8	9	5589	14173	32768	8	88.79	Local congestion detection
9	6	932	15086	32768	8	97.50	Local congestion detection
10	7	979	14617	32768	8	97.66	Local congestion detection
Stat.	Average	92.08	Stdev.	5.38	Confidence interval	3.33	Statistics for accuracy
1	6	353	13659	128	8	97.56	Global congestion detection
2	6	340	12536	32	2	97.42	Global congestion detection
3	6	2134	14917	32768	8	93.08	Global congestion detection
4	9	923	13549	8192	8	98.32	Global congestion detection
5	10	75	14563	32	2	99.54	Global congestion detection
6	6	2060	14821	32768	2	93.21	Global congestion detection
7	7	243	11197	32768	2	97.84	Global congestion detection
8	9	1072	14173	8192	8	97.95	Global congestion detection
9	6	2269	15086	32768	8	91.54	Global congestion detection
10	7	52	14617	512	2	99.69	Global congestion detection
Stat.	Average	96.61	Stdev.	2.9	Confidence interval	1.8	Statistics for accuracy
1	3	126	11872	32768	8	99.55	Local loss detection
2	3	196	9570	32768	2	97.63	Local loss detection
3	5	98	11935	8192	8	99.18	Local loss detection
4	5	164	11863	0.031 25	0.00781	98.62	Local loss detection
5	5	268	11813	32768	8	98.32	Local loss detection
6	4	81	11916	2048	8	99.72	Local loss detection
7	5	188	9897	32768	8	98.36	Local loss detection
8	3	204	11903	2048	8	98.31	Local loss detection
9	4	178	11894	8192	8	99.04	Local loss detection
10	5	158	11992	32768	8	99.02	Local loss detection
Stat.	Average	98.77	Stdev.	0.64	Confidence interval	0.40	Statistics for accuracy

Table 6.1: Statistics of the generated training sets in various scenarios, including ID of the slowest group member, number of congestions, number of samples, SVM control parameters c and g, and classification accuracy at the slowest group member.

6.4.3 Classification Accuracy Estimation for WMCD

In order to estimate the classification accuracy of the WMCD scheme, a set of simulations were implemented which compared the classification results of the WMCD scheme to the detection results of the MAC layer queue state measure method. After off-line training, a QualNet (Scalable Networks) simulation is run to test the performance of WMCD. LIBSVM (Chang & Lin, 2001) is used for SVM training and classification. The same QualNet (Scalable Networks) configuration used by training set generation is implemented during SVM classification. The senders multicast data packets to other group members, and then the group members detect incipient congestions using SVM classifications instead of MAC layer queue state measure. The slowest group member collects the samples during the simulation. The sampling time is labelled as "congested" or "uncongested" depending on the results of the SVM classification. These labelled samples are then compared to the labelled samples generated by the MAC layer queue state measure. We changed the seed of the random node placement model in the Qualnet (Scalable Networks) simulations. The experiment was repeated ten times for various scenarios, including local congestion detection ($congestion\_threshold = 95\%$), global congestion detection ($congestion\_threshold = 95\%$), and local congestion loss detection ($congestion\_threshold = 100\%$). Figure 6.9 clearly demonstrates that WMCD can achieve good accuracy in predicting incipient wireless multicast congestion by SVM classification. The accuracy of our SVM classification is about 90%. For example, in Simulation 10 of the local congestion detection scenario, the classification accuracy of the slowest group member is 97.7% by using SVM control paramter $c = 32768$ and $g = 8$ (see Table 6.1). Failing includes either missing congestion or predicting congestion while there is none.

6.4.4 Congestion Control with Group Structure Adaptation

To estimate the effect of the unified modelling framework with WMCD, we compared the average receiving rate of the slowest group member derived from WMCD with the results collected by the MAC layer queue state measure (Rajen-

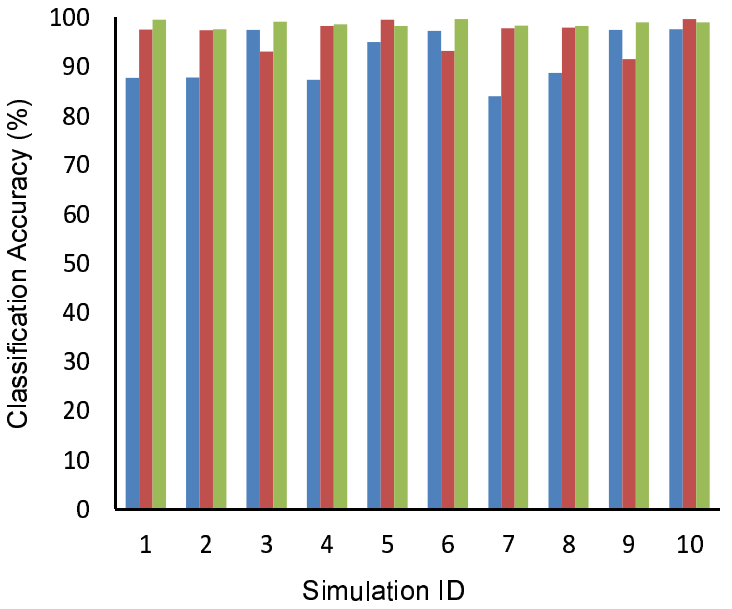

Mean	Std.	Confid-ence interval	Scen-arios
92.08	5.38	3.33	L. C.
96.61	2.9	1.8	G. C.
98.77	0.64	0.4	L. L.

Figure 6.9: Statistics of classification accuracy estimation of WMCD scheme in various scenarios, including local congestion detection, global congestion detection, and local congestion loss detection. It clearly demonstrates that WMCD can achieve great accuracy in predicting incipient wireless multicast congestion by SVM classification.

dran et al., 2004) in different scenarios. In this experiment, the incipient congestions are detected by using SVMs and structural situation information of packet streams in the WMCD scheme, while the congestion states are generated by monitoring the MAC layer queue state in (Rajendran et al., 2004). We used a simple node and link update rule for the generation of the instances of the wireless adaptive network model. When a incipient congestion is detected at the slowest group member, all ten group members leave the current group and join the group with lower transmission rate by modifying their group memberships from the group with high transmission rate ($packet\_transmission\_interveal = 1ms$) to the group with low transmission rate ($packet\_transmission\_interveal = 2ms$). If there is no congestion within $50ms$ at the slowest group member, all group members can update their group memberships and join the group with higher transmission rate. Thus, through using the current congestion states of group memberships, the current network topology and group structure, and the current control parameters, an instance of the wireless

adaptive network model with updated group structure is generated in each time step. Depending on the generated instance, the multicast group structures of the mobile ad hoc network are automatically adjusted by modifying the memberships of the group members in order to relieve the high load.

We changed the seed of the random node placement model in the Qualnet (Scalable Networks) simulations. The simulation was repeated ten times for various scenarios, including local congestion detection ($congestion\_threshold = 95\%$), global congestion detection ($congestion\_threshold = 95\%$), and local congestion loss detection ($congestion\_threshold = 100\%$). As illustrated in Table 6.2, the maximum receiving rates (0.9991 Mbps, 0.8345 Mbps, and 0.8096 Mbps) and the maximum percentage increases (2.5%, 25.7%, and 23%) at the slowest group members generated by the simulations with WMCD scheme are higher than MAC layer queue state measure in all three scenarios. In Figure 6.10, the mean values of the average receiving rates at the slowest group member derived from the ten simulations with WMCD increased 0.7%, 22.1% and 14.4% in three scenarios respectively. Moreover, in Figure 6.11, we also observe that our WMCD scheme achieved higher average receiving rate at the slowest group member than the MAC layer queue state measure scheme in all ten simulations of congestion loss detection. The possible reason is that the WMCD can detect incipient congestion before the MAC layer queue state measure and produce less congestion indications. Thus, the multicast group members can stay in the group with higher transmission rate for a longer time and thus increase their average receiving rates. In local congestion detection scenario, the average receiving rates at the slowest group member derived from the WMCD scheme and the MAC layer queue state measure are very close. It may imply that congestion time measured by the two methods are also very close.

The above simulation result clearly shows that our WMCD scheme achieves better performance than the MAC layer queue state measure scheme, where the unified modelling framework were used for multicast congestion control in MANETs. It also means that the SVM-based adaptive control structure can drive the multicast group structure of the wireless adaptive network model towards a desired state.

Simulations	Local congestion detection			Global congestion detection			Local loss detection		
	WMCD	MAC	Increment	WMCD	MAC	Increment	WMCD	MAC	Increment
1	0.9696	0.9464	2.45%	0.8243	0.6702	22.99%	0.7896	0.7048	12.03%
2	0.9345	0.9329	0.17%	0.7862	0.6609	18.96%	0.6451	0.5743	12.33%
3	1.0245	1.0236	0.09%	0.8297	0.6608	25.56%	0.795	0.6551	21.36%
4	0.9495	0.932	1.88%	0.8039	0.6586	22.06%	0.8096	0.6582	23.00%
5	0.984	0.9897	-0.58%	0.7929	0.6515	21.70%	0.7897	0.6596	19.72%
6	1.014	1.0135	0.05%	0.8119	0.6583	23.33%	0.7886	0.6785	16.23%
7	0.7918	0.7862	0.71%	0.7195	0.6442	11.69%	0.7385	0.6518	13.30%
8	0.9977	0.973	2.54%	0.8311	0.6616	25.62%	0.7932	0.7034	12.77%
9	1.0317	1.0311	0.06%	0.8345	0.664	25.68%	0.7865	0.7261	8.32%
10	0.9991	0.9989	0.02%	0.8054	0.6542	23.11%	0.8	0.7619	5.00%
Mean	0.9696	0.9627	0.74%	0.8039	0.6584	22.07%	0.7736	0.6774	14.41%
Std	0.0699	0.0718	0.011254	0.034	0.0071	0.04202	0.0489	0.051	0.057074
Confidence interval	0.0433	0.0445	0.006975	0.0211	0.0044	0.026044	0.0303	0.0316	0.035374

Table 6.2: Statistics of average receiving rates (Mbps) at the slowest group members generated by the simulations with WMCD scheme and MAC layer queue state measurement scheme in various scenarios, including local congestion detection, global congestion detection, and local congestion loss detection. The maximum values of average receiving rates and percentage increase between two congestion detection schemes (increment) in the three scenarios are highlighted in bold.

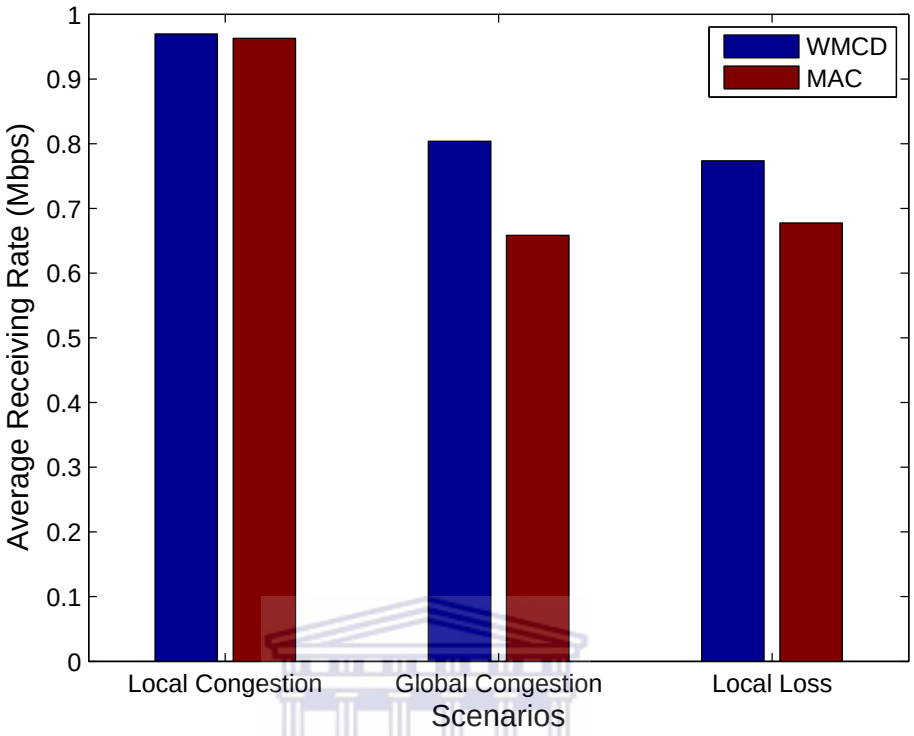

Figure 6.10: The mean values of the average receiving rates at the slowest group member derived from the ten simulations with WMCD scheme and the MAC layer queue state measure scheme in various scenarios, including local congestion detection, global congestion detection, and local congestion loss detection. The mean values of the average receiving rates at the slowest group member derived from the ten simulations with WMCD increased 22.1% and 14.4% in global congestion detection scenario and congestion loss detection scenario respectively. However, in local congestion detection scenario, the average receiving rates at the slowest group member derived from the WMCD scheme and the MAC layer queue state measure are very close.

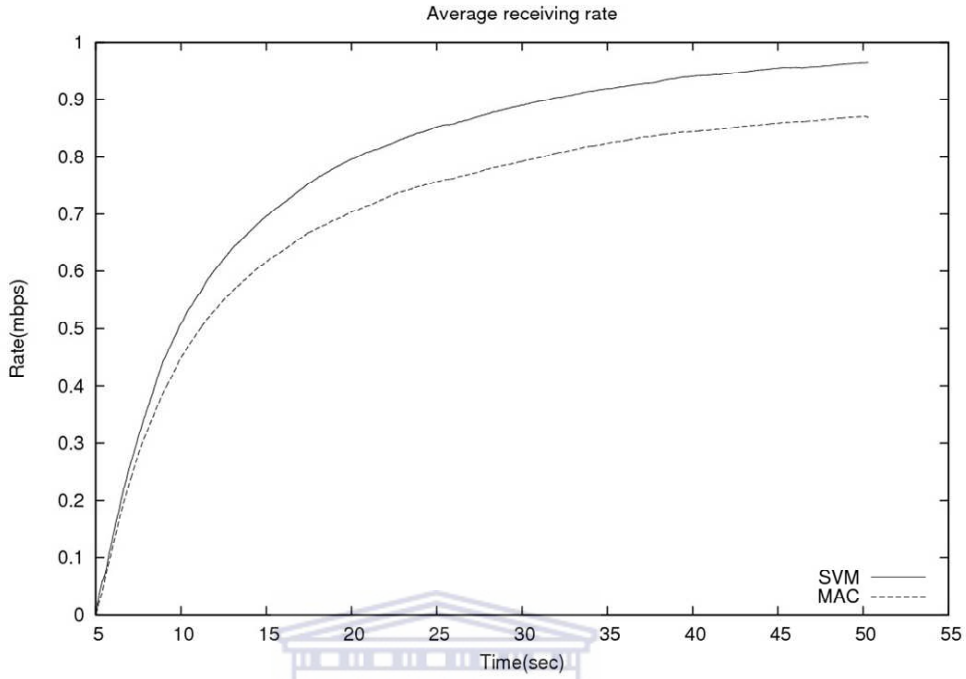

(a) Two average receiving rate curves generated by Simulation 1.

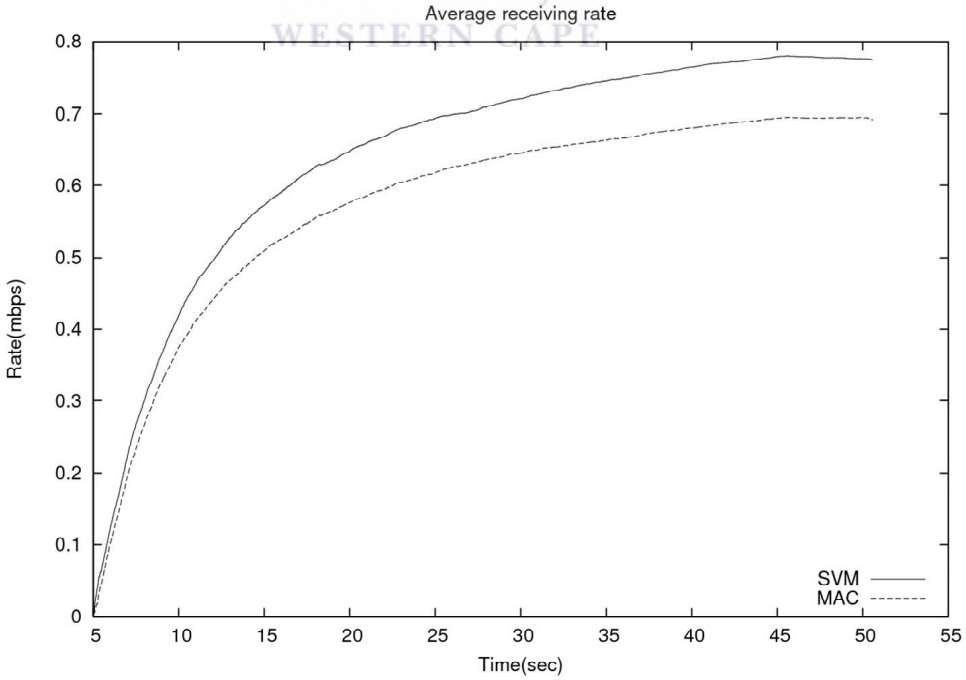

(b) Two average receiving rate curves generated by Simulation 2.

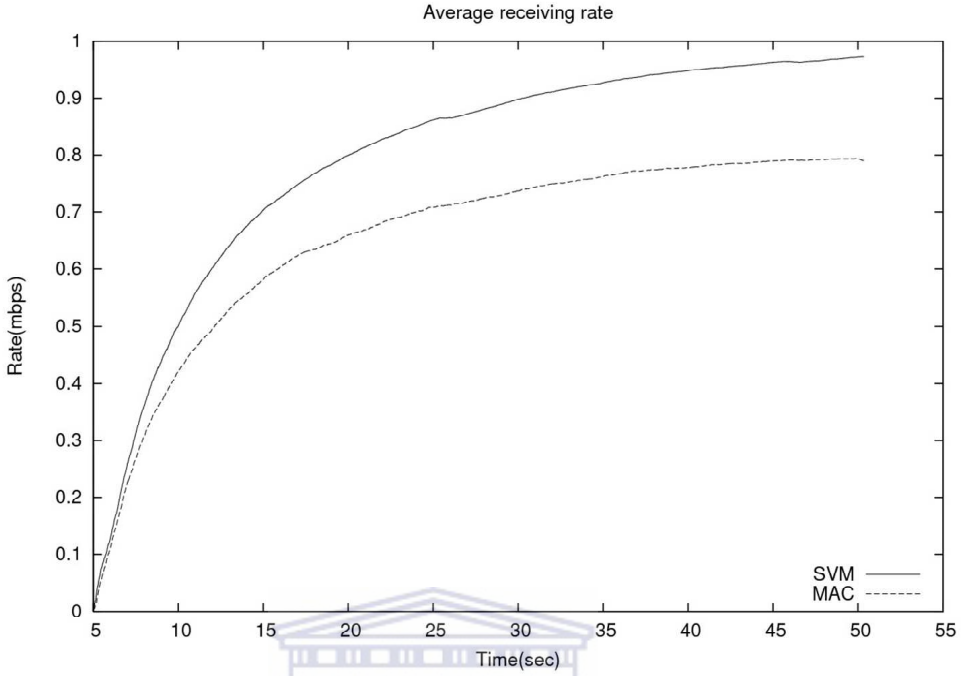

(c) Two average receiving rate curves generated by Simulation 3.

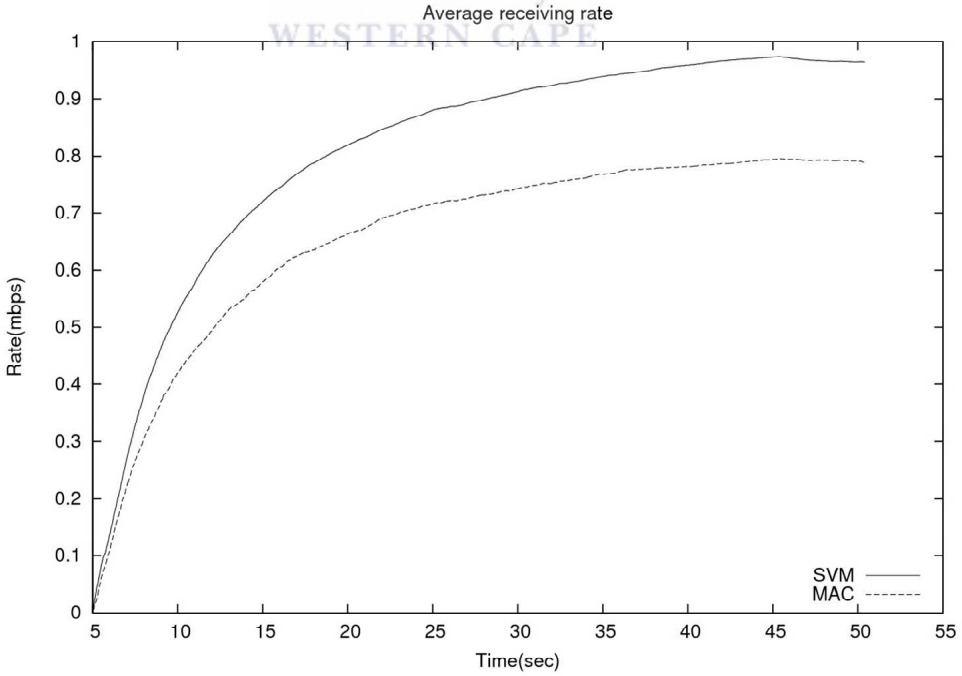

(d) Two average receiving rate curves generated by Simulation 4.

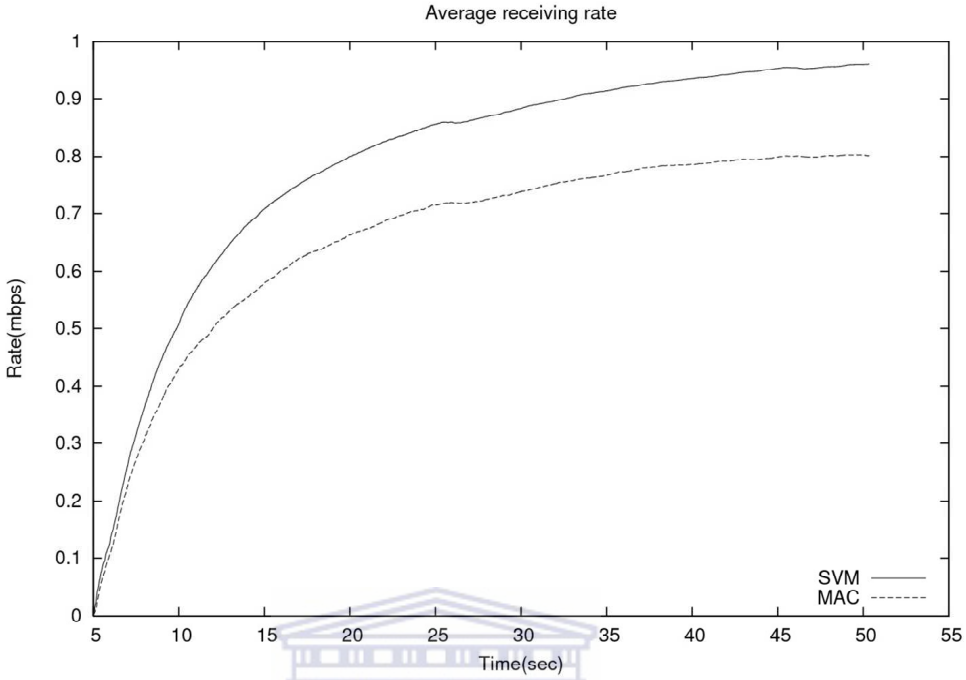

(e) Two average receiving rate curves generated by Simulation 5.

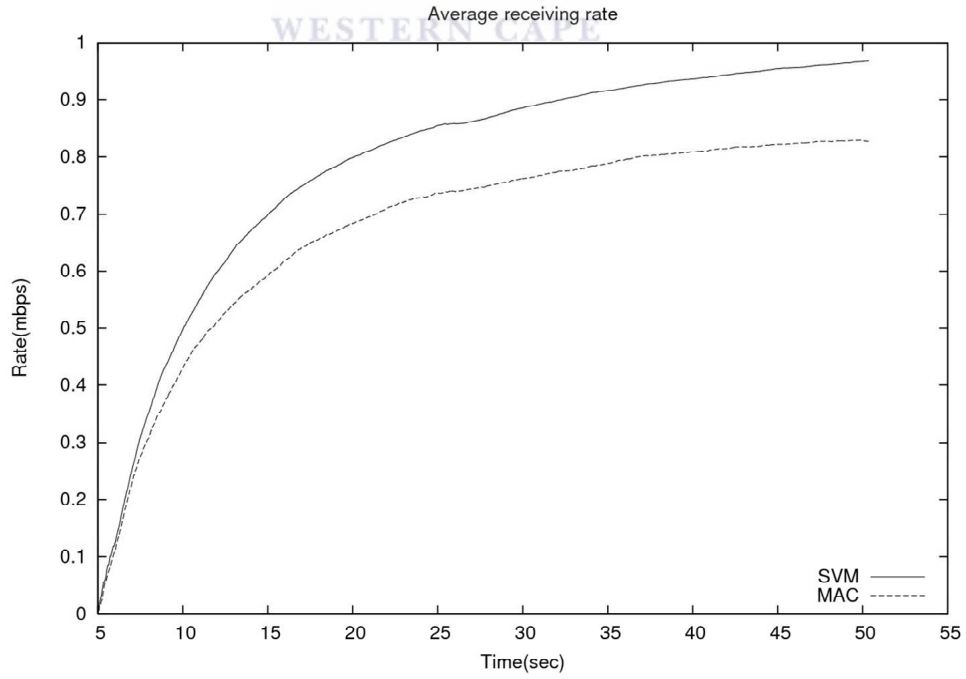

(f) Two average receiving rate curves generated by Simulation 6.

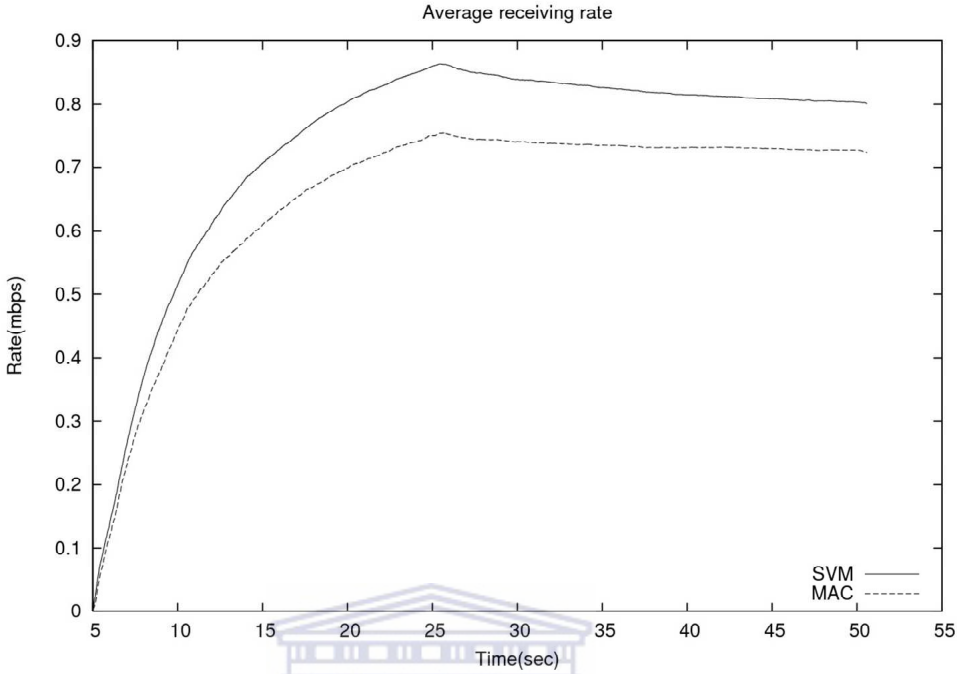

(g) Two average receiving rate curves generated by Simulation 7.

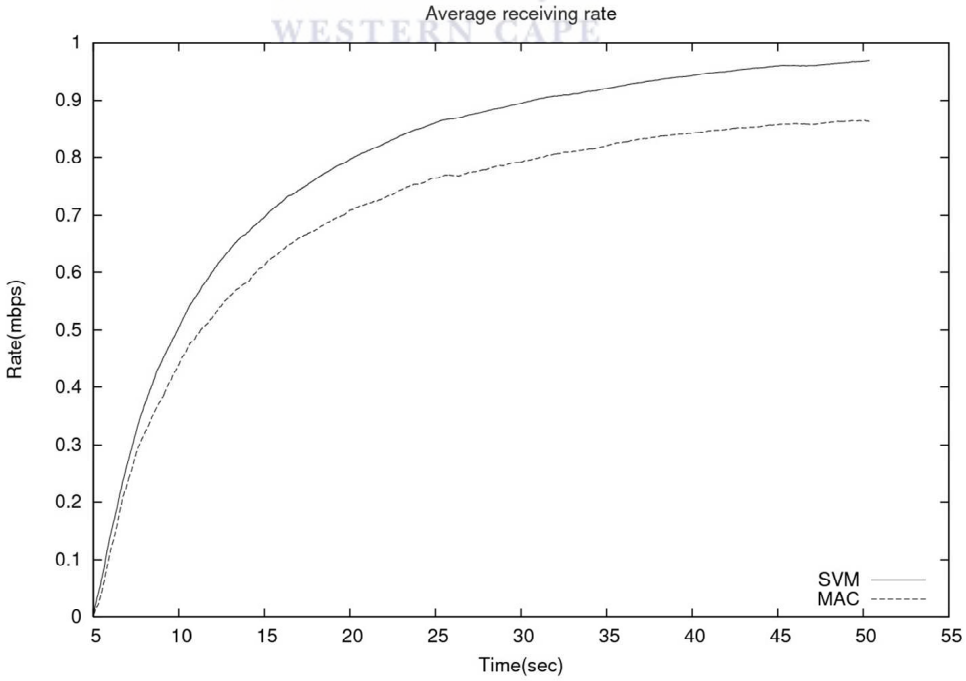

(h) Two average receiving rate curves generated by Simulation 8.

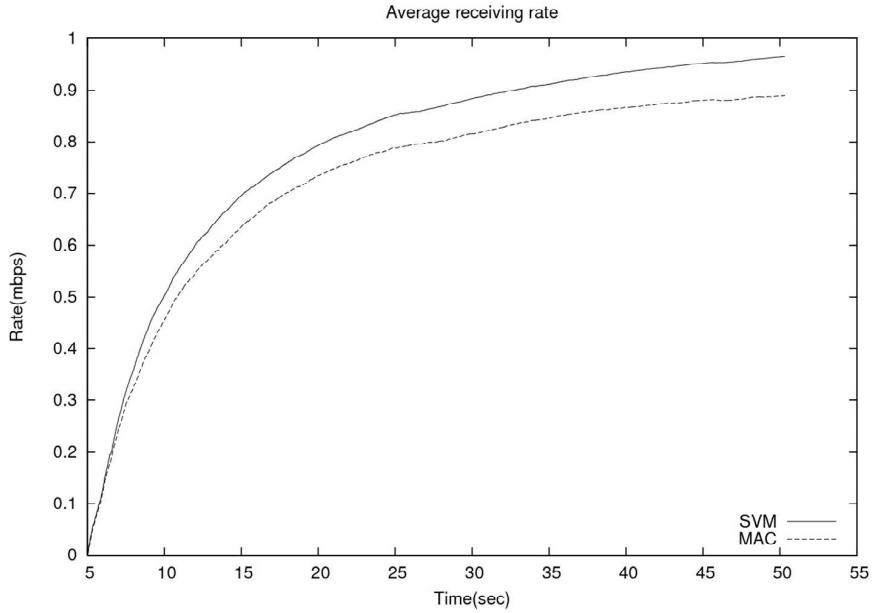

(i) Two average receiving rate curves generated by Simulation 9.

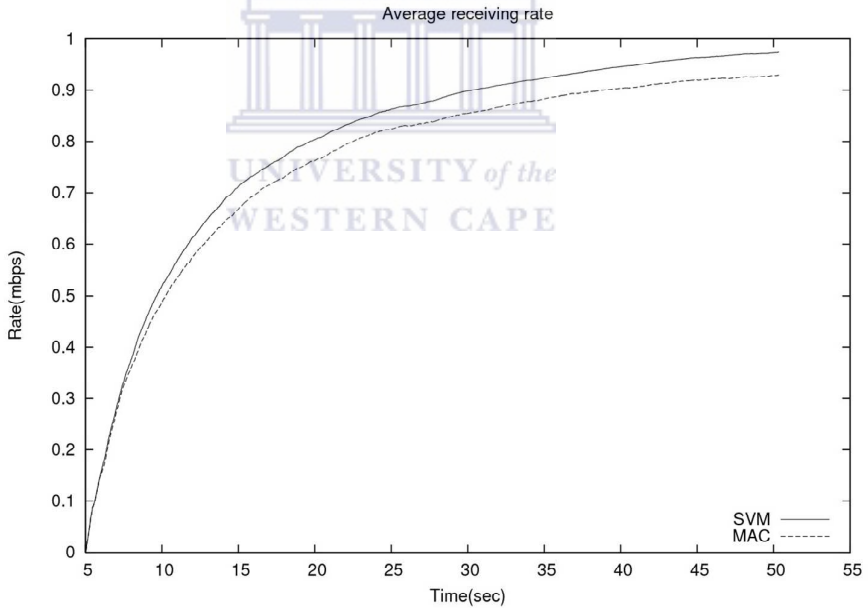

(j) Two average receiving rate curves generated by Simulation 10.

Figure 6.11: Two average receiving rate curves generated by ten simulations with WMCD scheme and MAC scheme at the slowest group member in local congestion loss detection scenario. The WMCD scheme achieve higher average receiving rate at the slowest group member than the MAC layer queue state measure scheme in all ten simulations of congestion loss detection.

6.5 Summary

In this work, we have described a unified framework which combines adaptive network models and support vector machine-based adaptive control structures for modelling and simulation of multicast congestion in mobile ad hoc network systems. By automatically adjusting network structures according to the dynamics of multicast packet streams, this framework allows researchers to adopt a suitable framework level on the basis of available network performance metrics, computational models of network management, their research study objectives and expected outcomes, thus allowing them to better understand, describe, predict, and control the multicast congestion in mobile ad hoc network systems. In this framework, a mobile ad hoc network system can be represented as an agent-based adaptive network which is defined by a feedback loop between the congestion states of group members and the group structure of the network, where the support vector machine-based adaptive control structures are used for driving the group structure of the wireless adaptive network model towards a desired state based on the prediction of incipient congestions. By using such a unified modelling framework, a set of instances of the wireless adaptive network model can be automatically generated through using structural situation information about the multicast packet streams. The generated instances with various group structures can improve the multicast transport performance in mobile ad hoc network systems because the high load can be relieved by group structure adaptation.

In the present work, a multicast congestion detection scheme, WMCD, has been developed for the unified modelling framework, in which the incipient congestions of group members can be predicted by using support vector machine-based prediction models and current traffic states. In this scheme, a congestion prediction model is created by SVMs which quantifies the dynamics of multicast packet flows. The multicast group members then automatically update their congestion states based on the congestion prediction model. By using the updated congestion states, a set of instances of the wireless adaptive network model with updated group structures are generated for dynamically adjusts the network topology and group structure of the mobile ad hoc network system and relieving the high load.

Our WMCD scheme can estimate the congestions before packet loss occurs at each group member using a SVM. Therefore, WMCD does not require acknowledge equivalent and negatively acknowledge equivalent feedbacks from receivers. Additionally, WMCD scheme requires no computation procedure for congestion estimation at the multicast source. While our scheme detects the congestion without introducing packet loss, other congestion control approaches only do the simplest packet loss detection at the group members. WMCD only updates the congestion states of group members for group structure adaptation according to the results of the SVM classification. Wireless losses are suppressed to prevent adjusting group structure improperly. The simulation results illustrate that our SVM-based WMCD scheme achieves great accuracy in predicting multicast congestion. Furthermore, the network's throughput capacity is efficiently improved through using the unified modelling framework, which dynamically adjusting the group structures according to the updated congestion states of group members generated by the WMCD scheme in order to relieve the high load.

Some approaches with machine learning have been applied to tackle network congestion management problems, such as Wang et al.'s scheme (Wang et al., 2007), Kang et al.'s work (Kang et al., 2009), and EI Khayat et al.'s work (EI Khayat et al., 2010). In comparison, our scheme is a receiver-based end-to-end multicast congestion detection scheme for MANETs. It does not require special support from other network management protocols. Furthermore, WMCD uses structural situation information (average number of the packets and variance) as the input data for SVM, while the methods mentioned above collect the traffic patterns (including packet delay, link quality indication metrics, etc.) for supervised learning. Our previous work (Liu & Omlin, 2010) also uses structural stream information to detect incipient multicast congestion. However it only works in wired networks. We realize that many problems still exist for which this approach is applicable, however, predicting congestion is the first step towards a unified framework for modelling and simulation of multicast congestion in mobile ad hoc network systems.

Wireless network congestion is a problem that changes very quickly. Any algorithm detecting congestion would have to render the decision before the problem has

changed to a degree that the decision is no longer relevant to the environment. Once trained, a SVM can render decisions very quickly. Therefore, the SVM is an appropriate mechanism for decision making in proactive wireless multicast congestion detection, and should be the target of more research. Moreover, the network performance can be effectively improved through using the unified modelling framework which combines adaptive network models and support vector machine-based adaptive control structures. Although the interaction between the dynamics of packet streams and the complex topologies in mobile ad hoc networks has not been studied in much detail in this work, it seems to provide a powerful modelling tool to build up large-scale structures from simple building blocks .

In the future work, we will investigate how different machine learning algorithms affect the performance of WMCD, such as neural networks, decision tree, etc. We will also investigate the temporal correlation of network congestions and improve the performance of WMCD with better congestion prediction models. Moreover, we also plan to update the WMCD scheme with a cost estimator, in which the routing and congestion control costs of a set of instances are measured, in order to generate the enhanced wireless adaptive network models with the minimum routing and congestion control costs.

CHAPTER 7
Conclusion and Future Work

This thesis represents the first steps towards the solution of modelling and simulation of various real-world adaptive networks within a unified framework which combines adaptive network models and adaptive control structures. In this framework, the state-topology coevolution of an adaptive network model is specified by various adaptive control structures. Moreover, through dynamically adjusting the controller parameters in terms of the observations of a real-world complex system, the adaptive interplay between state and topology as a dynamic feedback can drive an adaptive network model towards desired target states. Having such an automated modelling framework would greatly reduce the human effort and provide a valuable tool for better understanding, description, prediction, and control of the real-world complex systems around us. This unified modelling framework can also allow implementing comprehensive complex network system inter-/multi-disciplinary research studies based on available empirical data and computation models from different research fields. It has brought a unique approach to modelling and simulation of real-world complex systems.

In Chapter 3, a unified framework was proposed for modelling and simulation of complex systems using a combination of adaptive network models and adaptive control structures. While the process of modelling and simulation is considered as a control system with a state-topology feedback, this framework is not only able to automatically generate enhanced adaptive network models based on the observations of real-world complex systems, but also provide a systematic approach for automatic adjustment of control parameters in order to achieve or to maintain a desired topological property for the corresponding adaptive network models. Moreover, through tracing various reference values, the generated adaptive network models can have different structures which are similar to the studied complex systems when the systems change. While this chapter can be considered a generalized methodology, we discussed how this unified framework can be useful for modelling and simulation

of complex systems by the combination of adaptive network models and adaptive control structures.

In Chapter 4, a unified framework which combines adaptive network models and adaptive control structures was proposed for modelling and simulation of fractured-rock aquifer systems. In this framework, the adaptive control structures with iterative parameter identification were used to identifying an instance of an fracture adaptive network model with the desired topological characteristics, where the natural fracture network can be represented by the fracture adaptive network models with "state-topology" coevolution. By using this modelling framework, a user-friendly modelling tool, Fracture3D, has been developed for automatically building enhanced fracture adaptive network models, in which the fracture statistics and the structural properties can both follow the observed statistics from natural fracture networks. Through using simple field data and measurements taken on site or in-situ such as length, orientation, and density of measured fractures, the enhanced fracture adaptive network models can be built for rapidly evaluating the connectivity of the studied aquifers on a broad range of scales. For illustration purpose, we have applied the proposed unified modelling framework and automatic modelling tool Fracture3D on a real-world fractured-rock aquifer systems, and a set of the enhanced 3–D fracture adaptive network models with desired topological characteristics has been created by using Fracture3D. Through using label-propagation based cluster identification and Fracture fMRI techniques, the quantitative topological information extracted from these fracture adaptive network models have been used for understanding, description, and prediction of the groundwater flow and transport processes. Moreover, these quantitative data have also been used for studying parameter uncertainty of modelling and simulation in the studied fractured-rock aquifer systems. The simulations clearly show that the coupling between the fracture adaptive network models and the adaptive control structures with iterative parameter identification can drive the network topology towards a desired state by dynamically updating the geometrical states of fractures (size and profile of fractures) with a proper adaptive control structure.

In Chapter 5, a unified framework which combines adaptive network models

and multiple model adaptive control structures was proposed for modelling and simulation of social network systems. In this framework, a real-world social network system can be represented as an agent-based adaptive network which are defined by a feedback loop between behavioural state of individuals and community structure of the studied system, where a multiple model adaptive control structure is used for the predetermination of suitable computational models of behavioural state update and social interaction update in order to improve the performance of modelling and simulation. By using such a unified modelling framework, an automatic modelling tool, SMRI, is developed for automatically building enhanced social adaptive network models through using mobile-phone-centric multimodal data with suitable computational models of behavioural state update and social interaction update. We have applied our SMRI on a real-world social network system by using a mobile-phone-centric multimodal dataset. Two experiments were performed for demonstrating how to conduct a research case study on social network modelling by using the automatic modelling tool. In the first experiment, a set of enhanced social adaptive network models were automatically generated based on various periodic social contact data and different computation models of social interaction strength. The simulation results demonstrate that the enhanced social adaptive network models whose community structures are similar to the studied real-world social network systems can be automatically built through using SMRI and periodic social contact histories of individuals, when these social contact data are generated from various mobile-sensing based data sources. In the second experiment, the experimental results with different social adaptive network models having different computation models of data and feature processing show that our automatic modelling tool SMRI with data-fusion based and feature-fusion based feature enhancement methods can be used for improving the performance of certain computational models when raw data are noisy. Moreover, the results of both two experiments also demonstrated that the coupling between the social adaptive network models and the multiple model adaptive control structures can drive the community structure of a social adaptive network model towards a desired state through using suitable computational models of behavioural state update and social interaction update predetermined by the

multiple model adaptive control structure.

In Chapter 6, a unified framework which combines adaptive network models and support vector machine-based adaptive control structures for modelling and simulation of multicast congestion in mobile ad hoc network systems was introduced. In this framework, a mobile ad hoc network system can be represented as an agent-based adaptive network which is defined by a feedback loop between congestion states of group members and group structure of the network, where the support vector machine-based adaptive control structures are used for the prediction of incipient congestions. Moreover, a multicast congestion detection scheme, WMCD, has been developed for the unified modelling framework, in which the incipient congestions of group members can be predicted by using support vector machine-based prediction models and current traffic states. In this scheme, a congestion prediction model is created by SVMs which quantifies the dynamics of multicast packet flows. The multicast group members then automatically update their congestion states based on the congestion prediction model. By using the updated congestion states, a set of instances of the wireless adaptive network model with updated group structures are generated for dynamically adjusting the network topology and group structure of the mobile ad hoc network system and relieving the high load. In order to estimate the classification accuracy of the WMCD scheme, a set of simulations was implemented which compared the classification results of the WMCD scheme to the detection results of the MAC layer queue state measure method. We also performed a set of simulations with group structure adaptation for evaluating the performance of our WMCD scheme, while the unified modelling framework was used for multicast congestion control in MANETs. The simulation results illustrate that our SVM-based WMCD scheme achieves great accuracy in predicting multicast congestion. Furthermore, the network's throughput capacity is efficiently improved through using the unified modelling framework, which dynamically adjusts the group structures according to the updated congestion states of group members generated by the WMCD scheme in order to relieve the high load.

The results represented in this work demonstrated the applicability and use of the unified framework with the combination of adaptive network models and

adaptive control structures for modelling and simulation of different real-world complex systems, including fractured-rock aquifer systems, social network systems, and mobile ad hoc network systems. Moreover, adaptive control techniques provide a systematic approach for automatic adjustment of control parameters of adaptive network models in order to generate a set of the enhanced adaptive network models which follow the observations from real-world complex systems, while the adaptive network models provide an abstraction of complex systems allowing to draw high-level analogies between seemingly different research fields and phenomena. We have used this unified modelling framework to develop three automatic modelling tool for different real-world complex systems, namely Fracture3D for fractured-rock aquifer systems, SMRI for social network systems, and WMCD for mobile ad hoc network systems. In all these case studies, our unified modelling framework has provided a systematic approach for automatically generating the enhanced adaptive network models, which follow the observations of studied systems, on the basis of available empirical data and computational models from different research fields, research study objectives, and expected outcomes.

The adaptive network model-based approach provides a powerful abstraction of many different real-world complex systems, which targets the interplay between local dynamics and topological coevolution and its implications for system behaviour. More insights of complicated system behaviours can be gained from the adaptive network modes because it present more realistic coevolutionary dynamics between the node states and the network topology in the system. In this work, a unified modelling framework is established by considering different complex systems as adaptive networks, while a suitable adaptive control structure can drive the dynamical network structure towards a desired state. Moreover, the combination of adaptive network models and adaptive control structures can deepen our understanding of complex systems.

Although an agent-based modelling approach can simulate very intricate dynamical processes while fully incorporating stochastic effects, the agent-based models are often very complicated and it is difficult to study the impact of any given modelling assumption or parameter. Moreover, the adaptive network models may be

rendered impractical due to the unrealistic assumptions and poor sample quality, and their accuracy suffers significantly from a lack of knowledge about the conditions of real-world complex systems or other useful information related to the assumptions. In order to improve the performance of the adaptive network models, a set of adaptive control technologies have been used for automatic control parameter adjustment of the adaptive network models to drive the network structures towards a desired state. In recent years, adaptive control methodologies have become more and more popular as a way of improving performance and functionality of control systems, because it provides a systematic approach for automatic adjustment of controllers in non-linear dynamical systems. Moreover, a desired level of control system performance can be achieved or maintained through modifying a controller's behaviour in response to changes in the dynamics of the studied systems. In the present work, three different adaptive control structures, including iterative parameter identification, multiple model adaptive control, and support vector machine-based adaptive control, have been used for automatically generating enhanced adaptive network models with suitable control parameters in various complex systems. In these case studies, the control parameters of adaptive network models were included as a part of the state-topology coevolution, while they are considered as internal parameters and automatically adjusted according to the observations of the studied complex systems. We conducted a set of experiments and simulations in different real-world complex systems in order to verify the validity of the proposed unified modelling framework and three automatic modelling tools, namely Fracture3D, SMRI, and WMCD. The simulation results demonstrated that the adaptive control approach is a useful tool for the performance improvement of the adaptive network models which allows us to gain more insights into the dynamical mechanisms behind the observed system behaviour in these models.

In order to generate meaningful adaptive network models from large-scale temporal network data, a set of analytical modelling approaches have been developed. In more complicated adaptive network models, however, the analytical approaches might not lead to solvable equations. Moreover, these analytical modelling approaches cannot provide a complete picture of the studied complex system because

individual heterogeneity or other possible fluctuations are ignored. In this situation, agent-based models can be applied. In this work, we have presented detailed agent-based modelling and simulations with the combination of adaptive network models and adaptive control structures in various real-world complex systems. A set of enhanced adaptive network models was generated based on the coevolution of the node (agent) state dynamics and topological dynamics with suitable control parameters. Through using the generated enhanced adaptive network models, better understanding, description, prediction, and control of the complicated system behaviours can be gained in the studied complex systems.

While the current adaptive network models remain mostly theoretical and conceptual, how to consolidate these models with empirical data of real-world complex systems is one of key challenges in adaptive network research. In this work, our unified modelling framework and three automatic modelling tools have shown how to generate meaningful adaptive network models from empirical data of real-world complex systems. Furthermore, network sampling, network measuring, network modelling, and model validation can be automatically implemented within this unified framework for modelling and simulation of different real-world complex systems. Although small-scale simulations with relatively simple operation rules of the models were performed in the present work, we hope that the techniques presented here may help multidisciplinary researchers for developing more complex and more accurate adaptive network models through using appropriate empirical data and computation models from different research fields.

Many areas of complex system research have adopted the "network perspective" and are advancing the state of the art. However, one of the biggest challenges that has to be faced in the future is how to make the real world complex systems "cognitive" by perceiving current network conditions and automatically adjusting system behaviour appropriately in order to improve the system performance. To address this challenge, "network learning" might be a key technology. We have demonstrated network sampling, network measuring, network modelling, and model validation can be automatically implemented within a unified framework which combines adaptive network models and adaptive control structures. Thus,

the performance of the studied complex systems can be improved by topological adaptation according to the enhanced adaptive network models. We expect that further integrating adaptive network models with adaptive control theory will open new avenues to transform “complex networks” towards “cognitive networks”.

List of Abbreviations

AODV	ad hoc on-demand distance vector routing
CDR	call detail records
CFD	clustered fracture density
CFS	contact frequency strength
CTS	contract trust strength
DCS	direct contact strength
DFN	discrete fracture network
FMRI	fracture mapping and realization imaging
Fracture3D	3–D fracture adaptive network modelling
GPS	global positioning system
ICS	indirect contact strength
MAC	media access control
MANET	mobile ad hoc network
MCBR	multicast constant bit rate
MRAC	model reference adaptive control
ODMRP	on-demand multicast routing protocol
PTS	propagation trust strength
RSPM	relative social pressure metric
SMRI	social relationship mapping and realization imaging
SIS	susceptible-infected-susceptible
Social MRI	social relationship imaging
SPM	social pressure metric
STR	self-tuning regulators
SVC	support vector classification
SVM	support vector machine
SVR	support vector regression
TFS	trust frequency strength
WMCD	wireless multicast congestion detection

REFERENCES

Adali, S., Escriva, R., Goldberg, M. K., Hayvanovych, M., Magdon-Ismail, M., Szymanski, B. K., Wallace, W. A., & Williams, G. (2010). Measuring behavioral trust in social networks. In *Proceedings of the IEEE International Conference on Intelligence and Security Informatics* (pp. 150–152). Vancouver, Canada.

Adali, S., Sisenda, F., & Magdon-Ismail, M. (2012). Actions speak as loud as words: Predicting relationships from social behavior data. In In *Proceedings of the 21st International Conference on World Wide Web* (pp 689–698). Lyon, France.

Aharony, N., Pan, W., Ip, C., Khayal, I., & Pentland, A. (2011a). Social fMRI: Investigating and shaping social mechanisms in the real world. *Pervasive and Mobile Computing*, *7*(6), 643–659.

Aharony, N., Pan, W., Ip, C., Khayal, I., & Pentland, A. (2011b). The social fmri: measuring, understanding, and designing social mechanisms in the real world. In *Proceedings of the 13th International Conference on Ubiquitous Computing* (pp. 445–454). Beijing, China.

Airoldi, E. M., Bai, X., & Carley, K. M. (2011). Network sampling and classification: An investigation of network model representations. *Decision Support Systems.51*(3) 506–518.

Alava, M. J., Nukala, P. K. V. V., & Zapperi, S. (2006). Statistical models of fracture, *Advances in Physics*, *55*(3–4), 349–476.

alla, G., Barabási, A. L., & Vicsek, T. (2007). Quantifying social group evolution. *Nature*, *446*(7136), 664–667.

Arenas, A., Díaz-Guilera, A., & Pérez-Vicente, C. J. (2006). Synchronization reveals topological scales in complex networks. *Physical Review Letters*, *96*, 114102 .

Aström, K. J., & Wittenmark, B. (2013). *Adaptive control* (2nd ed.). Mineola, NY: Dover Publications, Inc.

Axtell, R. L. (1999). *The emergence of firms in a population of agents: Local increasing returns to scale, unstable nash equilibria, and power law size distributions*. Center on Social and Economic Dynamics, Brookings Institution, Washington, D.C.

Axtell, R. L., Epstein, J., & Young, H. (1999). The emergence of classes in a multiagent bargaining model. *Social Dynamics*, 191–211.

Böhme, G. A., & Gross, T. (2011). Analytical calculation of fragmentation transitions in adaptive networks. *Physical Review E*, *83*, 035101.

Börner, K., Sanyal S., & Vespignani, A. (2007). Network science. *Annual Review of Information Science & Technology*, *41*, 537–607.

Baecher, G. B. (1983). Statistical analysis of rock mass fracturing. *Mathematical Geology*, *15*(2), 329–348.

Bagrow, J., Bollt, E., & Costa, L. d. F. (2006). Network structure revealed by short cycles. eprint arXiv:cond-mat/0612502.

Bailey, A. M., Lawrence, M. B., Shang, H., Katz, A. J., & Peirce, S. M. (2009). Agent-based model of therapeutic adipose-derived stromal cell trafficking during ischemia predicts ability to roll on P-selectin. *PLoS Computational Biology*, *5*(2), e1000294.

Bala, V. & Goyal, S. (2001). Conformism and diversity under social learning. *Economic Theory*, *17*, 101–120.

Baldi, P., Frasconi, P., & Smyth, P. (2003). *Modeling the Internet and the Web: Probabilistic methods and algorithms*. Hoboken, NJ: Wiley.

Ball, P. (2002). The physics of society. *Nature*, *415*, 371.

Bankes, S. C. (2002). Agent-based modeling: A revolution? *proceedings of the national academy of sciences*, *99*(Suppl 3), 7199–7200.

Barabási, A. L., & Albert, R. (1999). Emergence of scaling in random networks. *Science*, *286*(5439), 509–512.

Barabási, A. L., Hövel, P., Musella, G., & Martino, M. (2014). *Network science*. http://barabasilab.neu.edu/networksciencebook/.

Barrat, A., Barthélemy, M., & Vespignani, A. (2008). *Dynamical processes on complex networks*. New York, NY: Cambridge University Press.

Barrat, A., Barthélemy, M., Pastor-Satorras, R., & Vespignani, A. (2004). The architecture of complex weighted network. /emphProceedings of the National Academy of Sciences, *101*(11), 3747–3752.

Barreteau, O. (2003). Our companion modelling approach. *Journal of Artificial Societies and Social Simulation*, *6*(1).

Barthelemy, M. (2010). Spatial networks. *Physics Reports*, *499*(1–3), 1–101.

Batty, M. (2007). *Cities and complexity: Understanding cities with cellular automata, agent-based models, and fractals*. Cambridge, MA: MIT Press.

Baumgart, I., Heep, B., Krause, S. (2007). Oversim: A flexible overlay network simulation framework. In *Proceedings of the 10th IEEE Global Internet Symposium* (pp. 79–84). Anchorage, AK.

Baumung, P. (2005). Stable, congestion-controlled application-layer multicasting in pedestrian ad-hoc networks. In *Proceedings of the Sixth IEEE International Symposium on World of Wireless Mobile and Multimedia Networks* (pp. 57–64). Taormina, Italy.

Baumung, P., Zitterbart, M., & Kutzner, K. (2004). Improving delivery ratios for application layer multicast in mobile ad-hoc networks. *Computer communications*, *28*(14), 1669–1679.

Beggs, J., & Plenz, D. (2003). Neuronal avalanches in neocortical circuits. *Journal of Neuroscience*, *23*, 11167-11177.

Bennett, K., & Blue, J. (1997). *A Support Vector Machine Approach to Decision Tree*. (Math report), Rensselaer Polytechnic Institute, Troy, NY.

Berkowitz B., & Adler, P. M. (1998). Stereological analysis of fracture network structure in geological formations. *Journal of Geophysical Research: Solid Earth*, *103*(B7), 15339–15360.

Berkowitz, B. (1995). Analysis of fracture network connectivity using percolation theory. *Mathematical Geology*, *27*(4), 467–483.

Berkowitz, B., Bour, O., Davy, P., & Odling, N. (2000). Scaling of fracture connectivity in geological formations. *Geophysical Research Letters*, *27*(14), 2061–2064.

Bettencourt, L. M. A., Cintron-Arias, A., Kaiser, D. I., & Castillo-Chavez, C. (2005). The power of a good idea: quantitative modeling of the spread of ideas from epidemiological models. eprint arXiv:physics/0502067.

Bitmead, R. R. (1993). Iterative control design approaches. In *Proceedings of the 12th IFAC World Congress*, *9*, 381–384.

Blasius, B., & Gross, T. (2009). Dynamic and topological interplay in adaptive networks. *Annual Reviews of Nonlinear Dynamics and Complexity*, *2*, 63–106.

Blondel, V. D., Guillaume, J. -L., Lambiotte, R. & Lefebvre, E. (2008). Fast unfolding of communities in large networks. *Journal of Statistical Mechanics: Theory and Experiment*, *2008*(10), P10008.

Boccaletti, S., Latora, V., Moreno, Y., Chavez, M., & Hwang, D. (2006). Complex networks: Structure and dynamics.*Physics Reports. 424*(4–5), 175–308.

Boccaletti, S., Latora, V., & Moreno, Y. (2010). *Handbook on Biological Networks*. Singapore, SN: World Scientific Publishing Company.

Bollobás, B. (1998) *Modern graph theory*. Berlin, Germany: Springer-Verlag GmbH, 1998.

Bonabeau, E. (2002). Agent-based modeling: Methods and techniques for simulating human systems.*Proceedings of the National Academy of Sciences*, *99*(Suppl 3), 7280–7287.

Bonamy D., & Bouchaud, E. (2011). Failure of heterogeneous materials: A dynamic phase transition? *Physics Reports*, *498*(1), 1–44.

Bornholdt, S., & Roehl, T. (2003). Self-organized critical neural networks. *Physical Review E*, *67*, 066118.

Bornholdt, S., & Rohlf, T. (2000). Topological evolution of dynamical networks: Global criticality from local dynamics. *Physical Review Letters*, *84*, 6114–6117.

Bour, O. (2002). A statistical scaling model for fracture network geometry, with validation on a multiscale mapping of a joint network (Hornelen Basin, Norway). *Journal of Geophysical Research*, *107*(B6), 2113.

Bradbury, K. R., & Muldoon, M. A. (1994). Effect of fracture density and anisotropy on delineation of wellhead protection area in fractured-rock aquifers. *Applied Hydrogeology*, *2*(3), 17–23.

Brandes, U., & Wagner, D. (2000). *Graph-Theoretic concepts in computer science: 26th international workshop, WG 2000 Konstanz, Germany, June 15–17, 2000 Proceedings*. New York, NY: Springer,

Bulut, E., & Szymanski, B. K. (2012). Exploiting friendship relations for efficient routing in mobile social networks. *IEEE Transactions onParallel and Distributed Systems*, *23*(12), 2254–2265.

Bulut, E., Geyik, S. C., & Szymanski, B. K. (2014). Utilizing correlated node mobility for efficient DTN routing. *Pervasive and Mobile Computing*, *13*, 150–163.

Buskens, V., & van de Rijt, A. (2008). Dynamics of networks if everyone strives for structural holes. *American Journal of Sociology*, *114*(2), 371–407.

Butz, M. V., Herbort, O., & Hoffmann J. (2007). Exploiting redundancy for exible behavior: Unsupervised learning in a modular sensorimotor control architecture. *Psychological Review*, *114*(3), 1015-1046.

Cacas, M. C., Ledoux, E., de Marsily, G., & Tilli, B. (1990a). Modeling fracture flow with a stochastic discrete fracture network: Calibration and validation: 1. The flow model. *Water Resources Research*, *26*(3), 479–489.

Cacas, M. C., Ledoux, E., de Marsily, G., Barbreau, A., Calmels, P., Gaillard, B., & Margritta, R. (1990b). Modeling fracture flow with a stochastic discrete fracture network: Calibration and validation: 2. The transport model. *Water Resources Research*, *26*(3), 491–500.

Calise, A. J., Hovakimyan, N., & Idan, M. (2001). Adaptive output feedback control of nonlinear systems using neural networks. *Automatica*, *37*(8), 1201–1211.

Calliess, J., Papachristodoulou, A., & Roberts, S. J. (2013). Stochastic processes and feedback-linearisation for online identification and Bayesian adaptive control of fully-actuated mechanical systems. In *Proceedings of the Advances in Machine Learning for Sensorimotor Control.* Stateline, NV.

Camacho, J., Guimerá, R., & Amaral, L. A. N. (2002). Robust patterns in food web structure. *Physical Review Letters*, *88*, 228102.

Cao C., & Hovakimyan, N. (2007). Novel L1 neural network adaptive control architecture with guaranteed transient performance. *IEEE Transactions on Neural Networks*, *18*(4), 1160–1171.

Cao, C., & Hovakimyan, N. (2008). Design and analysis of a novel adaptive control architecture with guaranteed transient performance. *IEEE Transactions on Automatic Control*, *53*(2), 586–591.

Carpenter, C., & Sattenspiel, L. (2009). The design and use of an agent-based model to simulate the 1918 influenza epidemic at Norway House, Manitoba. *American Journal of Human Biology*, *21*(3), 290–300.

Carrington, P., Scott, J., & Wasserman, S. (2004). *Models and methods in social network analysis*. New York: Cambridge University Press.

Centola, D. (2010). The spread of behavior in an online social network experiment. *Science*, *329*, 1194–1197.

Centola, D. (2011). An experimental study of homophily in the adoption of health behavior. *Science*, *334*, 1269–1272.

Centola, D., Gonzalez-Avella, J. C., Eguiluz, V. M., & San Miguel, M. (2007). Homophily, cultural drift, and the co-evolution of cultural groups. *Journal of Conflict Resolution*, *51*, 905–929.

Chang, C. & Lin, C. (2001–2004). *LIBSVM: A library for support vector machines*. (Technical report), National Taiwan University, Republic of China. http://www.csie.ntu.edu.tw/ cjlin/libsvm/.

Chen, X., & Zhan, F. (2008). Agent-based modelling and simulation of urban evacuation: Relative effectiveness of simultaneous and staged evacuation strategies. *Journal of the Operational Research Society*, *59*(1), 25–33.

Chialvo, D. R., & Bak, P. (1999). Learning from mistakes. *Neuroscience*, *90*, 1137–1148.

Chowdhary, G., How, J. P., & Kingravi, H. (2012). Model reference adaptive control using nonparametric adaptive elements. In *Proceedings of the Conference on Guidance Navigation and Control* (pp. 1–24). Minneapolis, MN.

Christensen, K., Donangelo, R., Koiller, B., & Sneppen, K. (1998). Evolution of random networks. *Physical Review Letters*, *81*, 2380–2383.

Costa, L. d. F., Oliveira, O. N., Travieso, G., Rodrigues, F. A., Villas Boas, P. R., Antiqueira, L.,Viana, M. , & Correa Rocha, L. E. (2011). Analyzing and modeling real-world phenomena with complex networks: a survey of applications. *Advances in Physics*. *60*(3), 329–412.

Costa, L. d. F., Rodrigues, F. A., Travieso, G., & Villas Boas, P. R. (2007). Characterization of complex networks: A survey of measurements. *Advances in Physics*. *56*(1), 167–242.

Couzin, I. D., Ioannou, C. C., Demirel, G., Gross, T., Torney, C. J., Hartnett, A., Conradt, L., Levin, S. A., & Leonard, N. E. (2011). Uninformed individuals promote democratic consensus in animal groups. *Science*, *334*, 1578–1580.

Daley, D. J., Gani, J., & Cannings, C. (1999). *Epidemic modeling: An introduction*. Cambridge, UK: Cambridge University Press.

Dancik, G. M., Jones, D. E., & Dorman, K. S. (2010). Parameter estimation and sensitivity analysis in an agent-based model of Leishmania major infection.*Journal of Theoretical Biology*, *262*(3), 398–412.

Danon, L., Diaz-Guilera, A., Duch, J., & Arenas, A. (2005). Comparing community structure identification. *Journal of Statistical Mechanics: Theory and Experiment*, /emph2005(09), P09008.

de Dreuzy, J. R., Davy, P., & Bour, O. (2000). Percolation parameter and percolation-threshold estimates for three-dimensional random ellipses with widely scattered distributions of eccentricity and size. *Physical Review*, *62*(5), 5948–5952.

Degenne A., & Forsé, M. (1999). *Introducing social networks*. London, UK: Sage Publications Ltd.

Delvenne, J. C., Yaliraki, S. N., & Barahona, M. (2010). Stability of graph communities across time scales. *Proceedings of the National Academy of Sciences*, *107*(29), 12755–12760.

Demirel, G., Prizak, R., Reddy, P. N., & Gross, T. (2011). Opinion formation and cyclic dominance in adaptive networks. *European Physical Journal B*, *84*, 541–548.

Devillers, H., Lobry, J. R., & Menu, F. (2008). An agent-based model for predicting the prevalence of Trypanosoma cruzi I and II in their host and vector populations.*Journal of Theoretical Biology*, *255*(3), 307–315.

Dionne, S. D., Sayama, H., Hao, C., & Bush, B. J. (2010). The role of leadership in shared mental model convergence and team performance improvement: An agent-based computational model. *The Leadership Quarterly*, *21*(6), 1035–1049.

Do A.-L. (2011). *Self-organization in continuous adaptive networks* (Doctoral dissertation). University of Oldenburg, Germany.

Do, A.-L., Rudolf, L., & Gross, T. (2010). Patterns of cooperation: Fairness and coordination in networks of interacting agents. *New Journal of Physics*, *12*, 063023.

Dorogovtsev, S. N., Goltsev, A.V., & Mendes, J. F. F. (2002). Ising model on networks with an arbitrary distribution of connections. *Physical Review E*, *66*, 016104.

Dorogovtsev, S. N., Goltsev, A.V., & Mendes, J. F. F. (2008). Mendes, Critical phenomena in complex networks. *Reviews of Modern Physics*, *80*, 1275–1335.

Dorogovtsev, S., & Mendes, J. (2002). Evolution of networks. *Advances in physics*, *52*(4), 1079–1187.

Dubois-Ferriere, H., Grossglauser, M. & Vetterli, M. (2003). Age matters: Efficient route discovery in mobile ad hoc networks using contact ages. In *Proceedings of the ACM International Symposium on Mobile Ad Hoc Networking and Computing* (pp. 257–266). Annapolis, MD.

Eagle, N. N. (2005). *Machine perception and learning of complex social systems* (Doctoral dissertation). Massachusetts Institute of Technology, Cambridge, MA.

Eagle, N. N., & Pentland, A. S. (2006). Reality mining: sensing complex social systems. *Personal and Ubiquitous Computing*, *10*(4), 255–268.

Eagle, N. N., Macy, M., & Claxton, R. (2010). Network diversity and economic development. *Science*, *328*(5981), 1029–1031.

Eagle, N. N., Pentland A. S., & Lazer, D. (2009). Inferring friendship network structure by using mobile phone data. *Proceedings of the National Academy of Sciences*, *106*(36), 15274–15278.

Eckmann, J. P., & Moses, E. (2002). Curvature of co-links uncovers hidden thematic layers in the World Wide Web. *Proceedings of the National Academy of Sciences*, *99*(9), 5825–5829.

Eguíluz, V. M., Zimmermann, M. G., Cela-Conde, C. J., & San Miguel, M. (2005). Emergence of role differentiation in the dynamics of social networks. *American Journal of Sociology*, *110* (4), 977–1008.

El Khayat, I., Geurts, P., & Leduc, G. (2010). Enhancement of TCP over wired/wireless networks with packet loss classifiers inferred by supervised learning. *Wireless Networks*, *16*(2), 273–290.

Epstein, J. M., Parker, J., Cummings, D., & Hammond, R. A. (2008). Coupled contagion dynamics of fear and disease: mathematical and computational explorations. *PLoS one*, *3*(12), e3955.

Erdös, P., & Rényi, A. (1959). On random graphs, I. *Publ. Math. Debrecen*, *6*, 290–297.

Erdös, P., & Rényi, A. (1960). On the evolution of random graphs. *Publ. Math. Inst. Hungar. Acad. Sci*, *5*, 17–61.

Fagiolo, G., Birchenhall, C., & Windrum, P. (2007). Empirical validation in agent-based models: Introduction to the special issue. *Computational Economics*, *30*(3), 189–194.

Fan, Y., Li, M., Zhang, P., Wu, J., & Di, Z. (2007). Accuracy and precision of methods for community identification in weighted networks. *Physica A: Statistical Mechanics and its Applications*. *377*(1), 363–372.

Folcik, V. A., An, G. C., & Orosz, C. G. (2007). The basic immune simulator: An agentbased model to study the interactions between innate and adaptive immunity. *Theoretical Biology and Medical Modelling*, *4*, 39.

Fortunato, S. (2010). Community detection in graphs. *Physics Reports*, *486*(3–5), 75–174.

Fortunato, S., & Barthélemy, M. (2007). Resolution limit in community detection. *Proceedings of the National Academy of Sciences*, *104*(1), 36–41.

Fowlkes, E. B., & Mallows, C. L. (1983). A method for comparing two hierarchical clusterings. *Journal of the American Statistical Association*, *78*(383), 553–569.

Freeman, L. C. (1977). A set of measures of centrality based on betweenness. *Sociometry*, *40*, 35–41.

Freeman, L. C. (1979). Centrality in social networks: Conceptual clarification. *Social Networks*, *1*, 215–239.

Funk, S., Gilad, E., Watkins, C., & Jansen, V. A. A. (2009). The spread of awareness and its impact on epidemic outbreaks, *Proceedings of the National Academy of Sciences*, *106*, 6872–6877.

Funk, S., Salathé, M., & Jansen, V. A. A. (2010). Modelling the influence of human behaviour on the spread of infectious diseases: a review. *Journal of the Royal Society Interface*, *7*, 1247–1256.

Galvao, V., & Miranda, J. G. (2010). A three-dimensional multi-agent-based model for the evolution of Chagas disease. *Biosystems*, *100*(3), 225–230.

Galvao, V., Miranda, J. G., & Ribeiro-dos-Santos, R. (2008). Development of a twodimensional agent-based model for chronic chagasic cardiomyopathy after stem cell transplantation *Bioinformatics*, *24*(18), 2051–2056.

Garrido, P. P., Malumbres, M. P., & Calafate, C. T. (2008). ns-2 vs. OPNET: a comparative study of the IEEE 802.11 e technology on MANET environments. In *Proceedings of the First International Conference on Simulation Tools and Techniques for Communications, Networks and Systems* (p. 37). Marseille, France.

Gershenson, C. (2005). Self-organizing traffic lights. *Complex Systems*, *16*(1), 29–53.

Ghaffari, H. O., Nasseri, M. H. B., & Young, R. -P. (2011). Fluid Flow Complexity in Fracture Networks: Analysis with Graph Theory and LBM. e-print arXiv:1107.4918.

Gil, S., & Zanette, D. (2006). Coevolution of agents and networks: Opinion spreading and community disconnection. *Physics Letters*, *356*(2), 89–94.

Gilbert, N., & Troitzsch, K. G. (2005) *Simulation for the social Scientist* (2nd ed.). Columbus, OH: McGraw Hill Education.

Girvan, M., & Newman, M. E. J. (2002). Community structure in social and biological networks. *Proceedings of the National Academy of Sciences. 99*(12), 7821–7826.

Glauche, I., Krause, W., Sollacher, R. & Greiner, M. (2004). Distributive routing and congestion control in wireless multihop ad hoc communication networks. *Physica A*, *341*, 677–701.

Gong, P., & van Leeuwen, C. (2004).Evolution to a small-world network with chaotic units. *Europhysics Letters*, *67*(2), 328–333.

González M. C., & Barabási, A. L. (2007). Complex network: From data to models. *Nature Physics*, *3*, 224–225.

González, M. C., Hidalgo, C. A., & Barabási, A. L. (2008). Understanding individual human mobility patterns. *Nature*, *453*(7196), 779–782.

Gossain, H., Nandiraju, N., Anand, K., & Agrawal, D. (2004). Supporting MAC layer multicast in IEEE 802.11 based MANETs: issues and solutions. In *Proceedings of the 29th Annual IEEE International Conference on Local Computer Networks* (pp. 172–179). Tampa, FL.

Grimm, V., Berger, U., Bastiansen, F., Eliassen, S., Ginot, V., Giske, J., ... & DeAngelis, D. L. (2006). A standard protocol for describing individual-based and agent-based models. *Ecological Modelling. 198*(1–2), 115–126.

Gross, T., & Blasius, B. (2008). Adaptive coevolutionary networks: a review. *Journal of the Royal Society Interface*, *5*(20), 259–271.

Gross, T., & Kevrekidis, I. G. (2008). Robust oscillations in SIS epidemics on adaptive networks: Coarse graining by automated moment closure. *Europhysics Letters*, *82*, 38004.

Gross, T., & Sayama, H. (2009). *Adaptive networks: Theory, models and applications* (Understanding Complex Systems). New York, NY: Springer.

Gross, T., Dommar D'Lima, C., & Blasius, B. (2006). Epidemic dynamics on an adaptive network. *Physical Review Letters*, *96*, 208701.

Gross, T., Rudolf, L., & Levin, S. A. (2009). Generalized models reveal stabilizing factors in food webs. *Science*, *325*, 747–750.

Guerra, B., & Gomez-Gardenes, J. (2010). Annealed and mean-field formulations of disease dynamics on static and adaptive networks. *Physical Review E*, *82*, 035101.

Guo, Z., Sloot, P. M. A., & Tay, J. C. (2008). A hybrid agent-based approach for modeling microbiological systems. *Journal of Theoretical Biology*, *255*(2), 163–175.

Gusfield, D. (2002). Partition-distance: A problem and class of perfect graphs arising in clustering. *Information Processing Letters*, *82*(3), 159–164.

Gustafsson, M., Hörnquist, M., & Lombardi, A. (2006). Comparison and validation of community structures in complex networks. *Physica A: Statistical Mechanics and its Applications. 367*, 559–576.

Haggle, (2006-2010). A European Union funded project in Situated and Autonomic Communications, www.haggleproject.org.

Halihan, T., Love, A., & Sharp, J. M. (2005). Identifying connections in a fractured rock aquifer using ADFTs. *Ground Water*, *43*(3), 327–335.

Haykin, S. (1999). *Neural networks: A comprehensive foundation*. Upper Saddle River, NJ: Prentice Hall.

Holme, P., & Ghoshal, G. (2006). Dynamics of networking agents competing for high centrality and low degree. *Physical Review Letters*, *96*, 098701.

Holme, P., & Newman, M. E. J. (2006). Nonequilibrium phase transition in the coevolution of networks and opinions. *Physical Review E*, *74*, 056108.

Holthoefer, J. B. (2011). *Complex networks theory and its application to language* (Doctoral dissertation). Universitat Rovira i Virgili, Spain.

Hossmann, T., Spyropoulos, T., & Legendre, F. (2011). A complex network analysis of human mobility. In *Proceedings of the Third International Workshop on Network Science for Communication Networks* (pp. 876–881). Shanghai, China.

Hovakimyan N., & Cao, C. (2010). *L1 adaptive control theory: Guaranteed robustness with fast adaptation*. Philadelphia, PA: SIAM.

Hu, Y., Li, M., Zhang, P., Fan, Y., & Di, Z. (2008). Community detection by signaling on complex networks. *Physical Review E*, *78*, 016115.

Huang, C. F., Kaur, J., Maguitman, A., & Rocha, L. M. (2007). Agent-based model of genotype editing. *Evolutionary Computation*, *15*(3), 253–289.

Huepe, C., Zschaler, G., Do, A.-L., & Gross, T. (2011). Adaptive-network models of swarm dynamics. *New Journal of Physics*, *13*, 073022.

Hui, P., Crowcroft, J., & Yoneki, E. (2011). Bubble rap: Social-based forwarding in delay tolerant networks. *IEEE Transactions on Mobile Computing*, *10*(11), 1576–1589.

IEEE Standard 802.11b, (1999). *IEEE: Wireless LAN medium access control (MAC) and physical layer specifications*. (ANSI/IEEE Standard), IEEE, New York, NY.

Ioannou, P. A., & Kokotovic, P. V. (1984). Instability analysis and improvement of robustness of adaptive control. *Automatica*, *20*(5), 583–594.

Ioannou, P. A., & Kokotovic, P. V. (1984). Robust redesign of adaptive control. *IEEE Transactions on Automatic Control*, *29*(3), 202–211.

Ioannou, P. A., & Sun, J., (1996). *Robust adaptive control*. Upper Saddle River, NJ: Prentice Hall.

Isidori, A. (1995). *Trends in control: A European perspective*, Heidelberg, Germany: Springer-Verlag GmbH.

Itakura, J., Kurosaki, M., & Itakura, Y. (2010). Reproducibility and usability of chronic virus infection model using agent-based simulation; comparing with a mathematical model. *Biosystems*, *99*(1), 70–78.

Ito, J., & Kaneko, K. (2011).Spontaneous structure formation in a network of chaotic units with variable connection strengths. *Physical Review Letters*, *88*, 028701.

Jain S., & Krishna S. (2001). A model for the emergence of cooperation, interdependence, and structure in evolving networks. *Proceedings of the National Academy of Sciences*, *98*, 543–547.

Jain, S. & Das, S. (2006). MAC layer multicast in wireless multihop networks. In *Proceedings of the First International Conference on Communication System Software and Middleware* (pp. 1–10). Delhi, India.

Kachanov, M. (1987). Elastic solids with many cracks: A simple method of analysis, *International Journal of Solids and Structures*, *23*(1), 23–43.

Kang, Q., Wang, J., & Meng, X. (2009). TCP Vegas-like expert-controlled multicast congestion control algorithm for wireless networks. In *Proceedings of the International Conference on Artificial Intelligence and Computational Intelligence*, *4*, 50–54.

Karasaki, K., Freifeld, B., Cohen, A., Grossenbacherb, K., Cook, P., & Vasco, D., (2000). A multidisciplinary fractured rock characterization study at Raymond field site, Raymond, CA. *Journal of Hydrology*, *236*(1–2), 17–34.

Karimi, A., & Landau, I. D., (2000) Robust adaptive control of a flexible transmission system using multiple models. *IEEE Transactions on Control Systems Technology*, *8*(2), 321–331.

Karimi, A., Landau, I. D., & Motee, N. (2001). Effects of the design parameters of multimodel adaptive control on the performance of a flexible transmission system. *International Journal of Adaptive Control Signal Process*, *15*(3), 335–352.

Karrer, B., Levina, E., & Newman, M. E. J. (2008). Robustness of community structure in networks. *Physical Review E*, *77*(4), 046119.

Keeling, M. J., & Eames, K. T. D. (2005). Networks and epidemic models. *Journal of the Royal Society Interface*, *2*(4), 295–307.

Kim, B. S. & Calise, A. J., (1997). Nonlinear flight control using neural networks. *AIAA Journal of Guidance, Control, and Dynamics*, *20*(1), 26–33.

Kimura, D., & Hayakawa, Y. (2008). Coevolutionary networks with homophily and heterophily. *Physical Review E*, *78*, 016103.

Kiran, M., Coakley, S., Walkinshaw, N., McMinn, P., & Holcombe, M. (2008). Validation and discovery from computational biology models. *Biosystems*, *93*(1–2), 141–150.

Kitzbichler, M., Smith, M., Christensen, S., & Bullmore, E. (2009). Broadband criticality of human brain network synchronization. *PLoS Computational Biology*, *5*, e1000314.

Kovács, I. A., Palotai, R., Szalay, M. S., & Csermely, P. (2010). Community landscapes: an integrative approach to determine overlapping network module hierarchy, identify key nodes and predict network dynamics. *PloS one*, *5*(9), 25.

Kozma, B., & Barrat, A. (2008). Consensus formation on adaptive networks. . *Physical Review E*, *77*, 016102.

Krause, W., Scholz, J., & Greiner, M. (2006). Optimized network structure and routing metric in wireless multihop ad hoc communication. *Physica A: Statistical Mechanics and its Applications*, *361*(2), 707–723.

Krstic, M., Kanellakopoulos, I. & Kokotovic, P. (1995). *Nonlinear and adaptive control design*. New York, NY: John Wiley & Sons, Inc.

Kumar, R., Raghavan, P., Rajagopalan, S., Sivakumar, D., Tomkins, A., & Upfall, E. (2000). Stochastic models for the Web graph. In *Proceedings of the 41st Annual Symposium on Foundations of Computer Science* (pp. 57–65). Redondo Beach, CA.

Kumpula, J. M., Saramäki, J., Kaski, K., & Kertész, J. (2007). Limited resolution in complex network community detection with Potts model approach. *European Physical Journal B*, *56*, 41–45.

Kuramoto, Y. (2003). *Chemical oscillations, waves, and turbulence*. Mineola, NY: Dover Publications, Inc.

Lancichinetti, A., & Fortunato, S. (2009). Community detection algorithms: A comparative analysis. *Physical review E*, *80*(5), 056117.

Lancichinetti, A., Fortunato, S., & Kertész, J. (2009). Detecting the overlapping and hierarchical community structure in complex networks. *New Journal of Physics*, *11*(3), 033015.

Lancichinetti, A., Radicchi, F., & Ramasco, J. J. (2010). Statistical significance of communities in networks. *Physical Review E*, *81*(4), 046110.

Landau, I. D., Lozano, R., M'Saad, M. & Karimi, A. (2011). *Adaptive Control: Algorithms, Analysis and Applications* (2nd ed.). London, UK: Springer London, Limited, 2011.

Lao, B. J., & Kamei, D. T. (2008). Investigation of cellular movement in the prostate epithelium using an agent-based model. *Journal of Theoretical Biology*, *250*(4), 642–654.

Lavretsky, E. (2009). Combined/Composite model reference adaptive control. *IEEE Transactions on Automatic Control*, *54*(11), 2692–2697.

Lee, S., Gerla, M., & Chiang, C. (1999). On-demand multicast routing protocol. In *Proceedings of the IEEE Wireless Communications and Networking Conference*, *3*, 1298–1302.

Leidl, R., & Hartmann, A. K. (2009). *Modern computational science 09*. Oldenburg, Germany: University of Oldenburg Press.

Levina, A., Herrmann, J. M., & Geisel, T. (2009). Phase transitions towards criticality in a neural system with adaptive interactions. *Physical Review Letters*, *102*, 118110.

Levis, P., Lee, N., Welsh, M., & Culler, D. (2003). TOSSIM: Accurate and scalable simulation of entire TinyOS applications. In *Proceedings of the ACM Conference on Embedded Networked Sensor Systems* (pp. 126–137). Los Angeles, CA.

Liljeros, F., Edling, C. R., Amaral, L. A. N., Stanley, H. E., & Aberg, Y. (2001). The web of human sexual contacts. *Nature.411*, 907 .

Lim, M., Braha, D., Wijesinghe, S., Tucker, S. & Bar-Yam, Y. (2007). Preferential detachment in broadcast signaling networks: connectivity and cost trade-off. *Europhysics Letters*, *79*(5), 58005.

Lin, L. (2007). Hydraulic properties of the Table Mountain Group (TMG) aquifers (Doctoral dissertation). University of the Western Cape, South Africa.

Lin, L. & Xu, Y. (2006). A tensor approach to the estimation of hydraulic conductivities in Table Mountain Group aquifers of South Africa. *Water SA*, *32*(3), 371–378.

Lin, Y., & Desouza, K. C. (2010). Co-evolution of organizational network and individual behavior: An agent-based model of interpersonal knowledge transfer. In *Proceedings of the International Conference on Information Systems*. Saint Louis, MO.

Liu X. & Omlin, C. (2010). MCD: An end-to-end multicast congestion scheme using Support vector machines. In *Proceedings of the Southern Africa Telecommunication Networks and Applications Conference*. Cape Town, South Africa.

Liu, M., & Bassler, K. E. (2006). Emergent criticality from coevolution in random Boolean networks. *Physical Review E*, *74*, 041910.

Ljung, L. (2004). *System identification: Theory for the user*. Upper Saddle River, NJ: Prentice Hall.

Long, J. C. S., & Billaux, D. H. (1987). From field data to fracture network modeling: an example incorporating spatial structure. *Water Resources Research*, *23*(7), 1201–1216.

Lopes, M., Damas, B. (2007). A learning framework for generic sensory-motor maps. In *Proceedings of the IEEE/RSJ International Conference on Intelligent Robots and Systems*. San Diego, CA.

Lu, H., Yang, J., Liu, Z., Lane, N. D., Choudhury, T., & Campbell, A. T. (2010). The jigsaw continuous sensing Engine for mobile phone applications. In *Proceedings of the ACM Conference on Embedded Networked Sensor Systems* (pp. 71–84). Zurich, Switzerland.

Luce, R. D., & Perry, A. D. (1949). A method of matrix analysis of group structure. *Psychometrika*, *14*(2), 95–116.

Luo. J. (2013). *Adaptive control for distributed multi-agent coordination* (Doctoral dissertation). University of Connecticut, Storrs, CT.

Möller, T. (1997). A fast triangle-triangle intersection test. *Journal of Graphics Tools*, *2*(2), 25–30.

Macal, C. M. & North, M. J. (2007). Agent-based modeling and simulation: desktop ABMS. In *Proceedings of the 39th conference on Winter simulation* (pp. 95–106). Washington, DC.

Mackay, D. J. C. (2003). *Information theory, inference, and learning algorithms*. Cambridge, UK: Cambridge University Press.

Madan, A., Cebrian, M., Lazer, D., & Pentland, A. S. (2010). Social sensing for epidemiological behavior change. In *Proceedings of the 12th ACM International Conference on Ubiquitous Computing* (pp. 291–300). Copenhagen, Denmark.

Madan, A., Farrahi, K., Gatica-Perez, D., & Pentland, A. S. (2011). Pervasive sensing to model political opinions in face-to-face networks. In *Proceedings of the Ninth International Conference on Pervasive Computing* (pp. 214–231). San Francisco, CA.

Maiya, A. S. (2011). *Sampling and inference in complex networks* (Doctoral dissertation). University of Illinois at Chicago, Chicago, IL.

Makowsky, M. (2006). An agent-based model of mortality shocks, intergenerational effects, and Urban Crime. *Journal of Artificial Societies and Social Simulation*, *9*(2).

Marceau, V., Noël, P. -A., Hébert-Dufresne, L., Allard, A., & Dube, L. J. (2010). Adaptive networks: coevolution of disease and topology. *Physical Review E*, *82*, 036116.

Margolin, G., Berkowitz, B., & Scher, H. (1998). Structure, flow, and generalized conductivity scaling in fracture networks. *Water Resources Research*, *34*(9), 2103–2121.

Maruo, M. H., Lopes, H. S., & Delgado, M. R. (2005). Self-adapting evolutionary parameters: Encoding aspects for combinatorial optimization problems. *Lecture Notes in Computer Science*, *3448*, 155–166.

Maslov, S., & Sneppen, K. (2002). Specificity and stability in topology of protein networks.*Science*. *296*(5569), 910–913.

Meilă, M. (2007). Comparing clusterings–An information based distance.*Journal of Multivariate Analysis*, *98*(5), 873–895.

Meilă, M., & Heckerman, D. (2001). An experimental comparison of model-based clustering methods. *Machine learning*, *42*(1-2), 9–29.

Meisel, C., & Gross, T. (2009). Adaptive self-organization in a realistic neural network model. *Physical Review E*, *80*, 061917.

Meisel, C., Storch, A., Hallmeyer-Elgner, S., Bullmore, E., & Gross, T. (2012). Failure of adaptive self-organized criticality during epileptic seizure attacks. *PLoS Computational Biology*, *84*, e1002312.

Michel, O. (2004). WebotsTM: Professional mobile robot simulation. *International Journal of Advanced Robotic Systems*, *1*(1), 39–42.

Milgram, S. (1967). The small world problem. *Psychology Today*, *1*(1), 61–67.

Milo, R., Shen-Orr, S., Itzkovitz, S., Kashtan, N., Chklovskii, D., & Alon, U. (2002). NetworkMotifs: Simple building blocks of complex networks. *Science*, *298*(5594), 824.

Mirkin, B. G. (1996). *Mathematical classification and clustering*. Norwell, MA: Kluwer Academic Publishers.

Mitchell, M. (2006). Complex systems: Network thinking. *Artificial Intelligence*, *170*(18), 1194–1212.

Mondada, F., Pettinaro, G. C., & Guignard A. (2004). SWARM-BOT: A new distributed robotic concept. *Autonomous Robots*, *17*(2), 193–221.

Montoliu, R., & Gatica-Perez, D. (2010). Discovering human places of interest from multimodal mobile phone data. In *Proceedings of the 9th International Conference on Mobile and Ubiquitous Multimedia* (pp. 12:1–12:10). Limassol, Cyprus.

Montresor, A., & Jelasity, M. (2009). PeerSim: A scalable P2P simulator. In *Proceedings of the Ninth International Conference on Peer-to-Peer Computing* (pp. 99–100). Seattle, WA.

Moreno, Y., & Pacheco, A. F. (2004). Synchronization of Kuramoto oscillators in scale-free networks. *Europhysics Letters*, *68*(4), 603–609.

Morse, A. (1980). Global stability of parameter-adaptive control systems. *IEEE Transactions on Automatic Control*, *25*(3), 433–439.

Moss, S. (2008). Alternative approaches to the empirical validation of agent-based models. *Journal of Artificial Societies and Social Simulation*, *11*(1), 5.

Mourzenko, V. V., Thovert, J. F., & Adler, P. M. (1998). Percolation and conductivity of self-affine fractures. *Physical Review*, *59*(4), 4266–4284.

Narendra, K. S., & Annaswamy, A. M. (1989). *Stable adaptive systems*, Upper Saddle River, NJ: Prentice Hall.

Narendra, K. S., & Balakrishnan, J. (1997). Adaptive control using multiple models. *IEEE Transactions on Automatic Control*, *42*, 171–187.

Narendra, K., & Annaswamy, A. (1987). A new adaptive law for robust adaptation without persistent excitation. *IEEE Transactions on Automatic Control*, *32*(2), 134–145.

Narendra, K., Lin, Y. H., & Valavani, L. (1980) Stable adaptive controller design, part II: Proof of stability. *IEEE Transactions on Automatic Control*, *25*(3), 440–448.

National Research Council, (1996). Rock fractures and fluid flow: Contemporary understanding and applications. Washington D.C.: National Academy Press.

Nayak, P. C., Sudheer K. P., & Jain, S. K. (2012). Water resources management and modeling. Rijeka, Croatia: InTech Europe.

Newman M. E. J. (2003). The structure and function of complex networks. *SIAM Review*, *45*, 167–256 .

Newman, M. E. J. (2002). Assortative mixing in networks. *Physical Review Letters*, *89*(20), 208701.

Newman, M. E. J. (2010). *Networks: An introduction*. Oxford, UK: Oxford University Press.

Newman, M. E. J. (2011). Complex Systems: A Survey. *American Journal of Physics*, *79*(10), 800–810.

Newman, M. E. J., Barabási, A. L., Watts, D. J. (2006). *The structure and dynamics of networks*. Princeton, NJ: Princeton University Press.

Newman, M., & Girvan, M. (2004). Finding and evaluating community structure in networks. *Physical Review E*, *69*(2), 026113.

Nguyen-Tuong, D., & Peters, J. (2011). Model learning for robot control: A survey. *Cognitive Processing*, *12*(4), 319–340.

Niazi, M. A. K. (2011). *Towards a novel unified framework for developing formal, network and validated agent-based simulation models of complex adaptive systems* (Doctoral dissertation). University of Stirling, UK.

North, M. J., & Macal, C. M. (2007). *Managing business complexity: Discovering strategic solutions with agent-based modeling and simulation*. Oxford, UK: Oxford University Press.

Odell, G. M., & Foe, V. E. (2008). An agent-based model contrasts opposite effects of dynamic and stable microtubules on cleavage furrow positioning. *Journal of Cell Biology*, *183*(3), 471–483.

Pacheco J. M., Traulsen, A., & Nowak, M. A. (2006). Active linking in evolutionary games. *Journal of Theoretical Biology*, *243*(3), 437–443.

Pacheco, J. M., Traulsen, A., & Nowak, M. A. (2006). Coevolution of strategy and structure in complex networks with dynamical linking, *Physical Review Letters*, *97*, 258103.

Paczuski, M., Bassler, K. E., & Corral, A. (2000) Self-organized network of competing Boolean agents. *Physical Review Letters*, *84*, 3185–3188.

Palla, G., Derényi, I., Farkas, I., & Vicsek, T. (2005). Uncovering the overlapping community structure of complex networks in nature and society. *Nature*. *435*(7043), 814–818.

Panait, L., & Luke, S. (2005). Cooperative multi-agent learning: The state of the art. *Autonomous Agents and Multi-Agent Systems*, *11*(3), 387–434.

Park, S., Savvides, A., & Srivastava, M. B. (2000). SensorSim: a simulation framework for sensor networks. In *Proceedings of the 3rd ACM International Workshop on Modeling, Analysis and Simulation of Wireless and Mobile Systems* (pp. 104–111). Boston, MA.

Pastor-Satorras, R., & Vespignani, A. (2001). Epidemic spreading in scale-free networks. *Physical Review Letters. 86*, 3200–3203.

Pastor-Satorras, R., & Vespignani, A. (2004). *Evolution and structure of the Internet: A statistical physics approach*. Cambridge, UK: Cambridge University Press.

Pearlmutter, B. A., & Houghton, C. J. (2009). Tuning for criticality: A new hypothesis for sleep. *Neural Computation. 21*, 1622–1641.

Peng, J., & Sikdar, B. (2003). A multicast congestion control scheme for mobile ad-hoc networks. In *Proceedings of the Global Telecommunications Conference* (pp. 2860–2864). San Francisco, CA.

Perkins, C. E., & Royer, E. M. (1999). Ad-hoc on-demand distance vector routing. In *Proceedings of the 2nd Workshop on Mobile Computing Systems and Applications* (pp. 90–100). New Orleans, LA.

Pimm, S. L. (2002). *Food webs*. Chicago, IL: University of Chicago Press.

Podani, J., Oltvai, Z. N., Jeong, H., Tombor, B., Barabáasi, A. L., & Szathmary, E. (2001). Comparable system-level organization of Archaea and Eukaryotes. *Nature Genetics*, *29*(1), 54–56.

Polley, J., Blazakis, D., McGee, J., Rusk, D., & Baras, J. S. (2004). ATEMU: a fine-grained sensor network simulator. In *Proceedings of the First Annual IEEE Communications Society Conference on Sensor and Ad Hoc Communications and Networks* (pp. 145–152). Santa Clara, CA.

Poncela, J., Gomez-Gardenes, J., Traulsen, A., & Moreno, Y. (2009). Evolutionary game dynamics in a growing structured population. *New Journal of Physics*, *11*, 083031.

Price, D. J. D. S. (1965). Networks of scientific papers. *Science*, *149*, 510–515.

Price, D. J. D. S. (1976). A general theory of bibliometric and other cumulative advantage processes. *Journal of the American Society for Information Science*, *27*, 292–306.

Quera, V., Beltran, F. S., & Dolado, R. (2010) Flocking behaviour: Agent-based simulation and hierarchical leadership. *Journal of Artificial Societies and Social Simulation*, *13*(2), 8.

Raghavan, U., Albert, R., & Kumara, S. (2007). Near linear time algorithm to detect community structures in large-scale networks. *Physical Review E*, *76*(3), 036106.

Railsback, S. F., & Grimm, V. (2011). *Agent-based and individual-based modeling: A practical introduction*. Princeton, NJ: Princeton University Press.

Rajendran, V., Obraczka, K., Yi, Y., Lee, S., Tang, K., & Gerla, M. (2004). Combining source- and localized recovery to achieve reliable multicast in multi-hop ad hoc networks. In *Proceedings of the Networking Technologies, Services, and Protocols; Performance of Computer and Communication Networks; Mobile and Wireless Communication, Third International IFIP-TC6 Networking Conference* (pp. 112–124). Athens, Greece.

Rand, W. M. (1971). Objective criteria for the evaluation of clustering methods.*Journal of the American Statistical Association*, *66*(336), 846–850.

Rasmussen, C. E., Williams, C. K. (2006). *Gaussian processes for machine learning*. Cambridge, MA: MIT Press.

Ravasz, E., Somera, A. L., Mongru, D. A., Oltvai, Z. N., & Barab, A. L. (2002). Hierarchical organization of modularity in metabolic networks. *Science*. *297*(5586), 1551–1555.

Reichardt, J., & Bornholdt, S. (2004). Detecting fuzzy community structures in complex networks with a potts model. *Physical Review Letters*, *93*, 218701.

Reichardt, J., & Bornholdt, S. (2006). Statistical mechanics of community detection. *Physical Review E*, *74*(1), 16110.

Renshaw C. E., & Pollard, D. D., (1994). Numerical simulation of fracture set formation: A fracture mechanics model consistent with experimental observations. *Journal of Geophysical Research: Solid Earth*, *99*(B5), 9359–9372.

Resnick, M. (1996). StarLogo: An environment for decentralized modeling and decentralized thinking. In *Proceedings of the Conference on Human Factors in Computing Systems* (pp. 11–12). Vancouver, Canada.

Robinson, E. J., Ratnieks, F. L., & Holcombe, M. (2008). An agent-based model to investigate the roles of attractive and repellent pheromones in ant decision making during foraging. *Journal of Theoretical Biology*, *255*(2), 250–258.

Rohrs, C., Valavani, L., Athans, M., & Stein, G. (1985). Robustness of continuoustime adaptive control algorithms in the presence of unmodeled dynamics. *IEEE Transactions on Automatic Control*, *30*(9), 881–889.

Rosvall, M., & Bergstrom, C. T. (2007). An information-theoretic framework for resolving community structure in complex networks. *Proceedings of the National Academy of Sciences*, *104*(18), 7327–7331.

Rosvall, M., & Bergstrom, C. T. (2011). Multilevel compression of random walks on networks reveals hierarchical organization in large integrated systems. *PloS one*, *6*(4), e18209.

Rouleau, A., & Gale, J. (1985). Statistical characterization of the fracture system in the Stripa granite, Sweden. *International Journal of Rock Mechanics and Mining Science & Geomechanics Abstracts*, *22*(6), 353–367.

Ruan, J., & Zhang, W. (2008). Identifying network communities with a high resolution. *Physical Review E*, *77*(1), 016104.

Rubin, M. A., Mayer, J., Greene T. (2008). An agent-based model for evaluating surveillance methods for catheter-related bloodstream infection. *AMIA Annual Symposium Proceedings*, 631–635.

Rumelhart, D. E., & Hinton, G. E. (1986). *Parallel distributed processing: explorations in the microstructure of cognition* (Volume 1). Cambridge, MA: MIT Press.

Sahin, E., Girgin, S., Bayindir, L., & Turgut, A. E. (2008). Swarm robotics. *Swarm Intelligence*, *1*, 87–100.

Sales-Pardo, M., Guimerà, R., Moreira, A. A., Amaral, L. A .N. (2007). Extracting the hierarchical organization of complex systems. *Proceedings of the National Academy of Sciences*, *104*(39), 15224–15229.

Santoni, D., Pedicini, M., & Castiglione, F. (2008). Implementation of a regulatory gene network to simulate the TH1/2 differentiation in an agent-based model of hypersensitivity reactions. *Bioinformatics*, *24*(11), 1374–1380.

Santos, F. C., Pacheco, J. M., & Lenaerts, T. (2006). Cooperation prevails when individuals adjust their social ties. *PLoS Computational Biology*, *2*(10), e140.

Sayama, H., Pestov, I., Schmidt, J., Bush, B. J., Wong, C., Yamanoi, J., & Gross, T. (2013). Modeling complex systems with adaptive networks. *Computers & Mathematics with Applications*, *65*, 1645–1664.

Schölkopf, B., Smola, A. (2002). *Learning with kernels: Support vector machines, regularization, optimization and beyond*. Cambridge, MA: MIT Press.

Schölkopf, B., Sung, K. K., Burges, C. J. C., Girosi, F., Niyogi, P., Poggio, T., & Vapnik, V. (1997). Comparing support vector machines with gaussian kernel to radial basis function classifiers. *IEEE Transactions on Signal Processing*, *45*(11), 2758–2765.

Schaper, W., & Scholz, D. (2003). Factors regulating arteriogenesis. *Arteriosclerosis, Thrombosis, and Vascular Biology*, *23*, 1143–1151.

Scheuermann, B., Transier, M., Lochert, C., Mauve, M., & Effelsberg, W. (2007). Backpressure Multicast congestion control in mobile ad-hoc networks. In *Proceedings of the 3rd International Conference on Emerging Networking Experiments and Technologies* (pp. 265–275). New York, NY.

Schmid, A. (2005). What is the Truth of Simulation? *Journal of Artificial Societies and Social Simulation*, *8*(4), 5.

Schuster, H. G. (2009), *Reviews of nonlinear dynamics and complexity* (Volume 2). Berlin, Germany: Wiley-VCH.

Scirè, A., Tuval, I., & Eguluz, V. M. (2005). Dynamic modeling of the electric transportation network. *Europhysics Letters*, *71*, 318–424.

Scott, J. (2012). *Social network analysis*. Thousand Oaks, CA: SAGE Publications.

Shaw, L. B., & Schwartz, I. B. (2008). Fluctuating epidemics on adaptive networks. *Physical Review E*, *77*, 066101.

Shaw, L. B., & Schwartz, I. B. (2010). Enhanced vaccine control of epidemics in adaptive networks. *Physical Review E*, *81*, 046120.

Simon, H. A. (1955). On a class of skew distribution functions. *Biometrika*, *42*(3–4), 425–440.

Skyrms, B., & Pemantle, R. (2000). A dynamic model of social network formation, *Proceedings of the National Academy of Sciences*, *97*, 9340–9346.

Sobeih, A., Hou, J. C., Kung, L. C., Li, N., Zhang, H., Chen, W. P., Tyan, H. Y., & Lim, H. (2006). J-Sim: A simulation and emulation environment for wireless sensor networks. *Wireless Communications*, *13*(4), 104–119.

Social Network Journal, 2007. http://www.elsevier.com/locate/inca/505596.

Sornette, A., Davy, P., & Sornette, D. (1993). Fault growth in brittle-ductile experiments and the mechanics of continental collisions. *Journal of Geophysical Research: Solid Earth*, *98*(B7), 12111–12139.

Stanley, R. P. (1997). *Enumerative combinatorics* (Volume 1). Cambridge, UK: Cambridge University Press.

Stauffer, D. & Aharony, A., (1992). Introduction to percolation theory. London, UK: Taylor and Francis.

Steil, J. J. (2004). Backpropagation-decorrelation: online recurrent learning with O(N) complexity. In *Proc. IJCNN Conf.*

Streit, R. E., & Borenstein, D. (2009). An agent-based simulation model for analyzing the governance of the Brazilian Financial System. *Expert Systems with Applications*, *36*(9), 11489–11501.

Szolnoki, A., & Perc, M. (2009). Resolving social dilemmas on evolving random networks. *Europhysics Letters*, *86*(3), 30007.

Tabah, A. N. (1999). Literature dynamics: Studies on growth, diffusion, and epidemics. *Annual Review of Information Science & Technology*, *34*, 249–286.

Takaguchi, T., Nakamura, M., Sato, N., Yano, K., & Masuda, N. (2011). Predictability of conversation partners. *Physical Review X 1*(1), 011008.

Tang, K., Obraczka, K., Lee, S., & Gerla, M. (2002). A reliable, congestion-controlled multicast transport protocol in multimedia multi-hop networks, In *proceedings of the 5th International Symposium on Wireless Personal Multimedia Communications* (pp. 252–256). Honolulu, HI.

Tang, K., Obraczka, K., Lee, S., & Gerla, M. (2002). Congestion controlled adaptive lightweight multicast in wireless mobile ad hoc networks. In *Proceedings of the Seventh IEEE Symposium on Computers and Communications* (pp. 967–972). Taormina, Italy.

Tang, K., Obraczka, K., Lee, S., & Gerla, M. (2003). Reliable adaptive lightweight multicast protocol. In *Proceedings of the International Cnference on Communications* (pp. 1054–1058). Anchorage, AK.

Tao, G. (2003). *Adaptive control design and analysis*. Hoboken, NJ: Wiley.

Traud, A. L., Kelsic, E. D., Mucha, P. J., & Porter, M. A. (2011). Comparing community structure to characteristics in online collegiate social networks. *SIAM Review*, *53*(3), 526–543.

Travers, J., & Milgram, S. (1969). An experimental study of the small world problem. *Sociometry*, *32*(4), 425–443.

Trentelman H. L., Willems J. C. (1993). *Essays on control: Perspectives in the theory and its applications*.Cambridge, MA: Birkhäuser Boston.

van den Berg, D., & van Leeuwen, C. (2004). Adaptive rewiring in chaotic networksrenders small-world connectivitywith consistent clusters. *Europhysics Letters*, *65*(4), 459–464.

van den Hof, P., Schrama, R. (1995). Identification and control–closed-loop issues. *Automatica*, *31*(12), 1751–1770.

van Dongen, S. (2000). *Performance criteria for graph clustering and Markov cluster experiments*. (Technical report), National Research Institute for Mathematics and Computer Science in the Netherlands, Netherlands.

van Segbroeck, S., Santos, F. C., Lenaerts, T., & Pacheco, J. M. (2011). Selection pressure transforms the nature of social dilemmas in adaptive networks. *New Journal of Physics*, *13*, 013007.

van Segbroeck, S., Santos, F. C., Lenaerts, T., & Pacheco, J. M., (2009). Reacting differently to adverse ties promotes cooperation in social networks. *Physical Review Letters*, *102*(5), 058105.

Vapnik, V. (1998). *Statistical Learning Theory*. New York, NY: Wiley Inter-Science.

Vazquez, F., Eguíluz, V. M., & San Miguel, M. (2008). Generic absorbing transition in coevolution dynamics. *Physical Review Letters*, *100*, 08702.

Villas Boas, P. R., Rodrigues, F. A., Travieso, G., & Costa, L. d. F. (2008). Chain motifs: The tails and handles of complex networks. *Physical Review E*, *77*(2), 026106.

Volz, E., Frost, S. D. W., Rothenberg, R., & Meyers, L.A. (2010). Epidemiological bridging by injection drug use drives an early HIV epidemic. *Epidemics*, *2*, 155–164.

Wallace, D. L. (1983). A method for comparing two hierarchical clusterings: Comment. *Journal of the American Statistical Association*, *78*(383), 569–576.

Wang, L., Yan, J., Zhang, J., & Liu, Z. (2007). Controlling disease spread on networks with feedback mechanism. *Chinese Physics*, *16*(9), 2498–2502.

Wang, Y., Martonosi, M., & Peh, L. (2007). Predicting link quality using supervised learning in wireless sensor networks. *ACM SIGMOBILE Mobile Computing and Communications Review*, *11*(3), 71–83.

Wasserman, S., & Faust, K. (1994). *Social network analysis: Methods and applications*. Cambridge, UK: Cambridge University Press.

Watts, D. J. (1999). *Small Worlds: The dynamics of networks between order and randomness*. Princeton, NJ: Princeton University Press.

Watts, D. J. (2003). *Six degrees: The science of a connected age*. New York, NY: W. W. Norton and Company.

Watts, D. J., & Strogatz, S. H. (1998). Collective dynamics of 'small-world' networks. *Nature*. *393*(6684), 440–442.

Watts, J. D. (2007). A twenty-first century science. *Nature*, *445*, 489.

Waxman, B. M. (1988). Routing of multipoint connections. *IEEE Journal on Selected Areas in Communications*, *6*(9), 1617–1622.

Wellman, B. (1926). The school child's choice of companions. *Journal of Educational Research*, *14*, 126–132.

Wellman, B. (2001). Computer networks as social networks. *Science*, *293*(5537), 2031–2034.

Wellman, B., Salaff, J., Dimitrova, D., Garton, L., Gulia, M., & Haythornthwaite, C. (1996). Computer networks as social networks: collaborative work, telework, and virtual community. *Annual Review of Sociology*, *22*(1), 213–238.

Wieland, S., Aquino, T., & Nunes, A. (2012). The structure of coevolving infection networks. *Europhysics Letters*, *97*, 18003.

Wilensky, U. (1999). NetLogo. Center for Connected Learning and Computer-Based Modeling, Northwestern University, Evanston, IL.

Wilensky, U., & Rand, W. (2007). Making models match: Replicating an agent-based model. *Journal of Artificial Societies and Social Simulation*, *10*(4), 2.

Willis-Richards, J., Watanabe, K., & Takahashi, H. (1996). Progress toward a stochastic rock mechanics model of engineered geothermal systems. *Journal of Geophysical Research*, *101*(B8), 17481–17496.

Zanette, D. H., & Gil, S. (2006). Opinion spreading and agent segregation on evolving networks. *Physica D*, *224*, 156–165.

Zanette, D. H., & Risau-Gusmán, S. (2008). Infection spreading in a population with evolving contacts. *Journal of Biological Physics*, *34*, 135–148.

Zarandi, M. H. F., Pourakbar, M., & Turksen, I. B. (2008). A fuzzy agent-based model for reduction of bullwhip effect in supply chain systems. *Expert Systems with Applications*, *34*(3), 1680-1691.

Zhang, P., Li, M., Wu, J., Di, Z., & Fan, Y. (2006). The analysis and dissimilarity comparison of community structure. *Physica A: Statistical Mechanics and its Applications*, *367*, 577–585.

Zimmermann, M. G., Eguíluz, V. M., & San Miguel, M. (2004). Coevolution of dynamical states and interactions in dynamic networks. *Physical Review E*, *69*, 065102R.

Zimmermann, M. G., Eguíluz, V. M., San Miguel, M., & Spadaro, A. (2000). Cooperation in an adaptive network. *Advances in Complex Systems*, *3*, 283–297.

Zschaler, G. (2012). Adaptive-network models of collective dynamics. *European Physical Journal Special Topics*, *211*, 1–101.

Zschaler, G., Böhme, G. A., Seißinger, M., Huepe, C., & Gross, T. (2012). Early fragmentation in the adaptive voter model on directed networks. *Physical Review E*, *85*, 046107.

Zschaler, G., Traulsen, A., & Gross, T. (2010). A homoclinic route to full cooperation in adaptive networks and its failiure. *New Journal of Physics*, *12*, 93015.

APPENDIX A
Measurement of Structure Properties in Complex Networks

In this section, we review only some basic quantities of network measurement, such as average node degree, average clustering coefficient and average shortest path length, etc. The *degree* (or *connectivity* (Dorogovtsev & Mendes, 2002)) k_i of a node i is the number of links connected to the node. For undirected networks, using the adjacency matrix, it can be computed as

$$k_i = \sum_{j=1}^{N} a_{ij}. \tag{A.1}$$

The *average node degree* of a network is the average of k_i for all nodes in the network,

$$\langle k \rangle = \frac{1}{N} \sum_{i=1}^{N} k_i. \tag{A.2}$$

In the case of directed networks, for each node i, its *in-degree* is

$$k_i^{in} = \sum_{j=1}^{N} a_{ji}, \tag{A.3}$$

and *out-degree* is

$$k_i^{out} = \sum_{j=1}^{N} a_{ij}. \tag{A.4}$$

The total degree of a node i is $k_i = k_i^{in} + k_i^{out}$. The average in- and out-degrees are the same

$$\langle k^{out} \rangle = \langle k^{in} \rangle = \frac{1}{N} \sum_{ij} a_{ij}. \tag{A.5}$$

Degree distribution $P(k)$ is another important measurement related to con-

nectivity, i.e. as the probability that a node chosen uniformly at random has degree k (Boccaletti et al., 2006). Power law degree distribution has been found for many real world networks (Barabási & Albert, 1999), while three distributions have been observed in directed networks, including incoming links, $P(k^{in})$, outgoing links, $P(k^{out})$, and joint distribution $P(k^{in}, k^{out})$. Clustering, also known as *transitivity* T (Newman & Girvan, 2004), is the relative number of transitive triples,

$$C = \frac{3N_\Delta}{N_3}, \tag{A.6}$$

where N_Δ is the number of triangles in the network and N_3 is the number of connected triples. The *clustering coefficient* (Watts & Strogatz, 1998) of a node i is given by the ratio of the number of links between the neighbours of i and the maximum number of such links,

$$c_i = \frac{2e_i}{k_i(k_i-1)} = \frac{\sum_{j=1}^{N}\sum_{m=1}^{N} a_{ij}a_{jm}a_{mi}}{k_i(k_i-1)}. \tag{A.7}$$

The *average clustering coefficient* C of the graph is given by

$$C = \langle c \rangle = \frac{1}{N}\sum_{i=1}^{N} c_i. \tag{A.8}$$

The length of a path between nodes i and j is the number of links in the path. A shortest path between nodes i and j is one of the paths connecting these nodes with minimum length (Watts, 1999). All the shortest path lengths of a network can be represented by a distance matrix D whose elements are the length of the shortest paths between any two nodes. The *average shortest path length* (Erdös & Rényi, 1959; Brandes & Wagner, 2000) is given as

$$L = \frac{1}{N(N-1)}\sum_{i,j\in\mathcal{N}, i\neq j} d_{ij}. \tag{A.9}$$

All the measurements mentioned above can be extended from unweighted networks to weighted networks with the weight matrix W (Barrat et al., 2004). The strength of node i is given as the sum of the weights of the corresponding links,

$$s_i = \sum_{i=1}^{N} w_{ij}. \tag{A.10}$$

The average strength is given as:

$$\langle s \rangle = \frac{1}{N} \sum_{i=1}^{N} s_i. \tag{A.11}$$

The *weighted clustering coefficient* (Barrat et al., 2004) of a node i is given by,

$$C_i^w = \frac{1}{s_i(k_i - 1)} \sum_{j>k} \frac{w_{ij} + w_{ik}}{2} a_{ij} a_{ik} a_{jk}, \tag{A.12}$$

where the normalizing factor $s_i(k_i - 1)$ assures that $0 \leq C_i^w \leq 1$. The average weighted clustering coefficient is,

$$\langle C^w \rangle = \frac{1}{N} \sum_{i} C_i^w. \tag{A.13}$$

The correlations between the degrees of different nodes can be quantified by considering the Pearson correlation coefficient of the degrees at both ends of the links (Newman, 2002):

$$r = \frac{\frac{1}{M} \sum_{j>i} k_i k_j a_{ij} - [\frac{1}{M} \sum_{j>i} \frac{1}{2}(k_i + k_j) a_{ij}]^2}{\frac{1}{M} \sum_{j>i} \frac{1}{2}(k_i^2 + k_j^2) a_{ij} - [\frac{1}{M} \sum_{j>i} \frac{1}{2}(k_i + k_j) a_{ij}]^2}, \tag{A.14}$$

where M is the total number of links. If $r > 0$ the network is assortative; if $r < 0$, the network is disassortative; for $r = 0$ there are no correlation between node degrees.

APPENDIX B
Network Models

- *Erdös-Rényi random graph*: A network with random distribution of connections is generated by connecting each pair of vertices in the network with a fixed probability p (Erdös & Rényi, 1960). The degree distribution of this model follows a Poisson like distribution (Bollobás, 1998).

- *Small-world model of Watts and Strogatz*: The networks generated by this model have small-word property and a high clustering coefficient (Watts & Strogatz, 1998). The starting point is a N nodes ring, where all vertices are symmetrically connected to their nearest neighbours in each direction (Costa et al., 2011). Each link is then randomly rewired with probability q (Watts & Strogatz, 1998).

- *Barabási-Albert scale-free model*: This model generates networks with power law degree distribution. A network is generated by starting with m_0 isolated nodes, at each time step, a new node with m links is added to the network (Boccaletti et al., 2006). The vertices which receive the new edges are chosen following a linear preferential attachment rule, i.e. the probability of the new node j to connect with an existing node i is linearly proportional to the degree of j, $\mathcal{P}(i \to j) = k_j / \sum_u k_u$ (Barabási & Albert, 1999).

- *Waxman geographical model*: In a generated geographical network, the nodes have a random distribution in a 2–D space, and the probability of connecting two nodes decays with their distance as $p = e^{-\lambda d}$, where d is their geographic distance, and λ is a constant adjusted to achieve the desirable average degree (Waxman, 1998).

APPENDIX C
Adaptive Control

In the section, a brief introduction of these methodologies and some examples will be given, closely following and summarizing the review in (Luo, 2013). Further details can be found in (Kuramoto, 2011; Aström & Wittenmark, 2013; Luo, 2013;).

The early development of adaptive control theory was motivated by stability theory and system identification (Luo, 2013). Model Reference Adaptive Control scheme, for instance, was developed and analyzed by using the Lyapunov theory for stability analysis (Morse, 1980; Narendra et al., 1980). Adaptive control schemes were traditionally classified as two classes: "Lyapunov-based schemes" in which adaptive laws were derived from the Lyapunov stability analysis, and "estimation-based schemes" in which adaptive laws were generated from gradient or least-squares optimization algorithms (Krstic et al., 1995). Although they were able to provide stability and asymptotical tracking, these traditional schemes may lack robustness in the presence of unmodeled dynamics or bounded disturbances (Rohrs et al., 1985). Some modifications have been proposed for the improvement of robustness, such as σ-modification (Ioannou & Kokotovic, 1984a; Ioannou & Kokotovic, 1984b) and e-modification. In addition, an adaptive-control based backstepping approach has been proposed for more complex nonlinear systems with parametric uncertainty (Krstic et al., 1995), in which a recursive Lyapunov-based scheme was used for adaptive control. Although it can provide global or regional regulations as well as tracking capabilities for systems in a strict-feedback form, this approach fails to address the handling of non-smooth nonlinearities (Narendra & Annaswamy, 1987; Luo, 2013). In order to control nonlinear unknown systems with guaranteed closed-loop performance, neural network-based adaptive control scheme has been developed because of its excellent universal function approximation ability (Calise et al., 2001; Cao & Hovakimyan, 2007). In time-varying systems, however, this approach cannot be implemented directly because the desired weights of the neural network changes

over time (Luo, 2013).

To solve the problem of the trade-off between fast adaptation and robustness, the $\mathcal{L}_1$ adaptive control theory was introduced by Hovaimyan and Cao (2010). The trade-off occurs when high frequencies were introduced to the control signals by fast adaption which increases the systems sensitivity to time delays, and thus decreases the systems robustness. However, $\mathcal{L}_1$ adaptive control can provide a decoupling between robustness and the fast adaptation by using a low-pass filtering system to resolve robustness, as well as using the computational ability of hardware to limit the adaptation (Luo, 2013). A detailed review of $\mathcal{L}_1$ adaptive control theory and its applications can be found in (Hovakimyan & Cao, 2010).